



Intensification of Microalgae Harvesting using a Foam Column

A Thesis Submitted By

Prayoon Enmak

For the degree of Doctor of Philosophy

School of Chemical Engineering and Advanced Materials

Newcastle University

December 2024

Abstract

Large-scale production of microalgae for commercialisation still needs to be improved by challenges in downstream processes, particularly harvesting. This study investigated the feasibility of foam flotation as a cost-effective harvesting technology using a foam riser design. The harvesting of the microalgae *Chlorella vulgaris* was systematically examined within the foam column. The primary result showed that installing risers in the column significantly increased harvesting efficiency.

A flow map was developed showing the relationships between foam structures (discontinuous/continuous), air flow rate, and the CTAB and microalgae concentration. It was found that higher microalgae concentrations required more CTAB and approximately 30% of the free CTAB content remained in the solution.

A foam riser with a diameter ratio of 0.25 increased the pressure and liquid fraction within the column. It leads to reduced foam water content and a 95.6% higher concentration factor than the operation without a riser which using air flow rate of 1 L min^{-1} . Notably, the foam's velocity and bubble size increased significantly as it approached and entered the riser. However, the angle of the riser did not have a significant effect on the process due to the foam naturally formed its own angle under the riser.

The implementation of a double-stage foam flotation process at an air flow rate of 2 L min^{-1} resulted in a 30% increase in efficiency compared to a single-stage process. This suggests that using multistage foam flotation as the preferred method for microalgae harvesting can significantly improve the overall efficiency of the process.

Overall, a foam riser can be optimized for microalgae harvesting by having a constriction ratio of 0.25, a length of 15 cm, and an angle of 90 degrees. Additionally, a two-stage foam flotation process can enhance its effectiveness and offer the potential for scalability in microalgae harvesting technology.

Acknowledgements

I would like to express my deepest appreciation to Professor Adam Harvey and Dr. Jonathan G.M. Lee who accepted me as their student. It was incredibly inspiring and encouraging to work under your supervision during my PhD study. This thesis would not have been completed without your kindly support. Additionally, I could not have undertaken this journey without Dr. Gary S. Caldwell at the School of Natural and Environmental Science, Newcastle University, who provided me with hands-on experiences in algae culture and analysis throughout this study.

I would like to extend my sincere thanks to Dr. Jonathan McDonough, a member of Lab C125 and my lovely PhD office colleagues. It was my pleasure to work with you.

I would like to acknowledge the help I have received from the School of Chemical Engineering and Advanced Materials (CEAM) support staff, including Rob Dixon, Michael Percival, David Whitaker, Paul Roberts, and Paul Sterling. Marine technicians Peter McParlin and Tony Baker also provided valuable support along with all the CEAM administrative staff. I am hugely appreciative of all of you.

Special thanks to the Enmak family, including my parents, sisters, and my beloved wife, Pattarawadee Pannetra. They are always by my side, even when we are apart. Thank you to my friends, especially Bancha and Duangchan, for giving me moral support and being there for me. Thank you to my master's degree supervisor, Professor Pakawadee Kaewkannetra, for giving me countless valuable advice and always backing me up.

Finally, but most importantly, I am deeply indebted to the Royal Thai Government, the Office of the Civil Service Commission (OCSC) and the Ministry of Agriculture and Cooperatives, Thailand which funded my PhD scholarship. None of this would have been possible without their funding and resources,

Table of contents

Abstract.....	i
Acknowledgements	ii
Table of contents	iii
Table of figures.....	vi
Table of tables	x
Abbreviations and notation.....	xi
Chapter 1	1
Introduction.....	1
1.1 Project overview.....	1
1.2 Project development.....	4
1.3 Aims and objectives	5
1.4 Thesis plan.....	5
Chapter 2	6
Literature Review	6
2.1 Algae	6
2.1.1 <i>Definition</i>	6
2.1.2 <i>Classification</i>	7
2.1.3 <i>Habitat</i>	12
2.1.4 <i>Green algae</i>	14
2.2 Microalgae cultivation.....	16
2.2.1 <i>Growth pattern of microalgae</i>	16
2.2.2 <i>Growth conditions and factors for microalgae</i>	17
2.2.3 <i>Commercial microalgae biomass production</i>	21
2.3 Microalgae harvesting technology	32
2.3.1 <i>Coagulation/flocculation</i>	34
2.3.2 <i>Sedimentation</i>	36
2.3.3 <i>Filtration</i>	39
2.3.4 <i>Centrifugation</i>	40
2.3.5 <i>Flotation</i>	41
2.3.6 <i>Comparisons</i>	44

2.4	Foam flotation technique.....	45
2.4.1	<i>Mechanism of CTAB and microalgae cells</i>	46
2.4.2	<i>Foam formation</i>	47
2.4.3	<i>Foam Stability and Destabilisation Process</i>	49
2.4.4	<i>Evaluating Performance of flotation</i>	55
2.4.5	<i>Parameters</i>	55
2.5	Microalgae roles in circular bio-economy	68
2.5.3	<i>Algal-based bioresource cycle</i>	68
2.5.4	<i>Global production of algae</i>	70
2.5.5	<i>Microalgae applications</i>	74
2.6	Summary	85
Chapter 3	86
	Materials and Methods.....	86
3.4	Experimental flow diagram.....	86
3.5	Microalgae cultivation.....	87
3.6	Foam riser design	89
3.7	Foam flotation experiment	91
3.7.3	<i>Foam column structure</i>	91
3.7.4	<i>Foam flotation process</i>	93
3.7.5	<i>Foam visualisation</i>	94
3.7.6	<i>Process analysis</i>	95
Chapter 4	98
	Results and Discussion	98
4.1	Growth of microalgae.....	98
4.2	Microalgal cells in foam flotation process	100
4.3	Development of an Algae/Surfactant (<i>CTAB</i>) “Flow Map”.....	103
4.3.1	<i>Pressure profile</i>	103
4.3.2	<i>A correlation between algal biomass and CTAB concentrations</i>	105
4.3.3	<i>Efficacy of microalgae harvesting based on optimization of flotation factors</i>	110
4.4	Foam riser design and evaluation.....	115
4.4.1	<i>Effect of constriction ratio</i>	115
4.4.2	<i>Effect of angle</i>	119
4.4.3	<i>Effect of riser length</i>	120

4.5	Foam visualisation.....	122
4.5.1	<i>Bubble formation and shape</i>	122
4.5.2	<i>Bubbles size</i>	124
4.5.3	<i>Foam Velocity</i>	128
4.6	Process Development	129
4.6.1	<i>Riser position</i>	129
4.6.2	<i>Double-stage operation</i>	133
Chapter 5	138
Conclusions and Further Work	138
5.1	Conclusions	138
5.1.1	<i>Algae/surfactant/flow rate “Flow map” and suitable conditions</i>	139
5.1.2	<i>Foam riser design</i>	139
5.1.3	<i>Process development</i>	140
5.2	Suggestions for future work	141
Conferences attended and publication submitted	143
Conference	143
Publication.....	143
References	144

Table of figures

Figure 2.1: Number and arrangement of flagella in microalgae cell (Wehr et al., 2015).....	8
Figure 2.2: An illustration of the chloroplast structure (Blankenship, 2002).....	9
Figure 2.3: A schematic representation of the general growth pattern of microalgae in batch culture (Lavens & Sorgeloos, 1996)	16
Figure 2.4: Diagram of an extensive or unmixed pond (A) production site for the cultivation of <i>Dunaliella salina</i> with 250 ha of artificial ponds operated by BASF Health and Nutrition in Hutt Lagoon, Western Australia. Photos courtesy of BASF. (B) The cultivation of <i>Dunaliella salina</i> in Abu Dhabi, U.A.E. Photos courtesy of Ronald Loughland.....	22
Figure 2.5: (A) Schematic diagram of circular ponds. (B) Circular ponds are used for growing <i>Spirulina</i> and <i>Chlorella</i> operated by Far East Bio-Tec, Taiwan. Photos courtesy of FEBICO. (C) The <i>Chlorella</i> cultivation site for beta-carotene production on Ishigaki Island, operated by Yaeyama, Japan. Photos courtesy of Yaeyamachlorella.....	23
Figure 2.6: Some of examples of microalgae culture in open pond system. (A-B) Open pond culture of GIEC-CAS, China (Alam et al., 2017; Qin et al., 2019). (C) Open raceway ponds culture of Department of Agriculture, Ministry of Agriculture and Cooperatives, Bangkok and (D) the largest <i>Spirulina</i> raceway ponds in Chiang Mai, Thailand.	24
Figure 2.7: Schematic diagram and experiment of an outdoor thin- layer cascade system with a working volume of 220 L (top) and a large-scale system for <i>Chlorella</i> cultivation with an area of 650 m ² (bottom) in the Center Algatec, Institute of Microbiology of the Czech Academy of Sciences, Třeboň, Czech Republic (Grivalský et al., 2019; Masojídek et al., 2023).....	26
Figure 2.8: (A) a schematic of flat panel PBR (Gupta et al., 2015) and (B) a large-scale flat-panel PBRs at Guangzhou Institute of Energy Conversion, Chinese Academy of Sciences (GIEC-CAS), China (Qin et al., 2019) and (C) the Arizona Centre for Algae Technology and Innovation (AzCATI) facility in Mesa, Arizona.....	29
Figure 2.9: (A) the schematics of a bubble column photobioreactor (Gupta et al., 2015) and (B) The closed-loop vertical photobioreactor from GreenTech Ventures Inc., Virginia (Photo courtesy of TrueAlgae).	29
Figure 2.10: (A) a schematic of a tubular PBRs system, (B) a pilot-scale vertically stacked tubular photobioreactor in Almera, Spain (Fernández et al., 2014), (C) a horizontal tubular photobioreactor at AlgaePARC, Wageningen UR, Netherlands (Placzek et al., 2017) and (D) a commercial <i>Haematococcus pluvialis</i> production facility at Algatechnologies Ltd. in Kibbutz Ketura, Israel. (Photo courtesy of Solabia-Algatech Nutrition).....	30
Figure 2.11: An overview of the main biomass harvesting approaches in microalgae production.	33
Figure 2.12: Schematic diagram of conventional clarification tanks (A) and lamella-type sedimentation tanks (B). [Source: (Roselet et al., 2019)]	37
Figure 2.13: Harvesting <i>Spirulina</i> sp. using a filtration technique from open pond cultures in Chiang Mai, Thailand.	39

<i>Figure 2.14: Schematic and photo of the microalgal centrifuge (A) Westfalia self-cleaning disk stack centrifuge with pressure-discharged by using a centripetal pump, Source: GEA Westfalia Separator (https://www.gea.com/en/binaries/CP_Chemical_Industry_EN_tcm11-29028.PDF) (B) microalgal biomass harvesting from open raceway pond at Department of Agriculture, Ministry of Agriculture and Cooperatives, Bangkok, Thailand.</i>	<i>40</i>
<i>Figure 2.15: The process of froth flotation (Crawford & Quinn, 2017)</i>	<i>45</i>
<i>Figure 2.16: The molecular structures of cetyltrimethylammonium bromide (CTAB) and microalgae cell. (The following diagram was modified in accordance with the reports of Machado et al., 2022; Kumar, 2021; Vahidi et al., 2017).</i>	<i>46</i>
<i>Figure 2.17: The column pressure profiles at different heights above the interface (A) and a typical curve of surface liquid velocity versus liquid fraction in a two-layer foam column without wash water injection (B), (Modified from: Ireland & Jameson, 2007).</i>	<i>52</i>
<i>Figure 2.18: The profile of the typical curve of superficial liquid velocity versus liquid fraction in a two-layer froth column without wash water injection (Ireland & Jameson, 2007).</i>	<i>53</i>
<i>Figure 2.19: A foam riser plate is installed in the liquid discharge column between the interstitial spaces (Li et al., 2011).</i>	<i>59</i>
<i>Figure 2.20: Equilibrium of solutes around the reflux column (Brunner & Lemlich, 1963) ..</i>	<i>61</i>
<i>Figure 2.21: The cycle of algal-based bioresource, Illustration by Wilkie et al., (2011)</i>	<i>68</i>
<i>Figure 2.22: World aquaculture productions, 1991-2020.</i>	<i>70</i>
<i>Figure 2.23: The global market value of algae products worldwide from 2018 to 2025</i>	<i>73</i>
<i>Figure 2.24: Commercial applications of algae biomass produced by European companies (Vazquez Calderon & Sanchez Lopez, 2022). (Note: not by biomass volumes)</i>	<i>75</i>
<i>Figure 2.25: Transesterification reaction of triglycerides. [Adapted from (Zhao et al., 2020)]</i>	<i>84</i>
<i>Figure 3.1: The experimental flow diagram.....</i>	<i>86</i>
<i>Figure 3.2: The process of algae starter product enhanced in BG-11 medium under autotrophic conditions. A single healthy colony was picked from the agar plate (left), dropped into 10 ml of culture medium and left for 30 days (middle). After 30 days, the cultured algae were further cultured in 1 litre and 10 litre scales (right).</i>	<i>87</i>
<i>Figure 3.3: Side view of some of 51 variable modules of the foam riser, (A) variable lengths and constriction ratios, (B) angles and constriction ratios, (C) as desired, a combination of variable length and variable angle was constructed to form a type of riser and (D) the desired riser was then inserted into the transparent acrylic tube.</i>	<i>89</i>
<i>Figure 3.4: Photograph and schematic diagram of the continuous foam flotation unit. (A) The column for foam equilibrium experiment. (B) The column for foam riser optimization experiment.</i>	<i>92</i>
<i>Figure 3.5: Schematic representation of the continuous foam flotation system.</i>	<i>92</i>
<i>Figure 3.6: Diagram and the photograph of the continuous foam flotation set up with a high speed camera for foam visualisation.</i>	<i>94</i>

Figure 4.1: The growth profile of <i>Chlorella vulgaris</i> cultivated in BG-11 medium pH 7.1 under an autotrophic condition with 16 h of light and 8 h of dark cycles in the presence of cool white fluorescent lights with 2,500 lux of light intensity and continuous aeration for 30 days.....	99
Figure 4.2: The characteristics of <i>C. vulgaris</i> cells as observed under 40x magnification microscopes (A) Feed solution (B) discharged stream or underflow solution and (C) Final product or foamate.	101
Figure 4.3: The physical characteristics of the solution in each part of the foam flotation process with (A) 0.2 g L ⁻¹ algal biomass at 150 mg L ⁻¹ of CTAB concentration and (B) 0.4 g L ⁻¹ algal biomass at 200 mg L ⁻¹ of CTAB concentration.....	102
Figure 4.4: Time-dependent pressure profiles at different heights within the column.	103
Figure 4.5: The pressure profiles at different heights in the column during steady state for 15 minutes of foam flotation process.	104
Figure 4.6: The correlations between CTAB concentration and algal biomass as a function of foam residence time at a column height of 146 cm under operating conditions of 0.1 L min ⁻¹ feed flow rate, 1 L min ⁻¹ air flow rate and 25 cm liquid pool depth.	106
Figure 4.7: Foam behaviour in the column during the foam flotation process.	107
Figure 4.8: The correlation between CTAB concentration and microalgae biomass concentration under the operating conditions of 0.1 L min ⁻¹ feed flow rate, 1 L min ⁻¹ air flow rate, 146 cm column height and 25 cm liquid pool depth.	108
Figure 4.9: An analysis of the free CTAB profile in a feed culture solution at various algal biomass concentrations.	109
Figure 4. 10: The volume profile of foamate as a function of residence times (0.8, 1.2, and 2.3 minutes) in a column of 146 cm height with a liquid pool depth of 25 cm at different CTAB and microalgae biomass concentrations, operating under a feed flow rate of 0.1 L min ⁻¹ . Mean ± standard deviation.	111
Figure 4. 11: The harvesting performance profile as a function of residence times (0.8, 1.2, and 2.3 minutes) in a column of 146 cm height with a liquid pool depth of 25 cm at different CTAB and microalgae biomass concentrations, operated at a feed flow rate of 0.1 L min ⁻¹ . Mean ± standard deviation.	112
Figure 4. 12: Pressure and liquid fraction profiles of the foam at different heights within the column as a function of various constriction ratios (0.25, 0.50, and 0.75) of the foam riser.	113
Figure 4. 13: Pressure and liquid fraction profiles of the foam at different heights within the column as a function of various constriction ratios (0.25, 0.50, and 0.75) of the foam riser.	116
Figure 4. 14: The flotation efficiency as a function of the variations of the constriction ratios (0.25, 0.50 and 0.75) with an angle of 60° and a length of the foam riser of 7 cm.	117
Figure 4. 15: The flotation efficiency profile as a function of the variation of the riser angle (30°, 45°, 60° and 90°) with 5, 10 and 15 cm riser length.....	119
Figure 4. 16: The flotation efficiency profile as a function of variation of riser lengths (5, 7, 10, 15 cm and flat riser) between (A) 0.2 gL ⁻¹ algal biomass and 150 mgL ⁻¹ CTAB and (B) 0.4 gL ⁻¹ algal biomass, 200 mgL ⁻¹ CTAB.....	121

<i>Figure 4. 17: The formation and shape of bubble appearance under the riser with a constriction ratio of 0.25, an angle of 90° and a length of 15 cm.</i>	<i>122</i>
<i>Figure 4. 18: Photo of the foam bubble under the riser with a constriction ratio of 0.25, an angle of 90° and a length of 15 cm</i>	<i>124</i>
<i>Figure 4. 19: Bubble size profile under the riser with a constriction ratio of 0.25, an angle of 90° and a length of 15 cm.</i>	<i>125</i>
<i>Figure 4. 20: Bubble size profile and the appearances, (A) before and (B) after passing through the riser of 0.25 constriction ratio, 90° of angle and 15 cm length.</i>	<i>126</i>
<i>Figure 4. 21: Bubble velocity profile before and after passing through the riser with a constriction ratio of 0.25, an angle of 90° and a length of 15 cm.</i>	<i>128</i>
<i>Figure 4. 22: The characteristics of algal cells attached to bubbles in the column below the riser while rising between 50 and 90 cm above the pulp phase (mixed level solution). .</i>	<i>130</i>
<i>Figure 4. 23: The flotation efficiency profile as a function of the position of a flat riser with an angle of 90° and a constriction ratio of 0.25 at different heights on the column (A) and the sets of multiple risers (B) at 0.1 gL⁻¹ algal biomass, 100 mgL⁻¹ CTAB.</i>	<i>131</i>
<i>Figure 4. 24: Free CTAB profile in the multistage flotation process solution.</i>	<i>133</i>
<i>Figure 4. 25: The physical appearance of the multi-stage flotation process solution at different air flow rates, (A) 1 L min⁻¹ and (B) 2 L min⁻¹</i>	<i>135</i>
<i>Figure 4. 26: The flotation efficiency profile as a function of multi-stage flotation using 90° of angle, 15 cm in length and 0.25 constriction ratio with 1 L min⁻¹ air flow rate (A) and 2 L min⁻¹ air flow rate (B) at 0.2 gL⁻¹ algal biomass, 150 mgL⁻¹ CTAB.</i>	<i>137</i>

Table of tables

<i>Table 2.1: Classification of algae based on evolution and chloroplast structure (Chapman & Chapman, 1973; Bold & Wynne, 1985; Lee, 2008).</i>	10
<i>Table 2.2: Algae and the cell compositions (Bold & Wynne, 1985; Sheehan et al., 1998; Taylor et al., 2008; Leliaert et al., 2012; Baweja & Sahoo, 2015; Hoef-Emden & Archibald, 2017).</i>	11
<i>Table 2.3: A simplified overview of the classification system for Chlorophyta (green algae).</i>	15
<i>Table 2.4: General autotrophic conditions for microalgae cultivation (Baert et al., 1996).</i> ...	17
<i>Table 2.5: Characteristics comparison of growth conditions for microalgae cultivation.</i>	20
<i>Table 2.6: The comprehensive parameter comparison between open systems and photobioreactors for large-scale microalgae cultivation.</i>	31
<i>Table 2.7: Comparison of different harvesting methods (Adapted from: Barros et al., 2015)</i>	44
<i>Table 2.8: World aquaculture production and growth</i>	71
<i>Table 2.9: Commercial microalgae production in 2019</i>	72
<i>Table 2.10: The composition of conventional food sources and microalgae (Becker, 2007; Von Der Haar et al., 2014; Rösch et al., 2019; Diaz et al., 2023).</i>	76
<i>Table 2.11: Comparison of lipid production and land requirements between commercial oil crops and microalgae. Source: (Chisti, 2007)</i>	77
<i>Table 2.12: Commercial products from microalgae and applications. [Adapted from (Spolaore et al., 2006; Rosenberg et al., 2008; Pires, 2017; Barkia et al., 2019)]</i>	80
<i>Table 2.13: Producing biofuels from microalgae through thermochemical conversion processes [source: (López Barreiro et al., 2013)].</i>	82
<i>Table 2.14: Oil content in microalgal biomass (Chisti, 2007).</i>	83
<i>Table 3.1: The composition of BG-11 medium and the amount of compounds for stock preparation (Stanier et al., 1971).</i>	88
<i>Table 3.2: A 51-module riser designed in Google SketchUp Make 2016 and printed on a desktop 3D printer.</i>	90

Abbreviations and notation

ABC	Algae-based bioresource cycle
ABS	Acrylonitrile butadiene styrene
BASF	Badische Anilin- und Sodafabrik
BG-11	Blue Green-11 medium
CAGR	Compound annual growth rate
CNCs	Cellulose nanocrystals
CO ₂	Carbon dioxide
CTAB	Cetyl-trimethyl ammonium bromide
DAH	1,6-diaminohexane
DHA	Docosahexaenoic acid
DCW	Dry cell weight
EPA	Eicosapentaenoic acid
EPS	Extracellular polymeric substance
FAME	Fatty Acid Methyl Ether
GC	Gas Chromatography
GC-MS	Gas Chromatography-Mass Spectrometry
HTC	Hydrothermal carbonization
HTG	Hydrothermal gasification
HTL	Hydrothermal liquefaction
LC	Load Centre / Level control
MDE	Margaritaria discoidea
OD	Optical density
PBR	Photobioreactor
PC	Polycarbonate
PolyDADMAC	Polydiallyldimethylammonium chloride
PUFA	Polyunsaturated fatty acid
SDS	Sodium dodecylsulfate
TG	Triglyceride
TAG	Triacylglycerol
TLC	The thin-layer cascade system
TSS	Total suspended solids
VFA	Volatile fatty acid

UHMWPE Ultra-high molecular weight polyethylene

Notation

CF	Concentration factor
C_x	Cell concentration (cells mL ⁻¹)
D	Diameter of the foam column
DWC	Dry weight concentration
ha	Hectare
RE	Recovery efficiency
(°)	Degree of riser angle
°C	Celsius
ε_L	Liquid fraction in the foam
g	Gravitational field strength
j_d	Superficial drainage velocity
J_g	Superficial gas velocity
J_l	Superficial liquid velocity
n	Fluid dynamic viscosity
p	Pressure
ρ_g	Gas densities
ρ_L	Liquid densities
ρ_l	Liquid medium densities
ρ_s	Microalgae cell densities
r	Radius of the microalgal cell
τ_w	Wall shear stress
y	Positive upward length

Chapter 1

Introduction

1.1 Project overview

Microalgae are single-celled organisms that can use CO₂ as a carbon source for their growth through photosynthesis (Trentacoste *et al.*, 2015). Microalgae play a role in various biotechnology-based industries, especially in use as food additives and health supplements such as fatty acids, proteins and high-value chemicals due to their rapid growth, high productivity per area and ability to grow in various conditions (Borowitzka, 2013; Yan *et al.*, 2013). In addition, they can be used in agriculture as soil conditioners, biofertilizers, pesticides and for biological control of phytopathogens (Abdel-Raouf *et al.*, 2012). Interestingly, there are some species, such as *Nannochloropsis*, *Botryococcus braunii* or *Chlorella* sp., that can accumulate lipids in their cells and thus be used as raw material for biofuel production (Masojídek and Torzillo, 2014). In addition, microalgae can produce biodiesel via one of three methods: using the direct transesterification reaction to convert algae oil into biodiesel (fatty acid methyl esters: FAMES), through direct conversion from wet algae biomass, or via a two-step method of oil extraction followed by conversion directly into algae oil using the hydrothermal liquefaction (HTL) process (Chisti, 2007; Johnson and Wen, 2009; López Barreiro *et al.*, 2013).

A key factor that has made microalgae applications less economically attractive is their operating costs, particularly the cost of the harvesting process. In particular, the dewatering of microalgae from culture media represents a major obstacle to large-scale production due to high energy consumption (Bhatia & Bhatia, 2014). Currently, conventional microalgae harvesting techniques include sedimentation, flocculation with chemical flocculants, filtration and centrifugation (Alam *et al.*, 2017). The disadvantages of these methods are as follows:

- Sedimentation is the simplest method for separating and harvesting microalgae, but it is the slowest process and is ineffective in mass production (Allnut & Kessler, 2015).
- Due to metal contamination in the products, flocculation is limited in food and pharmaceutical product applications as it involves the use of chemical flocculants such as aluminium sulfate. Furthermore, production costs increase because a surfactant removal step is required (Alam *et al.*, 2017).

- Filtration is suitable for harvesting large species of microalgae, such as *Spirulina* sp., where the problem of clogging occurs, and backwashing is required (Packer, 2009; Alam *et al.*, 2017).
- Centrifugation is an efficient harvesting method that results in very high recovery of biomass but has the disadvantage of high capital cost, intensive energy consumption and complicated handling (Chen *et al.*, 2015)

Flotation is a type of particle separation technique based on the attachment of air bubbles to particular particles and is widely used in the mineral industry and wastewater treatment to separate suspended solids, fibres and other low-density solids (Wang, 2010; Alam *et al.*, 2017). Commonly, this method is used in combination with flocculation harvesting (Pahl *et al.*, 2013). In general, this method consists of three main phases: air bubbles, water or media (where the air bubble has been introduced into the flotation reactor) and particles in suspension (Alhattab & Brooks, 2017). According to Shammas and Bennett (2010), the flotation process consists of four basic steps:

1. Air bubbles are created by passing air into water or medium through a porous membrane in the reactor.
2. Contact or collision between the air bubbles and particles suspended in the water or medium.
3. Adhesion and adhesion of the particles to the air bubbles.
4. The air-solid particles float up to the top of the reactor surface.

During foam flotation for microalgae harvesting, microalgae cells are captured by air bubbles in the culture medium (containing surfactant) and then transported to the surface (Allnut & Kessler, 2015). Air bubble-algal cell attachment occurs due to the electrostatic interaction between the positive charge of the surfactants and the negative charge of the algal cell along with the hydrophilic force (Zhang *et al.*, 2019). Among these approaches, flotation is the most effective method for large-scale production due to its simple operation and low energy requirements. However, appropriate harvesting techniques must be selected depending on the microalgae strains, cultivation conditions and end-product requirements (Packer, 2009).

Foam flotation in Thailand

Flotation techniques have been applied in Thailand for several purposes. Dissolved air flotation (DAF), for instance, is used in the production of tap water supplies because it can purify water three times more quickly and effectiveness than the clarifier and pressure sand filter methods (Kittirattanachai, 2016). In addition, Thai ports, food factories, petrochemical facilities, and natural gas separation plants also apply foam flotation in wastewater treatment to eliminate suspended materials like oil and solids. Based on its numerous benefits as mentioned above and its economical process, grease and oil are predominantly separated from wastewater using this method, which achieves a removal rate of around 80–95% while requiring less installation space and enabling the design of compact equipment that is portable to the field (Pothong et al., 2012; Team group, 2012). Typical operating pressure conditions for this system are 4 - 6 barg, and a 10-30% recirculation ratio is reported (Pothong *et al.*, 2012; Srirathchatchawarn & Petiruksakul, 2016). Despite its effectiveness, this system still has comparatively high running costs. There are costs related to chemicals such as PAC (poly aluminum chloride) polymer and NaOH, which aid in the flocculation and coagulation process by assisting suspended particles in the water to form larger particles (Team group, 2012).

Despite the well-recognized advantages of microalgae as a sustainable raw material, increasing scale as commercialization faces obstacles, in particular downstream processes such as harvesting techniques. Microalgae are unique in their ability to thrive in a variety of environments and utilize CO₂ to grow. Bioactive compounds and lipid content yields are significantly higher than those of conventional crops (Masojídek and Torzillo, 2014). Furthermore, cultivation techniques for high-yield microalgae biomass and application technologies are well-established and adaptable to various environments and investment capacities. About 20–30% of the cost of algae production is the harvesting process (*Molina Grima et al.*, 2003). At present, filtration, flotation, and centrifugation are common methods used for commercial microalgae harvesting. These methods, however, are usually expensive, complex, and often require a combination of methods. However, the critical downstream process of harvesting remains a significant bottleneck that limits the commercial viability of microalgae production (Shen *et al.*, 2009). For large-scale microalgae production, the development of cost-effective and energy-efficient harvesting reactors is of utmost importance.

However, the critical downstream process of harvesting remains a significant bottleneck, introducing challenges and incurring substantial costs that limit the commercial viability of microalgae production (Shen *et al.*, 2009). For large-scale microalgae production, the development of cost-effective and energy-efficient harvesting reactors is of utmost importance.

Innovative approaches are essential to overcome these challenges, including novel strategies and the development of integrated harvesting systems that remove and recirculate water from the culture medium. In addition, innovative approaches to address a decrease in labour requirements will also be considered. These efforts will direct investments in the most promising approaches and accelerate the transition to a sustainable and economically viable microalgae-based industry.

In this project, the performance of flotation separation was evaluated based on the percentage of recovery efficiency (biomass removal from the medium) and degree of concentration. Here, research focused on optimizing the estimated chemical concentration and biomass removal via developing and evaluating a new design of foam columns.

1.2 Project development

In this study, the design of a continuous foam flotation model column was refined and evaluated for harvesting the freshwater microalga *Chlorella vulgaris*. The influence of the constriction parameters of the foam riser model was studied, including:

- Angle (30°, 45°, 60° and 90°)
- Constriction ratio (0.25, 0.5 and 0.75)
- Length (5 cm, 10 cm, 15 cm and 0.2 cm (disc shape))
- Processes evaluation (the fitted model columns were evaluated in the context of the effectiveness of microalgae harvesting, including multi-riser and multi-stage flotation)
- In addition, the behaviour of the foam from a fine-tuned model column, including size, shape and velocity, was examined by visualisation with a high-resolution camera.

1.3 Aims and objectives

This project focused on harvesting microalgae using the foam flotation column technique to increase the recovery of microalgae biomass and investigate the influences of constriction parameters on foam column concentration. A modified model column was investigated and studied to adjust the angle, constriction ratio and length of the column.

Accordingly, the aim of this research was:

1. To develop and evaluate a continuous foam flotation for cost-effective application of microalgae biomass harvesting processes.
2. To study the effectiveness of an optimised model column after varying the angle, constriction ratio and length of the foam risers.
3. To study the mechanism of foam flotation through the foam riser (i.e. size, shape and velocity of the bubble) using image visualization with a high-resolution camera.
4. To perform a process design study including multi-riser and multi-stage flotation modifications.

1.4 Thesis plan

This work is presented as a series of chapters formatted according to journal style. The introduction and literature review are first (Chapters 1 and 2), in order to create a solid foundation for subsequent research. Chapter 3 then describes the methodology for microalgae cultivation and the design of a riser in a flotation column and further examines the effects on the system. In addition, foam visualisation and process development are presented in this chapter. Chapter 4 presents the research results and discussions and covers a range of topics including the growth of microalgae and the flow map of the relationship between algal biomass and surfactant concentration. The chapter also discusses foam risers, foam visualizations, and process development. Finally, Chapter 5 provides a comprehensive conclusion, summarises the overall implications of the research, and offers recommendations for future work.

Chapter 2

Literature Review

This chapter provides comprehensive information about microalgae and covers the general aspects of algae and green algae through their definition and classification. Then, the cultivation of microalgae is discussed, including the growth pattern of microalgae, microalgae growth conditions and factors, and commercial microalgae biomass production.

The narrative then moves to the integral roles of microalgae in the context of the circular bioeconomy, which includes the algae-based bioresource cycle, global algae production and various applications of microalgae. Finally, the chapter deals with technologies for harvesting microalgae, exemplified by coagulation/flocculation, sedimentation, filtration, centrifugation and flotation.

2.1 Algae

2.1.1 *Definition*

Algae are photosynthetic organisms containing chlorophyll that, like land plants (*Embryophyta*), rely on sunlight as an energy source, to fix carbon dioxide via photosynthesis. The reaction produces organic macromolecules, such as glucose (sugar) and several kinds of lipids that are used in their metabolic mechanisms and release useful oxygen as a by-product to the environment (Sumi, 2009; Ferrell *et al.*, 2010; Raven & Giordano, 2014).

Algae cells have a wide range of sizes and shapes. Some exist as simple structures or individual cells, while others form colonies together. Some species of algae have large, visible cells (macroalgae) that resemble roots, leaves, and stems called thallus but lack a vascular system (xylem and phloem) and the zygote does not develop into an embryo. However, many types of microalgae are microscopic (called microalgae) and difficult to see without a microscope (Brodie & Lewis, 2007; Biris-Dorhoi *et al.*, 2020).

2.1.2 Classification

Algae have a wide range of morphologies, including single cells, colonies, pseudo filaments, and filaments (Wehr *et al.*, 2015). Phycologists use various criteria to categorize algae. For instance, the primary classification factors focus on specific characteristics of algae, including the number and arrangement of flagella, the composition of cell walls or membranes, intracellular nutrient reserve products, and the pigmentation present within the cells (Wehr *et al.*, 2015; Lee, 2018).

2.1.2.1 Intracellular nutrient storage-products

Groups of algae have been observed that have different amounts of nutrient storage compounds from photosynthesis process accumulated in intracellular cells. For example, green algae and blue-green algae typically accumulate carbohydrates such as starch, amylose and amylopectin. Brown algae and golden algae store nutrient compounds in the form of laminarin, leucosin and mannitol. Meanwhile, euglenoids contain specific nutrients such as lipids and paramylons (Lee, 2018).

2.1.2.2 Composition of cell walls or membranes

Algae have a variety of cell wall structures. Some of them are cell wall-free, while others have complex structures that consist of a variety of compounds incorporated to create their cell wall. The microalgae cell wall composition can be utilised for grouping. For example, green algae cell walls are mainly composed of cellulose, similar to the cell walls of land plants.

Diatoms consist mainly of silica and brown algae possess cell walls composed of alginic acid or alginate. Microalgae with robust cell wall structures, such as red algae, consist of calcium, galactans, agar and carrageenan in their cell walls (Lee, 2018; Nash *et al.*, 2019).

2.1.2.3 Number and arrangement of flagella

Algae exhibit varying mobility depending on the presence or absence of a flagellum. Those that have a flagellum are able to move, while algae without a flagellum remain immobile. Each type of algae has unique characteristics, including the number and placement of flagella, which provide valuable criteria for taxonomic classification.

Figure 2.1 shows different categories: algae with flagella such as *Ceratium rhomvoides*, *Euglena* and *Carteria* sp.; colonial algae with flagella such as *Eudorina elegant* and *Astrephomene gubernaculifera*; and non-motile colonial algae without flagella such as *Scenedesmus bernardii*, *Pediastrum boryanum* and *Pediastrum simplex* etc (Wehr *et al.*, 2015).

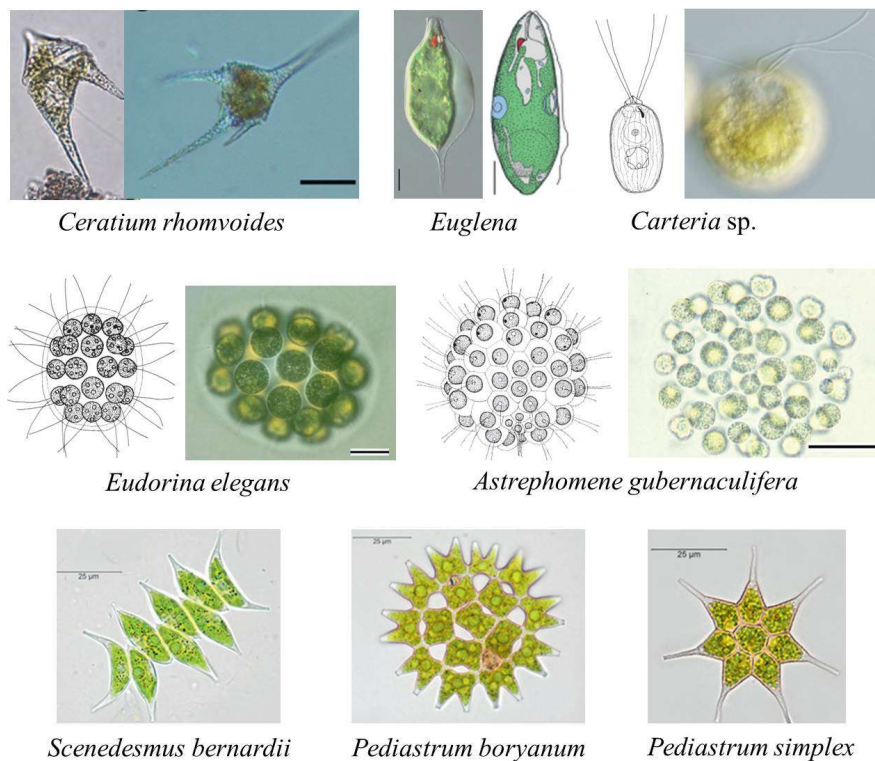


Figure 2.1: Number and arrangement of flagella in microalgae cell (Wehr *et al.*, 2015)

2.1.2.4 Pigmentation within algal Cells.

Chlorophyll A is a universal primary pigment found in all algal species. However, secondary pigments vary depending on the type of algae. For example, blue-green algae and red algae contain phycocyanin and phycoerythrin pigments, respectively, while green algae contain carotenoid pigments. Pigments are localized in special double-membrane structures called chloroplasts, as shown in **Figure 2.2** (Blankenship, 2002).

Within these chloroplasts are stacks of membrane-bound structures called thylakoids, which are made up of protein and lipid compounds used in photosynthesis reactions. Chlorophyll and pigment molecules are distributed throughout the thylakoid membranes. These pigments play an important role in the algal photosynthesis processes and are crucial for the storage of food in the algae cells. In particular, certain pigments can give the algae different colour. It is important to note that each type of algae has a unique pigment profile that varies in both type and quantity.

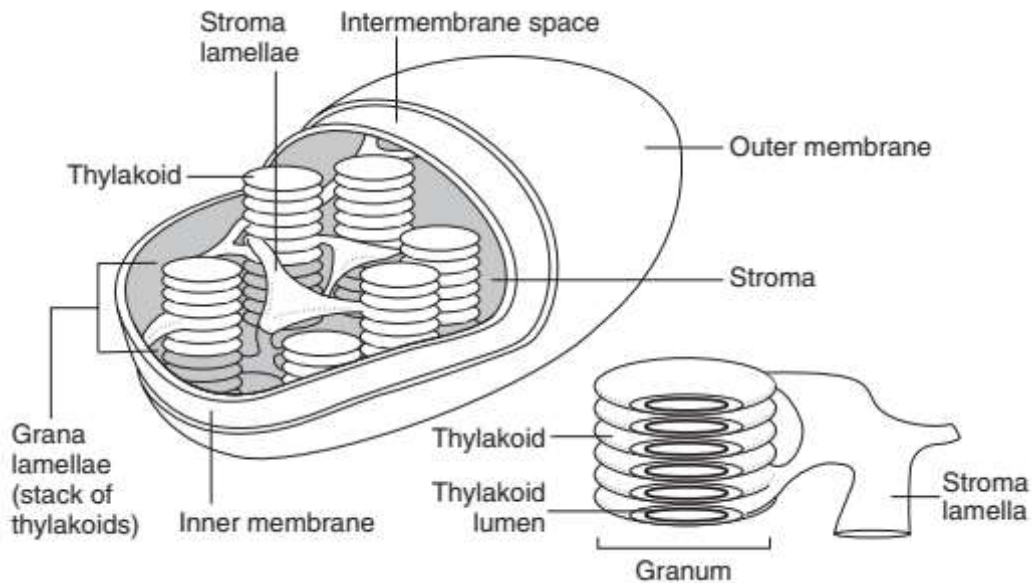


Figure 2.2: An illustration of the chloroplast structure (Blankenship, 2002)

Algae are difficult to assign to a clear system. This is because ongoing discoveries are being made, causing classification at higher levels to change based on genetic and structural considerations. However, the basic information of traditional taxonomy remains useful in modern classifications. Based on evolution and chloroplast structure, **Table 2.1** compares the classifications of algal groups proposed by Lee (2008), Bold and Wynne (1985), and V. J. Chapman (1973). In terms of evolution, it can be divided into Prokaryota and Eukaryota. The Prokaryota group has only one division, Cyanophyta, which consists of blue-green algae.

Groups		Divisions			Algae
Evolutionary	Chloroplast membrane	R. E. Lee (2008)	Bold and Wynne (1985)	V. J. Chapman (1973)	
Prokaryota	I	Cyanophyta	Cyanophyta	Cyanophyta	Blue Green Algae
Eukaryota	II. Chloroplast surrounded by one membrane of chloroplast endoplasmic reticulum	Euglenophyta	Euglenophyta	Euglenophyta	Euglenoids
		Dinophyta	Pyrrophyta	Pyrrophyta	Dinoflagellates
	III. Chloroplast surrounded by two membranes of chloroplast endoplasmic reticulum envelope	Prymnesiophyta Cryptophyta Heterokontophyta	Cryptophyta	Cryptophyta Xanthophyta	Haptophytes Cryptomonads Yellow-green algae
				Chloromonadophyta	Raphidophytes
IV. Chloroplast surrounded by the two membranes of the chloroplast envelope	Chlorophyta	Chlorophyta	Chlorophyta	Green algae	
	Rhodophyta	Charophyta Rhodophyta Phaeophyta Chrysophyta	Charophyta Rhodophyta Phaeophyta Chrysophyta Bacillariophyta	Stone worts Red algae Brown algae Golden algae Diatoms	
	Glaucoephyta			Glaucoephyte algae	

Table 2.1: Classification of algae based on evolution and chloroplast structure (Chapman & Chapman, 1973; Bold & Wynne, 1985; Lee, 2008).

Eukaryota, on the other hand, can be divided into three main groups according to the nature of the chloroplast membrane: Eukaryotic algae, which contain chloroplasts surrounded by one membrane of chloroplast endoplasmic reticulum, can be divided into two divisions: Euglenophyta and Dinophyta. Eukaryotic algae with two membranes of chloroplast endoplasmic reticulum can be divided into two divisions: Cryptophyta and Heterokontophyta. Eukaryotic algae is characterized by a chloroplast surrounded by two membranes, such as: Chlorophyta, Charophyta, Rhodophyta, Phaeophyta and Chrysophyta.

Based on the information in **Table 2.2**, it is noteworthy that the Chrysophyta group (golden algae and diatoms) has the largest number of algae species. Another major category of algae, the Chlorophyta group (green algae), is commonly found in various bodies of water, including freshwater, brackish water, and seawater. Each group of algae exhibits different pigments and cellular nutrient component. In addition, habitats also cause algae to differ.

Division		Known species	Pigments	Nutrient reserve products	Habitat
1	Cyanophyta (Blue Green Algae)	2,000	chlorophyll a, phycocyanin, allophycocyanin, phycoerythrin, β - carotene, xanthophyll	Cyanophycean starch, granules, glocogen	different habitats, freshwater, brackish water
2	Chlorophyta (Green Algae)	8000-12,000	chlorophyll a, b, carotenoids, xanthophyll	Starch, lipids	freshwater, marine, brackish water
3	Charophyta (Stone worts)	over 700	chlorophyll a, b, carotenoids	Starch	freshwater, brackish water
4	Euglenophyta (Euglenoid)	over 1,000	chlorophyll a, b, β - carotene, xanthophylls, zeaxanthin	Starch, paramylon, lipids	freshwater
5	Phaeophyta (Brown Algae)	over 1,800	chlorophyll a, c, β - carotene, fucoxanthin, xanthophylls	Laminarin (β 1,3 glucan polymer), Mannitol, Alginic acid	marine
6	Chrysophyta (Golden Algae, Diatom)	100,000	fucoxanthin, diatoxanthin, chlorophyll a, c, β - carotene, xanthophylls	lipids (TAGs), β -1,3-linked carbohydrate (chrysolaminarin), silica	marine, freshwater, brackish water
7	Pyrrophyta (Dinoflagellates)	over 2,000	Chlorophyll a, c, β - carotene, xanthophylls	Starch, α -1,4- glucan and lipids	marine, freshwater, brackish water
8	Cryptophyta (Red Flagellates)	over 100	chlorophyll a, c, α -and β -carotene, xanthophylls, phycocyanin, phycoerythrin	Starch, α -1,4- glucan	freshwater, marine, brackish water
9	Rhodophyta (Red Algae)	4000	chlorophyll a, α -and β -carotene, xanthophylls, phycobilin, phycocyanin, phycoerythrin	Floridian starch (amylopectin- like), agar, carrageenan	mostly marine, few freshwater (2%)

Table 2.2: Algae and the cell compositions (Bold & Wynne, 1985; Sheehan et al., 1998; Taylor et al., 2008; Leliaert et al., 2012; Baweja & Sahoo, 2015; Hoef-Emden & Archibald, 2017).

2.1.3 *Habitat*

Algae are found anywhere in the world where moisture, nutrients, and environmental conditions are sufficient for growth. Their habitats are extremely diverse: freshwater, mangrove forests, brackish water, seawater, soil, surface area etc. (Yan *et al.*, 2013). Their different habitats are classified as follow (Joubert & Rijkenberg, 1971; Lewin, 1995; Lee, 2008; Wehr *et al.*, 2015; Brooks *et al.*, 2015):

2.1.3.1 *Hard surfaces environment*

Drought-tolerant algae are group that thrive on solid substrates and are typically exposed to atmospheric conditions. Typically, these algae exist as spores or a slick mucilaginous layer, the advantage of them is that they adapt to adverse environment due to capable of surviving and thriving in low-humidity conditions. When the humidity in the environment is sufficient, these algae perform transformation and further develop to thalli or typical cell structure (vegetative cell).

A group of algae called epiphytic algae are able to colonize rigid surfaces such as bark and wood or adhere to rocks and cliffs. Furthermore, another group called terrestrial algae thrive primarily in terrestrial or soil-based environments (Hoffmann, 1989; Sheath & Wehr, 2015).

2.1.3.2 *Freshwater*

- 1) ***Running water*** means water in rivers, streams, waterfalls, and canals. Algae in these habitats are able to adapt to living in a flowing water environment. Their cells' physical structures contribute to them adhering to the ambient substrates.
- 2) ***Stagnant water*** means water in lakes, reservoirs, ponds, and wetlands. In this habitat, algae can grow either free-floating in the water (phytoplankton) or attach themselves to plant stems and roots, or to soil or sand.

2.1.3.3 *Seawater*

- 1) ***Coastal areas***, there are several types of algae that prefer to grow in this habitat, such as brown algae, red algae and green algae. Some of them attach to rocks or sand.

Ocean: a high concentration of free-floating algae (phytoplankton) that usually grow in low number of density.

2.1.3.4 *Extreme environmental conditions*

1) *Snowy Environment*

Algae living in snowy environments have evolved fascinating ability to thrive in such unusual habitats. A common feature of snow-dwelling algae is high carotenoid pigment content, which play important role to protect algae against the intense lighting of snowy landscapes. This group is called Cryoflora algae, or “rd snow algae”.

2) *Geothermal Spring*

In contrast to the cold environments, some algae thrive in geothermal springs, where water temperatures can reach up to 80°C. These resilient algae are called thermophilic algae, including green algae and blue-green algae.

3) *Symbiotic livelihood*

Algae coexist harmoniously with other living organisms or live within their host structures. Notable examples include the relationship between algae and *Azolla sp.* or cycad, where algae inhibit plant root growing. In addition, certain algae can be found associated with animals, as illustrated in sea urchins (*Echinoidea*).

4) *Parasitic livelihood*

Some algae have adopted a parasitic lifestyle. Algal parasites can be observed on both green and blue-green algae, with *Cephaleuros sp.* is an example of an algae parasite. These parasitic algae thrive by growing on the leaves and fruits of host organisms. An algal spot, a yellowish orange fuzzy thalli on the leaves and fruit of the guava (*Psidium guajava*), or red rust on the leaves of the avocado (*Persea Americana*) are typical symptoms of *Cephaleuros virescens*.

2.1.4 *Green algae*

Green algae, a member of the plant kingdom, is classified under the division Chlorophyta. It has a broad spectrum of forms, ranging from single cells and colonies to filamentous structures and thallus (Garcia-Pichel & Belnap, 2021). Within these cell structures, the pigments chlorophyll A and B are particularly widespread and outperform all other pigment types. In addition, the cells contain a variety of carotenoids and xanthophyll pigments. All of these pigments are enclosed in chloroplasts that assume different shapes, and these characteristic features serve as valuable criteria for the systematic classification of green algae (Leliaert, 2019). Additionally, it is worthy that green algae typically contain pyrenoids in their chloroplasts, which harbour a starch-producing enzyme called amylose synthetase, which plays a central role in starch production in algal cells (Wang & Jonikas, 2020).

Green algae have a wide distribution, with an estimated 90% of all green algae thriving in freshwater environments. They can adapt to a range of aquatic habitats, from shallow to deep waters where light can penetrate. The remaining 10% of green algae are marine in nature and their growth patterns vary depending on factors such as water temperature, light availability and nutrient availability (Chapman & Chapman, 2013). Furthermore, green algae can also be located in terrestrial environments, referred to as terrestrial algae. Specific varieties of green algae form symbiotic associations with other plants by either living on their surfaces are called epiphyte algae, or within their tissues referred to as endophyte algae (Wehr & Sheath, 2015).

Chlorophyta species are categorized based on various criteria, including mitosis, cytokinesis, type of gametes, life cycle, cell wall, and more recently genetic information etc. **Table 2.3** provides a simplified overview of the Chlorophyta (green algae) phylogeny, based on the classifications of Bold & Wynne (1985) and Lewis & McCourt (2004). This table lists major groups with informal names in parentheses and order names. When classifying it is very important to note that they are very different from each other. Bold & Wynne presented only one class within this division, Chlorophyceae, which includes 16 orders (Bold & Wynne, 1985). In contrast, Lewis & McCourt divides Chlorophyta into four classes: Chlorophyceae, Ulvophyceae, Trebouxiophyceae and Prasinophyceae, comprising a total of 18 orders (Lewis & McCourt, 2004).

Bold and Wynne 1985	Lewis & McCourt 2004
<p>Kingdom Plantae (Chlorobionta)</p> <p>Division Chlorophyta (green algae)</p> <p>Class Chlorophyceae (chlorophytes)</p> <ul style="list-style-type: none"> Order Volvocales Order Tetrasporales Order Chlorococcales Order Chlorosarcinales Order Ulotrichales Order Sphaeropleales Order Chaetophorales Order Trentepohliales Order Oedogoniales Order Ulvales Order Cladophorales Order Acrosiphoniales Order Caulerpales Order Siphonocladales Order Dasycladales Order Zygnematales 	<p>Kingdom Plantae (Chlorobionta)</p> <p>Division Chlorophyta (green algae)</p> <p>Class Chlorophyceae (chlorophytes)</p> <ul style="list-style-type: none"> Order Chlamydomonadales Order Sphaeropleales Order Oedogoniales Order Chaetopeltidales Order Chaetophorales <p>Class Ulvophyceae (ulvophytes)</p> <ul style="list-style-type: none"> Order Ulotrichales Order Ulvales Order Siphonocladales/Cladophorales Order Caulerpales Order Dasycladales <p>Class Trebouxiophyceae (trebouxiophytes)</p> <ul style="list-style-type: none"> Order Trebouxiales Order Microthamniales Order Prasiolales Order Chlorellales <p>Class Prasinophyceae (prasinophytes)</p> <ul style="list-style-type: none"> Order Pyramimonadales Order Mamiellales Order Pseudoscourfieldiales Order Chlorodendrales

Table 2.3: A simplified overview of the classification system for Chlorophyta (green algae).

Regarding the size variation among green algae, these organisms exhibit a range of cell sizes. Some green algae are composed of simple structures or individual cells, while others aggregate into colonies that can only be observed with a microscope and are often referred to as microalgae. On the other hand, specific types of green algae have relatively large, visible cells, known as macroalgae (Khan *et al.*, 2018). Therefore, in the context of this work, the focus is on microalgae when talking about green algae, and future mentions of green algae refer specifically to microalgae.

2.2 Microalgae cultivation

2.2.1 Growth pattern of microalgae

The growth of microalgae in batch cultures can be divided into distinct phases. **Figure 2.3**, provides a schematic of the algal growth rate in a batch culture as described by Fogg and Thake (1987) consisting to five well-defined stages namely:

- 1) *Lag or induction phase*: this initial phase represents a period of slow growth as the culture adapts to the new conditions.
- 2) *Exponential phase*: rapid growth occurs in this phase, where cell density increases significantly over time.
- 3) *Phase of declining growth rate*: this is where cell division slows down due to various limiting factors, such as nutrient availability, light, pH, carbon dioxide or other environmental factors.
- 4) *Stationary phase*: at this point, the growth rate and the limiting factors reach equilibrium, resulting in a relatively constant cell density within the culture.
- 5) *Death phase*: the culture experiences a decline in cell density as water quality deteriorates and essential nutrients are depleted, rendering the environment unable to support further growth.

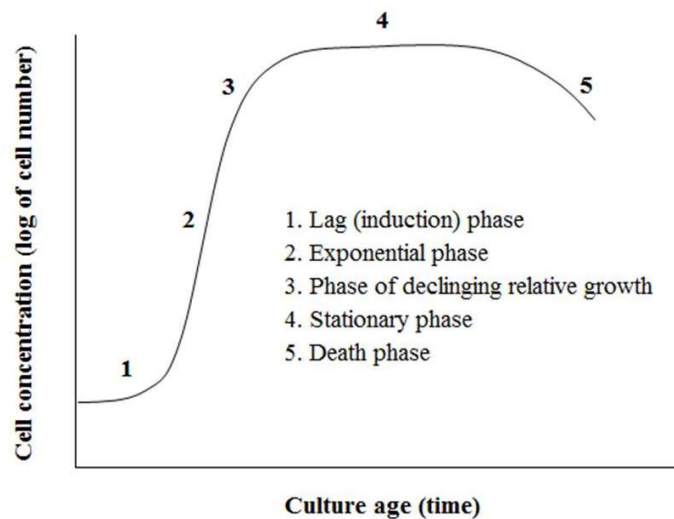


Figure 2.3: A schematic representation of the general growth pattern of microalgae in batch culture (Lavens & Sorgeloos, 1996)

2.2.2 Growth conditions and factors for microalgae

2.2.2.1 Growth factors

Algal growth is influenced by a range of physical and chemical factors. These factors include nutrient quantity and quality, light intensity, pH levels, aeration/mixing, salinity and temperature etc. **Table 2.4** provides a general overview of the key parameters (Baert *et al.*, 1996).

Parameters	Range	Optimal
Temperature (°C)	16-27	18-24
Salinity (g L ⁻¹)*	12-40	20-24
Light intensity (lux)	1,000-10,000 (depends on volume and density)	2,500-5,000
Photoperiod (light: dark, hours)		16:8 (minimum) 24:0 (maximum)
pH	7-9	8.2-8.7

*marine species

Table 2.4: General autotrophic conditions for microalgae cultivation (Baert *et al.*, 1996).

It is crucial to recognize that optimal conditions and acceptable distribution areas vary from one algal species to another. These conditions affect the growth rate of algae overall and are highly specific to each species. Therefore, it is important to consider their interaction in the effective cultivation of different types of algae. Several factors significantly influence microalgae growth and can be described as follows:

- 1) **Nutrient availability and pH balance:** microalgae require essential nutrients and a specific pH range for optimal growth. For autotrophic growth they require carbon dioxide as a carbon source, hydrogen, oxygen, nitrogen, phosphorus, sulfur, iron and trace elements. The pH level of the culture medium also impacts growth. Most microalgae typically thrive in a pH range between 7 and 9, with the most favorable range being between 8.2 and 8.7.

- 2) **Temperature requirements:** the optimal temperature for microalgae growth varies depending on the species. For microalgae cultures, it is generally between 16 and 27°C. The most commonly cultivated microalgae species tolerate temperatures between 18 and 24 °C. However, extreme temperatures, particularly those above 35°C, can damage various types of algae, particularly green microalgae, while temperatures below 16°C tend to slow growth.
- 3) **Salinity:** marine algae show remarkable tolerance to changes in salinity. They often thrive best at slightly lower salinity levels than in their natural habitat. This can be achieved by diluting seawater with tap water, with optimal salinity typically being between 20 and 24 g/L.
- 4) **Light intensity:** light intensity is a critical factor for algae growth. It should not be excessively strong or weak. The optimal light intensity is typically between 1,000 and 10,000 lux, with the most effective results often achieved at 2,500 to 5,000 lux. A minimum of 16 h of artificial illumination per day is recommended for phytoplankton cultivation. Microalgae typically only require one-tenth the intensity of direct sunlight to grow. In natural aquatic microalgae systems, light penetration is limited to the upper 7-10 cm due to the presence of bulk microalgae biomass that blocks light from reaching deeper into the water.
- 5) **Aeration and mixing:** adequate mixing is essential to prevent algal sedimentation, ensure uniform exposure to light and nutrients, prevent thermal stratification (especially in outdoor cultures), and facilitate gas exchange between the culture medium and the air. Effective mixing is particularly important because it provides the carbon source necessary for photosynthesis in the form of carbon dioxide. Mixing methods vary depending on the scope of the culture system. These methods include manual stirring, aeration, or the use of specialized equipment such as agitators, paddle wheels, and pump circulation. It is important to note that not all algal species can tolerate vigorous mixing.

2.2.2.2 Growth conditions

The growth patterns of microalgae are particularly influenced by the cultivation conditions. It is crucial to select the most appropriate microalgae cultivation conditions to achieve maximum productivity while maintaining cost-effectiveness. There are three main conditions for cultivating microalgae: photoautotrophic, heterotrophic and mixotrophic cultivation (Wang *et al.*, 2014).

1) Photoautotrophic condition

Phototrophic cultures are a method of cultivating microalgae that utilizes light such as sunlight as an energy source and carbon dioxide (CO₂) as an inorganic carbon source for photosynthesis (Cruz *et al.*, 2018). This approach offers significant environmental benefits as it has the potential to convert atmospheric CO₂ into various forms of chemical energy, including polysaccharides, proteins, lipids and hydrocarbons for microalgae biomass production (Huang *et al.*, 2010). Consequently, photoautotrophic cultivation is the most widely used method for the growth of microalgae and can be carried out in either open ponds or closed photobioreactors (Medipally *et al.*, 2015). However, there are certain limitations such as low biomass productivity and longer culture periods (Dragone, 2022).

2) Heterotrophic condition

The heterotrophic process in microalgae is the process by which they use organic substrates as a source of both energy and carbon under aerobic conditions. Depending on the type of microalgae, various organic compounds, including sugars, organic acids, acetate, glycerol, and volatile fatty acids (VFAs), can be used in heterotrophy (Huang *et al.*, 2010; Bashan & Perez-Garcia, 2015; Ahmad *et al.*, 2021). Among these, sugars and organic acids are the most commonly chosen and effective sources. Unlike autotrophic cultivation, heterotrophic cultivation does not require light. This flexibility allows heterotrophic microalgae to play a crucial role in the large-scale production of microalgae in regions with long winters and limited sunlight, such as boreal areas (Nzayisenga *et al.*, 2020). While heterotrophic cultivation yields higher biomass than autotrophic cultivation, the effort required to add external organic carbon sources is higher compared to using CO₂. To address the challenge of this limitation, utilizing organic carbon from wastewater sources is a viable solution (Wang *et al.*, 2014; Cruz *et al.*, 2018).

3) *Mixotrophic condition*

Mixotrophic condition is a growth scenario in which microalgae effectively utilize both inorganic CO₂ and organic carbon sources while exposed to light. This condition signifies the ability of microalgae to enter into both photoautotrophic and heterotrophic conditions (Chen *et al.*, 2011). In this process, inorganic carbon fixation takes place through photosynthesis, which responds to light conditions, while the absorption of organic compounds occurs through aerobic respiration, depending on the availability of organic carbon (Hu *et al.*, 2012; Wang *et al.*, 2014). Some microalgae species such as *Spirulina sp.* (Cyanobacteria) and *Chlamydomonas sp.* (Green algae) have the ability to alternate between photo-autotrophic and heterotrophic growth conditions (Bashan & Perez-Garcia, 2015; Medipally *et al.*, 2015). Due to their adaptability to mixotrophic conditions, where they can achieve higher biomass yields than autotrophic algae, making them an excellent approach for the commercial production of microalgae products (Kang *et al.*, 2004).

A comparison of different growing conditions, including phototrophic, heterotrophic and mixotrophic approaches, as shown in **Table 2.5**. Suggests that heterotrophic growth has the potential to offer significantly higher biomass productivity compared to other methods (Chen *et al.*, 2011). For this reason, heterotrophic cultivation has attracted great interest. Nevertheless, under phototrophic conditions, relatively slow cell growth and low biomass productivity are limiting factors. This condition still has a unique advantage because microalgae can effectively capture CO₂ emissions from industrial flue gases. Consequently, phototrophic conditions are widely preferred due to their cost-effectiveness and ease of scaling, especially in open pond systems, making this method extremely attractive.

Cultivation condition	Energy source	Carbon source	Cell density	Reactor scale-up	Operation cost
Phototrophic	Light	Inorganic	Low	Open pond or photo-bioreactor	Low
Heterotrophic	Organic	Organic	High	Conventional fermentor	Medium
Mixotrophic	Light and organic	Inorganic and organic	Medium	Closed photo-bioreactor	High

Table 2.5: Characteristics comparison of growth conditions for microalgae cultivation.

On the other hand, heterotrophic and mixotrophic conditions come with concerns about the cost of acquiring a pond organic carbon source, which represents a significant economic challenge. Additionally, factors such as contamination risks, light requirements, and further complicating the potential need for dedicated photo-bioreactors for scale-up can increase operational costs (Chen *et al.*, 2011; Barbosa *et al.*, 2023).

2.2.3 Commercial microalgae biomass production

Large-scale production of microalgae biomass is only economically feasible through phototrophic cultivation. This is primarily because microalgae have a remarkable ability to efficiently absorb atmospheric carbon dioxide, a resource readily available from power plant emissions (Medipally *et al.*, 2015). Selecting a suitable site is a crucial aspect in designing a microalgae farm for commercial cultivation. It is important to identify regions that provide consistent sunlight throughout the year, especially in tropical and subtropical climates. In addition, this choice of location ensures stable and moderate temperatures all year round, which are ideal for successful microalgae cultivation (Lee *et al.*, 2014).

Phototrophic conditions apply to both indoor and outdoor microalgae cultivation systems as long as an adequate light source is present. For outdoor facilities, natural sunlight serves as the primary light source (Mata *et al.*, 2010). Novel artificial lighting technologies such as LEDs and optical fibres are being explored for indoor systems. Additionally, it is possible to transmit solar energy from external sources to illuminate indoor photo-bioreactors, such as fibre optic sunlight systems (Chen *et al.*, 2011). This approach not only enhances cost-effectiveness, but also allows production to be easily scaled. Under these conditions, two main categories of microalgae cultivation technologies are used for biomass production: open cultivation systems and close cultivation systems, also known as enclosed photo-bioreactor (Y. Shen *et al.*, 2009), as described below:

2.2.3.1 Open cultivation systems

The most basic and oldest approach to cultivating microalgae is open systems in which sunlight provides the energy required for their growth. In open systems, microalgae are grown outdoors and exposed to natural environmental factors such as light, temperature, evaporation and potential contamination (Cruz *et al.*, 2018). These systems can be installed in a variety of locations, including natural bodies of water such as lakes, ponds and lagoons, as well as man-made water containers such as tanks, circular ponds and raceway ponds, which can either be

covered by greenhouse or uncovered (Tan *et al.*, 2018). Over time, numerous designs for open pond systems have been developed. Three main types have proven successful and continue to be used on a commercial scale: extensive ponds, circular ponds, and raceway ponds.

1) *Extensive ponds*

Extensive, also known as unstirred or unmixed ponds represent the most cost-effective and least complex method for commercial cultivation (Y. Shen *et al.*, 2009). These pond systems can cover areas from 1 to over 200 ha and are essentially either natural lakes or artificially created water bodies. Typically, these ponds are shallow, with a of less than 50 cm, with an average depth of 20 to 30 cm (Borowitzka, 2005).

Figure 2.4 shows an example of the use of such ponds for growing *Dunaliella salina* to produce beta-carotene. For this purpose, BASF Health and Nutrition operates a 250-ha artificial pond system in Hutt Lagoon, Western Australia. Likewise, extensive pond systems are used for the cultivation of *Dunaliella salina* in the Arabian Gulf region, particularly in Abu Dhabi, United Arab Emirates (Loughland *et al.*, 2018).

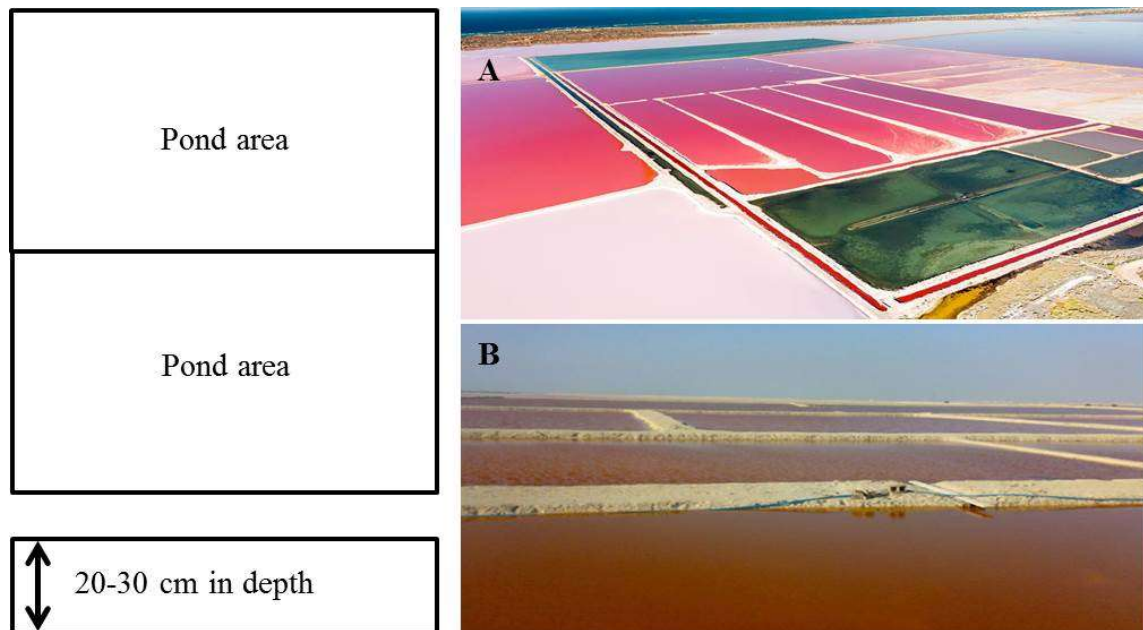
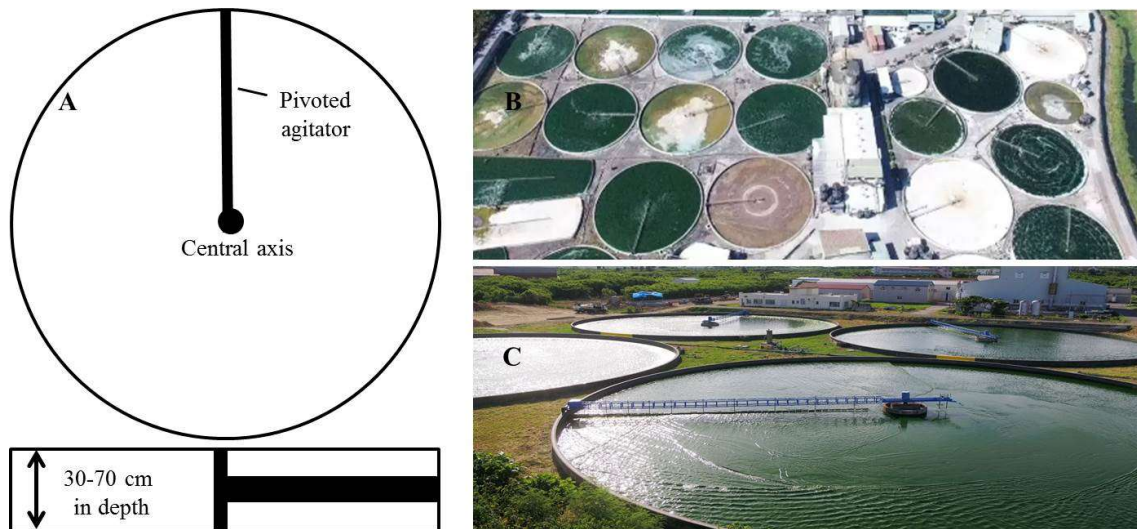


Figure 2.4: Diagram of an extensive or unmixed pond (A) production site for the cultivation of Dunaliella salina with 250 ha of artificial ponds operated by BASF Health and Nutrition in Hutt Lagoon, Western Australia. Photos courtesy of BASF. (B) The cultivation of Dunaliella salina in Abu Dhabi, U.A.E. Photos courtesy of Ronald Loughland.

2) Circular ponds

Circular ponds, one of the earliest large-scale microalgae cultivation systems, are similar in design to conventional raceway ponds. Typically, these ponds have a diameter of up to 45 m and a depth of 30 to 70 cm. They have a centrally pivoting agitator, as shown in **Figure 2.5A**. However, one limitation of circular ponds is their size, typically limited to around 10,000 m², as mixing efficiency decreases when the rotating arm becomes too long.

These ponds are often used in Southeast Asia to produce nutritional supplements such as beta-carotene (Borowitzka, 2005; Y. Shen *et al.*, 2009). For example, **Figure 2.5B** shows the utilization of circular ponds for growing *Spirulina* and *Chlorella* by Far East Bio-Tec (FEBICO) in Taiwan. Similarly, **Figure 2.5C** showcases a *Chlorella* cultivation site on Ishigaki Island by Yaeyama, Japan, for beta-carotene production. In addition, these algae circular ponds can be integrated into wastewater treatment processes to provide a multi-purpose solution (García *et al.*, 2000).



*Figure 2.5: (A) Schematic diagram of circular ponds. (B) Circular ponds are used for growing *Spirulina* and *Chlorella* operated by Far East Bio-Tec, Taiwan. Photos courtesy of FEBICO. (C) The *Chlorella* cultivation site for beta-carotene production on Ishigaki Island, operated by Yaeyama, Japan. Photos courtesy of Yaeyamachlorella.*

3) Raceway ponds

Raceway ponds are widely used open systems for commercial algae cultivation due to their cost-effectiveness in construction and maintenance (Borowitzka, 2005). **Figure 2.6** illustrates the typical structure of raceway ponds designed in a closed loop configuration with oval-shaped recirculation channels. These ponds can be either single units or groups of channels formed by connecting individual raceway channels. They are equipped with paddle wheels to ensure continuous water circulation and mixing, as well as baffles to direct the flow around curves (Y. Shen *et al.*, 2009; Ahmad *et al.*, 2021). Raceway ponds can be constructed from materials such as concrete, fiberglass or polycarbonate with either ground bottom or plastic coating to allow constant circulation of algae cultures. These ponds are generally shallow and typically have a depth of 15 to 30 cm (Schenk *et al.*, 2008; Cruz *et al.*, 2018). An overview of raceway ponds used for the large-scale cultivation of microalgae, such as for the production of beta-carotene and nutritional supplements which are intended for human consumption. **Figure 2.6 (A-B)** shows the raceway pond culture at GIEC-CAS, China (Alam *et al.*, 2017; Qin *et al.*, 2019). **Figure 2.6 (C)** shows the raceway ponds culture in the Department of Agriculture, Ministry of Agriculture and Cooperatives, Bangkok and **Figure 2.6 (D)** shows the largest *Spirulina* raceway ponds in Chiang Mai, Thailand.

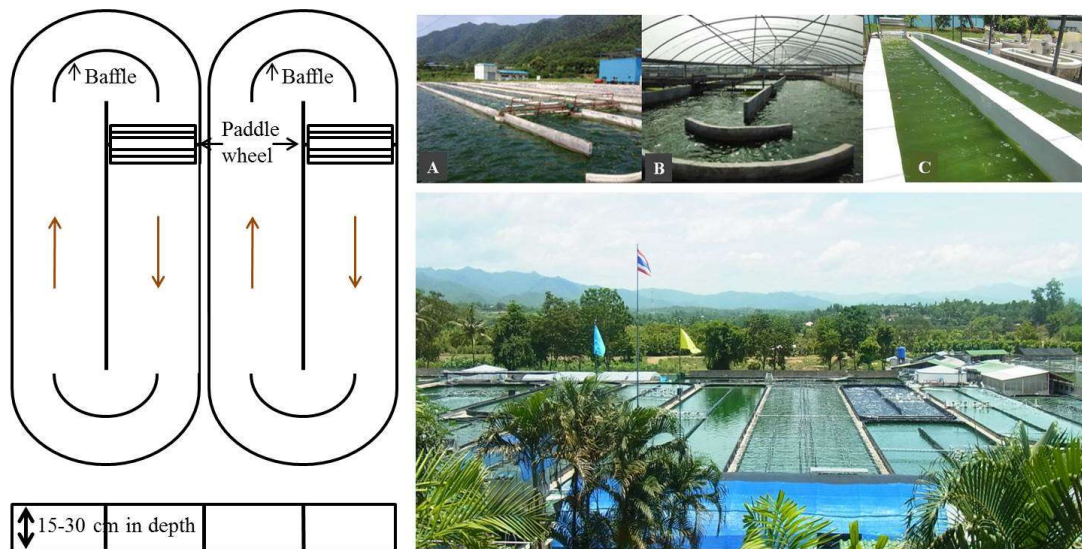


*Figure 2.6: Some of examples of microalgae culture in open pond system. (A-B) Open pond culture of GIEC-CAS, China (Alam *et al.*, 2017; Qin *et al.*, 2019). (C) Open raceway ponds culture of Department of Agriculture, Ministry of Agriculture and Cooperatives, Bangkok and (D) the largest *Spirulina* raceway ponds in Chiang Mai, Thailand.*

However, although commonly used for commercial algae cultivation, raceway ponds suffer from relatively low productivity, typically yielding an average microalgae biomass of only 0.5 g/L. It is important to recognize that raceway ponds have limitations associated with the effects of seasonal light and temperature variations. These fluctuations make it difficult to maintain consistent levels of productivity throughout the year. In addition, in this context, managing contamination becomes increasingly difficult and the intensity of light is limited when a high concentration of algal cells accumulates (Y. Shen *et al.*, 2009).

To address these limitations, researchers have sought solutions by introducing new designs that improve on the conventional raceway pond concept. One of the most successful and practical designs for commercial cultivation is the thin-layer cascade raceway. This innovative approach combines pumps and gravity flow to increase efficiency and productivity.

Thin-layer cascade raceway ponds

The thin-layer cascade system (TLC) is an open microalgae cultivation method that consists of a retention tank connected to a horizontal area exposed to sunlight via a pump and pipes (CG *et al.*, 2014). This system features a series of shallow, inclined troughs, typically 1 to 5 cm deep, arranged one below the other to maximize light utilization (**Figure 2.7**). Microalgae grow in these troughs while a pump continuously circulates the culture from bottom to top, allowing the culture to flow down the troughs (Grivalský *et al.*, 2019). Therefore, TLC systems are particularly suitable for algae strains such as *Chlorella*, *Nannochloropsis* and *Scenedesmus*, which can be resistant to the repeated pumping and shearing stresses associated with the process (Borowitzka, 2005; Masojídek *et al.*, 2023).

This design ensures that all microalgae cells have access to light, maximizing photosynthesis and efficient light utilization resulting in very high cell densities of up to 35 g L⁻¹ (Masojídek *et al.*, 2011; CG *et al.*, 2014). Additionally, the lower total culture volume in TLC systems compared to traditional raceway ponds means less water and nutrients are required (Masojídek *et al.*, 2011). These can reduce harvesting costs and make them an attractive option for commercial microalgae production.

However, there are some limitations to consider. Similar to raceway ponds, TLC systems are open systems and therefore more susceptible to contamination from external microorganisms (Cruz *et al.*, 2018). Furthermore, TLC systems require higher initial investment than raceway ponds. Therefore, the introduction of cheaper materials has significantly reduced the cost of TLC systems, making them more competitive with raceway ponds.

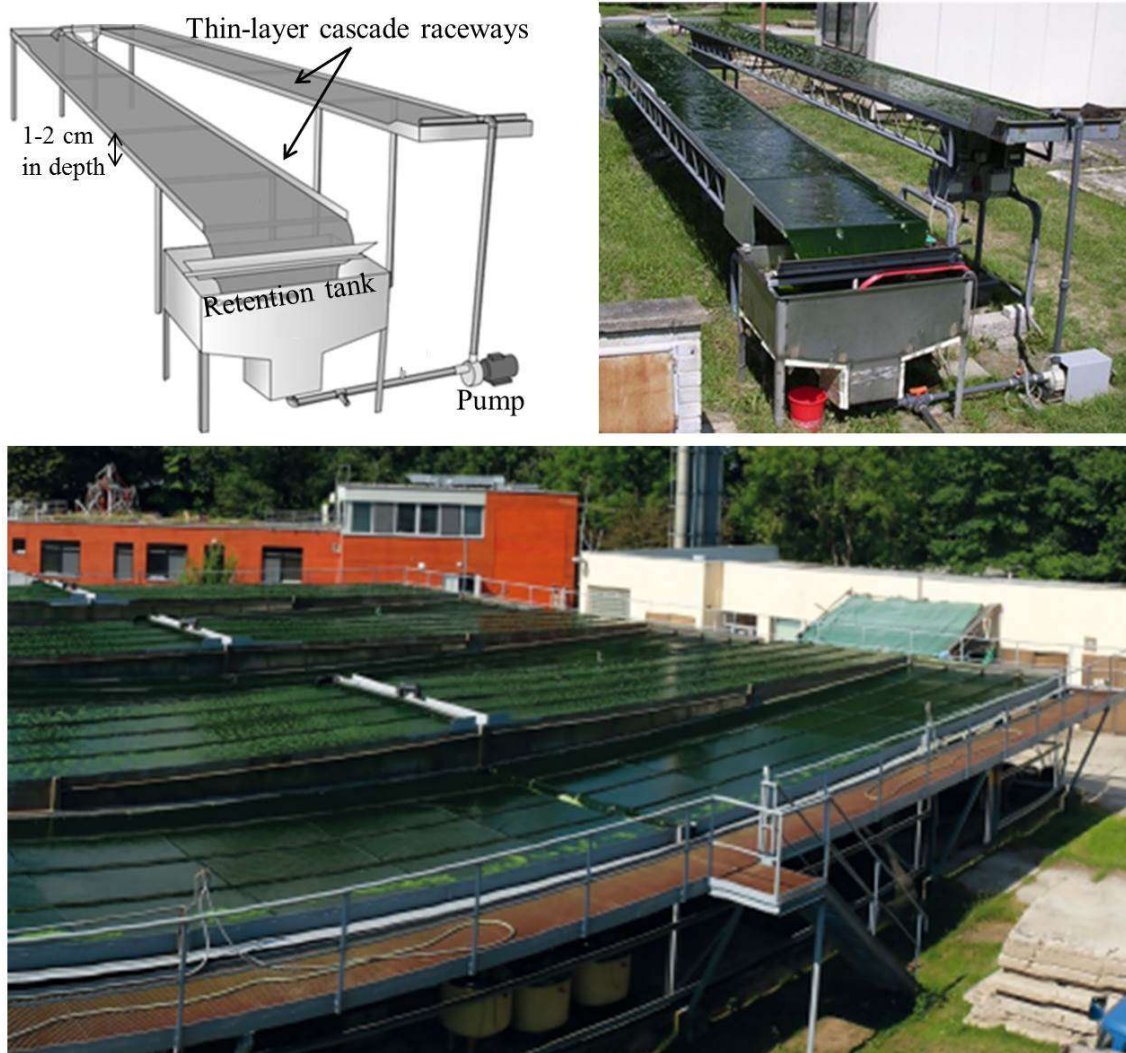


Figure 2.7: Schematic diagram and experiment of an outdoor thin-layer cascade system with a working volume of 220 L (top) and a large-scale system for *Chlorella* cultivation with an area of 650 m² (bottom) in the Center Algatec, Institute of Microbiology of the Czech Academy of Sciences, Třeboň, Czech Republic (Grivalský *et al.*, 2019; Masojídek *et al.*, 2023).

2.2.3.2 Closed cultivation systems

Closed microalgae cultivation systems, also known as photobioreactors (PBRs), are typically enclosed structures that provide a controlled environment for microalgae growth (Y. Shen *et al.*, 2009). These systems offer a more controlled and efficient approach to microalgae production over open systems such as raceway ponds (Masojídek *et al.*, 2023), including:

- **Enhanced productivity:** Closed systems allow for precise control of environmental parameters such as temperature, light intensity, pH and nutrient levels, which can result in higher biomass yields.
- **Reduced contamination:** Closed systems minimize the risk of contamination from external factors such as pests and unwanted microorganisms such as bacteria, fungi and other microalgae species. This is crucial for maintaining stable cultures and preventing the production of unwanted biomass.
- **Year-round cultivation:** Closed systems can operate regardless of outdoor conditions, enabling year-round production and reducing dependence on seasonal fluctuations.

In the context of closed microalgae cultivation systems, various photobioreactor designs have been developed. There are three primary categories commonly used (Wang *et al.*, 2012): flat panels, vertical columns, and tubular photoreactors.

1) Flat Panel PBRs

Flat panel photobioreactors are transparent, flat structures that can be placed either vertically or horizontally. These panels are typically made from transparent materials such as glass or polycarbonate. **Figure 2.8 (A)** illustrates the operating principle of a flat panel PBR, which consists of a frame surrounded by transparent panels on both sides (Gupta *et al.*, 2015). To circulate the algal cell suspension, a pump is used that injects air through a perforated tube on one side, which can reduce the light penetration depth across the culture surface similar to vertical column PBRs (Singh & Sharma, 2012; Gupta *et al.*, 2015). **Figure 2.8 (B)** provides an example of large-scale flat-panel photobioreactors at Guangzhou Institute of Energy Conversion, Chinese Academy of Sciences (GIEC-CAS), China and **Figure 2.8 (C)** the Arizona Centre for Algae Technology and Innovation (AzCATI) facility in Mesa, Arizona.

2) *Vertical Column PBRs*

Vertical column PBRs are most suitable for outdoor mass cultivation and are characterized by their tall and slim design. **Figure 2.9 (A)** demonstrates the principle of a bubble column photobioreactor used in these systems. Cultures are introduced from the bottom and circulated using an air pump or airlift system, improving gas exchange and minimizing sedimentation. Vertical columns can be categorized as bubble columns or airlift reactors based on their liquid flow mode (Gupta *et al.*, 2015). An example of a closed-loop vertical photobioreactor from GreenTech Ventures Inc., Virginia, is presented in **Figure 2.9 (B)**.

3) *Tubular PBRs*

A tubular photobioreactor (PBR) can be configured in various orientations such as horizontal, vertical or inclined forming parallel tubes arranged in loops, alpha shapes or inclined tube configurations depending on the specific design requirements. **Figure 2.10 (A)** provides a schematic representation of a tubular PBRs system. This system consists of two main components: the solar receiver section, which is made of transparent tubes designed to maximize the absorption of solar radiation, and the bubble column section, which is used for mixing, degassing and heat exchange during the cultivation process. The microalgae culture circulates within the system through a centrifugal pump located between the bubble column and the solar receiver (Fernández *et al.*, 2014).

In these tubular PBRs, microalgae cultures are contained within elongated tubes, allowing efficient light utilization and ensuring uniform illumination throughout the culture. The tubular shape offers advantages for outdoor cultivation, as it allows the system to be aligned with sunlight and provides a higher surface area to volume ratio compared to vertical setups. This alignment results in superior light conversion efficiency (Wang *et al.*, 2012; Singh & Sharma, 2012).

Tubular systems are highly scalable and find extensive applications in large-scale microalgae cultivation for biofuel production and various other applications. Figure 2.10 shows examples such as **Figure 2.10(B)** a pilot-scale vertically stacked tubular photobioreactor in Almera, Spain (Fernández *et al.*, 2014), **Figure 2.10(C)** a horizontal tubular photobioreactor at AlgaePARC, Wageningen UR, Netherlands (Płaczek *et al.*, 2017) and **Figure 2.10(D)** a commercial *Haematococcus pluvialis* production facility at Algatechnologies Ltd. in Kibbutz Ketura, Israel.

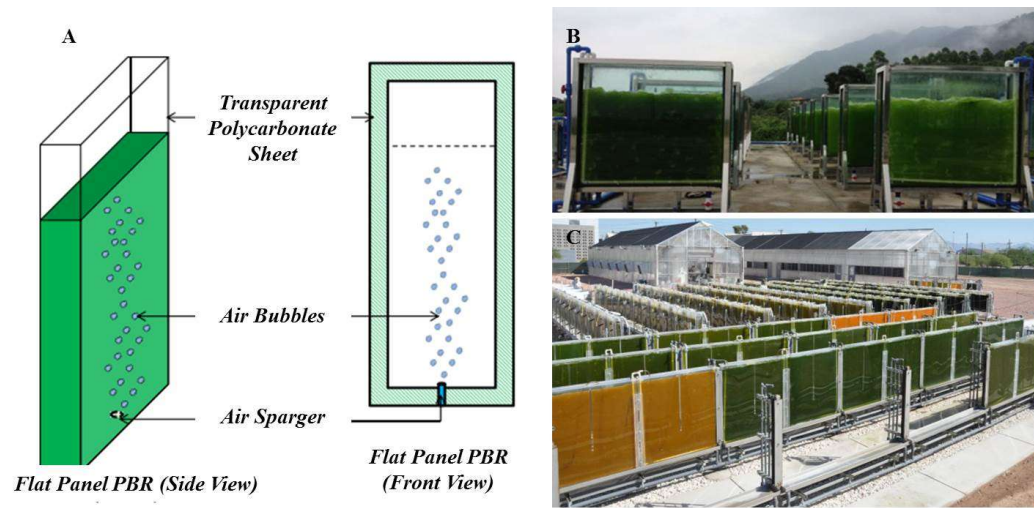


Figure 2.8: (A) a schematic of flat panel PBR (Gupta et al., 2015) and (B) a large-scale flat-panel PBRs at Guangzhou Institute of Energy Conversion, Chinese Academy of Sciences (GIEC-CAS), China (Qin et al., 2019) and (C) the Arizona Centre for Algae Technology and Innovation (AzCATI) facility in Mesa, Arizona.

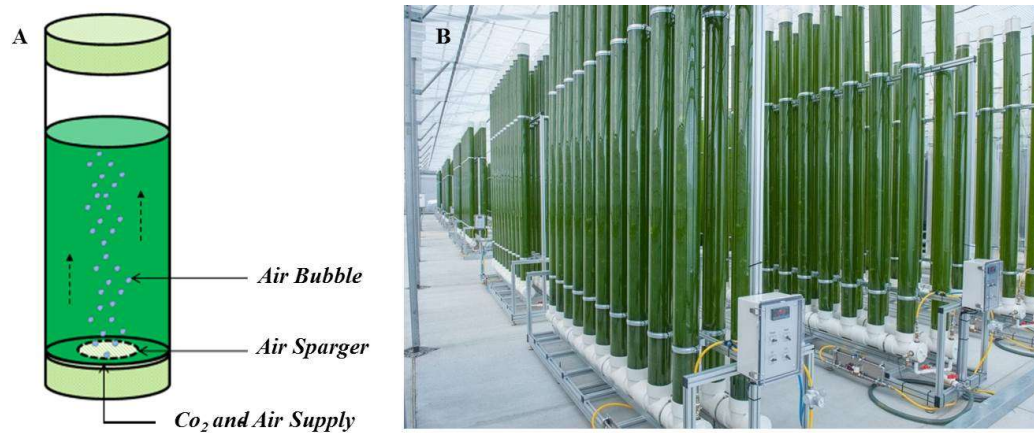


Figure 2.9: (A) the schematics of a bubble column photobioreactor (Gupta et al., 2015) and (B) The closed-loop vertical photobioreactor from GreenTech Ventures Inc., Virginia (Photo courtesy of TrueAlgae).



Figure 2.10: (A) a schematic of a tubular PBRs system, (B) a pilot-scale vertically stacked tubular photobioreactor in Almera, Spain (Fernández *et al.*, 2014), (C) a horizontal tubular photobioreactor at AlgaePARC, Wageningen UR, Netherlands (Placzek *et al.*, 2017) and (D) a commercial *Haematococcus pluvialis* production facility at Algatechnologies Ltd. in Kibbutz Ketura, Israel. (Photo courtesy of Solabia-Algatech Nutrition).

However, it is important to note that due to the high surface-to-volume ratio of tubular PBRs, it is critical to address issues such as photo inhibition caused by oxygen accumulation and intense light exposure. To effectively manage these factors, appropriate cooling mechanisms must be in place (Gupta *et al.*, 2015).

Table 2.6 shows a comprehensive comparison of parameters between open systems and closed systems (PBRs) for large-scale microalgae cultivation. In general, closed systems (PBRs) offer numerous advantages over open systems, such as superior contamination control, improved mixing, enhanced operational flexibility and higher productivity. However, these systems also come with drawbacks, including higher initial investment and operating costs. In addition, they exhibit reduced light utilization efficiency under conditions where the photobioreactor surfaces are obscured or cloudy and challenges associated with scaling up. Conversely, open systems are more cost-effective and scalable. Nevertheless, they present difficulties in process control and typically yield lower productivity than closed systems (Mata *et al.*, 2010; Qin *et al.*, 2019; Masojídek *et al.*, 2023).

Parameters	Open systems	Closed systems (PBRs)
Contamination risk	High	Low
Process control	Difficult	Easy
Mixing	Not uniform, Poor	Uniform
Area requirements	High	Low
Capital cost	Low	High
Operation cost	Low	High
Water losses	Very high	Low
Light utilization	Low	High
Biomass concentration/productivity	Low	High (3-5 times)
Scale-up	Easy	Difficult

Table 2.6: The comprehensive parameter comparison between open systems and photobioreactors for large-scale microalgae cultivation.

2.3 Microalgae harvesting technology

One of the most crucial stages of mass microalgae production is harvesting that is the process of microalgae biomass removal from their culture medium suspension. This process represents a significant challenge in large-scale commercial production, potentially accounting for 20-30% of the overall microalgae production cost (Ghosh & Das, 2015). However there is no one-size-fits-all harvesting method applied to all microalgae species as well as all other products. The complexity of microalgae harvesting is influenced by several factors such as media composition, microalgae species, cultivation conditions, desired end products, and associated costs (Mata *et al.*, 2010).

Despite these challenges, research efforts aimed to improve harvesting methods is on-going. When selecting a harvesting method, several factors must be considered. This includes the physical characteristics of the microalgae (shape, size, density) and the intended end products (Brennan & Owende, 2010). Additionally, any one chosen method should avoid damage of microalgae biomass to enable its use for proceed purposes. Furthermore, the efficiency and cost-effectiveness of the harvesting method are crucial as it aims to remove microalgae from the culture suspension with minimal energy consumption and costs (N. Kumar *et al.*, 2022).

General effective requirements of microalgae harvesting include optimization of both recovery efficiency (RE) and concentration factor (CF) (Lee *et al.*, 2009). The RE is proportion of microalgae cells in the final product obtained from the initial feed culture (Equation 2.1), while the CF indicates the ratio of biomass concentration in the final product compared to its initial concentration in the feed culture as shown in Equation 2.2 (Pahl *et al.*, 2013). A high CF indicates a significant increase in biomass concentration. These two parameters are equally important for assessing the effectiveness of a microalgae harvesting method. In an ideal harvesting process, both RE and CF should be maximized while minimizing energy consumption (Vandamme, 2017).

$$\text{Recovery efficiency (RE)} = \frac{\text{Mass of Cells recovered in foamate}}{\text{Mass of Cells initial feed culture}} \dots\dots\dots 2.1$$

$$\text{Concentration factor (CF)} = \frac{\text{concentration of algae in final product (foamate)}}{\text{initial concentration of algae in feed culture}} \dots\dots\dots 2.2$$

Typically, harvesting processes involve chemical, biological and mechanical (physical) techniques to maximise the recovery efficiency of the product, called algal biomass. It is important to note that these methods can be applied either independently or in combination, offering flexibility in optimising the harvesting process (Milledge & Heaven, 2013; Barros *et al.*, 2015). Harvesting of microalgae generally involves a two-step concentration process, consisting of thickening and dewatering (Brennan & Owende, 2010).

Figure 2.11 illustrates an overview of the main biomass harvesting approaches in the microalgae production process. In bulk harvesting, microalgae are removed from the diluted culture medium and concentrated to obtain a microalgae slurry containing 2-7% total suspended solids (TSS). Thickening takes one step further by increasing the concentration of the microalgae slurry. This achieves higher dewatering with 15-25% TSS, which requires relatively higher energy input. From the initial suspension, these stages play a critical role in achieving concentrated algal slurry and thereby facilitating drying and downstream processing (Ghosh & Das, 2015).

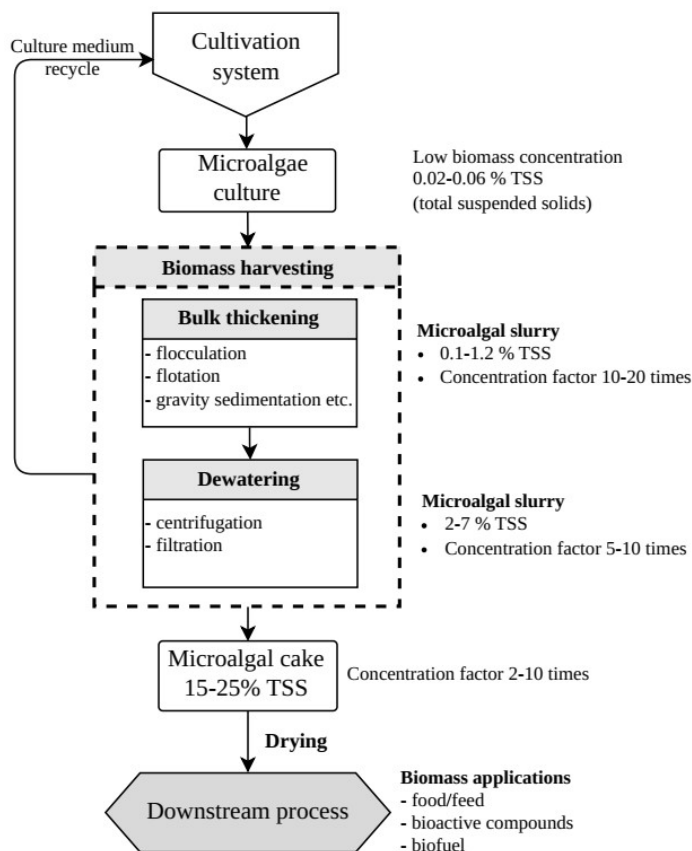


Figure 2.11: An overview of the main biomass harvesting approaches in microalgae production. (Adapted from: Mata et al., 2010; Barros et al., 2015; Ghosh & Das, 2015; N. Kumar et al., 2022)

Ongoing efforts by researchers and practitioners are focused on exploring and refining these methods to increase efficiency, reduce costs, and maximize biomass processing volume. Here is an overview of various microalgae harvesting methods. Coagulation/flocculation, sedimentation, flotation, filtration and centrifugation are common techniques in this context.

2.3.1 Coagulation/flocculation

Coagulation/flocculation is a widely used method for microalgae harvesting. This is the first step in the bulk harvesting process, involving the aggregation of microalgae cells into larger flocs, which can then be easily separated from the culture medium (Ghosh & Das, 2015). This method also serves as a preparation step for other harvesting methods such as filtration, flotation or gravity sedimentation (Brennan & Owende, 2010). There are two phases involved in this process: the coagulation phase and the flocculation phase (N. Kumar et al., 2022).

2.3.1.2 Coagulation phase

Coagulation is a step that destabilizes suspended particles and prepares them for aggregation by rapidly mixing coagulants into the culture suspension (N. Kumar et al., 2022). To initiate this process, multivalent cations or cationic polymers are added to neutralize or reduce the negative charge of the microalgal cells (Molina Grima *et al.*, 2003). This allows them to clump together.

2.3.1.1 Flocculation phase

Flocculation is the subsequent step in which gentle stirring facilitates the interaction of smaller flocs, leading to the formation of larger, well-defined aggregates (N. Kumar et al., 2022). Typically, these steps are followed by gravity sedimentation to improve separation and reduce the volume of concentrated microalgal biomass for cost-effective harvesting (Brennan & Owende, 2010).

Coagulation consists of several mechanisms, including charge neutralization, sweep coagulation, bridging, and patch flocculation, and can occur during floc formation. In charge neutralization, a coagulant or flocculant with a high positive charge is adsorbed on the surfaces of negatively charged colloids. The added chemicals penetrate the diffuse double layers surrounding the particles, making them denser and, therefore, thinner and smaller, allowing the particles to move closer together. Suppose a metal salt coagulant is added to the water at a high enough concentration to cause the precipitation of amorphous metal hydroxide. In that case,

colloid particles can become trapped in these precipitates. This process is called sweep coagulation (Gheraout *et al.*, 2020).

Several flocculation harvesting methods have been studied, each with unique properties and applications. The ideal flocculants depend on factors such as cost, toxicity, effectiveness, and compatibility with downstream applications (Molina Grima *et al.*, 2003). There are several inorganic coagulants that are particularly effective, such as ferric chloride, aluminium sulphate, and ferric sulphate (Brennan & Owende, 2010). The optimum dose of between 50-250 mg L⁻¹ with recovery achievement is around 90% (Gerardo *et al.*, 2015). Additionally, biological flocculation can also be used in microalgae harvesting process. A variety of biological flocculants have been studied, including natural biopolymers such as cationic starch, chitosan, microorganism-produced extracellular biopolymers, plant extracts, and synthetic polymers such as polydiallyldimethylammonium chloride (PolyDADMAC) and glycine betaine-grafted cellulose nanocrystals (CNCs) (Saliu *et al.*, 2022). Secondary metabolites from bacteria or fungi such as extracellular polymeric substances (EPS) are utilized as flocculants (Ghosh & Das, 2015).

According to Oh *et al.* (2001), *Paenibacillus* AM49 was used as a flocculant in *Chlorella vulgaris* harvests with a pH range between 5 and 11, resulting in a flocculation efficiency of 83%. Guo *et al.*, (2018) used a bioflocculant (MBF-G22) from *Pseudomonas boreopolis* G22 to harvest *Scenedesmus abundans* at a dosage of 60 to 90 mg L⁻¹ at an initial pH of 7. The highest flocculation efficiency was achieved at 80 mg L⁻¹ with 95.7% flocculation efficiency. Phytochemicals from plant seed extracts such as *Margaritaria discoidea* (MDE), which is rich in galactomannans, have been shown to be effective as environmentally friendly biocoagulants for microalgae biomass harvesting. The optimal MDE dosage was 16 ml L⁻¹, which resulted in 96% recovery efficiency (Saliu *et al.*, 2022).

Although flocculation harvesting is a simple and energy-efficient method, the operating cost is highly dependent on the type and dosage of flocculants used (Schenk *et al.*, 2008). However, the utilization of metal-based flocculants introduces significant drawbacks, including potential toxicity and metal contamination. In addition, the recycling of culture medium becomes more difficult and potentially facilitates the persistence of microbial contaminants within the medium (Barros *et al.*, 2015). Therefore, selecting the most appropriate method depends on factors such as the microalgae species, the growth medium and the desired biomass concentration.

2.3.2 Sedimentation

Gravity sedimentation is a commonly used method to separate microalgae from water and wastewater with a simple and inexpensive process. In this technique, microalgal cells settle under the influence of gravity force, resulting in the formation of concentrated slurry and a clear supernatant (Brennan & Owende, 2010).

The sedimentation process involves the interaction of two forces - the gravitational force (F_g) and the drag force (F_d) (Williams & Laurens, 2010). According to Stokes' law (Equation 1), there appears to be a direct relationship between the settling velocity and the density and radius of the microalgae cells.

$$\text{Sedimentation velocity} = \frac{F_g}{F_d} = \frac{2}{9} \times \frac{(\rho_s - \rho_l)}{n} g r^2 \dots\dots\dots 2.3$$

Where g is gravitational field strength, r radius of the microalgal cell, n is the fluid dynamic viscosity, and ρ_s and ρ_l are the microalgal cell and liquid medium densities, respectively.

Efficacy of sedimentation

The efficiency of gravity sedimentation relies on the density and radius of the microalgal cells. Microalgae typically have cytoplasm densities in the range of 1020 to 1130 kgm³. According to Equation 2.3, sedimentation occurs relatively slowly, with the settling rate being between 0.1 and 2.6 cm h⁻¹ depending on the density and size of the microalgae (Barros *et al.*, 2015). Those with higher densities settle more quickly, making separation more efficient. For instance, *Spirulina*, with its high-cell density and larger size, as well as colonial forms such as *Scenedesmus* and *Micractinium*, can be effectively harvested using gravity sedimentation. However, many microalgae species have lower densities and settle more slowly, limiting the reliability of sedimentation in routine harvesting (Milledge & Heaven, 2013).

To address this limitation, flocculants are often added to the coagulation/flocculation steps prior to sedimentation. This is to aggregate microalgal cells into larger flocs to improve sedimentation efficiency. The aggregation process increases settling velocity and improves removal efficiency, making sedimentation a more viable harvesting method for lower density microalgae (Chen *et al.*, 2011; Barros *et al.*, 2015).

Types of Sedimentation Systems

Several sedimentation methods are used in the microalgal harvesting process, including conventional clarification tanks and lamella-type sedimentation tanks as shown in **Figure 2.12** (Uduman *et al.*, 2010; Gerardo *et al.*, 2015). These systems concentrate cultures and achieve final total suspended solids (TSS) levels between 1.6% and 3% (Show & Lee, 2014).

- **Conventional clarification tanks:** These are large tanks used to separate microalgae from large volumes of feed suspension. The microalgae settle to the bottom of the tank while the clear liquid is removed from the top
- **Lamella separators:** These are tanks equipped with a series of angled plates that allow for a greater settling area, which enabling faster separation of the microalgae. The microalgae suspension is continuously pumped through the plates, where the microalgae settle at the bottom of the plates. The slurry is then removed discontinuously.

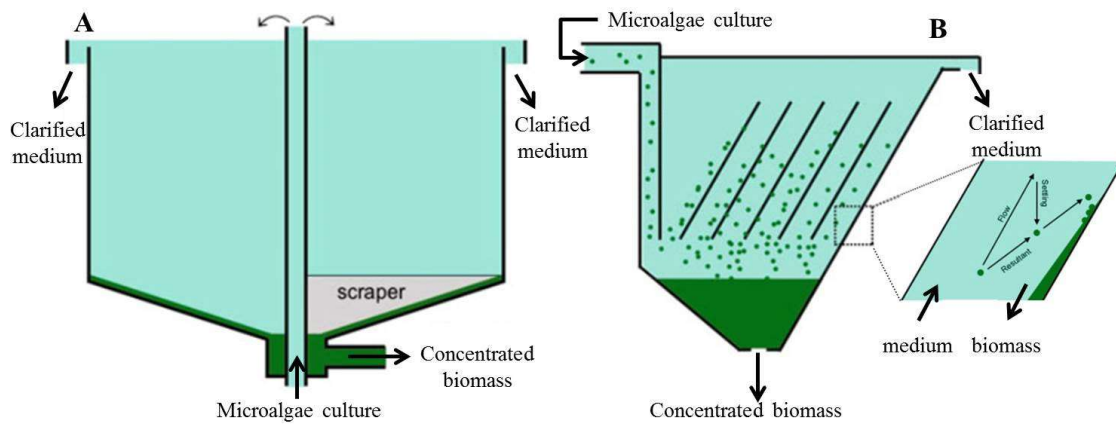


Figure 2.12: Schematic diagram of conventional clarification tanks (A) and lamella-type sedimentation tanks (B). [Source: (Roselet *et al.*, 2019)]

As a cost-effective and energy-efficient method for harvesting microalgae, gravity sedimentation is not widely implemented because of its limitation in low solids concentration and biomass recovery. The low solids concentration achieved through sedimentation often requires additional thickening steps, further complicating the process and increasing the overall cost (N. Kumar *et al.*, 2022). Despite these drawbacks, gravity sedimentation offers several advantages, including simplicity, low construction costs and minimal operator expertise requirements. However, the slow sedimentation rates and low solids concentration make it impractical for large-scale microalgae harvesting operations (Yin *et al.*, 2020).

Primary sedimentation used in wastewater treatment generally has a residence time of one to three hours, on average around two hours. On the other hand, the residence time for water treatment processes that use pure sedimentation is typically three to four hours. However, residence time is typically reduced to two to two and a half hours when coagulation is used to improve particle removal (Zamanikherad *et al.*, 2023).

2.3.3 Filtration

Filtration is a dewatering process that usually also involves coagulation or flocculation to improve harvesting performance (Barros *et al.*, 2015). Usually, filtration can be divided into two basic types: surface filter filtration and depth filter filtration:

Surface filter filtration: algae cells are retained and collected as a paste on the surface of the filter substrate.

Deep bed filtration: algae cells are absorbed into the filter (Alam *et al.*, 2017). The filtration process can be carried out both continuously and discontinuously.

Filtration is suitable for long length microalgae such as *Spirulina sp.* or large colonies (Zhou *et al.*, 2013) and can harvest the low concentration of cell culture. In contrast, other devices such as vacuum, pressure or centrifugal force are required to increase separation efficiency. Clogging of filter media is a significant problem in filtration processes (Barros *et al.*, 2015).



Figure 2.13: Harvesting *Spirulina sp.* using a filtration technique from open pond cultures in Chiang Mai, Thailand.

2.3.4 Centrifugation

Biomass harvesting by centrifugation is the fastest method using centrifugal force to increase sedimentation rate of biomass from the culture (Gerardo et al., 2015; Barros *et al.*, 2015). The biomass concentration from an open pond culture system has low concentration of approximately about 0.25 g L^{-1} (Shen *et al.*, 2009). In demonstration of centrifuge 13000xg, 6000xg and 1300xg can harvest microalgae in term of cell harvest efficiency >95, 60, and 40% at, respectively (Heasman *et al.*, 2000). Hence centrifugation is a suitable harvesting technique, since it has a relatively high recovery outcomes, fast and free of flocculants or chemical contamination used in biomass harvesting (Gerardo et al., 2015).

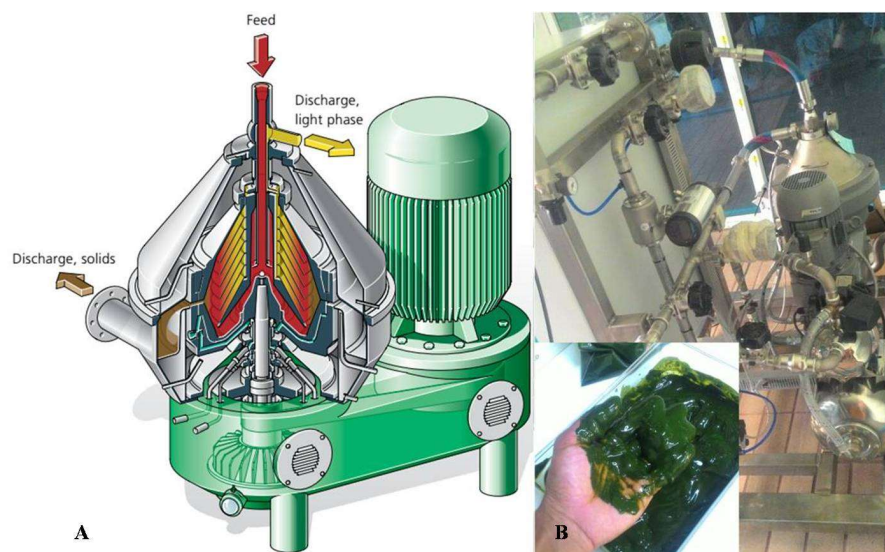


Figure 2.14: Schematic and photo of the microalgal centrifuge (A) Westfalia self-cleaning disk stack centrifuge with pressure-discharged by using a centripetal pump, Source: GEA Westfalia Separator (https://www.gea.com/en/binaries/CP_Chemical_Industry_EN_tcm11-29028.PDF) (B) microalgal biomass harvesting from open raceway pond at Department of Agriculture, Ministry of Agriculture and Cooperatives, Bangkok, Thailand.

Basically, the success of harvesting also depends on the microalgal species, size, and biomass concentration in culture solution and on the type of centrifuges in relation to the centrifuge condition especially energy consumption. For example, 1 kWhm^{-3} can separate *Scenedesmus* sp. and *Coelastrum* by using Self-cleaning disk-stack centrifuge (Molina Grima *et al.*, 2003), while harvesting *Nannochloropsis* sp need more retention time with low flow rate (0.94 Lmin^{-1}) in the bowl of continuous-flow centrifuge due to small size of cell need more energy intensive of 20 kWhm^{-3} (Dassey & Theegala, 2013).

Several centrifuges are examined for microalgae separation such as disk stack centrifuges, decanters and hydrocyclones (Pahl *et al.*, 2013). Disc stack centrifugation has a wide range of uses in commercial separation (**Figure 2.14**) in which it can obtain the concentration of dry algal biomass of up to 10-22% (Milledge & Heaven, 2011). Although centrifugation is an appropriate harvesting method, the complicate to operation and high maintenance costs as well as intensive energy consuming results in obstacle to scaling up.

2.3.5 Flotation

Flotation is one type of particle-separation process that utilises bubble forming that is generated through the culture media column. The bubbles carry any particles from the bottom to the top surface by airlifting force, where the concentrated particles can be harvested (Barros *et al.*, 2015; Alam *et al.*, 2017). This system uses less space compared with the sedimentation method. Because it takes less time to separate sludge from wastewater, this system requires more sophisticated machines and energy consuming. Frequently, this method is used in combination with flocculation harvesting (Pahl *et al.*, 2013). In some cases, chemicals may need to be added to help separate the sediment, such as alum, FeCl₃, etc. This system is preferred to remove solid waste with low density. Flotation systems can be divided into three main groups.

2.3.5.1 Air Flotation or Disperse Air Flotation

This method allows air to directly or blow air into the wastewater at atmospheric pressure. The blowing can create a large number of air bubbles with a diameter of approximately 2-3 mm. Consequence, various sediments float up to the surface of the water. The sediment that floats up can be carried away (Pawlik, 2022).

2.3.5.2 Vacuum Flotation

This method blows air into the wastewater until saturation. There are two methods of blowing air. The first is blowing directly to wastewater, and the second spontaneously letting the air enter the pump. Afterwards, inside the system, there is a vacuum, and then the dissolved air separates from the water in the form of small bubbles. These tiny air bubbles carry various sediments in the water. Waste floats up to the surface of the water which can be separated from the water by sweeping and or pumping out. This method requires less space for installing the system than the first two methods. This system is complicated and not very popular (Barrut *et al.*, 2013; Prakash *et al.*, 2018).

2.3.5.3 Dissolved-air Flotation (DAF)

This technique compresses air and water in a high-pressure tank about 2-4 times the atmosphere for 1-3 minutes before blowing air into the wastewater at a pressure of 2-3 atmospheres and releasing the pressure to atmospheric pressure. As a result, the air will float in the water for longer than usual when the water is passed into atmospheric pressure through the pressure valve to lower the pressure. Excess air floats and rises to the surface of the water, carrying suspended solid sediment with it (Wang *et al.*, 2005; Prakash *et al.*, 2018). There are two types of DAF systems:

1. The absence of a water circulation system makes it appropriate for non-brittle sediments.
2. The water circulation system is noteworthy because it uses pre-treated water to boost pressure. It is then combined with fresh wastewater and sent to the tank, where the sediment floats. This can increase the efficiency of the system more valuable and decrease time spent due to the decreasing concentration of wastewater from the dilution of mixed water.

Application of foam flotation

Foam flotation is widely used in a broad range of commercial industries to separate suspended solids, fibres, and other low-density solids, particularly in mineral processing, wastewater treatment, and chemical industries (Wang *et al.*, 2010). The following are examples of its applications on a commercial scale. Froth flotation is a critical method for separating valuable minerals from ore, especially for sulfide ores like copper, zinc, lead, and nickel in the mining industry. It's also used for non-sulfide minerals such as phosphate and fluorite (Zhang *et al.*, 2019). In gold recovery, it is used in the beneficiation of gold-bearing sulfide ores, where gold is associated with minerals like pyrite or arsenopyrite (Zhou *et al.*, 2020). In the coal cleaning industry, it is used to separate fine coal particles from impurities, such as clay and shale, to improve the quality of the coal for combustion or further processing (B. Kumar *et al.*, 2022). In water and wastewater treatment, oil and water are separated by employing continuous froth flotation in the removal of oil and grease (Seneesrisakul *et al.*, 2021). Heavy metals such as copper, zinc, and nickel can be removed as ion flotation that helps in the treatment of wastewater containing heavy metals by floating out insoluble hydroxides or sulphides (Vidu *et al.*, 2020).

In dissolved air flotation (DAF), the air is forced by high pressure, thereby generating a large number of tiny bubbles that dissolve particles in wastewater and are finally able to remove suspended solids, grease, and oils (Henderson *et al.*, 2008). Foam flotation with different types of surfactants, such as cationic, anionic or non-ionic, was employed in pulping and flotation processes to remove ink and other contaminants from recycled paper pulp (El-Khalek, 2012). In environmental remediation, particularly soil washing, foam flotation is occasionally used to separate organic and inorganic contaminants from soil in environmental clean-up projects (Tiwari & Tripathy, 2023). The versatility of froth flotation makes it indispensable in industries where fine particle separation is necessary. The technique is particularly favoured for its efficiency, cost-effectiveness, and ability to handle large volumes in continuous processing systems.

The main advantage of flotation on microalgae harvesting is that it is low energy consuming. Many reports suggest that this technique has low power for the operation system. For example, harvested *Chlorella* and *Scenedesmus* using dispersed air flotation with the lowest energy consumption of 0.003 kWhm⁻³ Wiley *et al.* (2009). the flotation process has lower equipment cost and low energy requirement (0.015 kWhm⁻³) than conventional processes, such as sedimentation and centrifugation Coward *et al.*, 2013. the harvesting of *C. vulgaris*, *I. galbana* and *T. suecica* using continuous foam flotation with low power consumption (0.052 kWhm⁻³) Alkarawi *et al.* (2018).

2.3.6 Comparisons

Concentration methods, for example, chemical concentration methods such as flocculation, are generally simple and rapid but can be toxic to the biomass and introduce contaminants such as metals into the culture medium. On the other hand, biological concentration methods are non-toxic to the biomass but may be limited by the culture medium used.

In terms of dewatering methods, centrifugation is the fastest, most expensive and energy-consuming method. It is also not suitable for all types of microalgae as it can damage the cells. Filtration, on the other hand, is a more cost-effective method that can achieve high recovery rates, but it can be prone to fouling and clogging, which can increase operating and maintenance costs.

Table 2.7 compares the advantages and disadvantages of different harvesting methods for microalgae, focusing mainly on concentration and dewatering methods. Each method has its own advantages and disadvantages.

Harvesting method			Advantages	Disadvantages
Concentration	Chemical flocculation	Cellana, Inc. TerraVia	simple and fast	toxic to biomass culture medium limited metal contamination
	Biological flocculation		non-toxic to biomass low cost	microbial contamination
Dewatering	Centrifugation	Westfalia Co., Ltd. US Filter-Maxx	fast high recovery suitable for all sp.	expensive high energy consumes cell damage
	Filtration	Litree Purifying Technology Co., Ltd. Green Diamond	high recovery	fouling/clogging operation cost pumping associate
Combine two steps above	Flotation	AlgaEnergy Ecologix Systems AWC Water	low cost and space requirements short operation times feasible for large-scale	use chemical flocculants marine strain limited

Table 2.7: Comparison of different harvesting methods (Adapted from: Barros et al., 2015)

It should be noted that a combined two-step method. Flotation, for example, is particularly noteworthy. This method offers the advantages of being low-cost, space-efficient, and requiring little operator effort. However, it still requires chemical flocculants and may not be suitable for all microalgae strains.

2.4 Foam flotation technique

Foam flotation is a technique in which particles are physically separated from a liquid phase. Air bubbles vary in their ability to selectively adhere to the surface of the particles due to their hydrophobicity. Air bubbles with attached hydrophobic particles are carried to the surface and form foam that can be removed, while hydrophilic materials remain in the liquid phase (**Figure 2.15**).

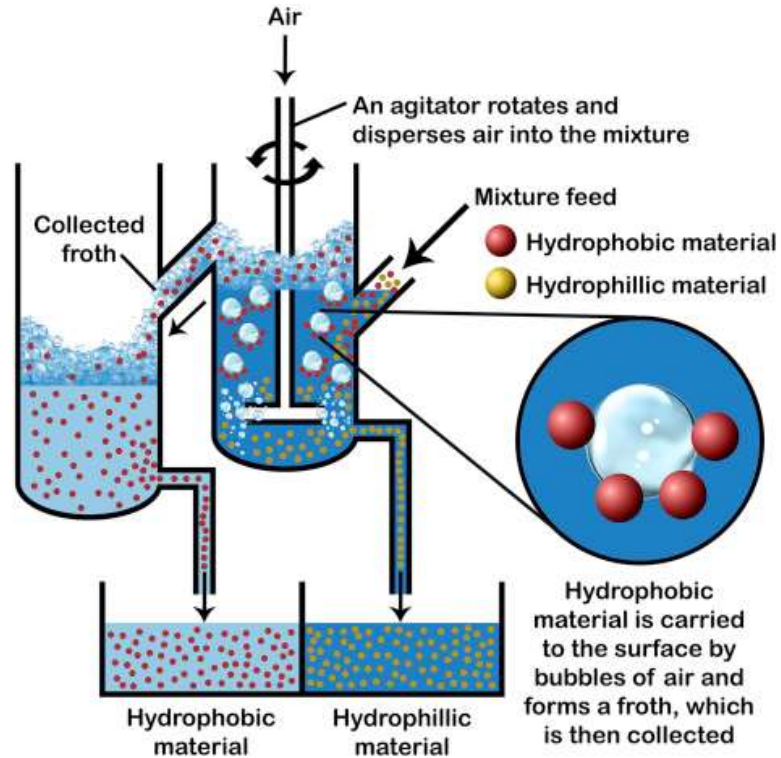


Figure 2.15: The process of froth flotation (Crawford & Quinn, 2017)

The flotation processes comprise of three main phases: *air bubbles*, *water or media* where the air bubble is introduced to the flotation column and *particle* in suspension (Alhattab & Brooks, 2017). According to Shamma and Bennett (2010), the separation mechanism of flotation consists of four basic steps as follows:

1. The bubble is generated into the water or medium using air generator.
2. Contraction or collision of air bubble and particles suspended in the water.
3. Attachment and adhesion between difference in surface charges of the particles and the gas bubble occurs.
4. The air-solid particles are carried to collect at the top surface of flotation device.

2.4.1 Mechanism of CTAB and microalgae cells

In general, microalgae cells have a negative charge. Cationic surfactants such as cetyltrimethylammonium bromide (CTAB) and dodecyl ammonium hydrochloride can be used to harvesting (Garg *et al.*, 2014). Among these surfactants, cetyltrimethylammonium bromide (CTAB) is a positively charged surfactant that is widely used in various scientific fields, including biochemistry and nanotechnology. Its molecular structure, shown in **Figure 2.16**, contains a positively charged trimethylammonium group (hydrophilic head) and a long straight hydrocarbon chain or hydrophobic tail (Vahidi *et al.*, 2017). CTAB is particularly effective in binding to negatively charged molecules and is used to improve the hydrophobicity of microalgae, resulting in better harvesting efficiency. Furthermore, it has applications in research involving the purification, isolation, and analysis of biological macromolecules.

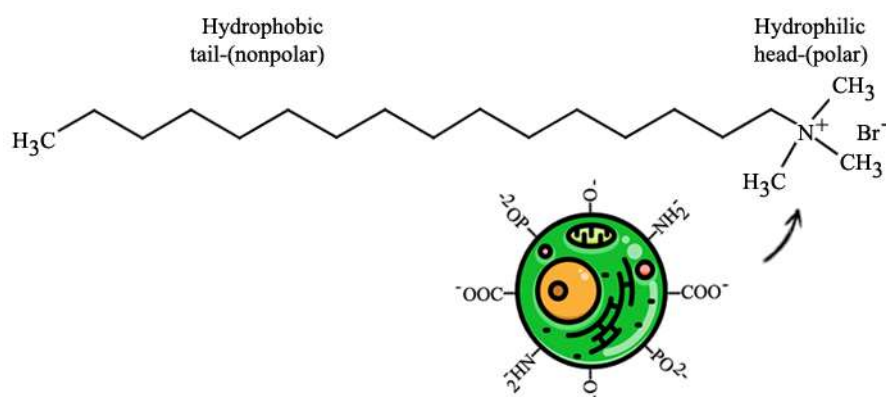


Figure 2.16: The molecular structures of cetyltrimethylammonium bromide (CTAB) and microalgae cell. (The following diagram was modified in accordance with the reports of Machado *et al.*, 2022; Kumar, 2021; Vahidi *et al.*, 2017).

The adsorption of CTAB on *C. vulgaris* is probably due to physical interaction between the two materials following a mechanism of multilayer adsorption involving electrostatic forces such as hydrogen bonding or van der Waals forces-driven process. The algal surface has many hydrophilic functional groups, such as protein and phospholipid layers (Hao *et al.*, 2017; van Oss, 1995) that form a high number of hydrogen bonds resulting in stronger van der Waals and electrostatic interactions (Li *et al.*, 2022). The interaction between algae and surfactants is supported by FT-IR spectrum measurements, which indicate no changes in the chemical groups on the surface of *C. vulgaris* when untreated and treated with CTAB (Shen *et al.*, 2018).

As part of the flotation, CTAB, as a cationic surfactant, interacts with *C. vulgaris* through a process of electric neutralization that involves the formation of hydrogen bonds. CTAB contains both hydrophilic and hydrophobic parts (Coward *et al.*, 2014). *C. vulgaris* adheres to the hydrophilic part due to its hydrophilic nature (Ozkan & Berberoglu, 2013). Consequently, the complex comprising CTAB and algae becomes more positively charged and hydrophobic on the surface. During flotation, the bubbles utilized are electronegative and hydrophobic, allowing the algal cells and surfactant particle complexes to easily attach to them (Kwak & Kim, 2015).

2.4.2 Foam formation

Bubbles form more easily when a surfactant is introduced into a liquid, leading to reduced surface tension and allowing air to penetrate and form bubbles (Pugh, 2016a). When gases are dispersed in a liquid along with surfactants the reduction in surface tension, can lead to formation of a stable network of bubble i.e. a foam. The general mechanism of foam formation involves the following steps:

1. **Bubble initiation.** The formation of bubbles begins with a gas pocket or cavity is created within a liquid using a variety of mechanisms, such as mechanical agitation (Scardina & Edwards, 2000).
2. **Bubble growth.** Once a gas pocket is created, gas molecules diffuse into the liquid to occupy the newly formed pockets. Several factors determine the growth rate of bubbles, including their size and shape, the pressure and concentration of the gas, the temperature, and the viscosity of the liquid (Hilton *et al.*, 1993; Hey *et al.*, 1994).
3. **Drainage.** During the growth of a bubble, the thin liquid film surrounding it begins to drain under the influence of gravity. Through this process, the thickness of the liquid film decreases, increasing the curvature of the bubble surface, which is referred to as the *drainage process* (Koehler *et al.*, 2000; Grassia *et al.*, 2006)
4. **Coalescence.** This occurs when bubbles grow and move in a liquid, eventually coming into contact with one another. A thin liquid film is redistributed or ruptured between two or more gas bubble pockets and merges to form a larger bubble (Marrucci, 1969; Ghosh, 2009).
5. **Finally, the foam stabilisation** can also be attributed to the properties of the liquid film surrounding the bubbles. The film must be strong enough to keep the bubbles from collapsing and hold them together (Pugh, 2016c).

It is common for bubbles to minimize their surface areas, which may result in them merging or sharing a common wall with one another. The shared wall is flat if the bubbles have the same size or symmetry. However, if they are unequal in size, the smaller bubble with more internal pressure will bulge into the larger bubble in accordance with Laplace's principle (Walstra, 1989).

Laplace pressure is a phenomenon in which the surface tension of a liquid is at an interface or curved surface. When a liquid contains two bubbles of different sizes, the pressure in the smaller bubble is higher than in the larger bubble because of its smaller radius of curvature. This pressure difference results in the diffusion of gas from the smaller bubble to the larger bubble until both bubbles reach pressure equilibrium (Pugh, 2016d). The Laplace pressure, ΔP , can be calculated using the equation:

$$\Delta P = P_{inside} - P_{outside} = \gamma \left(\frac{1}{R} + \frac{1}{R'} \right) \dots \dots \dots 2.4$$

Where, ΔP is the increase in hydrostatic pressure, γ is the surface tension, R and R' are the radii of curvature of the surface, and $C = 1/R + 1/R'$ is the curvature of the surface. For a spherical surface ($R = R'$), the equation simplifies to

$$\Delta P = \frac{2\gamma}{R} \dots \dots \dots 2.5$$

Where, R is the radius of curvature. This equation shows that the Laplace pressure is inversely proportional to the radius of curvature. In other words, the smaller the radius of curvature, the higher the Laplace pressure.

In symmetrical bubbles, the contact lines form a symmetrical shape, and they join together at a 120° angle at their common wall (Cohen-Addad & Pitois, 2012). It should be noted that when more than two bubbles encounter at a point, the walls of the bubbles are arranged in a hexagonal shape, with three bubble walls meeting along a line at the central of the meeting point. Because of the 120° angle, the bubbles are more likely to assemble efficiently with the least surface area. Therefore, no matter how the bubbles are arranged or shaped, the angle between two bubble walls at the central of a point where three bubble walls meet will always be 120° (Sullivan, 1999; Cohen-Addad & Pitois, 2012).

2.4.3 Foam Stability and Destabilisation Process

Foam stability refers to the ability of foams to resist collapse and maintain their structure and properties over time (Wierenga *et al.*, 2023). Several physical and chemical mechanisms interact to affect foam stability, including the properties of the gas and liquid phases, gas-liquid surface tension, liquid fraction or interfacial properties, surfactant concentration and environmental conditions such as temperature and pressure (Yu *et al.*, 2021). Foam ageing refers to the gradual change in the structure and properties of the foam, which is unstable and disappears over time, affecting its stability (Pugh, 2016b). It is important to understand that foam stability and ageing are due to three main mechanisms: drainage, coalescence and coarsening (Fameau and Salonen, 2014). The mechanisms that contribute to foam stability and ageing are explained in more detail below:

2.4.3.1 Foam drainage

Foam drainage is a phenomenon in which fluid gradually drains from the foam structure over time due to fluid boundary conditions and the permeability present at the bottom of the foam (Yazhgur *et al.*, 2016). A process where liquid flows within the foam structure as gas along with bubbles are dispersed in a liquid solution (Saint-Jalmes, 2006), resulting in changes in the amount of liquid inside the film. This phenomenon is because the film thickness decreases as the liquid drains away, affecting the foam's physical and chemical properties. For example, the stability of the foam may decrease as the film thickness decreases, which can lead to the collapse of the foam structure.

Drainage is the natural process of liquid draining out of the thin films between gas bubbles in the foam, caused by gravitational forces acting on the liquid within the foam. This drainage causes the liquid films to decrease in thickness and the liquid fraction to decrease (Pugh, 2016d). In response to the increased curvature, the Laplace pressure increases, this can destabilise the foam and ultimately rupture and collapse over time. It is also important to note that as the liquid drains from the foam, the concentration of surfactant increases, resulting in a change in surface tension that can cause the foam to lose its stability.

Several forces affect foam drainage, including gravity, capillary and viscous force. The liquid is pulled downward by gravity, while capillary forces arise due to the surface tension of the liquid, which causes it to adhere to the walls of the foam structure. Viscous forces can also prevent foam from draining (Stevenson (2007)). Foam drainage can occur naturally, called free foam drainage, or can be induced mechanically, called forced foam drainage. Free foam drainage occurs when fluid flows out of the foam through plateau boundaries (PBs) and nodes (Bhakta and Ruckenstein, 1997). Plateau borders are thin films of liquid that connect adjacent bubbles in the foam, while nodes are the points where three or more bubbles meet. These structures provide the pathway for a liquid to exit the foam, and as the dewatering process progresses, the foam structure becomes more solidified. In contrast, forced foam drainage creates foam within a column through mechanical agitation or gas sparging (Hutzler *et al.*, 2005), resulting in a more controlled and uniform drainage process that may be beneficial in specific applications.

Stevenson and Li, 2014, claim that if the drainage rate is high, the foam will become dry since the liquid leaves the foam rapidly. Consequently, dry foam promotes the following processes:

1. Coalescence of adjacent bubbles due to thinning of liquid films separating them. This makes bubbles more likely to rupture, allowing the bubbles to merge (Marrucci, 1969).
2. Inter-bubble gas diffusion between adjacent bubbles. A difference in pressure between irregular bubble sizes can also accelerate coalescence by diffusing gas. The gas diffuses from the interior of smaller bubbles to the surrounding larger bubbles (Etemad *et al.*, 2022).

The equation of foam drainage can be obtained from the continuity equation. In order to obtain the liquid velocity within a plateau border, the balance of gravity, viscosity, and capillarity forces are considered. One of the parameters that can be used to describe the behaviour of liquid drainage in a vertical foam column is the superficial drainage velocity (j_d), which can be calculated using an empirical equation:

$$j_d = \frac{\rho_f g r_b^2}{\mu} m \varepsilon^n \dots\dots\dots 2.6$$

Based on observations and experimental data, the equation involves foam properties and other parameters. The first two parameters are the interstitial liquid's density (ρ_f) and viscosity (μ). The two adjustable parameters (m and n) are determined experimentally by the forced drainage method. These parameters are specific constants for a particular system, and their values depend on the foam properties. Gravitational acceleration (g) is also necessary in the equation, as it also affects the drainage rate. The liquid fraction of the foam (ε) is the volumetric fraction of liquid in the foam column. The final parameter is the average bubble size (r_b).

Foam drainage generally depends on the size and inclination of plateau borders, influencing the bubble shape. In this regime, the foam is assumed to have a polyhedral structure when moving in the channels (Koehler *et al.*, 2000; Saint-Jalmes *et al.*, 2004; Pugh, 2016d). The mean of all possible orientations of the plateau borders in the foam expressed the drainage velocity (V_d):

$$V_d = \left(\frac{0.16R_{pb}^2}{150\eta_\ell} \right) (\rho_\ell g) \dots\dots\dots 2.7$$

Where R_{pb} is PB curvature radius, η_ℓ is dynamic viscosity, ρ_ℓ is liquid density and g is gravity. It is possible to express the drainage velocity when the surface is highly of moving foam (Koehler *et al.*, 1999; Pugh, 2016d) as follows:

$$V_d = \left(\frac{K_n^0 \rho_\ell g}{\eta_\ell} \right) \left(L_{pb}^2 \Phi_l^{1/2} \right) \dots\dots\dots 2.8$$

Where K_n^0 is dimensionless permeability, L_{pb} is PB length and Φ_l is liquid volume fraction

It is clear from this equation that changing the bubble size or liquid fraction is the only effective method for accelerating superficial drainage velocity without changing the liquid properties. If the density, viscosity and liquid fraction of the foam column remain the same, the superficial drainage velocity can be increased (Stevenson and Li, 2014).

As illustrated in **Figure 2.17**, the pressure profile measurement used to determine liquid holdup was described by (Ireland & Jameson, 2007). In a column with wet and dry areas of rising foam without coalescence, the liquid profile is preserved. At the wash water injection point and at the liquid-foam interface, the pressure gradient varies dramatically. While the liquid fraction for the wet foam phase increases, showing that the liquid content in each region quickly reaches an equilibrium value and remains constant, the liquid fraction for the dry foam phase remains approximately constant. The lowest two gas velocities agree well with the theoretical curves, suggesting strong agreement. The maximum gas velocity aligns acceptably with the model and shows a reasonable fit. The overflow rate and the liquid content of the upper foam layer change only to a limited extent with the wash water rate. This consistency reinforces the assumption that the upper froth layer is at the peak of the drift-flow curve.

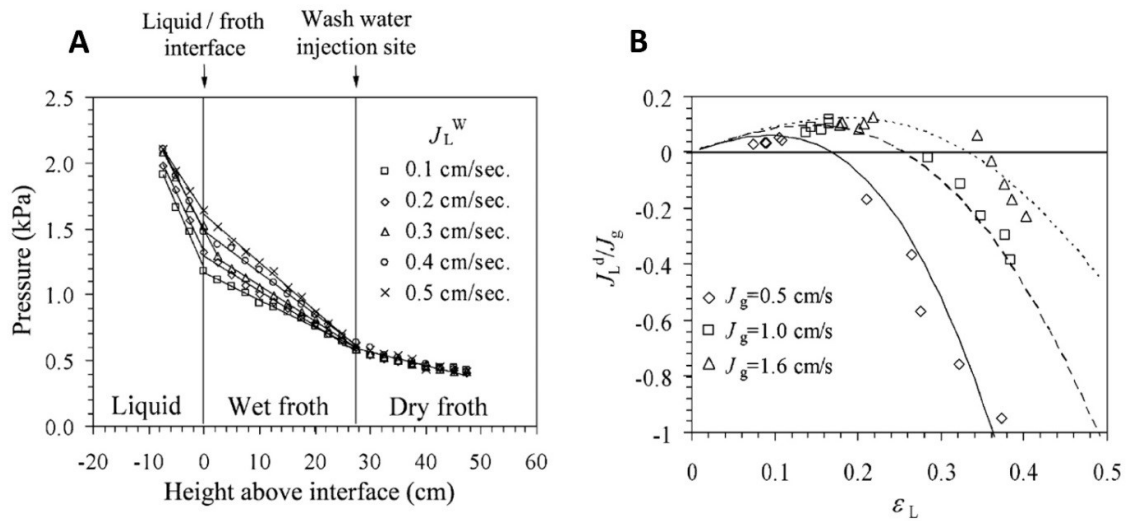


Figure 2.17: The column pressure profiles at different heights above the interface (A) and a typical curve of surface liquid velocity versus liquid fraction in a two-layer foam column without wash water injection (B), (Modified from: Ireland & Jameson, 2007).

According to the principle, the basic principles of rising foam drainage describe the concept presented in equation (2.9). The liquid that is carried upward by bubbles (the first term on the left) and the liquid that drains downward as a result of drainage through the foam (the second term on the left) balance the net upward flux of liquid. The relationship between the net flux of liquid rising in the column and the liquid hold-up can then be determined using a foam drainage model to find a function for (j_L) (Ireland & Jameson, 2007).

$$\frac{J_g}{1-\varepsilon_L} - \frac{J_L}{\varepsilon_L} = f(\varepsilon_L) \dots\dots\dots 2.9$$

Figure 2.18 shows the profile of the typical curve of superficial liquid velocity versus liquid fraction in a two-layer froth column without wash water injection.

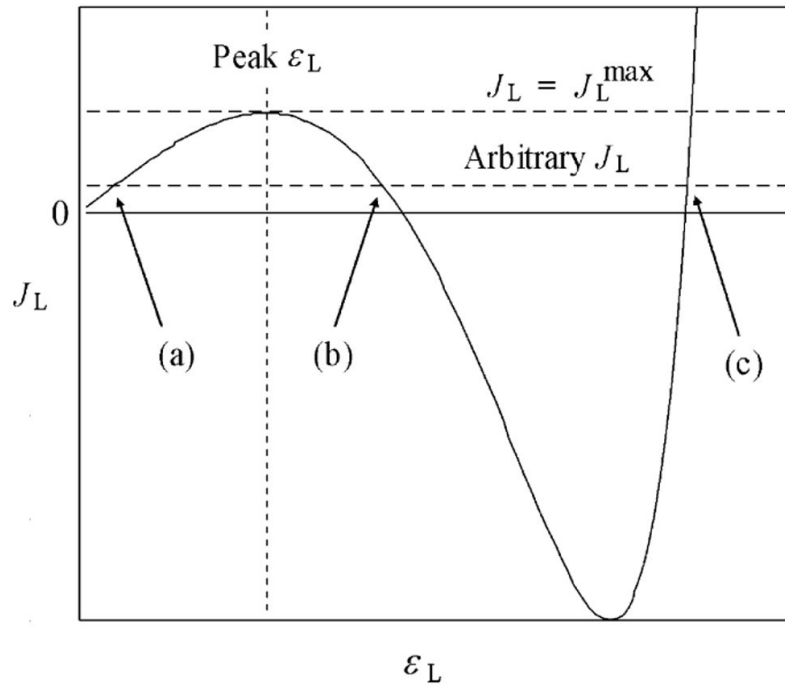


Figure 2.18: The profile of the typical curve of superficial liquid velocity versus liquid fraction in a two-layer froth column without wash water injection (Ireland & Jameson, 2007).

The liquid content in the foam layer corresponds to the peak value of the curve in the steady state. The liquid content should reach this peak value in a rising foam without reflux, wash water or coalescence (Ireland & Jameson, 2007). It has been suggested that in a rising foam without coalescence or any wash water or reflux, the liquid hold-up will reach this peak value (Tobin *et al.*, 2014).

Therefore, it is necessary to increase the size of gas bubbles to increase the superficial drainage velocity, which can be achieved either by increasing the number of larger gas bubbles in the foam column or by reducing the number of smaller bubbles in the foam column. Alternatively, increasing the liquid fraction of the foam column can also increase the superficial drainage velocity.

2.4.3.2 Coalescence

Coalescence is the process in which two or more bubbles merge, resulting in a larger bubble and a reduction in the overall number of bubbles in the foam structure. This phenomenon occurs when the liquid film separating the bubbles becomes too thin or when there is a significant pressure difference between bubbles (Langevin, 2019). When the bubbles merge, the liquid films between them rupture, causing the foam to collapse, giving rise to a larger bubble (Chaudhari & Hofmann, 1994; Drenckhan & Saint-Jalmes, 2015). Furthermore, the merging of bubbles through coalescence can also decrease the stability of the foam as the number of bubbles decreases and the size of the remaining bubbles increases (Fameau & Salonen, 2014). Several factors, such as the concentration and size of the bubbles, the viscosity of the liquid, and the surface tension between the liquid and gas phases, can influence the occurrence of coalescence. The nature of the surfactant and its concentration, as well as the size of the bubbles, can affect the stability and lifetime of the foam. It notes that coalescence events can lead to foam collapse as the liquid fraction in the foam decreases and that smaller bubbles are generally more stable and are likely to contribute to the stability of the foam (Carrier & Colin, 2003).

2.4.3.3 Coarsening

Coarsening, also known as Ostwald ripening, is the enlargement of foam bubbles through gas diffusion from smaller bubbles to larger ones (Hilgenfeldt *et al.*, 2001). This causes a decrease in the overall number of bubbles and an increase in their average size. The driving force behind this process is the pressure difference between the bubbles, which promotes gas exchange between them due to differences in Laplace pressure (Saint-Jalmes, 2006). As a result, smaller bubbles shrink and eventually disappear while larger bubbles grow. However, excessive coarsening can undermine the stability of the foam by thinning the liquid film separating the bubbles when they become too large (Fameau & Salonen, 2014). During coarsening, intermittent rearrangement of the bubbles occurs, leading to a local relaxation of the interfacial energy. This leads to changes in bubble size and distribution (Cohen-Addad and Pitois, 2012). The kinetics of foam coarsening (the growing size of the bubbles in the foam) is influenced by the permeability of the liquid film surrounding the bubbles, the tension between the gas and liquid phases, and the size of the bubbles. The lower foam quality is due to the fact that the film is less permeable and coarsens more slowly. Furthermore, surfactant concentrations significantly affect the coarsening rate by affecting the interfacial tension between phases (Yu *et al.*, 2022).

2.4.4 Evaluating Performance of flotation

The performance of foam flotation for microalgae harvesting indicate in two terms, the recovery efficiency and the concentration factor (Pahl *et al.* (2013):

The recovery efficiency (RE) is determined from the microalgae biomass in the recovered foam (foamate) presents in the initial feed suspension.

The concentration factor (CF) is explained as the ratio of the concentration of microalgae in foamate to the initial concentration of microalgae in culture suspension. An increase in the concentration factor (sometime called enrichment ratio) can increase in algae cell concentration between feed and foamate (Burghoff, 2012). The flotation performance depends on the optimal condition in the collision and adhesion phases (Ralston *et al.*, 1999).

2.4.5 Parameters

There are two main groups of factors affecting the effectiveness of flotation processes, as follows:

- **Physical and Chemical factors** consist of the type of surfactant, concentration, pH, etc.
- **Process factors** consist of the microalgae concentration, growth stage, air bubble size, time, air flow rate, feed rate, etc. (Alhattab & Brooks, 2017).

2.4.3.1 Physical factors

Surface properties of algae cells; the electrical properties of cell surfaces are primarily influenced by their surface structure and extracellular products. The cell wall of green algae is mainly composed of cellulose, a polysaccharide that provides structural support and protection (Ozkan & Berberoglu, 2013; Hao *et al.*, 2017). In addition the cell wall also has a high content of glycoproteins. These proteins contain a variety of functional groups such as amino, carboxyl, sulfate, and hydroxyl compounds. Cell wall electrical properties depend on protein functional groups (He & Chen, 2014) in *Chlorella vulgaris* and other green algae. These functional groups have chemical properties that allow them to interact with surfactant molecules, which can make the cell surface electronegative and naturally hydrophilic.

According to Hao *et al.* (2017), the surface of *Chlorella vulgaris* is electronegative, as the zeta potential values are below zero. In addition, the study also showed that *Chlorella vulgaris* has a naturally hydrophilic surface. This hydrophilic nature is believed to be due to the presence of oxygenated functional groups such as hydroxyl (-OH), carboxyl (-COOH), and aldehyde (-CHO) groups. Other studies, Callow *et al.* (2000) showed that *Botryococcus braunii* have extracellular hydrocarbons, called Botryococcenes, which constitute about 30% of their dry biomass.

Therefore, the hydrophilicity of green algae is expected to be influenced by the composition of their cell walls, which are mainly composed of hydrocarbon compounds. This potentially makes green algae amenable to the separation of cultures through the flotation process by introducing air bubbles that attach to the cell particles and cause them to rise to the surface.

2.4.3.2 Chemical factors

Surface-active agents, also known as surfactants, are chemical compounds that reduce the surface tension between a solution and other phases, such as gases or solids (Rosen & Kunjappu, 2012). This plays a crucial role in adhesion processes. There are two main molecular structures in surfactants: a hydrophobic “tail”, which repels water, and a hydrophilic “head”, which attracts water. Surfactants are used in various areas, including cleaning, emulsifying, wetting, foaming and dispersing. These compounds are commonly used in personal care products such as soaps, shampoos and detergents.

(1) Surfactants types

There are four main types of surfactants based on their ionic charge:

1. Anionic surfactants: have a negatively charged hydrophilic part, such as a sulfate (SO_4^{2-}) or carboxylate (COO^-) group. Examples include sodium lauryl sulfate, sodium laureth sulfate, and soap.
2. Cationic surfactants: have a positively charged hydrophilic part, e.g. an amine (NH_3^+) group or a quaternary ammonium (NR_4^+). Examples include benzalkonium chloride and cetyl trimethylammonium bromide.
3. Non-ionic surfactants: have no charged hydrophilic groups.
4. Amphoteric surfactants: have both positive and negative charges in their molecular structure, allowing them to act as both anionic and cationic surfactants.

Numerous surfactant selection studies have been conducted in microalgae harvesting applications, such as mixing CTAB with dodecyl ammonium hydrochloride (DAH), suggesting that CTAB and DAH are beneficial for improving harvesting efficiency. Ecover is a blend of biodegradable surfactants (15% anionic surfactant, 5% nonionic surfactant) made from yeasts, glucose and rapeseed oil, reaching an optimal concentration of 0.15 mgL^{-1} was used to harvest algae (Shen *et al.*, 2018). In addition, one type of biosurfactant, tea saponin, contains both hydrophilic and hydrophobic elements. This property strengthens the bond between algae and bubbles and acts as a bridge through hydrophobic attraction and van der Waals forces (Stamatis *et al.*, 1993). Supported by Shen *et al.*, 2018, CTAB achieved a maximum harvesting efficiency of 89.2% at 80 mgL^{-1} concentration. Additionally, the study found that CTAB had superior adsorption properties and formed a more stable interaction with *C. vulgaris* when compared to tea saponin.

In a previous study, Alkarawi *et al.* (2018) examined the effectiveness of three surfactants, namely CTAB, SDS, and TWEEN20, and discovered that only CTAB could enhance the hydrophobicity of algae. According to their findings, adding 20 mgL^{-1} of CTAB increased the hydrophobicity of the algal solution by 97%. Furthermore, the study by Kurniawati *et al.* (2014) revealed that the flotation separation efficiency of microalgae cells increased with the concentration of CTAB. Using CTAB at 60 mgL^{-1} resulted in excellent separation (>93.7%) of both *C. vulgaris* and *Scenedesmus obliquus*.

Therefore, several studies in foam flotation so far suggest that a chemical such as CTAB is an effective surfactant for microalgae harvesting (Kurniawati *et al.*, 2014; Shen *et al.*, 2018; Alkarawi *et al.*, 2018). Thus, this chemical was chosen as a surfactant for this study. A significant limitation of CTAB as a surfactant is that it destroys the algae cell, and its remaining turn turns into a contaminant in the final product, which can be a hurdle to further steps. Therefore, this surfactant should only be considered as a candidate for application in microalgae harvesting for non-food or non-feed supplements, such as in biofuel production and other similar applications.

(2) Surfactant concentration

Surfactants in foam flotation mainly are compound existing amphiphilic properties with hydrophobic (non-polar) and hydrophilic (polar) parts. Typically, an increase in surfactant concentration contributes to the foaming amount by reducing the surface tension of the liquids,

allowing air to disperse and form bubbles more easily when introduced. High surfactant concentration also increases the number of surfactant molecules at the air-liquid interface, thereby facilitating bubble formation. Foamability at low concentrations can result in insufficient surface tension reduction, while high concentrations could lead to saturation with little improvement in foam production.

The efficiency of microalgae harvesting is affected by the concentration of surfactant in the media because the cell-surfactant complex precipitates when the net charge is close to zero but disperses in the medium when a net charge is present (Huang & Kim, 2013).

Several studies have been conducted to determine the optimal surfactant concentration for harvesting microalgae. For example, Chen *et al* (1998) found that increasing the CTAB concentration from 10 to 40 mg L⁻¹ improved the removal efficiency of *Scenedesmus quadricauda* from 50% to 90% compared to Triton X-100 and SDS, which resulted in less than 10% removal. Similarly, Liu *et al.* (1999) 20% and 86% removal efficiencies were observed for *Chlorella sp.* using 40 mg L⁻¹ of SDS and CTAB, respectively. Additionally, Garg *et al* (2014) reported that the cell recoveries increased from 6.4% to 70% and 5% to 70% with increasing concentrations of CTAB and DAH from 0 to 50 mg L⁻¹, respectively. Coward *et al* (2014) found that using 10 mg L⁻¹ CTAB resulted in an increased concentration factor of up to 230 times within 30 min of the flotation process. In another study, Alkarawi *et al* (2018) found that the most significant enhancement of *Chlorella vulgaris* removal occurred at a concentration of 35 mg L⁻¹ CTAB, which yielded a recovery efficiency of 95% under an airflow rate of 1 L min⁻¹ using continuous column flotation.

Therefore, the required amount of surfactant for microalgae harvesting depends on the algae concentration needed for final products. A mount biomass concentration is proportional to the used surfactant concentration to ensure the stability of the foam in the system.

A surfactant should be selected based on the specific application and properties that enable to perform effectively. It is common to use surfactants to enhance the efficiency of foam flotation by altering the surface properties of algae and bubbles, which in turn affects their interaction. The type and concentration optimisation of the surfactant used can significantly impact the process's efficiency of microalgae harvesting, as some surfactants may be more effective than others in facilitating the attachment of algae to the bubbles. Investigation on the role of surfactants in bubble-algae interaction in flotation harvesting of *Chlorella vulgaris*.

(3) Operational parameters

(3.1) Constriction Ratio

The constriction ratio is the geometric narrowing of the foam column or the cross-sectional area of the vessel. This constriction affects airflow, foam stability and bubble dynamics. The constriction increases bubble rupture, creating smaller bubbles that increase the surface area for microalgae to adhere (Zhang & Zhang, 2019).

Previous studies, such as those by Li *et al.*, 2011, examined the effect of constriction in the riser as shown in **Figure 2.19**. A smaller cross-sectional area increases air velocity, which improves collision between bubbles and particles. However, if the velocity is too high, turbulence can occur, causing particles to detach from the bubbles, resulting in lower recovery rates. This suggests that excessive constriction may result in unstable foam and reduce the efficiency of particle-bubble interaction (Li *et al.*, 2011; Coward *et al.*, 2013; Alkarawi *et al.*, 2018). Finding an optimal constriction ratio is crucial as it contributes to the effective separation of microalgae from the liquid phase by promoting foam enrichment. This process ultimately leads to improved harvest efficiency without significantly increasing energy consumption.

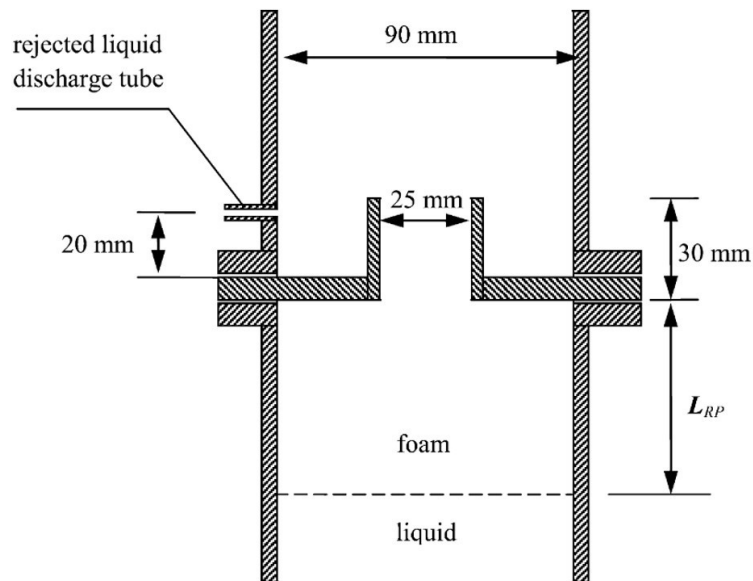


Figure 2.19: A foam riser plate is installed in the liquid discharge column between the interstitial spaces (Li *et al.*, 2011)

(3.2) Reflux and Internal reflux

Reflux refers to the recycling of a portion of the separated foam back into the flotation column. The process affects foam flotation by enriching the residence (foamate) time of particles, increasing their chance of attachment to bubbles and improving the concentration gradient, enhancing the selective separation of particles with different surface properties. The reflux can improve foam quality by concentrating target substances in the foam layer. Increasing the reflux ratio generally improves the purity of the collected material but may reduce the overall recovery if excessive liquid recycling dilutes the product stream. High reflux ratios promote the enrichment of the target component in the foam phase, as recycled liquid reintroduces particles for additional attachment opportunities. However, excessive reflux can lead to foam flooding or system inefficiency due to the saturation of the foam phase (Martin et al., 2010; Li et al., 2011; Stevenson, 2012).

Internal reflux refers to the downward flow of liquid within the column caused by liquid drainage from the foam layer. Its contribution to variations of the effectiveness of the accumulation and separation becomes substantial at low concentrations of surfactants only. Proper internal reflux ensures that the foam layer remains stable by maintaining an optimal liquid content, which is crucial for effective separation. Internal reflux improves separation by enhancing the interaction between rising bubbles and descending liquid, allowing for the reattachment of missed particles (Stevenson *et al.*, 2008).

However, excessive internal reflux can lead to the detachment of particles from the bubbles, reducing recovery efficiency. Internal reflux effect on several foam flotation parameters, such as particle separation, can enhance particle separation by allowing additional interactions between particles and bubbles (Stevenson *et al.*, 2008; Stevenson, 2012) . In terms of energy utilization, it can improve system efficiency by redistributing energy and bubble interactions without needing external input, and in terms of Selectivity, it can help refine the separation process, ensuring only target particles are enriched in the foam.

In order to reduce downstream processing costs and improve recovery efficiency and concentration factors, the effects of sudden expansion and contraction in flow areas were examined. Li *et al.*, 2011, showed that liquid flux is reduced by suddenly expanding the flow area. This reduction concentrates the liquid beneath the area of expansion and encourages external reflux, which enriches the foamate. On the other hand, sudden contraction has minimal effects on either liquid flux or surfactant concentration.

Reflux is the counter-current flow that results from returning collapsed foamate to the top of a rising foam column. This process allows rich collapsed foamate to drain down through the rising foam. The first detailed analysis of this phenomenon was conducted by Brunner and Lemlich in 1963.

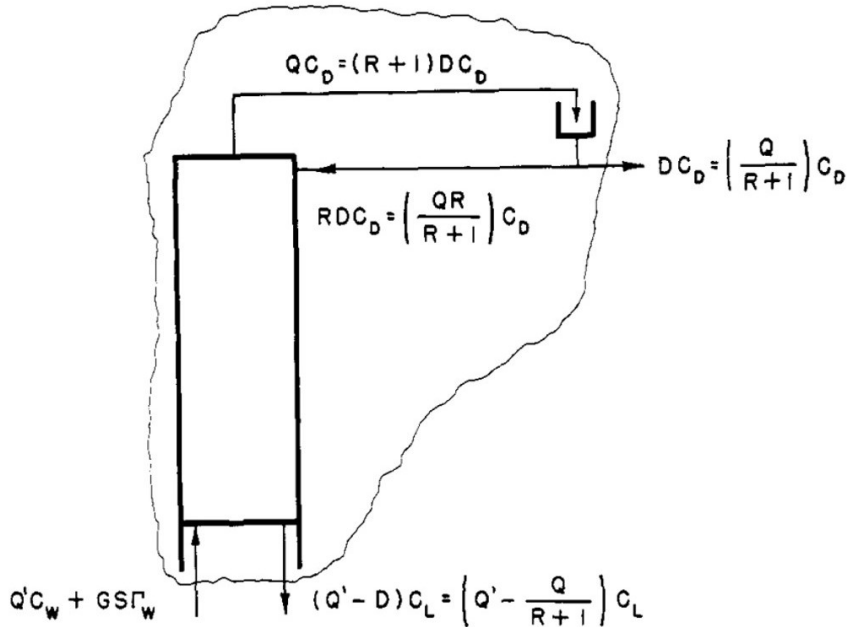


Figure 2.20: Equilibrium of solutes around the reflux column (Brunner & Lemlich, 1963)

$$\left(\frac{c_D}{c_w}\right)_{max} = \frac{(R+1)GS\Gamma_w}{Qc_w} + 1 \dots\dots\dots 2.10$$

Equation 2.10 illustrates how the foamate concentration rises as the reflux ratio R increases. The diagram as shown in **Figure 2.20** describes external reflux, where stable foam rises up the column before collapsing and then returning (Brunner & Lemlich, 1963). This has the same effect and also leads to less fluid retention, greater foam accumulation and a change in bubble size. (Li et al., 2011)

Previous studies that experimented with the geometry of the riser such as in 2018, Alkarawi *et al.*, investigated the use of foam risers with a contraction and expansion ratio of 0.25 in diameter to maximize microalgae harvesting. The study found that this method significantly increased algae concentration, achieving a 722-fold increase compared to a concentration factor of 173 without using a riser. However, the efficiency of biomass recovery fell slightly from 95% to 91%. Additionally, pressure and liquid fraction analysis when using risers with higher restriction ratios (e.g. 0.25) showed that these resulted in higher pressure and lower liquid fraction below the riser (Bumbieris, 2020).

2.4.3.3 Process factors

(1) Air flow rate

Air flow rate is a crucial factor in regulating the residence time of air bubbles in foam flotation. According to Weeks *et al* (1992), increasing the air flow rate can decrease the foam concentration factor. Liu *et al* (1999) demonstrated that changing the flow rate can also affect air bubble size. Merz *et al* (2011) investigated foam flotation with different flow rates ranging from 20 to 60 mL min⁻¹. They found that a 40 mL min⁻¹ flow rate resulted in the highest recovery, while a 20 mL min⁻¹ flow rate resulted in the highest enrichment ratio. Hosseini *et al.*, 2016, found that increasing cell concentrations of *Ochromonas danica* were associated with an approximately threefold increase in biomass harvest from 2.3×10^8 to 6.8×10^8 cells mL⁻¹, but resulted in low efficiency recovery. This was due to rapid foam formation in the medium even though low air flow rates (50 mLmin⁻¹) were used.

Moreover, a low flow rate promotes liquid drainage in the column, and air bubbles have an extended residence time, resulting in dry foams and a more prolonged process time. Conversely, high flow rates increased the number of larger bubbles, leading to wet foams and shorter residence times in the column (Alhattab & Brooks, 2017).

(2) Time

Longer running time gave higher recovery efficiency due to increased chances of air bubble-particle interaction (Alhattab & Brooks, 2017). Csordas and Wang (2004) noted that the harvesting efficiency of *Chaetoceros* sp. was increased within 30 min and afterwards increased by 10% when continuing the running time from 15-60 min, meaning that the optimum time was 30 min. Rosa *et al* (2007) stated that 40 min of running time reduced the concentration of bovine serum protein in solution from 100 to 5 mg L⁻¹ by semi-batch foam fractionation.

(3) Foam velocity

The Reynolds number is a dimensionless number used to characterize the flow patterns in fluids, including liquids and gases, whether the flow of the fluid will be laminar (smooth and predictable) or turbulent (chaotic and unpredictable) as a function of the fluid's density, velocity, viscosity, and characteristic length scale (Kulkarni & Joshi, 2005). Regarding flotation, the Reynolds number is used to determine whether viscous or inertial forces dominate

the bubble's motion, which, in turn, affects the behaviour of the bubble in the fluid. It is given by the following equation (Sommerfeld, 1908; Eckert, 2010):

$$Re = \frac{\text{inertial force}}{\text{viscous force}} = \frac{\rho v R}{\mu} \dots\dots\dots 2.11$$

Where Re is the Reynolds number, ρ is the density of the fluid, v is the velocity of the fluid, R is the characteristic length of the flow (e.g. diameter of a pipe or radius of a bubble), and μ is the kinematic viscosity of the fluid.

Bubble velocity is the speed at which a gas bubble rises through a liquid. Several factors affect the velocity at which a bubble rises, including the size and shape of the bubble, the properties of either gas or liquid, and the conditions under which the bubble is rising (e.g. temperature, pressure, and gravitational forces).

1. The bubble radius is less than 0.01 cm, which occur the Reynolds number (Re) is less than 1, an explanation for the effect of bubble size on the velocity of a rising bubble can be provided by Stokes Law. This regime is typically laminar and dominated by viscous forces, which assumes that the bubble is small and spherical and that the liquid is stationary (Shammas & Bennett, 2010). The motion of bubbles is usually slow and steady and can be described by:

$$v = \frac{gR^2(\rho_g - \rho_l)}{18\mu} \dots\dots\dots 2.12$$

Where v is the velocity of the bubble, ρ_g is the density of the gas, ρ_l is the density of the liquid, g is the acceleration due to gravity, R is the bubble's diameter (or radius), and μ is the viscosity of the liquid.

2. The bubble radius is between 0.01 cm and 0.1 cm, which occurs when $1 < Re < 800$. The motion of bubbles is usually vertical without an oscillating or transition regime and can be described with the following equation:

$$v \sim 2 \sqrt{\frac{gR}{0.9}} \dots\dots\dots 2.13$$

3. When the radius of bubbles exceeds 0.1 cm, and Reynolds numbers are higher than 800, the fluid flow can transition into a turbulent regime characterized by irregular flow patterns. In this regime, inertial forces become more significant, and the velocity of the bubble can be faster and more unpredictable.

However, the bubbles also become unstable and tend to break down into smaller bubbles. In order to calculate the velocity of each bubble, it is necessary to differentiate its position as a function of time using a central difference scheme (Ruth *et al.*, 2021) and to express it mathematically as follows:

$$v = d/t \dots\dots\dots 2.14$$

Where, bubble velocity is defined as v , the distance that the bubble has moved is defined as d and t is a bubble's time for moving that given distance. As described by the equations above, the velocity of a bubble in a fluid correlates with the square of the bubble's diameter as follows:

$$v \propto R^2 \dots\dots\dots 2.15$$

This equation suggests that larger bubbles will rise faster than smaller bubbles in the same liquid. It is important to note that this relationship between bubble size and velocity is not the only factor influencing bubbles' motion in fluids. The velocity is also directly proportional to the difference in density between the bubble and the liquid ($\rho_g - \rho_l$), which means that bubbles with a lower density than the liquid will rise faster than bubbles with a higher density.

Additionally, the velocity is inversely proportional to the viscosity of the liquid (μ), which means that bubbles will rise more slowly in more viscous liquids. However, the equation above provides a useful approximation of the relationship between bubble size and velocity in many fluid systems.

The impact velocity is crucial for the stability of bubbles and the formation of liquid films during bubble collisions. A higher bubble velocity improves the efficient drainage of liquid from the foam. Faster-moving bubbles create more turbulence within the foam, which helps break up existing liquid films. This process allows the liquid to drain more quickly, resulting in faster particle concentration and improved separation efficiency. Several demonstrate how bubble velocity can also affect foam flotation processes. For instance, a study using the Stefan-Reynolds model examines the influence of bubble approach velocity on the fluid drainage process between a bubble and a particle under constant conditions. The results suggest that higher bubble approach velocities lead to an increase in the critical thickness of the wet liquid film, which subsequently leads to reduced film stability (Albjanic *et al.*, 2018). Another study found that bubble coalescence occurs at approach velocities exceeding 1 mms^{-1} , consistent with the instability observed in pure water foams (Yaminsky *et al.*, 2010).

The relationship between superficial gas velocity and the bubble size distribution in an overflowing foam column indicates that the distribution of bubble sizes increases as the superficial gas velocity rises. The superficial gas velocity has been shown to influence the extent and location of bubble coalescence within the system (Cole & Cole, 2011). In addition, the diameter of the bubbles was altered to manipulate their impact velocity. The coalescence time was observed to increase with higher impact velocities. This increase was attributed to the greater deformation of the bubble shape and the larger radius of the liquid film (Zawala & Malysa, 2011).

(4) Foam Bubble

Foam bubbles are formed when gas bubbles are mixed and distributed throughout a liquid. The thin liquid layer that envelops each bubble stabilizes it and prevents it from collapsing (Walstra, 1989; Cantat *et al.*, 2013). Bubbles play a critical role in every bubble-particle attachment mechanism, including collision, attachment, and detachment (Tao, 2010). A bubble-particle collision is initiated by the boundary between long-range hydrodynamic forces and short-range interfacial interactions (Han *et al.*, 2014). In order for the particles to eventually be collected as a concentrate, the flotation process uses bubbles to selectively adhere to the microalgae and float up to the flotation cell's surface.

The size distribution of bubbles in both the froth zone and the mixing or liquid pool zone in the column is correlated with the foam flotation's efficacy.

Impact of bubble in the pulp phase (or liquid pool zone)

In a successful particle recovery, the pulp phase's bubble size has a significant impact on the collision of microalgae with bubbles and the attachment of microalgae to bubbles (Yoon, 2000; Hassanzadeh *et al.*, 2016). Comparing smaller bubbles to larger ones, the former increases the attachment probability and gives particles more places to collide (Hassanzadeh *et al.*, 2016). Additionally, the size distribution of bubbles in the pulp phase also affects the sizes of the bubbles that adhere to the microalgae. Therefore, the effectiveness of the flotation process can be impacted by managing the size distribution of bubbles in the pulp phase.

Impact of bubble in the froth phase (foam zone)

The froth phase plays several important roles in the flotation process, including transporting particles to the concentrated layer, maintaining froth stability, and influencing mobility and structure. These factors can significantly impact flotation performance. Consequently, bubble size in this phase is crucial to the effectiveness of the flotation process (Bhondayi, 2020). Additionally, the size distribution of bubbles in the froth phase can be utilized to help control flotation and determine the extent of the froth (Moolman *et al.*, 1996). Furthermore, the distribution of bubble sizes in the foam also affects its rheological characteristics. These characteristics are crucial for comprehending the characteristics of the foam and establishing connections between the distribution of bubble sizes and the liquid properties that make up the foam (Calvert & Nezhati, 1986).

Foam bubble size can be increased via various methods to make microalgae harvesting more efficient. These methods include:

1. Mechanical methods are used to generate turbulence or agitation in the liquid to produce larger bubbles. Examples: stirring, shaking, or using a mechanical mixer.
2. Thermal methods are used to heat the liquid. This increases the vapour pressure, forming larger bubbles.
3. Physicochemical methods: adding substances to the liquid to reduce surface tension or increase viscosity, such as surfactants, polymers, or salts.
4. Gas injection is used to inject gas into the liquid. It contributes to adjusting the gas flow rate, which can affect the size of the bubbles formed. By the way, a high gas flow rate can lead to the formation of large bubbles.

The influence of small bubble size in the froth phase

Small bubbles are more stable and less likely to merge and break apart than larger bubbles, so they help to make the flotation process more effective. Longer contact times are made possible by their decreased buoyancy and the fewer disturbances they cause in the water. A more efficient absorption process results from this prolonged interaction, which improves the bubbles in the column's ability to absorb algae cells (Ralston *et al.*, 1999). Smaller bubbles possess a larger surface area (Tao *et al.*, 2019), which raises the possibility of particle adhesion to the bubbles by dramatically increasing the likelihood of collisions between bubbles and particles (Yoon & Luttrell, 1989).

According to research, it is more efficient to use small bubbles (with a Sauter mean diameter $d_{32} < 300 \mu\text{m}$) to separate particles from a sample and achieve a high particle concentration (Reis *et al.*, 2023). One significant consequence of small bubbles is their low rise velocity, which increases the bubble residence time by prolonging the time the particle stays in contact with the bubble (Nguyen & Schulze, 2003). Bubbles, on the other hand, raise slowly, which results in low drag forces and ineffective recoveries. For example, in the case of P_2O_5 recovery, only 40% was retrieved because the bubble-particle aggregates were dragged down with the tailings (Miettinen *et al.*, 2010; Reis *et al.*, 2019). In addition, it was shown that as the bubble size decreases, the rise velocity also decreases. This results in more gas being collected in the collection zone (Han *et al.*, 2014).

Through the use of three distinct aerator pipe diameters, the study also investigated the impact of bubble size on flotation during microalgae harvesting. The findings showed that a 0.25 mm aerator produced smaller bubbles that were more efficient at recovering microalgae, with an efficiency of 33%. In comparison, the 0.5 mm aerator had an efficiency of 24%, whereas the 1 mm aerator only achieved 20% (Zhao *et al.*, 2022).

The influence of large bubbles in the froth phase

As the size of bubbles increases, the likelihood of bubble-particle collisions also rises (Hassanzadeh *et al.*, 2016), resulting in greater drainage and even drier foam. Consequently, the foam phases contain larger bubbles (Du *et al.*, 2002). This occurs despite larger bubbles having a reduced surface area and a higher rise velocity (Reis *et al.*, 2019). The increase in bubble size leads to greater superficial gas flow (Al-Thyabat *et al.*, 2011), which enhances the entrainment and transport of particles from the pulp phase to the foam (froth) phase. This transfer happens through the liquid between the rising bubbles, resulting in improved particle recovery (Reis *et al.*, 2023). Large bubble flotation ($d_{32} > 1000 \mu\text{m}$) achieved the highest P_2O_5 recovery; However, this also resulted in increased entrapment of unwanted particles, which reduced the purity of the product concentrate (Reis *et al.*, 2019).

According to the analysis of bubble distribution within the foam phase, larger bubbles were formed as airflow rates increased. , the sparger configuration significantly affected the size of the bubbles. In particular, the mixture of a fluidic oscillator and a ceramic plate sparger created an oscillatory flow (COF) at a rate of 100 Lh^{-1} , which resulted in the smallest bubbles in the liquid pool or pulp phase and the largest bubbles in the foam phase. Consequently, the COF configuration was the most successful in reaching the ideal bubble size combination, which improved the concentration factor and biomass yield (Coward *et al.*, 2015).

2.5 Microalgae roles in circular bio-economy

The unique characteristics of microalgae, such as high productivity, the ability to grow in diverse environments and the potential to produce a wide range of valuable products, make them an attractive resource for various industries. Their economic potential is expected to grow, leading to the development of new products and applications. Microalgae have the potential to revolutionize various industries and contribute to a more sustainable and resource-efficient economy. An integrated approach called the algal-based bioresource cycle, which focuses on utilizing microalgae for sustainable production and resource recovery, offers a promising pathway towards a circular bio-economy.

2.5.3 Algal-based bioresource cycle

The algae-based bioresource cycle (ABC) is a promising approach to utilizing algae as a sustainable source of food, energy and various valuable products. It contributes to resource diversification, environmental sustainability and revitalizes local economies through bio-based industries. **Figure 2.21** illustrates the ABC concept, which begins with the identification and isolation of locally occurring algae species with desirable characteristics. The selected strains are then cultivated under controlled conditions, typically in photobioreactors (PBRs) or open ponds, using sunlight and carbon dioxide (CO₂) as primary energy sources. The resulting algal biomass is a rich source of valuable biomolecules, including lipids, carbohydrates, proteins and pigments (Becker, 2007; Wilkie *et al.*, 2011).

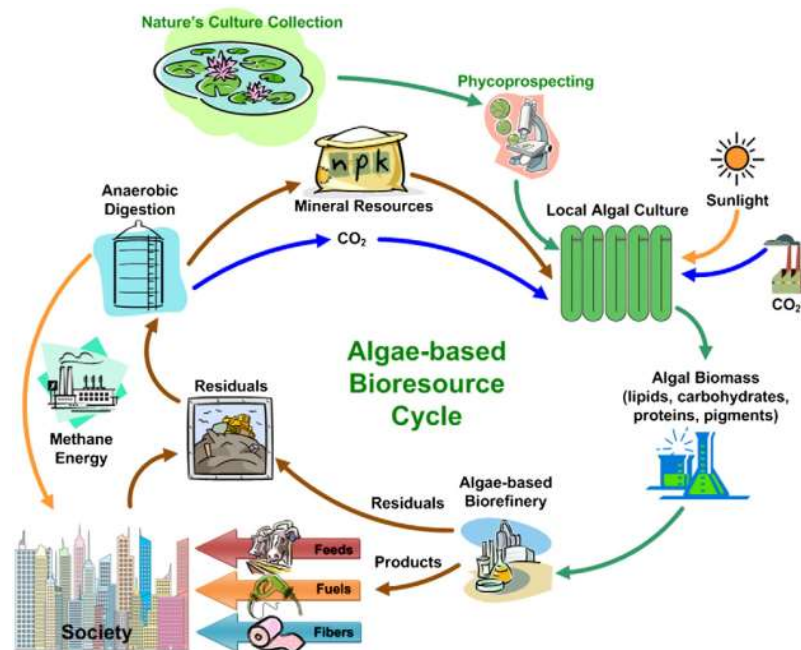


Figure 2.21: The cycle of algal-based bioresource, Illustration by Wilkie *et al.*, (2011)

The harvested algal biomass is subsequently processed in an algae-based biorefinery, where it undergoes various fractionation and conversion steps to produce a diverse range of marketable products. These products can broadly be categorized into three main groups:

- 1) **Food and feed:** microalgae are a rich source of protein and nutrients that can be processed into food supplements and feed products suitable for use in aquaculture and livestock.
- 2) **Fuels:** microalgae lipids can be converted into biodiesel, which provides a renewable replacement for fossil fuels, and biogas through the anaerobic digestion of biomass.
- 3) **Other Products:** microalgae can also be used to produce various products such as bioplastics, biofibers, fertilizers, pharmaceuticals and nutraceuticals.

Residues and by-products from the cultivation, processing refinery stages and general use of the products in daily life can be further utilized for resource recovery. These residuals can be anaerobically digested to produce methane energy. The remaining can be recycled as mineral resources for further microalgae production and other applications.

Therefore, from the analysis of this cycle, it can be concluded that the algae-based bioresource cycle (ABC) could contribute to a more sustainable society by providing alternative sources of food, energy and materials. It offers several benefits, including:

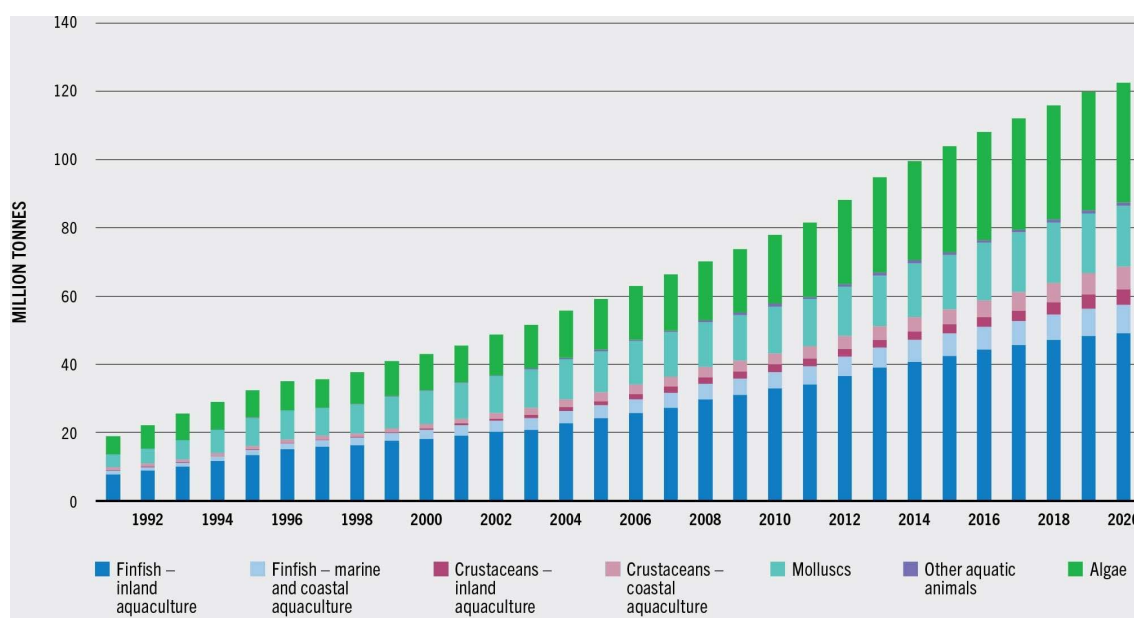
- 1) **Sustainability:** microalgae is a renewable resource that can be grown on non-arable land using sunlight, carbon dioxide and wastewater, reducing pressure on traditional agriculture.
- 2) **Versatility of applications:** microalgae can be used for the production of bioenergy and bioproducts, including animal feed, biofuels, fertilizers, food, cosmetics and pharmaceuticals.
- 3) **Environmental benefits:** microalgae absorb carbon dioxide during photosynthesis, reducing greenhouse gas emissions. In addition, microalgae can be used for wastewater treatment, reducing environmental pollution and providing a cost-effective source of nutrients for algae cultivation.

While the economic potential of microalgae appears promising, there are challenges that need to be addressed for large-scale commercialization. These include the development of cost-effective cultivation and harvesting technologies, optimization of strain selection to enhanced productivity and establishment of standardized production processes.

2.5.4 Global production of algae

Global aquaculture production is a growing industry that is playing an increasingly important role in providing food and nutrition for the world's population. This is due to its ability to do so in a variety of environments. **Figure 2.22** shows the overall production status and trend of global aquaculture from 1991 to 2020. It can be seen that global aquaculture production has grown steadily over the past three decades, and the growth rate has accelerated in recent years. In 2020, global aquaculture production reached a record 122.6 million tonnes, up 6.2% from the previous year.

The three largest aquatic animal species (finfish, crustaceans and molluscs) accounted for 87.5 million tonnes (72% of total production), mostly for human consumption. Among non-aquatic animal species, algae were the predominant species, producing 35.1 million tons (28% of total production) for both food and non-food purposes (FAO, 2022).



(Notes: Data exclude shells and pearls. Data expressed in live weight equivalent)

Figure 2.22: World aquaculture productions, 1991-2020.
Source: The State of World Fisheries and Aquaculture 2022 (FAO, 2022)

The data presented in **Table 2.8** illustrates global aquaculture production and its growth rate from 1990 to 2020 and covers various types of algae, including multicellular macroalgae (e.g. seaweed), unicellular microalgae (e.g. *Chlorella* spp.) and cyanobacteria commonly known as blue-green algae (e.g. *Spirulina* spp.). Overall global aquaculture experienced significant growth, increasing annual production by 609 percent over three decades, with an average annual growth rate of 6.7 percent. Notably, this growth rate has gradually declined from 9.5% in the 1990s to 4.6% in the 2010s and further to 3.3% in recent years (2015-2020).

Despite the decline in growth rate, it is important to recognize that aquaculture production has been steadily increasing in absolute terms, starting from 17.3 million tonnes in 1990 to 122.6 million tonnes in 2020. This growth is due to the continued growth of the world population and the resulting increase in food demand.

Production (A,B,C * million tonnes)	1990	1990	2000	2010	2015
	2020	2000	2010	2020	2020
All aquaculture					
A. Starting annual output	17.3	17.3	43	77.9	104
B. Ending year's annual output	122.6	43	77.9	122.6	122.6
C. Accumulated increase in annual output	105.3	25.7	34.9	44.6	18.6
D. Overall increase	609%	149%	81%	57%	18%
E. Average annual growth rate	6.70%	9.50%	6.10%	4.60%	3.30%
Algae (Note: algae include macroalgae, microalgae, and cyanobacteria)					
A. Starting annual output	4.2	4.2	10.6	20.2	31.1
B. Ending year's annual output	35.1	10.6	20.2	35.1	35.1
C. Accumulated increase in annual output	30.9	6.4	9.6	14.9	4
D. Overall increase	736%	153%	90%	74%	13%
E. Average annual growth rate	7.30%	9.70%	6.70%	5.70%	2.50%

Table 2.8: World aquaculture production and growth

Source: The State of World Fisheries and Aquaculture 2022 (FAO, 2022).

In this broader context, algae cultivation emerges as a dynamic segment within the aquaculture industry. Global algae production grew by 736% from 1990 to 2020, an average annual growth rate of 7.3%. Despite a recent slowdown in growth rate, it remains higher than total aquaculture production.

Forecasts indicate continued growth in algae cultivation in the coming years. This growth is driven by a number of factors, such as the versatility of algae, which can grow in different environments such as freshwater, saltwater and wastewater. High protein, vitamin, and mineral content in biomass enable it to be used as a source of biofuels, cosmetics, pharmaceuticals, and industrial products. In addition, sustainable food and feed sources are becoming increasingly important, so the use of algae in these applications will have a significant impact on the production of food and algae-based products in the future.

Table 2.9 shows commercial microalgae production in detail by country and species in 2019. The total production amount reached 56,456 tonnes, with *Spirulina (Arthrospira)* accounting for the majority at 56,208 tonnes (99.5%), and four green microalgae (*Chlorella vulgaris*, *Haematococcus pluvialis*, *Tetraselmis spp.* and *Dunaliella salina*) contributing 248 tonnes (0.5%). China emerged as the largest microalgae producer in 2019, contributing 97% of global production, particularly spirulina production. Other contributors to microalgae production include Chile, France, Greece, and Tunisia. Notably, FAO statistics also reflect microalgae production in three landlocked developing countries in Africa, namely Burkina Faso, Central African Republic and Chad (Cai *et al.*, 2021).

Country/area	Total Microalgae (tonnes)	Total <i>Spirulina/ Arthrospira</i> (tonnes)	Green microalgae (tonnes)				
			Total	<i>Haematococcus pluvialis</i>	<i>Chlorella vulgaris</i>	<i>Tetraselmis spp.</i>	<i>Dunaliella salina</i>
World	56,456	56,208	248	242	4.77	1.45	0.22
China	54,850	54,650	200	200			
Chile	903	861	42	42			
France	207	201	6.22	4.77	1.45		
Greece	142	142					
Tunisia	140	140					
Burkina Faso	140	140					
Central African Republic	50	50					
Chad	20	20					
Bulgaria	2.65	2.65					
Spain	1.52	1.3	0.22	0.22			

Table 2.9: Commercial microalgae production in 2019

Source: Seaweeds and microalgae: an overview for unlocking their potential in global aquaculture development. Fishery and Aquaculture Statistics (FishStatJ), Global production by production source 1950–2019 (Cai et al., 2021).

A notable observation from the table is that green microalgae production is significantly lower than *Spirulina (Arthrospira)*. It is likely that this difference can be attributed to *Spirulina*'s well-established commercial status and presence. However, the data also indicates a rising interest in green microalgae production due to their potential applications in food, feed, and biofuels. Although commercial microalgae production remains relatively small, their remarkable recent growth suggests that an industry is still in its early developmental stages. Nevertheless, there is substantial potential for future expansion and development.

According to the Statista database, as presented in **Figure 2.23** by Allied Market Research, the market value of algae products has been steadily increasing in recent years and is expected to continue to grow in the coming years. The global market value of algae products is expected to increase from 2.6 billion US dollars in 2018 to 3.45 billion US dollars by 2025, representing a compound annual growth rate (CAGR) of over 6% (Wunsch, 2020).

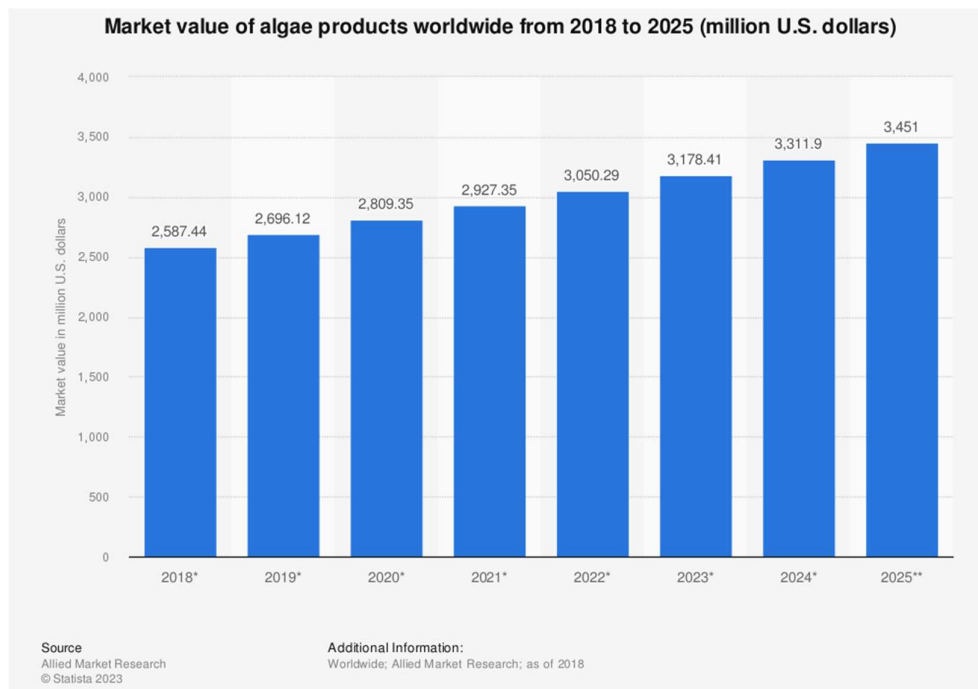


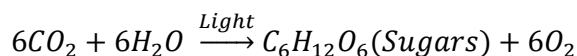
Figure 2.23: The global market value of algae products worldwide from 2018 to 2025

Source: Allied Market Research, Statista database

This indicates significant growth potential in the microalgae industry. In particular, microalgae represent a promising growth path due to their numerous advantages over traditional food sources and other products. These advantages include higher nutritional content, a highly sustainable source for various industries including food and beverages, cosmetics and pharmaceuticals, and reduced environmental impact.

2.5.5 Microalgae applications

Due to the diverse characteristics of microalgae, including a wide range of cell wall compositions, intracellular nutrient storage products, and pigmentation, they serve as an abundant source of proteins, lipids, carbohydrates, and pigments (Sathasivam *et al.*, 2017). Microalgae grow and reproduce through photosynthesis like land plants. This process involves the conversion of light energy into chemical energy by absorbing atmospheric CO₂ through the following reaction:



The sugars produced through photosynthesis play a crucial role in the synthesis of various cellular components such as lipids, carbohydrates and proteins, which together form biomass. These biochemical components stored in the microalgae cell serve as essential raw materials for various applications (Laurens, 2017). This diversity leads to various applications based on each algae species. Currently, whole microalgae biomass and purified extracts from microalgae find applications in various fields, including food, dietary supplements, feed and biofuels, etc (Barkia *et al.*, 2019).

Figure 2.24 illustrates the distribution of algae biomass producing enterprises in Europe, categorized according to various commercial applications of biomass and not by its volume. The information comes from a survey conducted in 2022 that included responses from 548 algae enterprises (Vazquez Calderon & Sanchez Lopez, 2022; Kuech *et al.*, 2023).

In the case of microalgae, the most common applications are food supplements and nutraceuticals, which account for 23% of enterprises. This is followed by animal feed at 19% and human food at 12%. In addition, cosmetics and wellbeing products prove to be a significant sector at 19%, followed by pharmaceuticals (8%) and fertilizers and biostimulants (7%). *Spirulina sp.*, a member of the cyanobacteria group, has long been a traditional component of diets in the Western world and is now recognized as a superfood due to its exceptional nutritional content (Jung *et al.*, 2019).

Mainly used for human food, food supplements and nutraceuticals, accounting for a significant 76% of enterprises in this field. Other marginal uses of this biomass include cosmetics and wellbeing products (6% of enterprises), animal feed (5%), pharmaceuticals (3%), fertilizers and biostimulants (2%) and bioremediation (1%).

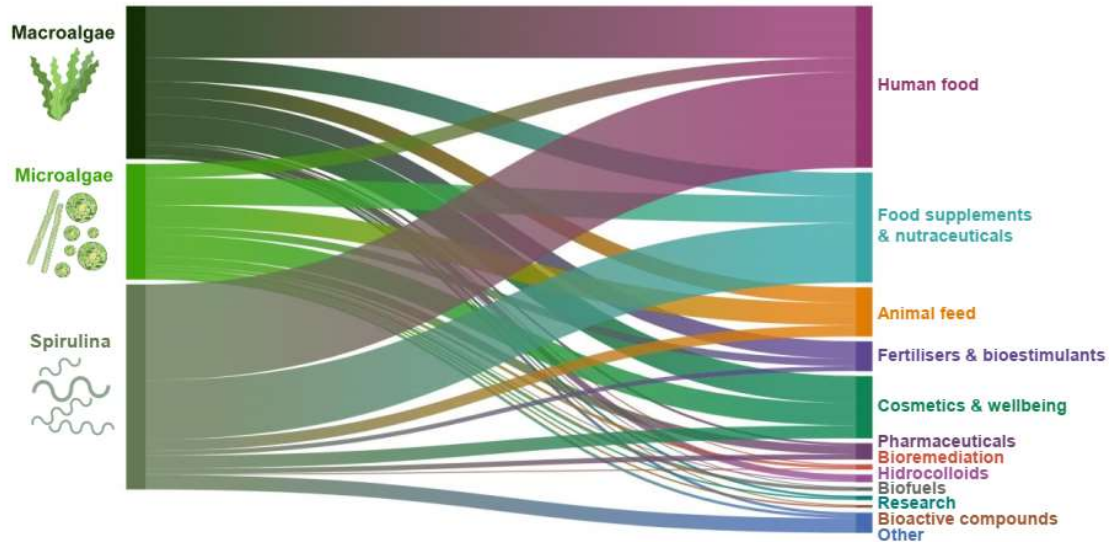


Figure 2.24: Commercial applications of algae biomass produced by European companies (Vazquez Calderon & Sanchez Lopez, 2022). (Note: not by biomass volumes)

2.5.5.1 Microalgae for human food and supplements

In general, the human food consists mainly of proteins, carbohydrates and lipids (fats and fatty acids). The global agricultural system produces an excess of carbohydrates because these are the main components of staple crops such as corn, rice, wheat and cassava. However, there is a deficiency in proteins and essential lipids. Soybeans are the main crop for these nutrients, while other sources come from animal products (Diaz *et al.*, 2023). Algae, on the other hand, represent a sustainable and nutritious source of proteins and lipids. Their biomass, which accumulates both proteins and lipids in abundance, addresses the scarcity of these essential nutrients in the global food system.

Table 2.10 shows the composition of conventional food sources and microalgae in terms of proteins, carbohydrates and lipids (adapted from Becker, 2007; Chisti, 2007; Von Der Haar *et al.*, 2014; Hadley *et al.*, 2017; Dilia *et al.*, 2018; Rösch *et al.*, 2019; Diaz *et al.*, 2023). Microalgae are generally higher in protein than traditional food sources. Some microalgae such as *Chlorella sp.*, *Scenedesmus sp.*, *Spirulina sp.* and *Dunaliella salina* have protein contents of over 50%. This is significantly higher than conventional food sources such as meat, eggs and milk. Microalgae are also reliable sources of lipids, with some species such as *Schizochytrium sp.* and *Botryococcus braunii* having high lipid contents in their cells. This is comparable to oilseeds such as rapeseed and oil palm kernels.

Commodity	Composition (% dry weight)		
	Protein	Carbohydrates	Lipids/fatty acids
Animal and plant products			
Wheat	13	73	1.5
Rice (<i>flour white</i>)	7	80	1.3
Corn (<i>flour, yellow, fine meal</i>)	6	81	1.7
Meat	43	1	34
Egg	47	4	41
Milk	26	38	28
Soybeans	37	30	20
Rapeseed (<i>defatted seeds</i>)	14–18	12–15	40–45
Oil palm kernel (<i>defatted kernels</i>)	16–27	6–11	50–70
Microalgae			
<i>Scenedesmus dimorphus</i>	60–71	13–16	6–7
<i>Chlorella pyrenoidosa</i>	57	26	2
<i>Chlorella vulgaris</i>	51–58	12–17	14–22
<i>Spirulina maxima</i>	46–63	8–14	4–9
<i>Spirulina platensis</i>	52	15	3
<i>Dunaliella salina</i>	39–61	14–18	14–20
<i>Haematococcus pluvialis</i>	48	27	15
<i>Chlamydomonas reinhardtii</i>	48	17	21
<i>Botryococcus braunii</i>	18–40	19–31	25–80
<i>Schizochytrium sp.</i>	12	32	45–77

Table 2.10: The composition of conventional food sources and microalgae (Becker, 2007; Von Der Haar *et al.*, 2014; Rösch *et al.*, 2019; Diaz *et al.*, 2023).

A comparison of lipid production and land requirements between commercial oil crops and microalgae, as shown in **Table 2.11**, was adapted from Chisti (2007). It is clear that microalgae produce significantly more lipids per hectare than all commercial oil crops. For example, microalgae with 70% of lipid by weight in the biomass can provide 136,900 L lipid /ha. In contrast, oil palm, the highest-yielding commercial oil crop, only produces 5,950 L lipid /ha (Chisti, 2007).

Raw Material	Lipid Yield (L/ha)	Land requirement (M ha)
Corn	172	1,540
Soybean	446	594
Canola flowers	1,190	223
Jatropha curcas	1,892	140
Coconut	2,689	99
Oil palm	5,950	45
Microalgae (30% lipid by wt. in biomass)	58,700	4.5
Microalgae (70% lipid by wt. in biomass)	136,900	2

Table 2.11: Comparison of lipid production and land requirements between commercial oil crops and microalgae. Source: (Chisti, 2007)

Based on land requirements, microalgae also have a significant advantage over commercial oil crops. They need much less land to produce the same amount of lipid as commercial oil crops. For example, to produce 136,900 L of lipid, microalgae with 70% lipid content would only require 2 ha of land, while oil palms would require 45 ha of land. Additionally, microalgae can be grown quickly, with some species doubling their biomass within a short period of time. Microalgae can also be cultivated in non-agricultural areas such as wastewater treatment ponds and deserts, while commercial oil crops require arable land (Chisti, 2007; Zullaikah *et al.*, 2019).

With regards to human nutrient composition, microalgae may be an alternative source of human calories. The data in Table 1 presents the main nutrient contents in microalgal biomass compared with the data from some conventional foods (Becker, 2007). The information suggesting some of microalgae are source of protein, carbohydrate and lipid that amount of them is higher or equal staple food. For example, high protein contents are found in some algae such as *Spirulina maxima*, *Synechococcus sp.*, *Scenedesmus obliquus*, *Chlorella vulgaris*, etc. Some species such as *Chlamydomonas reinhardtii* and *Chlorella vulgaris* have high levels of accumulated lipid in their cell. This information shows that microalgae are able to alterative food (Spolaore et al., 2006), compared to traditional crops and food stuffs, due to: (1) microalgae having a higher growth rate and productivity better than traditional crops per unit of area (Masojidek and Torzillo, 2014); and (2) ability to grow microalgae in several environments and less land use than conventional crops (Zullaikah et al., 2019).

To exploit microalgae for culture on an industrial scale, figure 2.1 illustrates industrial algal bioprocess concept including: selection and cultivation of high potential strains, biomass harvesting, extraction components (proteins, carbohydrates, lipids and pigments) and bio-refinery applications for feeds, foods, fuels, bioactive and pharmaceutical products which can integrated to the modern societies (Wilkie *et al.*, 2011).

To select new strains of microalgae to improve productivity, normally natural Microalgae are isolated and categorized following physiological and biochemical Rosenberg *et al.*, 2008 techniques. In addition biotechnology techniques, such as enzymatic bio-catalysis and biochemical assays can be used to evaluate the chemical and bioactive compounds in whole cell microalgal (Olaiyola, 2003). The interesting and selected species are further cultivated for biomass production using various systems particularly open raceway ponds or photobioreactors. CO₂, sunlight and wastewater which are main resources usually are used for microalgae cultivation, which can be harvested with suitable techniques (Wilkie *et al.*, 2011).

As mentioned earlier, algal biomass is well known a rich source of proteins, lipids, carbohydrates and pigments, depending on the characteristic of the algae species and the processing conditions (Sathasivam et al., 2017). Thus, it can be converted into a range of both low and high-value products, for example, foods, feed, fuels and fibres that can be used in daily life (Wilkie *et al.*, 2011; Sathasivam *et al.*, 2017). In addition The degraded consumable products and residuals from digestion or fermentation process can be reused as a raw material for algal cultivation (Wilkie *et al.*, 2011).

Depending on the microalgae species and growth conditions, the potential applications of microalgae biomass extend to the extraction of high-value products or bioactive molecules. Microalgae offer a diverse range of commercial products, including human and animal nutrition, polyunsaturated fatty acids (PUFAs), pharmaceuticals, antioxidants, anti-inflammatory agents and more (Loy & Chu, 2012; Mutanda *et al.*, 2020).

Table 2.12 outlines the main microalgae producers of commercial products with a focus on carotenoids such as beta-carotene and astaxanthin. In particular, *Dunaliella sp.* and *Haematococcus sp.* dominate the production of beta-carotene and astaxanthin (Suganya *et al.*, 2016). *Dunaliella salina*, known for its high beta-carotene content, reaches up to 16% of dry weight under semi-continuous conditions (Del Campo *et al.*, 2007). Cognis Nutrition and Health, the world's largest supplier of this strain, offers *Dunaliella* powder as an ingredient in functional foods and dietary supplements (Spolaore *et al.*, 2006). Astaxanthin, another valuable carotenoid from microalgae, is used in pharmaceuticals, cosmetics, nutraceuticals, and animal nutrition. *Haematococcus sp.* is a major producer of astaxanthin and contains up to 3% astaxanthin in a two-step culture process involving biomass induction and stress conditions (Spolaore *et al.*, 2006). Hawaii-based Cyanotech holds a dominant market share of over 95% in the animal feed market for algae-based astaxanthin products (Suganya *et al.*, 2016; Stachowiak & Szulc, 2021). In addition to carotenoids, cyanobacteria and microalgae such as *Schizochytrium sp.*, *Cryptocodinium sp.* and *Nitzschia sp.* contribute significantly to the commercial production of fats and oils as alternative sources to those of animal and plant. PUFAs, especially eicosapentaenoic acid (EPA) and docosahexaenoic acid (DHA), play a role in the prevention of cardiovascular disease. *Cryptocodinium cohnii*, for example, provides oil with 40–50% DHA and *Schizochytrium sp.* (40% DHA), which is crucial for brain and eye development in infants (Kroes *et al.*, 2003; Ward & Singh, 2005).

Product form	Microalgae	Application	Commercial Producer	Origin
Whole microalgae cell				
Dried biomass	<i>Spirulina sp. (arthrospira)</i>	Human food Nutritional supplements Animal feed Aquaculture	Cyanotech Corporation Far East Microalgae Ind. Hainan DIC Microalgae Japan Algae Co., Ltd. Biorigin TAAU Australia Pty Boonsom Farm	USA Taiwan China Japan Switzerland Australia Thailand
Dried biomass	<i>Chlorella sp.</i>	Human food Nutritional supplements Aquaculture	Taipei Roquette Klötze Earthise Nutritionals	Taiwan Germany USA
Extracted high-value co-products				
Carotenoids				
Beta-carotene	<i>Dunaliella sp.</i>	Antioxidant Nutritional supplements Aquaculture	Cognis Nutrition & Health Nature Beta Technology Cyanotech Corporation Tianjin Lantai Biotechnology	Australia Israel USA China
Astaxanthin	<i>Haematococcus sp.</i>	Antioxidant Nutritional supplements Aquaculture	Bioreal BlueBioTech Int. Parry's Pharmaceuticals Algatech DSM	Hawaii, USA Germany India Israel Netherlands
Lipid / Polyunsaturated fatty acids (PUFAs)				
Eicosapentaenoic acid (EPA)	<i>Nannochloropsis sp.</i> <i>Porphyridium sp.</i> <i>Phaeodactylum sp.</i> <i>Nitzschia sp.</i>	Nutritional supplements Phamaceutical Animal feed Aquaculture	AlgaeCytes AlgiSys BioSciences, Inc. Lyxia Xiaozao Tech Arizona Algae Products	UK USA China USA
Docosahexaenoic acid (DHA)	<i>Schizochytrium sp.</i> <i>Cryptocodinium sp.</i> <i>Ulkenia sp.</i>	Infant formula Nutritional supplements Phamaceutical Aquaculture	Veramaris Corbion Progress Biotech BIRAC DIC Asia Pacific Pte.	Netherlands Netherlands Netherlands India Singapore
Oil / Lipid	<i>Botryococcus sp.</i> <i>Chlamydomonas</i> <i>Chlorella sp.</i> <i>Neochloris sp.</i>	Biofuel	Cellana Renewable Algal Energy PetroAlgae	Hawaii, USA USA USA

Table 2.12: Commercial products from microalgae and applications. [Adapted from (Spolaore et al., 2006; Rosenberg et al., 2008; Pires, 2017; Barkia et al., 2019)]

2.5.5.2 *Microalgae for animal feed*

Microalgae are rich in essential biomolecules such as proteins, amino acids, polyunsaturated fatty acids (PUFAs), carotenoids and vitamins. These nutrients contribute to improved animal health, growth and product quality. This leads to microalgae being increasingly recognized as a promising alternative to traditional animal feed sources. Around 30% of global microalgae biomass production is currently used for animal feed applications. Companies actively cultivating microalgae for feed production can be found in China, Japan, Taiwan, Thailand, India, the United States and the United Kingdom (Saadaoui *et al.*, 2021).

Several studies have demonstrated the positive impact of microalgae-enriched feed on egg quality. Fredriksson *et al.*, (2006) found that adding 20% *Nannochloropsis oculata* to hen feed significantly increased lutein and zeaxanthin content in eggs. Several species of microalgae exhibit prebiotic properties that promote the population of beneficial intestinal bacteria and improve animal health. *Chlorella sp.* produces an immune-stimulating polysaccharide (Gupta *et al.*, 2017), while *Dunaliella salina* produces extracellular polysaccharides with immunostimulant, antiviral, and antitumor properties (Harvey & Ben-Amotz, 2020). In addition, microalgae play a crucial role in aquaculture by providing essential nutrients to zooplankton, molluscs, crustaceans, shrimp and fish (Dineshbabu *et al.*, 2019). Supplementation with 10 to 30 g of *Schizochytrium sp* per kg in the diet for *Leporinus friderici* and 16% dried whole cells for Nile tilapia significantly improved weight gain, protein efficiency ratio and overall health (Sarker *et al.*, 2016; Prates *et al.*, 2018).

2.5.5.3 *Microalgae for sustainable energy*

Cyanobacteria and microalgae have emerged as promising sources for biofuel production due to their ability to synthesize various biofuel-related compounds. Cyanobacteria have been modified to produce ethanol, butanol, isobutyl-aldehyde, ethylene, and isoprene (Nozzi *et al.*, 2013), while some species can be cultivated for hydrogen production (Azwar *et al.*, 2014). There are 3 main classes of production of biofuels from microalgae: biochemical conversion, thermochemical conversion and chemical conversion (Chisti, 2007; Brennan & Owende, 2010). They are discussed in detail in the following sections:

1) *Biochemical conversion*

The cyanobacterium *Synechococcus sp.* can accumulate a significant amount of carbohydrates, reaching up to 60% of its cell dry weight under nitrate-limited conditions. This carbohydrate can serve as a feedstock for yeast fermentation to produce bioethanol (Möllers *et al.*, 2014). The degradation of glycogen in the biomass of cyanobacteria, one of the major accumulations in the organism, can be converted into ethanol through saccharification and fermentation (Aikawa *et al.*, 2014; Diaz *et al.*, 2023). In addition, Badary *et al.*, (2018) investigated glycogen synthesis in *Synechococcus sp.* and found that this strain produced up to 23% of dry cell weight in glycogen.

2) *Thermo-chemical conversion*

Thermochemical conversion technologies are a promising route for biofuel production from microalgae. The substantial water content in microalgal feedstock significantly influences the operating parameters of thermochemical conversion processes (López Barreiro *et al.*, 2013). **Table 2.13** classifies different thermochemical conversion technologies for microalgae-based biofuel production according to the intended primary product and water content.

Hydrothermal liquefaction (HTL) is a thermochemical conversion process that uses high temperatures and pressure to convert biomass into liquid fuel. A particular advantage of HTL is its ability to convert algal biomass into bio-oil despite its high water content. HTL process involves heating wet biomass in a closed reactor at high temperatures (280-370°C) and pressures (10-25 MPa) In this process, the biomass is broken down into its constituent molecules, which subsequently recombine to produce liquid fuels or bio-oil (López Barreiro *et al.*, 2013). Numerous strains, including *Botryococcus braunii*, *Spirulina platensis*, *Chlorella vulgaris*, *Nannochloropsis sp.* and *Desmodesmus sp.* were examined in the context of HTL (Brown *et al.*, 2010; Jena *et al.*, 2011; Garcia Alba *et al.*, 2012). The specific products formed depend on the type of biomass and the reaction conditions.

Primary product	Feed stock state					
	Wet biomass			Dry biomass		
	Processes	Temperature	Pressure	Processes	Temperature	Pressure
Solid	Hydrothermal carbonization (HTC)	around 200 C	< 2 MPa	Torrefaction	200-300 C	atmospheric
Liquid	Hydrothermal liquefaction (HTL)	280-370 C	10-25 MPa	Pyrolysis	400-600 C	atmospheric
Gas	Hydrothermal gasification (HTG)	400-700 C	25-30 MPa	Gasification	> 700 C	atmospheric

Table 2.13: Producing biofuels from microalgae through thermochemical conversion processes [source: (López Barreiro *et al.*, 2013)].

Conversely, thermochemical conversion technologies with low water requirements, such as torrefaction, gasification and pyrolysis, are designed to operate under conditions that minimize or eliminate water requirements. The aim is to optimize the efficiency of converting raw materials into valuable products, including solid fuels, synthesis gas and bio-oil. Consequently, these low-water technologies are less suitable for biomass feedstocks with high water content, particularly microalgae.

3) *Chemical conversion*

Microalgae, on the other hand, can be utilized for biodiesel production due to their ability to store oil droplets within their cells through a process called transesterification. Several microalgae species exhibit a remarkable ability to store oil droplets, with oil content varying greatly between different strains (**Table 2.14**).

Microalgae	Oil content (% dry wt)
<i>Botryococcus braunii</i>	25-80
<i>Schizochytrium</i> sp.	50-77
<i>Neochloris oleoabundans</i>	35-65
<i>Nitzschia</i> sp.	45-47
<i>Chlorella vulgaris</i>	14-40
<i>Cylindrotheca</i> sp.	16-37
<i>Chlorella protothecoides</i>	23-30
<i>Phaeodactylum tricornerutum</i>	20-30
<i>Tetraselmis suecica</i>	15-23
<i>Cryptocodinium cohnii</i>	20
<i>Dunaliella salina</i>	14-20
<i>Spirulina maxima</i>	4 - 9

Table 2.14: Oil content in microalgal biomass (Chisti, 2007).

The amount of oil accumulated in the algal biomass is influenced by various factors: microalgae strain, cultivation conditions, and stress conditions such as nutrient deficiency, photooxidation,

pH and temperature (Hu *et al.*, 2008). Certain microalgae such as *Botryococcus braunii* and *Schizochytrium sp.*, have an exceptionally high oil content, accounting up to 25-80% or 50-77% of their total weight, respectively (Chisti, 2007). These oil-rich microalgae are particularly promising raw material sources for oil-derived biofuels.

Trans esterification is the reaction of an alcohol that converts algal oil into biodiesel via a two-step process of algal oil extraction and subsequent triglycerides conversion process into methyl esters (Chisti, 2007) or through direct conversion from wet algal biomass called in-situ transesterification (Teo & Idris, 2014).

Figure 2.25 presents the general equation for transesterification, in which the glycerol backbones of triglycerides (TG) is replaced by methanol; this causes fatty acids, the side chains of TG, to be esterified into methyl esters (biodiesel). Algal oils consist primarily of TG molecules that react with alcohols to form monoalkyl esters and the byproduct glycerin, which can be used in pharmaceuticals and cosmetics (Suganya *et al.*, 2016).

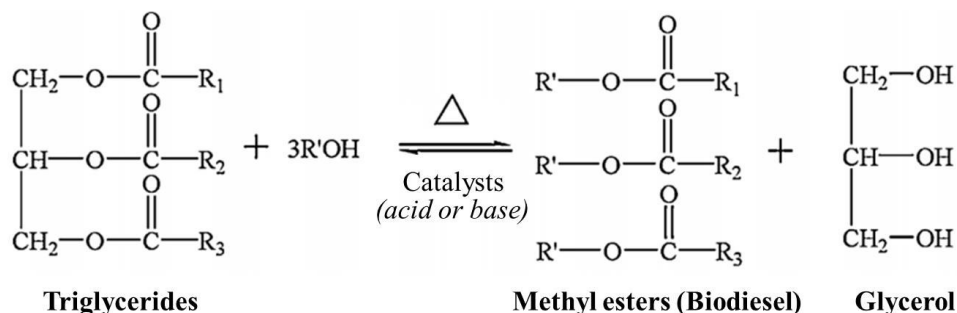


Figure 2.25: Transesterification reaction of triglycerides. [Adapted from (Zhao *et al.*, 2020)]

2.6 Summary

Microalgae are a potential feedstock for foods, feeds, biofuel and pharmaceuticals applications. The major stages of algal biomass production include as follows:

2.6.3 **Strain selection**, high-performance species including high growth rate, tolerance to the environment and high productivity of biochemical substance in their cells should be considered.

2.6.4 **Cultivation system**, the challenge of this system is low biomass yields and contamination. Open pond system is simple operation and low cost but has a risk of contamination and low biomass concentration. Photobioreactor systems operated in a closed condition are able to reduce contamination and give high productivity. However, these systems are considerably complicated and have high operating costs.

2.6.5 **Harvesting methods**, microalgae harvesting methods are an obstacle of large-scale production due to their high operating costs. The reasonable harvesting method that is cost-effective, rapid, and easy to scale up while giving high recovery efficiency should be considered.

Foam flotation as mentioned above is a promising method for microalgae harvesting. The advantage of this method includes high efficiency, simple and rapid operation and low power consumption. However, in foam flotation separations there is a trade-off between recovery efficiency and concentration factor. High recovery efficiencies are obtained using high air flow rates and high surfactant compositions. These conditions produce wet foams with low concentration factors. To overcome these, these studies propose to use high gas flow rate and surfactant concentrations along with column restrictions to enhance the dewatering of the foam.

Chapter 3

Materials and Methods

This chapter is separated into 5 main parts in this project that plays important roles in its overall success. They are: the experimental flow diagram, microalgae cultivation, the design of risers, foam flotation experiments and observation of foam formation. These sections will be described in more detail in the following sections.

3.4 Experimental flow diagram

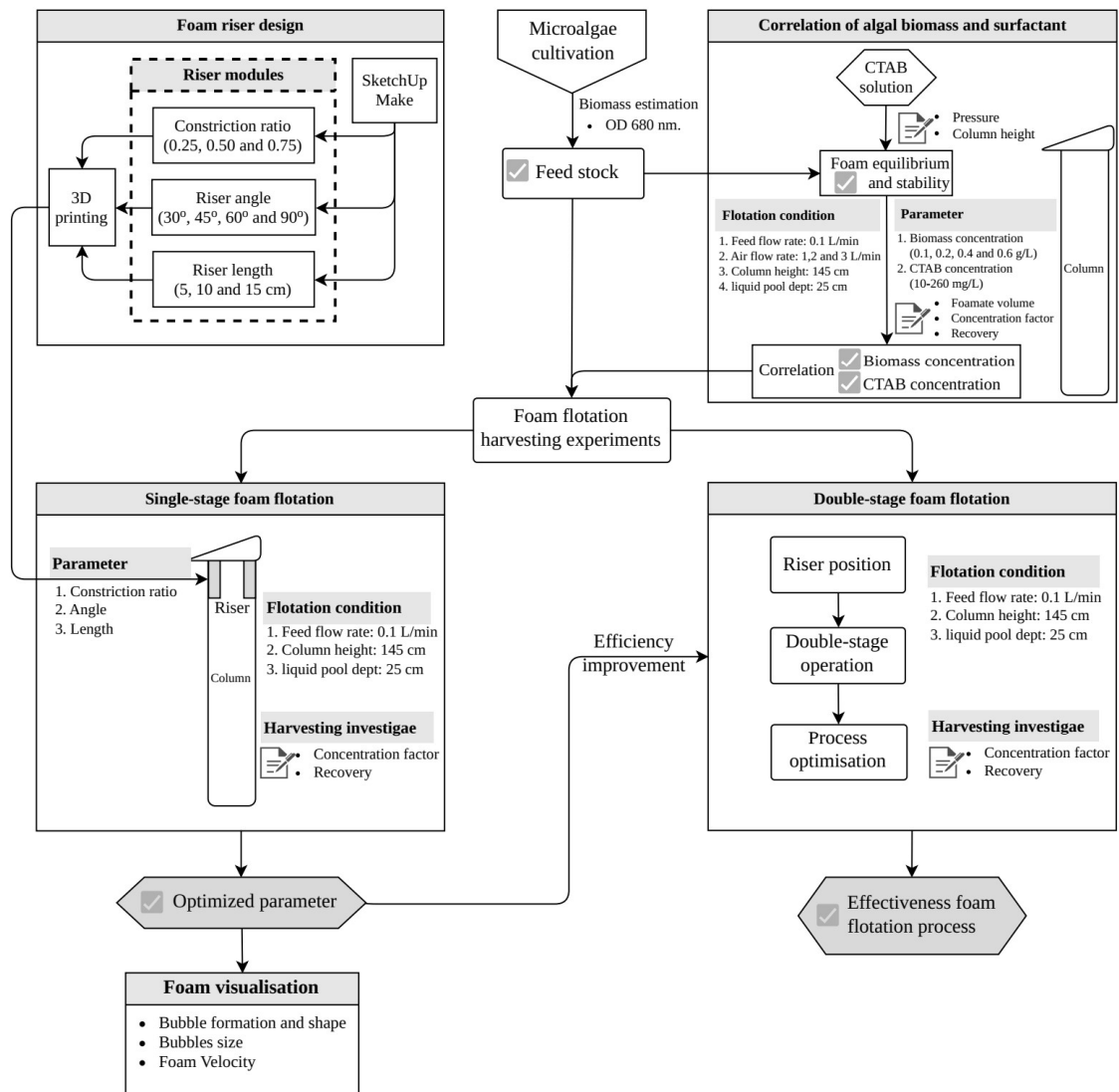


Figure 3.1: The experimental flow diagram

3.5 Microalgae cultivation

A pure algal strain of *Chlorella vulgaris*, supported by the algal culture laboratory at school of Natural and Environmental Sciences, Newcastle University was cultured in BG-11 medium for increasing algal biomass. The algae starter was cultured using the streak plate method with 10% agar in BG-11 broth for 30 days or until appearance of green colonies on the culture plate. A single colony was picked up and inoculated in 10 ml BG-11 medium to propagate algal cells under autotrophic conditions with 16 h light (cool white fluorescent light with 2,500 lux light intensity) and 8 h dark cycles and continuous aeration for 30 days. 1 L medium of algae culture was used as a starter culture for the experimental work (**Figure 3.2**).

The starter culture (approximately 10%) was inoculated into 10 L of Nalgene™ polycarbonate (PC) balloon tanks and cultured under autotrophic conditions for 15 days in the algae culture room at the School of Natural and Environmental Science, Newcastle University, UK. The culture conditions of Alkarawi *et al.* (2018) were followed. Briefly, the light source for algae cultivation was cool white LED (60 W LED Mirror stone, UK) with an average light density of 2,500 lux, 16 light hours: 8 dark hours photoperiod and continuous aeration with an air pump, 0.04 mPa, (Blagdon KA65, UK).

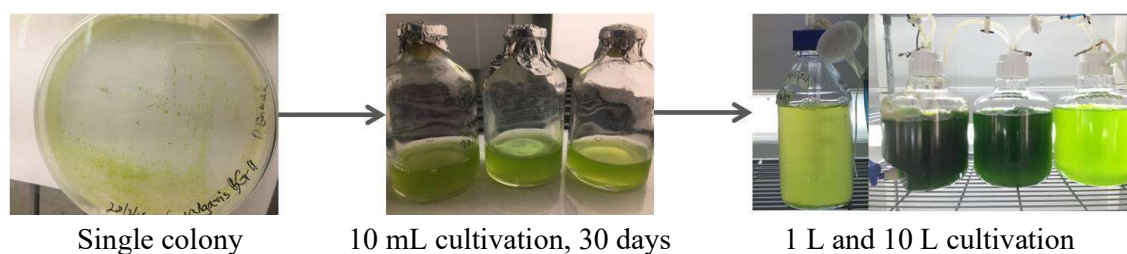


Figure 3.2: The process of algae starter product enhanced in BG-11 medium under autotrophic conditions. A single healthy colony was picked from the agar plate (left), dropped into 10 ml of culture medium and left for 30 days (middle). After 30 days, the cultured algae were further cultured in 1 litre and 10 litre scales (right).

The chemical composition of BG-11 medium consisted of NaNO₃, K₂HPO₄, MgSO₄.7H₂O, CaCl₂.2H₂O, Citric acid, Ammonium ferric citrate green, EDTANa₂, Na₂CO₃, Trace elements (H₃BO₃, MnCl₂.4H₂O, ZnSO₄.7H₂O, Na₂MoO₄.2H₂O, CuSO₄.5H₂O and Co(NO₃)₂.6H₂O). The medium was prepared according to the method of Stanier (Stanier *et al.*, 1971), See

Table 3.1.

To prepare the BG-11 medium, the volume was adjusted to any given volume with deionized water and the pH was adjusted to 7.1 with 1 M NaOH or HCl. Sterilisation was performed at 15 psi using autoclave (Ensign, Rodwell, UK) for 15 minutes and the medium was placed cooling at room temperature before use.

	Compound		Amount (mL/L)	Stock Solution	Final amount (g/L)
1	NaNO ₃		-	-	1.5
2	K ₂ HPO ₄		0.5	4.0 g/50 mL dH ₂ O	0.040
3	MgSO ₄ .7H ₂ O		0.5	7.5 g/50 mL dH ₂ O	0.075
4	CaCl ₂ .2H ₂ O		0.5	3.6 g/50 mL dH ₂ O	0.036
5	Citric acid		0.5	0.6 g/50 mL dH ₂ O	0.006
6	Ammonium ferric citrate green		0.5	0.6 g/50 mL dH ₂ O	0.006
7	EDTANa ₂		0.5	0.1 g/50 mL dH ₂ O	0.001
8	Na ₂ CO ₃		0.5	2.0 g/50 mL dH ₂ O	0.020
9	Trace metal solution:		0.5	Mix 9.1-9.6 in 50 mL dH ₂ O	
	9.1	H ₃ BO ₃		0.286 g	0.00286
	9.2	MnCl ₂ .4H ₂ O		0.181 g	0.00181
	9.3	ZnSO ₄ .7H ₂ O		0.022 g	0.00022
	9.4	Na ₂ MoO ₄ .2H ₂ O		0.039 g	0.00039
	9.5	CuSO ₄ .5H ₂ O		0.008 g	0.00008
	9.6	Co(NO ₃) ₂ .6H ₂ O		0.005 g	0.00005

Table 3.1: The composition of BG-11 medium and the amount of compounds for stock preparation (Stanier *et al.*, 1971).

3.6 Foam riser design

The aim of this study was to investigate the foam riser aspect to increase the algae harvesting capacity compared to the previous systems (Alkarawi *et al.*, 2018). The previous foam riser models were designed with diameter ratios of 0.25, 0.5 and 0.75, 60° transition sections on both sides and a length of 7 cm. Thus, foam risers by adjusting angles and length of riser as shown in **Figure 3.3**.



Figure 3.3: Side view of some of 51 variable modules of the foam riser, (A) variable lengths and constriction ratios, (B) angles and constriction ratios, (C) as desired, a combination of variable length and variable angle was constructed to form a type of riser and (D) the desired riser was then inserted into the transparent acrylic tube.

They were also assigned with wide range of both riser angle (30°, 45°, 60° and 90°) and riser length of 5, 10, 15 cm and 0.2 cm (disc shape). The foam constriction riser angle is the taper angle of the constriction section or riser where the foam containing the target material moves upward. The angle, measured in degrees, indicates how much the risers slope or deviate from the vertical axis of the column.

The designs were drawn in Google SketchUp Make 2016 program. The entire expansion riser design, which includes 51 modules (see **Table 3.2**), was printed using a uPrint SE Plus Desktop 3D printer (Stratasys, USA). A thermoplastic acrylonitrile butadiene styrene (ABS) building material (Stratasys uPrint P430 XL, USA) and a soluble support filament material (Stratasys SR 30XL) were used as model materials.

No.	Riser	No.	Riser	No.	Riser	No.	Riser
1	30°-0.25-5cm	2	30°-0.25-7cm	3	30°-0.25-10cm	4	30°-0.25-15cm
5	30°-0.50-5cm	6	30°-0.50-7cm	7	30°-0.50-10cm	8	30°-0.50-15cm
9	30°-0.75-5cm	10	30°-0.75-7cm	11	30°-0.75-10cm	12	30°-0.75-15cm
13	45°-0.25-5cm	14	45°-0.25-7cm	15	45°-0.25-10cm	16	45°-0.25-15cm
17	45°-0.50-5cm	18	45°-0.50-7cm	19	45°-0.50-10cm	20	45°-0.50-15cm
21	45°-0.75-5cm	22	45°-0.75-7cm	23	45°-0.75-10cm	24	45°-0.75-15cm
25	60°-0.25-5cm	26	60°-0.25-7cm	27	60°-0.25-10cm	28	60°-0.25-15cm
29	60°-0.50-5cm	30	60°-0.50-7cm	31	60°-0.50-10cm	32	60°-0.50-15cm
33	60°-0.75-5cm	34	60°-0.75-7cm	35	60°-0.75-10cm	36	60°-0.75-15cm
37	90°-0.25-5cm	38	90°-0.25-7cm	39	90°-0.25-10cm	40	90°-0.25-15cm
41	90°-0.50-5cm	42	90°-0.50-7cm	43	90°-0.50-10cm	44	90°-0.50-15cm
45	90°-0.75-5cm	46	90°-0.75-7cm	47	90°-0.75-10cm	48	90°-0.75-10cm
49	90°-0.25-0.2cm	50	90°-0.50-0.2cm	51	90°-0.75-0.2cm		

Table 3.2: A 51-module riser designed in Google SketchUp Make 2016 and printed on a desktop 3D printer.

3.7 Foam flotation experiment

A freshwater microalgae culture of *Chlorella vulgaris* was used throughout the experiment after 15 days of cultivation. To investigate the effectiveness of foam floating, there are 4 main parts, including foam equilibrium, influence of foam riser, foam visualisation and process evaluation were performed;

3.7.3 Foam column structure

The following procedure described the construction and operation of a laboratory-scale. The foam column made of poly(methyl methacrylate) tubes with an inner diameter of 51.5 mm. Additional tube modules were assembled to the column which were enable flexible height adjustment in the range of 50 to 250 cm. The purpose of the system setup was to systematically optimise various parameters as described below:

3.7.3.1 Column for foam equilibrium

A foam equilibrium experiment was carried out on the equipment as shown in **Figure 3.4 (A)**. The column was equipped with series of channel openings positioned along the side surface of the foam column module from a height of 45 cm. These connections facilitated the insertion of the pressure gauge tubing to enable precise measurements.

3.7.3.2 Column for the influence of riser

In **Figure 3.4 (B)** shows the use of the column for a flotation process, with particular emphasis on optimising parameters of the foam riser. In the experimental configuration, the riser was carefully positioned within the column, as depicted in **Figure 3.3 (D)**.

3.7.3.3 Column for the influence of riser position

The foam column was shown in **Figure 3.5 (A)**. It was used to perform a flotation process designed for both riser positioning and multiple riser processing. This undertaking required the use of flat riser with constriction ratio of 0.25 with the angle of 90°, placed at various heights within the column (45, 70, 90 and 120 cm).

3.7.3.4 Column for process evaluation

The foam column shown in **Figure 3.5 (B)** was used to carry out a flotation process focussing on multi-stage floatation. A riser module was used to characterise by a constriction ratio of 0.25, 90° angle with the length of 15 cm.

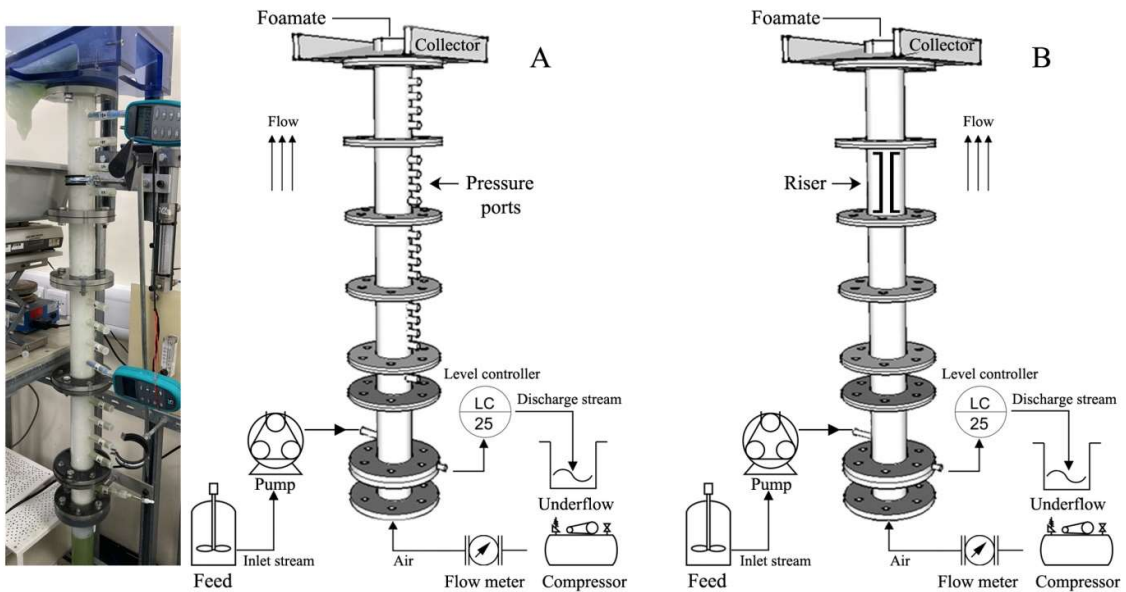


Figure 3.4: Photograph and schematic diagram of the continuous foam flotation unit. (A) The column for foam equilibrium experiment. (B) The column for foam riser optimization experiment.

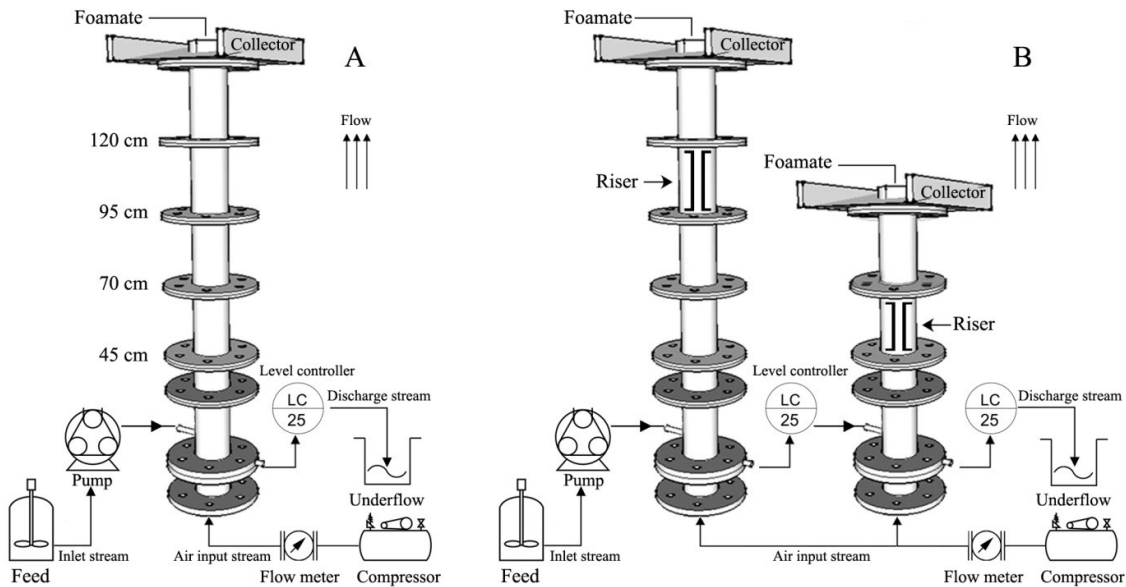


Figure 3.5: Schematic representation of the continuous foam flotation system. A: Column for riser position processing using a flat riser module with a constriction ratio of 0.25 and a 90 degree angle at different heights (45, 70, 90 and 120cm). B: Column series for multi-stage processing using a riser module with a constriction ratio of 0.25, a 90 degree angle and a length of 15cm.

To improve experimental versatility and precision, an instrumental, 15 cm deep cuboid trough with a length of 60 cm was used as the primary collection mechanism. The mechanism collected algal biomass or foamate, hereinafter referred to as collector of the column device. In particular, an additional air stream was placed near the collector as it was found to be particularly useful for breaking up foam. Peristaltic pumps (VWR PP3400, UK) were used to precisely control the flow rate of the sample solution in the inlet chamber to the column unit.

At the column base was an ultra-high molecular weight polyethylene (UHMWPE) gas diffuser, the dimensions of which were 6.0 mm thick, 6.0 mm diameter 51.5 mm and pore sizes of 30 μm . It should be noted that the diffuser assembled was inspired by the recommendations of Alkarawi *et al.* (2018) who suggested as a key component responsible for the generation of air bubbles that formed the dispersed phase. This was achieved by a vertical airflow carefully regulated via a rotameter from Dwyer Instruments, USA. To ensure precise control of liquid depth within the column, a level control valve was strategically integrated into an outlet port located at 1 cm above the gas diffuser. The mechanism contributed significantly to facilitating the discharge of the underflow solution. The growth medium solution will be throughout the foam column after the flotation process.

3.7.4 Foam flotation process

The flotation process was performed. Firstly, the solution introduced into the inlet chamber was a freshwater or an algae culture. Then, it was combined with a cationic surfactant of cetyltrimethyl ammonium bromide (CTAB) with various concentrations from 10 to 260 mg L^{-1} . The sample solution and surfactant were carefully achieved by using an overhead stirrer (VWR VOS14, UK) for a period of 10 min both before and during the flotation process. Thirdly, air bubbles were created and formed the dispersed phase using a gas diffuser (an ultra-high molecular weight polyethylene: UHMWPE) by introducing compressed air into the column from the base. An air compressor system was carefully set up to provide the required compressed air. A regulator was set in the range of 1 to 3 L min^{-1} , while a rota meter was judiciously used to carefully monitor the flow rate. A peristaltic pump system was used to continuously introduce the sample solution into the column, and maintained a feed flow rate of 0.1 L min^{-1} at the inlet. During the course of the flotation process, careful adjustments were made to the drain valve to effectively divert the underflow solution away from the bottom of the column, thereby ensuring the stability of the sample solution level at a constant 25 cm within the column. Subsequently, the foamate, after rising to the top surface of the column through the flotation process, was removed and collected using a dedicated collection device.

3.7.5 Foam visualisation

Several methods are available to quantify bubbles. The optical technique is the most common method for determining foam bubbles (Hanotu *et al.*, 2012). By measuring their size, speed or velocity and tracking where the bubbles are. The structure of the flotation unit for foam visualization was shown in **Figure 3.6** by dividing the inner diameter of 51.5 mm of a tubular poly(methyl methacrylate) into two halves and then using a constriction ratio of 0.25, an angle of 90° and a riser length of 15 cm placed at a height of 95 cm under the condition of an air flow rate of 1 L min⁻¹, a supply flow rate of 0.1 L min⁻¹ and a liquid pool depth of 25 cm.

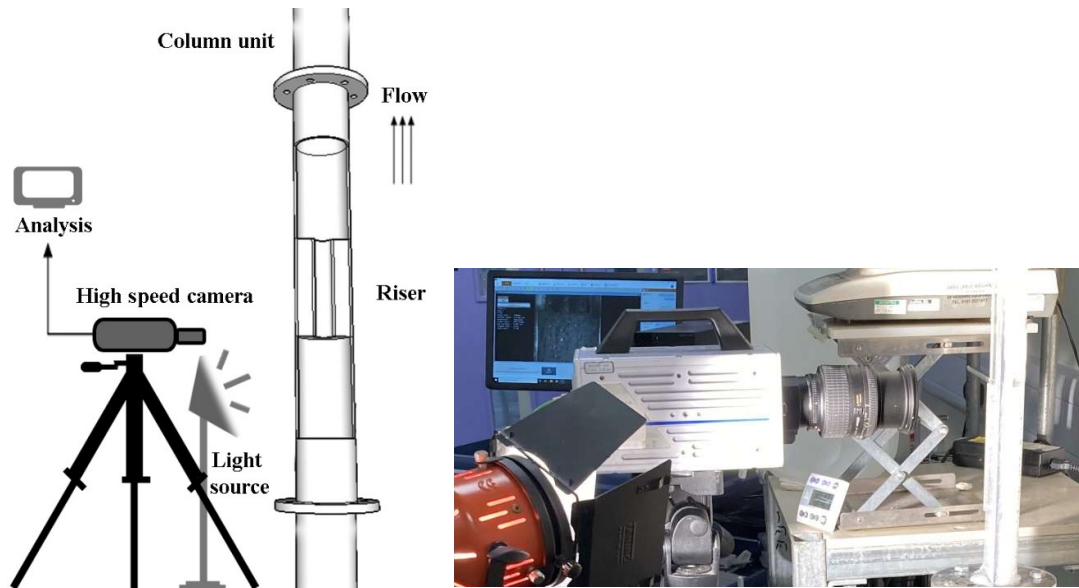


Figure 3.6: Diagram and the photograph of the continuous foam flotation set up with a high speed camera for foam visualisation.

To ensure that the images captured are accurate representations of the actual measurements in the column, at the position of riser, a ruler was attached to the outer wall of the column as a reference point for calibrating the images (pixels in mm). This allowed the images to be used as a reliable reference point when measuring the size and shape of foam bubbles in the column (Besagni *et al.*, 2016). Not only it was established the scale for all photos, but also it was mounted below and above the riser. For a high-speed camera (Photron FASTCAM SA3, USA) with a Nikon AF Nikkor 24-85 mm lens was used to photograph foam bubbles. The camera was placed in front of the column where the riser was installed and connected to a computer to record images. The backlight solution was used to illuminate the experimental trials to help focus the camera and obtain a clear image using a 650 W open tungsten light kit (Lanaro Lilliput150, Italy).

The experiments were conducted at a frame rate of 2000 frames per second (fps), with at least 250 high-quality images captured for each trial. Bubble sizes were measured using the open source software ImageJ 1.53T (National Institutes of Health, Maryland, USA). Bubble velocity is the rate at which the position of a bubble changes relative to a point in the surrounding medium. The movement of individual bubbles can be tracked by analysing video images captured at high speed, and their speed can be calculated based on their movement over time using high-speed digital imaging software Photron FASTCAM Viewer 4 (Coward *et al.*, 2015).

3.7.6 Process analysis

3.7.6.1 Cell density and biomass measurement

Cell number was counted in a Neubauer Improved Haemocytometer Counting Chamber, 0.1 mm depth, under a light microscope (Olympus BH-2 trinocular microscope, Japan) with 40× magnification. The number of cells per ml can be calculated as follows the **Equation 3.1** (Moheimani *et al.*, 2013):

$$\text{Cell Number (cells/mL)} = \left(\frac{\text{Total number of cells counted}}{\text{Number of squares counted}} \right) \times 1000 \dots\dots\dots 3.1$$

In the context of biomass or dry cell weight analysis, the gravimetric method was measured using a 4-decimal precision analytical balance (Kern ABS220-4N, Germany). Algal cells were dried at 65 °C for 24 h and stored in desiccators overnight. Dry weight concentration (DWC) was calculated as given in **Equation 3.2**.

$$\text{DWC (mg/mL)} = \frac{\text{Weight of tube containing algae cell (mg)} - \text{Weight of tube (mg)}}{\text{Volume of sample (mL)}} \dots\dots\dots 3.2$$

This was used together with the calibration curve of the correlation of their corresponding absorbance at 680 nm using a UV/Vis spectrophotometer (Biochrom Libra S12, 7315, UK).

3.7.6.2 Pressure measurement

A high precision differential pressure gauge (Kane 3500, UK) was used to measure the pressure gradient in this study at different heights in the column, between 45 cm and 250 cm. It was connected to a PE pipe with an inner diameter of 5mm. The pressure was measured by inserting a pressure measuring tube into the channel connections on the column at a height of 45 cm to 250 cm. Three replication of continuous flotation tests were performed for each experiment to get reproducibility.

3.7.6.3 Liquid fraction measurement

The liquid fraction is an influential factor to understand the effect of foam risers on the hydrodynamics of foams as well as the efficiency of liquid drainage in columns (Wang *et al.*, 2016). As described in **Equation 3.3** (Stevenson & Li, 2014), a pressure gradient was created in a foam column when the weight of the fluid and the shear of the wall interact. Since the wall shear stress of the foam column was negligible. It was assumed that the density of the microalgae *C. vulgaris* was equivalent to that of water. For the reason, the liquid fraction profile in the foam column was evaluated using pressure measurements according to **Equation 3.4**.

$$\frac{dp}{dy} = \rho_L g \varepsilon_L + \rho_g g (1 - \varepsilon_L) - \frac{4\tau_w}{D} \approx \rho_L g \varepsilon_L \dots \dots \dots (3.3)$$

$$\varepsilon_L = \frac{1}{\rho_L g} \frac{dp}{dy} \dots \dots \dots (3.4)$$

Where p : pressure (N.m²)

g : acceleration due to gravity (m.s⁻²)

y : positive upward length (m)

τ_w : wall shear stress (N.m²)

ε_L : liquid fraction in the foam

D : diameter of the foam column (m)

ρ_L : liquid densities (kg.m⁻³)

ρ_g : gas densities (kg.m⁻³)

3.7.6.4 Foam flow rate measurement

The term “foamate” refers to a flotation product commonly known as foam. This is obtained from a solution of CTAB and water or a microalgae culture that can be collected from the column's collector. By making the foam flotation process reach a steady state after more than 15 minutes of operation and then collecting the foam for 15 minutes. Using the gravimetric measurement method, the foamed weight was analysed to determine the flow rate using a precision analytical balance with four decimal places (A&D HF1200G, Japan). Again, a total of three replicates were performed for each continuous flotation experiment. The air flow rate in this experiment was controlled by an air flow meter to provide a flow rate of 1, 2 and 3 Lmin⁻¹, respectively.

3.7.6.5 Free CTAB measurement

In this study, the methyl orange method was used to quantify free CTAB in a sample mixture from a flotation process. Seven standard solutions of cationic surfactants (CTAB) with known concentrations (0, 50, 100, 150, 200, 250, 300 mg L⁻¹) were prepared and analysed at an absorbance of 415 nm. The absorbance data were used to create a calibration curve to convert the free CTAB concentration in the sample to mg L⁻¹. Both methyl orange and buffer solutions were prepared as described by Wang and Langley (1975). The analysis procedure included:

1. **Sample preparation:** diluting 10 ml of sample (standard or harvest water) with distilled water to 50 ml.
2. **Extraction:** adding 5 ml of buffer, 0.5 ml of methyl orange and 50 ml of chloroform, followed by vigorous shaking for 30 seconds and settling for 20 min.
3. **Measurement:** extraction of the chloroform layer, removal of water impurities and measurement of absorbance at 415 nm using a UV/Vis spectrophotometer (Biochrom Libra S12, 7315, UK).

3.7.6.6 Parameters

1. Surfactant concentration

Cetyl-trimethyl ammonium bromide (CTAB, CH₃(CH₂)₁₃N(CH₃)₃-Br) was used to provide foaming and stability in this experiment. Its concentration in tap water or microalgae cultures varied between 10 and 260 mg L⁻¹.

2. Microalgae concentration

The final concentrations of algae cells obtained by adding water to concentrated microalgae cultures were between 0.1, 0.2, 0.4 and 0.6 g L⁻¹ dry cell weight.

3. Constriction ratio

Various constriction ratios were evaluated including 0.25, 0.5, and 0.75, respectively.

4. Riser angle

Variations of riser angle at about 30°, 45°, 60° and 90°, respectively.

5. Riser length

The riser length was varied in 5, 7, 10 and 15 cm, respectively.

Chapter 4

Results and Discussion

4.1 Growth of microalgae

Several reports have investigated the impact of the duration of cultivation on the flotation process. A study by Danquah *et al.* (2009) found that microalgae harvested at low growth rates as they approach the stationary phase had reduced electrochemical properties compared to those harvested at high growth rates. As a result, intercellular interactions and cell agglomeration were improved, increasing harvesting efficiency. Coward *et al.* (2014) provides additional evidence supporting Danquah's findings, indicating that the most significant concentration factors were obtained from algae that had been harvested during the early stationary phase. Zhao *et al.*, 2022, found that decrease in algae concentration (microalgae recovery rates) after 5 min of flotation were affected by the cultivation period. Specifically, algae concentration declined to 0.23 g L⁻¹ for algae grown for 4 days, 0.22 g L⁻¹ for algae grown for 7 days, and 0.31 g L⁻¹ for algae grown for 10 days. This variation can be attributed to the higher concentration of hydrophobic algae in the 10-day cultivation period.

It is known that proteins are generally hydrophobic, so they tend to bind to the surface of air bubbles, whereas carbohydrates and polysaccharides are hydrophilic and do not have a significant impact on the flotation process (Qi *et al.*, 2022; Bertsch *et al.*, 2021). Ometto *et al.* (2014) showed that the surface activity of protein-like substances released by microalgae during the flotation process changes the characteristics of air bubbles. The proteins, when on the surface of air bubbles, become more hydrophilic, leading to increased adhesion of hydrophilic algae cells to the bubbles (Zhao *et al.*, 2022).

The growth profile of microalgae

In this work, the algal biomass production was cultured by using a starter algal cell culture around 10% obtained from a 1L stock culture was inoculated to 10 L BG-11 medium. The growth profile of *Chlorella vulgaris* was collected from three replications of the cultivation process as shown in **Figure 4.1**. The initial cell concentration was 9.0×10^5 cell mL⁻¹ at day 0. The cell growth rate rapidly increased in the first week between days 3 and 7. At day 15, the “log phase” ended, at $5.5 \times 10^7 \pm 8.2 \times 10^6$ cell mL⁻¹. The algal culture was carried out five times in succession.

It is evident from day 15 onward that there was no significant change in cell concentration, which indicates stationary phase. By the end of cultivation, it was estimated that the number of cells decreased by approximately 10% from the stationary phase due to the lack of nutrients enough in the system. These results suggest that the culture should be harvested at Day 15 of cultivation to be used as biomass to save time and cost.

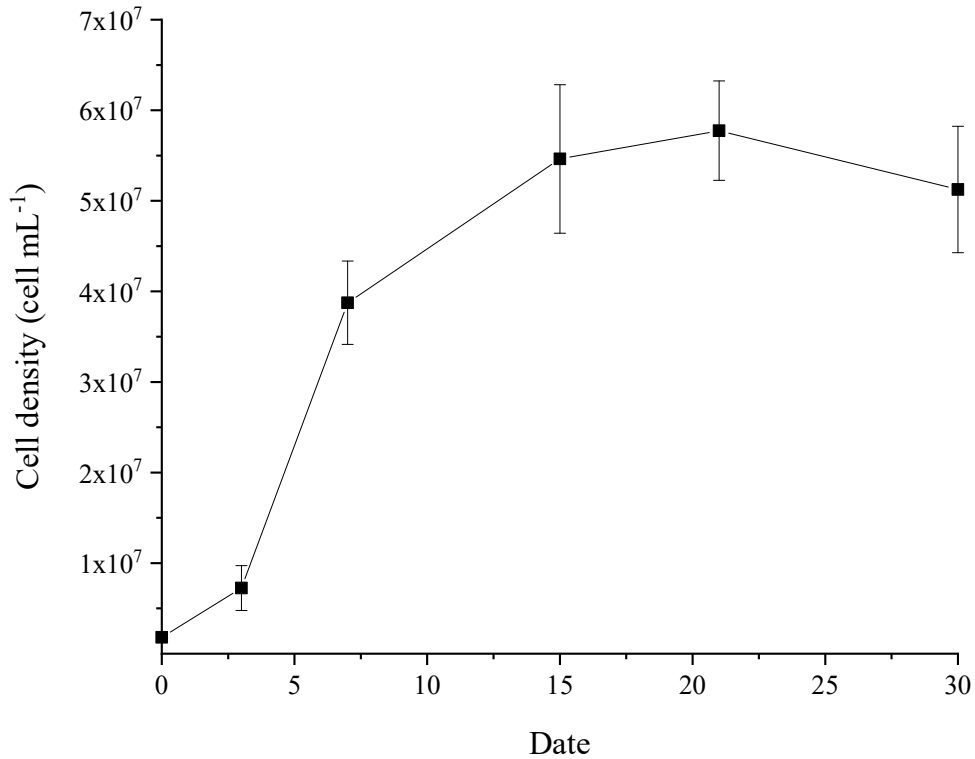


Figure 4.1: The growth profile of *Chlorella vulgaris* cultivated in BG-11 medium pH 7.1 under an autotrophic condition with 16 h of light and 8 h of dark cycles in the presence of cool white fluorescent lights with 2,500 lux of light intensity and continuous aeration for 30 days.

The microalgal culture that had been growing for 15 days was chosen due to its higher cell density compared to cultures that were less than 15 days old. However, it was observed that prolonging the cultivation period beyond 15 days did not significantly increase cell density, and the nutrient supply was exhausted. The correlation between optical density and cell concentration C_x (cells mL⁻¹), follows a linear relationship on OD 680 nm. ($R^2 = 0.99$, three replicates):

$$\text{Cell concentration } C_x(\text{cell mL}^{-1}) = 2 \times 10^7 \times OD_{680nm} - 1 \times 10^6 \dots \dots \dots (4.1)$$

4.2 Microalgal cells in foam flotation process

Figure 4.2, below, is a series of microscope images of *C. vulgaris* cells, at 40 x magnification. The microalgae here were a feed sample for the foam flotation process. In both the culture solution (A) and discharged stream (B), there was approximately 100% distribution of single cells inside each counting square. Clumps are clearly apparent in the final product (C), with a 40-50% distribution within the counting chamber, suggesting that the algae cells aggregated together. This aggregation was probably due to electrostatic interactions (Coward *et al.*, 2014) facilitated by the neutralization and hydrophobic bonding effects of CTAB (Shen *et al.*, 2018). The neutralization of the algal surface charge by CTAB would have allowed for the hydrophobic tails of the surfactant to interact with each other, causing the algae cells to aggregate and form clumps (Niecikowska *et al.*, 2011).

Figure 4.3 illustrates the physical characteristics of the sample solution as it passes through each stage of the foam column flotation process, including feed, underflow, and foamate. The characteristics were analysed under the specified operating conditions suggested in the optimized design of the previous study (Alkarawi *et al.*, 2018). These conditions were 0.1 L min⁻¹ feed flow rate, 1 L min⁻¹ air flow rate, 146 cm column height, and 25 cm liquid pool depth. Two different scenarios were evaluated: (A) 0.2 g L⁻¹ algal biomass at 150 mg L⁻¹ CTAB concentration. It is apparent that the underflow solution was clearer than the feed sample solution, whereas the final foamate product was darker green than the initial product. The absorbance supports this at 680 nm of the feed, underflow, and foamate, which were 1.75, 0.96, and 3.41, respectively. Similarly, in scenario (B), 0.4 g L⁻¹ algal biomass at 200 mg L⁻¹ CTAB concentration demonstrated absorbance values of 3.72, 1.99, and 28.3, respectively.

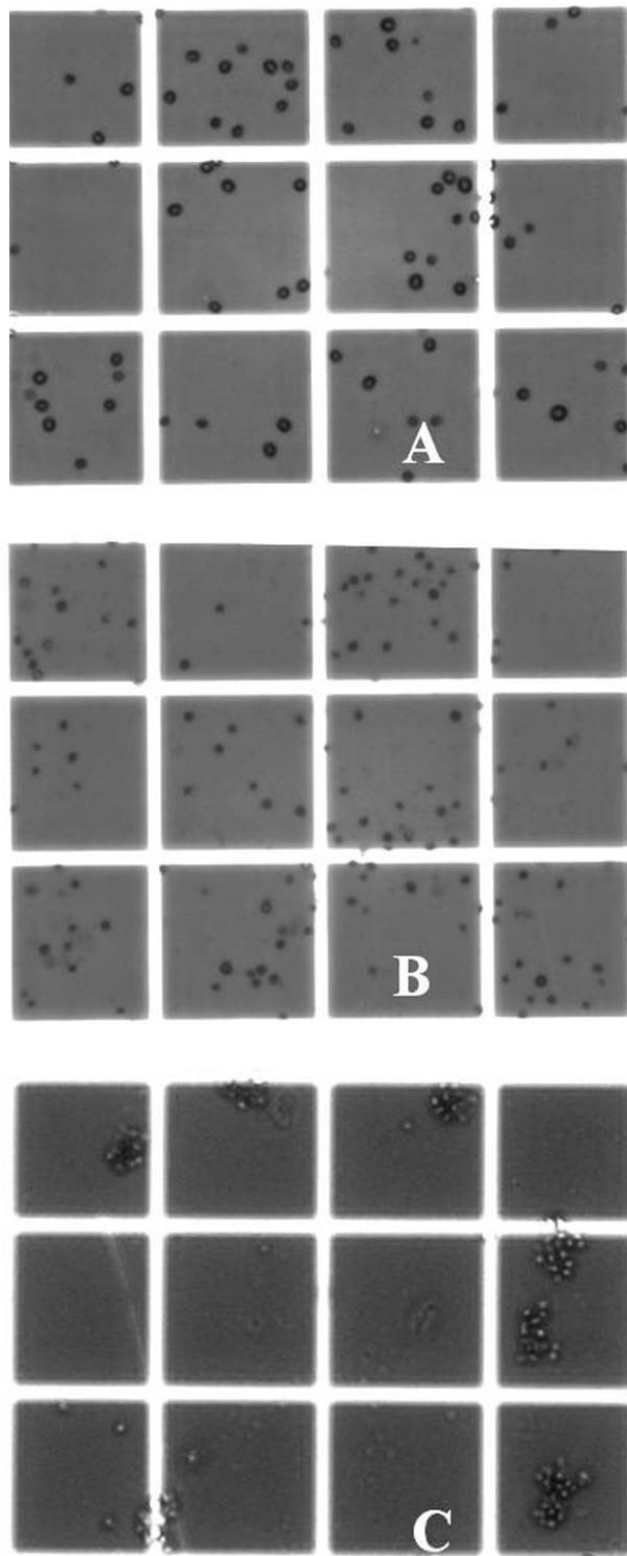


*Figure 4.2: The characteristics of *C. vulgaris* cells as observed under 40x magnification microscopes (A) Feed solution (B) discharged stream or underflow solution and (C) Final product or foamate.*

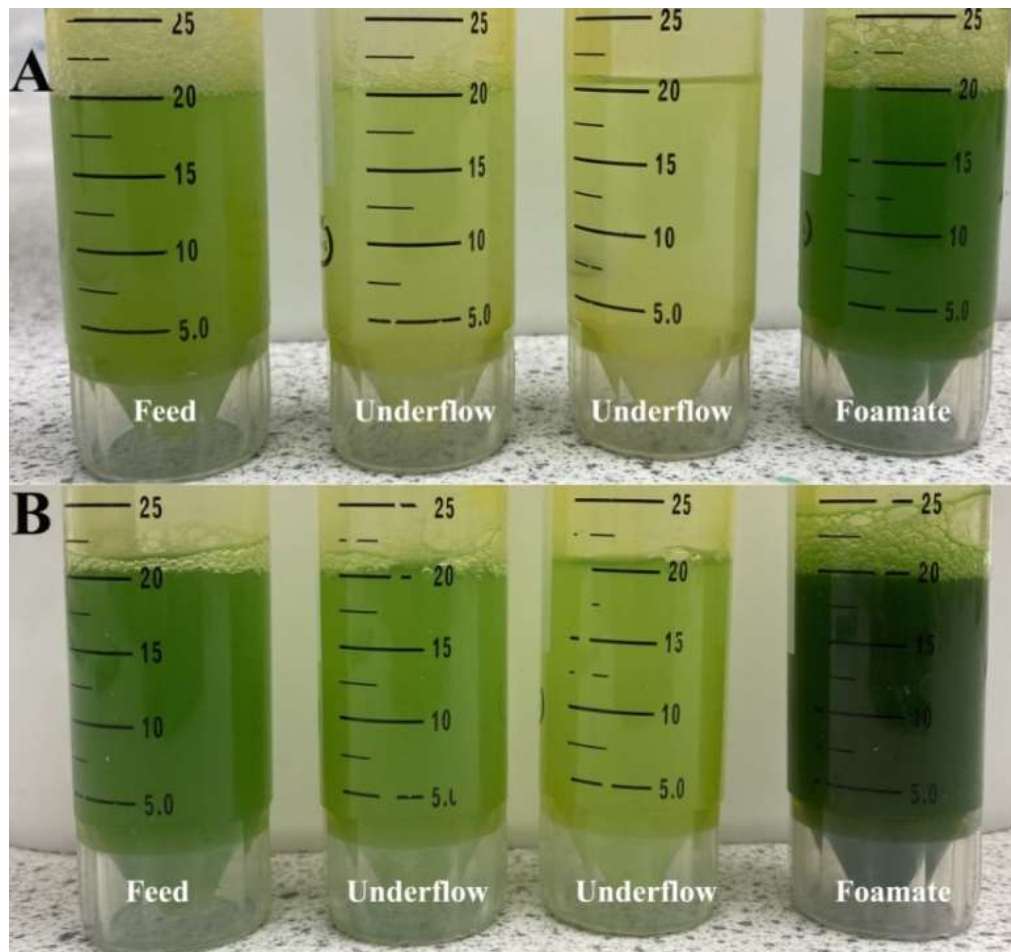


Figure 4.3: The physical characteristics of the solution in each part of the foam flotation process with (A) 0.2 g L^{-1} algal biomass at 150 mg L^{-1} of CTAB concentration and (B) 0.4 g L^{-1} algal biomass at 200 mg L^{-1} of CTAB concentration.

Data were obtained under the conditions: under the operating condition of 0.1 L min^{-1} feed flow rate, 1 L min^{-1} air flow rate, 25 cm liquid pool depth.

This outcome correlates with a higher algal biomass concentration in the final product (foamate). Clearly, microalgae surface characteristics, with hydrophobic attraction, are crucial in determining harvesting performance. Initially, algae cells adhere to hydrophobic surfaces due to their hydrophobicity (Ozkan & Berberoglu, 2013). According to Hao *et al.* (2017), adding a hydrophobic surfactant (CTAB) up to 80 mg L^{-1} can increase the hydrophobicity of hydrophilic microalgae cells by 2.37 times. This is achieved by promoting floc formation due to hydrophobic attraction between bubble-algal cells. The electrostatic interactions between them may play a role in neutralization and contribute to the clumping of the cells before transporting them to the surface for collection (Niecikowska *et al.*, 2011).

4.3 Development of an Algae/Surfactant (CTAB) “Flow Map”

Due to a cationic nature of CTAB, electrostatic interactions between CTAB and the negative cell interface facilitated the adhesion force from the CTAB to the negative surface of particles, thereby providing an improved flotation (Paria & Khilar, 2004). The results obtained was in agreement previous study (Liu *et al.*, 1999) who used a cationic surfactant that could be created electrostatic interactions between the harvested particles and gas bubbles during flotation.

4.3.1 Pressure profile

The purpose of this experiment was to determine the operating time related to the steady state of froth flotation. In order to obtain pressure profiles, different heights of the column were varied in a range of 45-245 cm under operating time at about 35 min. **Figure 4.4** below shows the pressure in the column as a function of time under the operating conditions outlined by Alkarawi *et al.* (2018): 0.1 L min^{-1} feed flow rate, 1 L min^{-1} air flow rate, 25 cm liquid pool depth and 35 mg L^{-1} of CTAB concentration). Notably, only fresh tap water and CTAB solution were used in this experiment, excluding any algal biomass from the mixture.

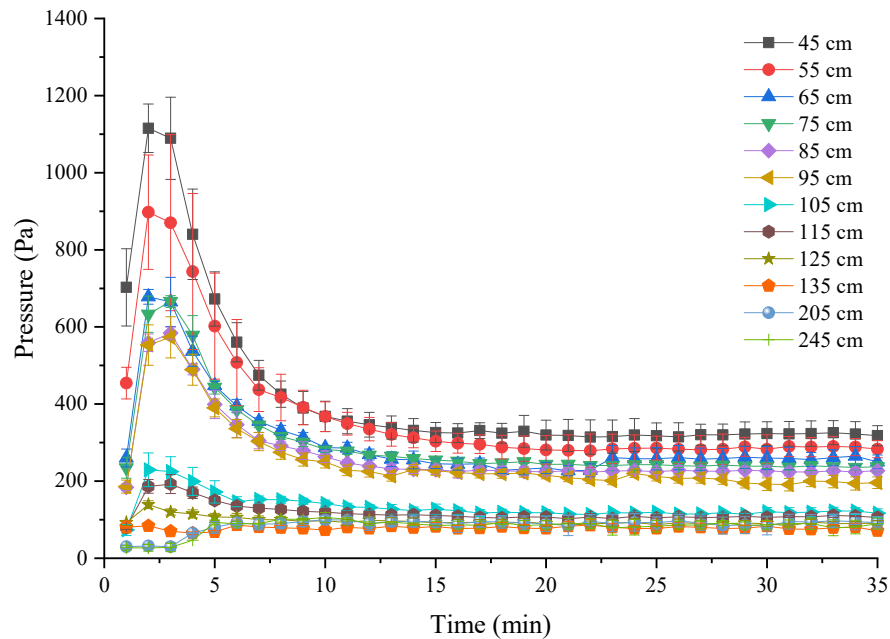


Figure 4.4: Time-dependent pressure profiles at different heights within the column. Data were obtained under the conditions: 0.1 L min^{-1} feed flow rate, 1 L min^{-1} air flow rate, 25 cm liquid pool depth and 35 mg L^{-1} CTAB concentration. Mean \pm standard deviation error.

In the initial phase, there was a rapid drop in pressure between the 3 and 7 min. From the graph, the pressure can be clearly divided into two groups, namely 45-95 cm and 105-245 cm height within the column. The data from column heights of 105 to 245 cm, suggested that a steady state was established after about 7 min. The low pressure at this time was between 120 and 70 Pa. However, it is important to note that the pressure tended to remain stable after 15 min of the process. The time required to establish a steady-state is very clear, hence samples were collected under these conditions for the froth flotation study.

Figure 4.5 shows the pressure measurements at different heights in the column after 15 minutes, of steady state under the operating conditions of 0.1 L min^{-1} feed flow rate, 1 L min^{-1} air flow rate and 25 cm liquid pool depth and 35 mg L^{-1} of CTAB concentration.

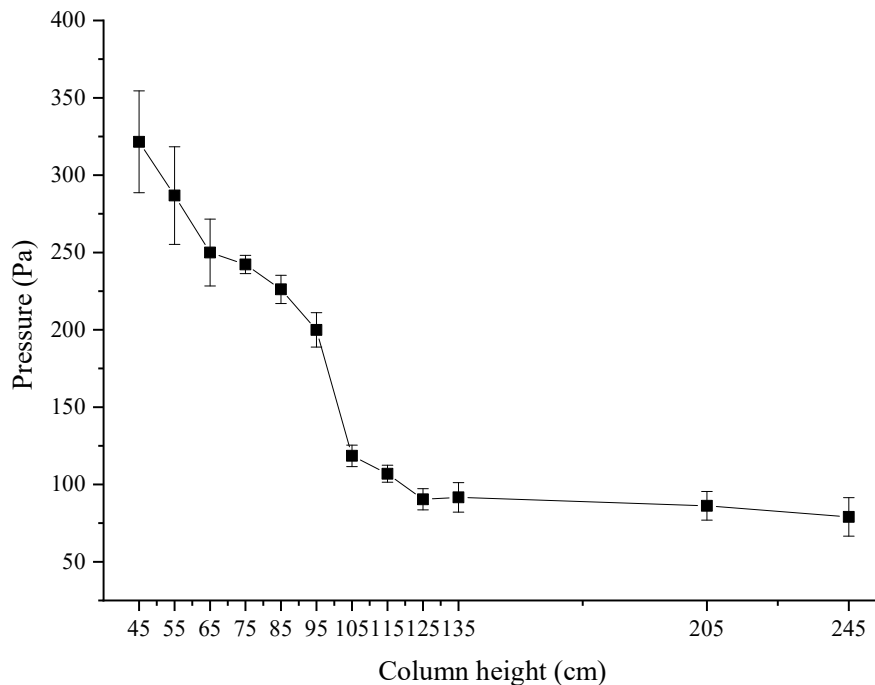


Figure 4.5: The pressure profiles at different heights in the column during steady state for 15 minutes of foam flotation process.

Data were obtained under the conditions: 0.1 L min^{-1} feed flow rate, 1 L min^{-1} air flow rate, 25 cm liquid pool depth and 35 mg L^{-1} of CTAB concentration. Mean \pm standard deviation error.

It was found that when the column height was increased by 105 cm, the pressure was significantly dropped to 120 Pa. The pressure was expected to gradually decrease in a few minutes until it reached to a height of 245 cm at 80 Pa. The observed variation of the pressure profile error bars across column height provided valuable insights into the stability of foam behaviour during the flotation process. The wider error bars observed below 75 cm and above

125 cm pointed to a less stable foam regime in these zones. This increased pressure variability indicates fluctuating foam behaviour. In contrast, the minimal error bars between 75 and 125 cm indicate a highly consistent and likely steady-state regime characterized by minimal pressure fluctuations. Therefore, minimal spreading can be interpreted as good stability in this area, indicating a well-controlled foam environment suitable for evaluating the influence of various parameters on the flotation process.

4.3.2 A correlation between algal biomass and CTAB concentrations

To determine the correlation between the concentrations of CTAB vs algae, in terms of the flow regimes produced, the experimental conditions of Alkarawi *et al.*, (2018) were followed. The operating conditions were: feed flow rate of 0.1 L min⁻¹, air flow rate of 1 L min⁻¹, liquid pool depth of 25 cm, and column height of 146 cm. CTAB concentrations ranged from 10 to 260 mgL⁻¹, and algae concentrations were adjusted to 0.1, 0.2, 0.4 and 0.6 gL⁻¹ with freshwater (tap water). The flotation process included air flow rates of 1, 2, and 3 Lmin⁻¹, corresponding to residence times of 2.3, 1.2, and 0.8 min, respectively.

Figure 4.6 presents a categorization of foam movement within the column, differentiated according to their respective foam flow rates. The experimental setup used a column with a height of 146 cm; operating under conditions of 146 cm; operated under conditions of 0.1 L min⁻¹ feed flow rate, 1 L min⁻¹ air flow rate and liquid pool depth of 25 cm.



Figure 4.6: The correlations between CTAB concentration and algal biomass as a function of foam residence time at a column height of 146 cm under operating conditions of 0.1 L min⁻¹ feed flow rate, 1 L min⁻¹ air flow rate and 25 cm liquid pool depth.

There is clearly an interplay between surfactant concentration, flow rate/residence time and microalgae concentration. The lower concentrations of algae resulted in continuous foam formation as a continuous flow without the appearance of discontinuous foam. This suggests that a microalgae biomass of 0.1 g L⁻¹ required CTAB at 100 mg L⁻¹. When the microalgae concentration increased to 0.2, 0.4 and 0.6 g L⁻¹, corresponding CTAB concentrations of 150, 200 and 250 mg L⁻¹ were required. In the absence of microalgae, a minimum CTAB concentration of 40 mg L⁻¹ was sufficient to maintain continuous foam formation in the column.

Expanding on the observations made in this study, **Figure 4.7** presents a detailed of the foam behaviour within the column during the foam flotation process. Through this analysis, four different types of foam behaviours were observed.

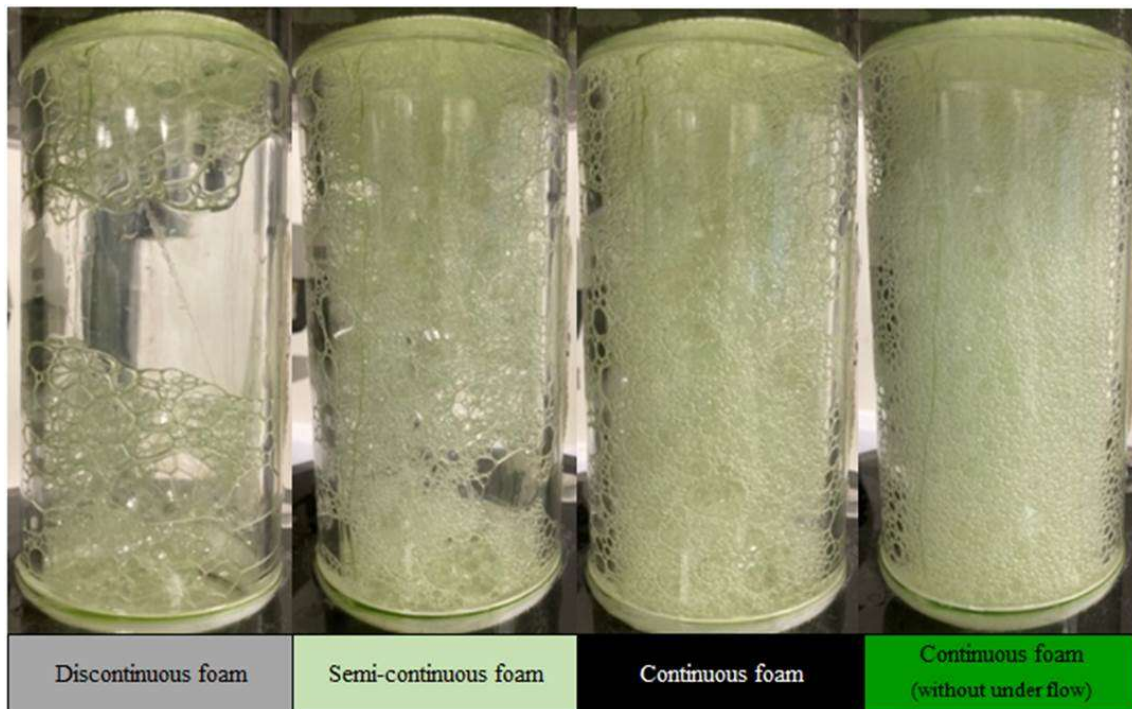


Figure 4.7: Foam behaviour in the column during the foam flotation process.

In this system, discontinuous foam occurs at a foam flow rate of $0-5 \text{ mL min}^{-1}$, semi-continuous foam occurs at $5-10 \text{ mL min}^{-1}$, and continuous foam has a foam flow rate of $10-80 \text{ mL min}^{-1}$. At foam flow rates exceeding 85 mL min^{-1} , the foam took on a continuous, fast-moving appearance and traversed the column without entraining any underflow. This behaviour suggests that the rapidly moving foam likely entrained and transported all microalgae cells and culture medium solution through the column, eventually to be collected by the collector at the top. Consequently, these conditions could not separate the algae from the culture medium.

Therefore, it is crucial to understand the conditions that lead to continuous foam movement in the column, without other forms such as discontinuous foam. Discontinuous foam could reduce the effectiveness of riser measurements and potentially affect precision in interpretation.

Based on the results of the study, it is obvious that the inclusion of algae in the flotation process requires a higher concentration of CTAB to maintain the foam in the system, as shown in **Figure 4.8**. Clearly there is a correlation between CTAB and algae concentration at an air flow rate of 1 L min^{-1} . Specifically, the graph reveals that an increased algae concentration requires an increased CTAB concentration to produce foaming in the column.

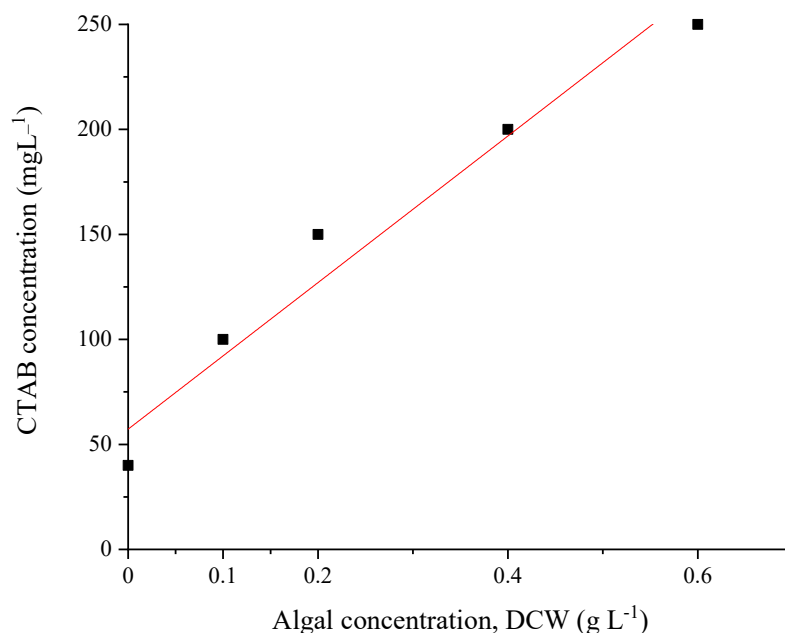


Figure 4.8: The correlation between CTAB concentration and microalgae biomass concentration under the operating conditions of 0.1 L min⁻¹ feed flow rate, 1 L min⁻¹ air flow rate, 146 cm column height and 25 cm liquid pool depth.

In summary, the study establishes a linear correlation that can be effectively used to determine the relationship between surfactant (CTAB) concentrations and algal biomass concentrations for microalgae harvesting by foam flotation.

Previously result obtained in form of linear pattern, when underflow product or discharge solution in each set was used to find a free CTAB that was remained in the system including non-adsorbed CTAB between CTAB and algal biomass. **Figure 4.9** shows an estimation of the remaining free CTAB in the underflow solution under operating conditions of 0.1 L min⁻¹ feed flow rate, 1 L min⁻¹ air flow rate and 25 cm liquid pool depth.

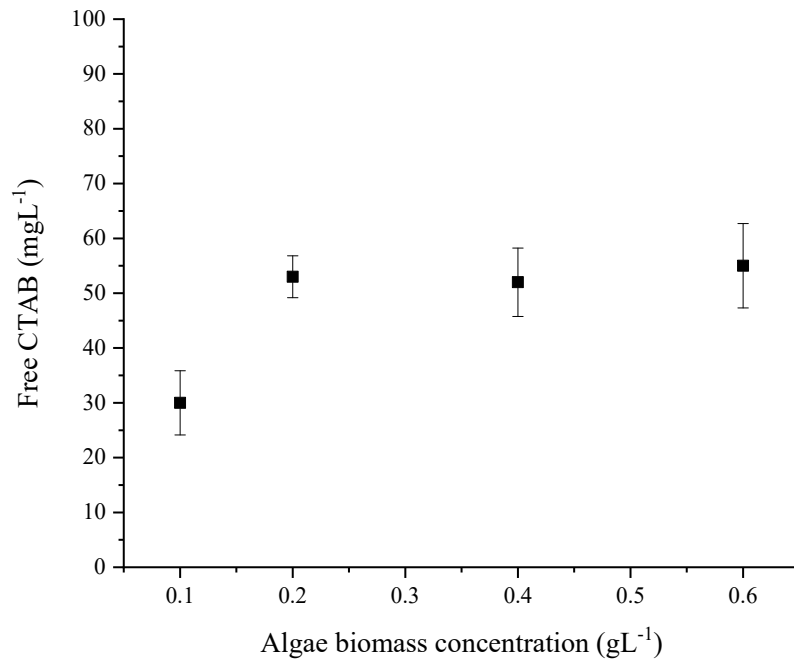


Figure 4.9: An analysis of the free CTAB profile in a feed culture solution at various algal biomass concentrations.

Data were obtained under the conditions: 0.1 Lmin⁻¹ feed flow rate, 1 L min⁻¹ air flow rate, 146 cm column height and 25 cm liquid pool depth. Mean ± standard deviation.

In the feed sample culture with 0.1 g L⁻¹ of algae biomass, the free CTAB content was 30 mg L⁻¹ at a CTAB concentration of 100 mg L⁻¹. However, using a feed sample culture with algae concentrations of 0.2, 0.4 and 0.6 gL⁻¹, the free CTAB content in the underflow solution ranged from 52 to 55 mg L⁻¹. As a result, it can be estimated that approximately 30–35% of the free CTAB content remained in the system, while around 70% was absorbed by the algal biomass.

Therefore, it is important to note that free CTAB plays a critical role in bubble formation in a foam flotation system. It facilitates the transport of air-solid particles (microalgae) to the top of the column device. Since, the remaining CTAB in the system could be bubbled in the same pattern every experiment set.

4.3.3 Efficacy of microalgae harvesting based on optimization of flotation factors

Various factors significantly influence the effectiveness of microalgae harvesting using flotation. This study focuses on optimizing two crucial parameters, residence time and column height, to enhance the overall efficiency of the process. Investigating the impacts of these parameters on microalgae recovery aims to establish a comprehensive understanding of their correlation and develop strategies to optimise flotation performance for improved microalgae harvesting.

4.3.3.1 Influence of residence time

This investigation explored the influence of residence time on the volume of the generated foam and their subsequent impact on the efficiency of the harvesting process. Five sets of Microalgae/CTAB concentrations were prepared to evaluate the effects on residence time. Each set varied in algae concentration (0, 0.1, 0.2, 0.4 and 0.6 g L⁻¹) and CTAB concentration (50, 100, 150, 200 and 250 mg L⁻¹), respectively. The CTAB concentration chosen for each algal biomass set was determined based on the experimental results presented in **Section 4.3.2**, specifically selecting the lowest concentration capable of maintaining continuous foam within the column.

Additional experimental conditions included a constant feed flow rate of 0.1 L min⁻¹ at three different air flow rates of 1, 2 and 3 L min⁻¹. These flow rates corresponded to foam residence times of 2.3, 1.2 and 0.8 min in the 146 cm height column with a liquid pool depth of 25 cm.

1) Impact on foam production

The study examined the impact of the residence time on the foam production volume generated in the flotation column at three different residence times of 2.3, 1.2 and 0.8 min in the 146 cm height column. **Figure 4.10** shows the final product volume as a function of the residence time of the foam in the column.

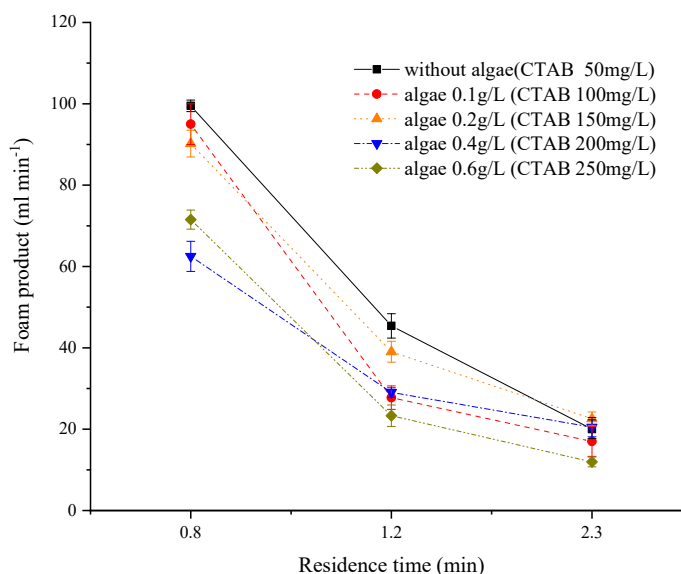


Figure 4. 10: The volume profile of foamate as a function of residence times (0.8, 1.2, and 2.3 minutes) in a column of 146 cm height with a liquid pool depth of 25 cm at different CTAB and microalgae biomass concentrations, operating under a feed flow rate of 0.1 L min^{-1} . Mean \pm standard deviation.

The total foam volume demonstrated a clear dependence on the air flow rate. Increasing the air flow rate or conversely decreasing the residence time led to a higher bubble surface area flux. This increase in surface area flux resulted in the formation of wetter foam and consequently a higher foam volume. Consequently, utilising a lower air flow rate of 1 L min^{-1} (corresponding to a residence time of 2.3 min) yielded a significantly lower foam production rate (approximately 21 mL min^{-1}) compared to higher airflow rates observed across all Microalgae/CTAB concentration samples.

The observed increase in foam volume with increasing airflow rate was consistent with established literature. Alhattab and Brooks (2017) reported that higher flow rates promote bubble formation and subsequently reducing residence times in the column, leading to wetter foams and increased final volume. Further supporting these findings, Swamy *et al.* (2010) observed that increasing gas flow rate impacts both bubble size and flow patterns within the column. Higher flow rates not only led to the formation of numerous smaller bubbles, but also shortened their residence time. This resulted in larger amounts of liquid being carried by the foam and consequently contributing to a greater final product volume. A development of the final product volume was reported by Wang *et al.* (2018), increasing the bubble residence time in the column resulted in a reduction in final product volume due to dehydration and increase in bubble size.

2) Impact on harvesting performance

This study investigated the influence of residence time on the performance of a foam fractionation column for harvesting microalgae biomass. Four different sets of microalgae/CTAB concentrations were utilized. **Figure 4.11** presents the observed effects on the concentration factor and the recovery efficiency for these algal sets as residence time varied.

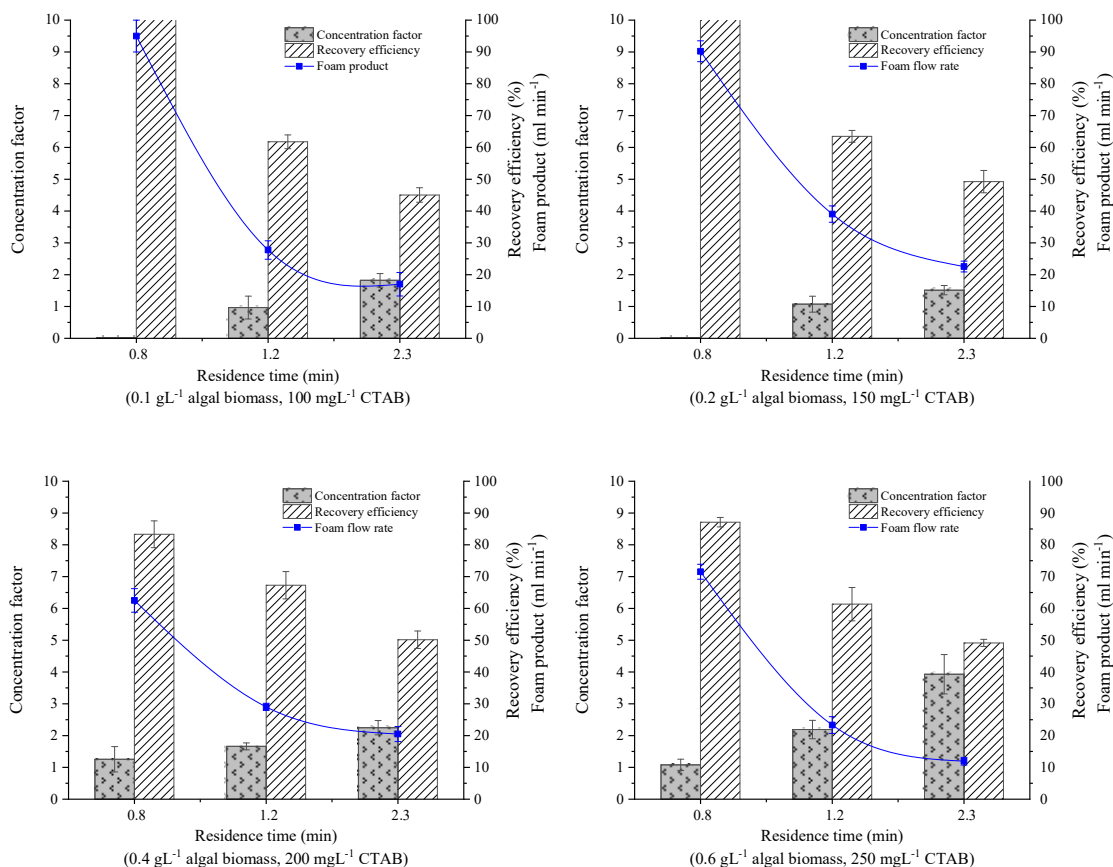


Figure 4. 11: The harvesting performance profile as a function of residence times (0.8, 1.2, and 2.3 minutes) in a column of 146 cm height with a liquid pool depth of 25 cm at different CTAB and microalgae biomass concentrations, operated at a feed flow rate of 0.1 L min⁻¹. Mean ± standard deviation.

Overall, it can be seen that production rates increased with increasing air flow, resulting in higher amounts of foam. The highest recovery efficiency of over 80% occurred when an air flow rate of 3 L min⁻¹ was used compared to 65% and 50% at 2 L min⁻¹ and 1 L min⁻¹, respectively. According to the results, algae harvesting at the lowest air flow rate of 1 L min⁻¹ (corresponding to a bubble residence time of 2.3 min in the column of 146 cm height) is more effective in terms of concentration factor than with 2 L min⁻¹ and 3 L min⁻¹ in all Microalgae/CTAB concentration

sample sets. As expected, the lowest concentration factor was found at an air flow rate of 3 L min^{-1} because the total volume of the final product (foamate) increased with increasing air flow rate. Furthermore, no underflow product with culture medium was observed at a high air flow rate of 3 L min^{-1} and microalgae biomass concentrations of 0.1 and 0.2 g L^{-1} . This phenomenon is due to the formation of excessively small bubbles due to their increased surface area. Therefore, these bubbles could have efficiently adsorbed on all microalgae cells with high water content in the column. The foam formation likely transported both microalgae and culture medium upwards, resulting in no medium left in the underflow. Therefore, efficient separation of the microalgae cells from the culture medium could not be achieved under these conditions.

4.3.3.2 Influence of column height

The study of foam flotation over different column heights (145, 170, 195, 220 and 245 cm) was carried out to evaluate its performance in foam flotation with algal biomass at a concentration of 0.1 g L^{-1} . **Figure 4.12** shows the performance profile of foam flotation as a function of column heights. The experiment was performed at a feed flow rate of 0.1 L min^{-1} , an air flow rate of 1 L min^{-1} , and a 25 cm liquid pool depth.

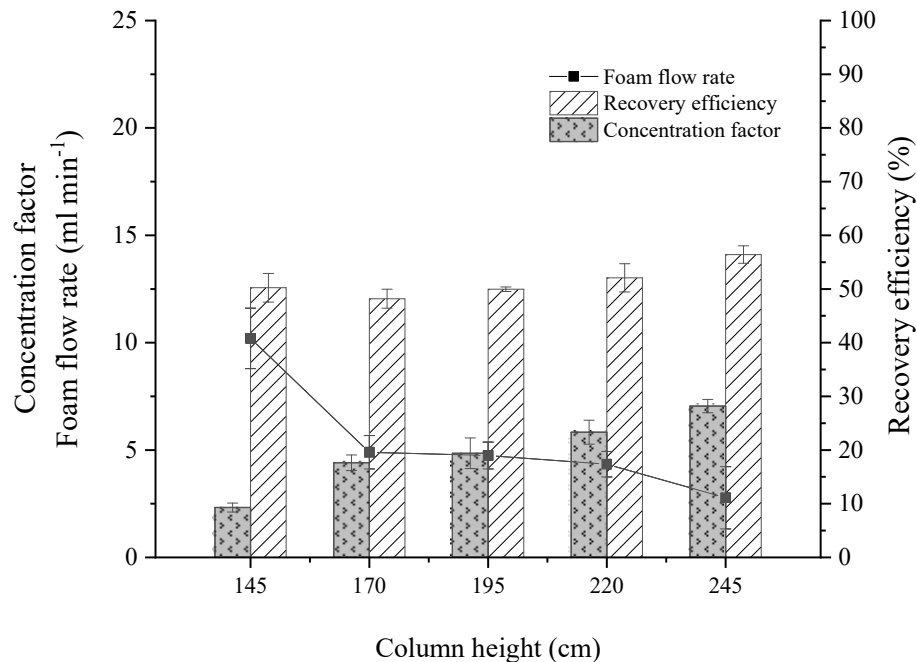


Figure 4. 12: Pressure and liquid fraction profiles of the foam at different heights within the column as a function of various constriction ratios (0.25, 0.50, and 0.75) of the foam riser.

Data were obtained under the conditions: 35 mg L^{-1} CTAB concentration, air flow rate of 1 L min^{-1} , feed flow rate of 0.1 L min^{-1} , column height of 146 cm, and liquid pool depth of 25 cm.

These results are consistent with the experimental results presented in **Section 4.3.2** concerning foam flow rate (**Figure 4.6**). A continuous foam flow was only observed at a column height of 145 cm, corresponding to a foam flow rate of 10 mL min⁻¹. On the other hand, at heights exceeding 145 cm, the final product flow rate dropped below 10 mL min⁻¹, resulting in discontinuous foam flow within the column. This phenomenon is due to the decreasing pressure with the increasing height of the column, which destabilises the movement of the foam.

An increase in the column height corresponded to an increase in the concentration factor (CF) due to the discontinuous flow, allowing for more residence time in the column and resulting in more dried foam. Interestingly, the recovery efficiency (RE) remained relatively constant at around 50-55% across all column heights. This observation suggests that a column height exceeding 145 cm may not be necessary to achieve optimal RE improvement while allowing continuous foam flow within the device. Therefore, balancing the requirements for a continuous foam flow to minimise the device footprint suggests that a column height of 145 cm could represent an optimal compromise for developing a compact and efficient flotation device.

This experiment was consistent with previous studies by Merz *et al.* (2011), who found that increasing air flow rates resulted in a reduction in the concentration factor and an increase in recovery. The maximum concentration factor (28.6) achieved at low gas flow rates is 20 m L min⁻¹. Correspondingly, in the study by Alkarawi *et al.* (2018), increasing air flow rates led to higher bubble surface area, resulting in wetter foam and a reduced concentration factor. Further supporting these results, Swamy *et al.* (2010), the formation of smaller bubble sizes observed even at higher flow rates slowed down the dewatering process and contributed to the reduction of the concentration factor due to the more significant liquid volumes transported by the foam. Furthermore, reducing gas flow rates resulted in longer bubble residence time to facilitate improved adsorption.

The findings of this study suggest that while increasing air flow rate led to higher recovery efficiency, it also resulted in a lower concentration factor. Consequently, a comprehensive understanding of the interdependence between these factors is crucial to achieving optimal harvest with both high concentration factors and recovery efficiency. This could be facilitated by systematic experimentation with varying column geometry designs and optimizing process parameters.

4.4 Foam riser design and evaluation

Foam riser models were created with diameter ratios of 0.25, 0.5 and 0.75 along with a wide range of riser angles (30°, 45°, 60° and 90°) and lengths (5, 10, 15 cm and a disc-shaped model with a height of 0.2 cm). These designs were drafted in Google SketchUp Make and subsequently fabricated using a uPrint SE Plus Desktop 3D printer using thermoplastic acrylonitrile butadiene styrene (ABS) as the building material. The influence of foam riser design on harvesting efficiency was investigated using the freshwater microalgae *Chlorella vulgaris*.

4.4.1 Effect of constriction ratio

Typically, liquid holdup is the proportion of liquid present in the foam per unit volume, which affects foam drainage results. In this experiment, the pressure profile was used to determine the total liquid fraction of the foam in the column by measuring the foam pressure at the side of the column using CTAB as a foaming agent. **Figure 4.13** shows the pressure profiles (top) and liquid fraction profiles (bottom) at different constriction ratios of the foam riser over the tubular part of the column under the operating condition of 0.1 L min⁻¹ feed flow rate, 1 L min⁻¹ air flow rate, 35 mg L⁻¹ CTAB with 146 cm column height.

The study found that increasing column height resulted in a reduction in both pressure and liquid holding profiles. Notably, the results at the highest pressure, corresponding to a constriction ratio of 0.25, exhibited the most favourable outcome. The liquid content at the bottom of the column was consistently higher than at the top due to the drying of the foam during its upward movement. Similarly, the liquid content at the bottom was higher with the riser than with constriction ratios of 0.5, 0.75 and without the riser. This finding is consistent with Alkarawi *et al.* (2018), who suggested that higher pressure in columns with risers can improve liquid drainage due to increased foam water content. Furthermore, the wet foam generated during the initial pneumatic transients, as Shaw *et al.* (2011) reported, probably contributed to improved fluid drainage.

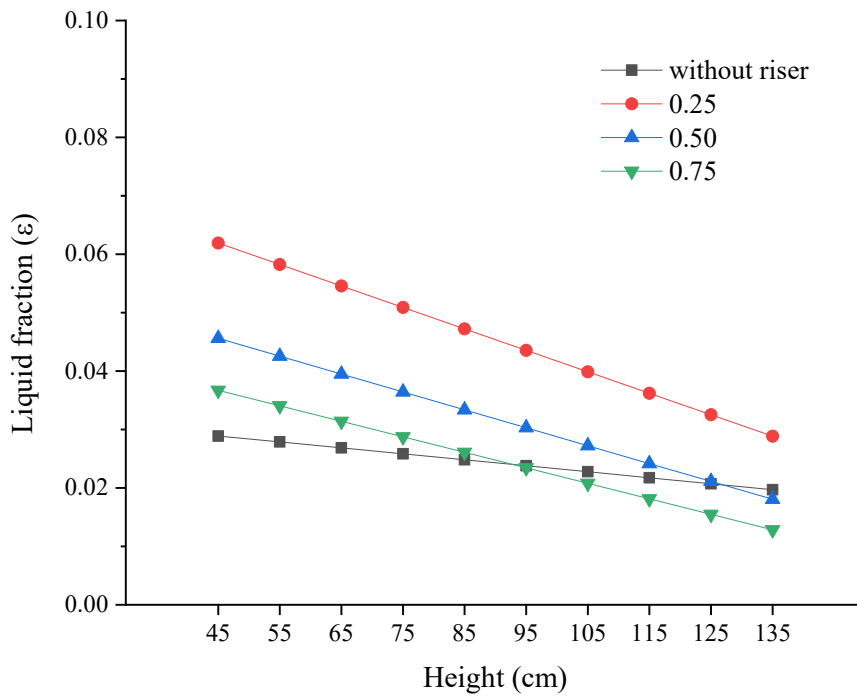
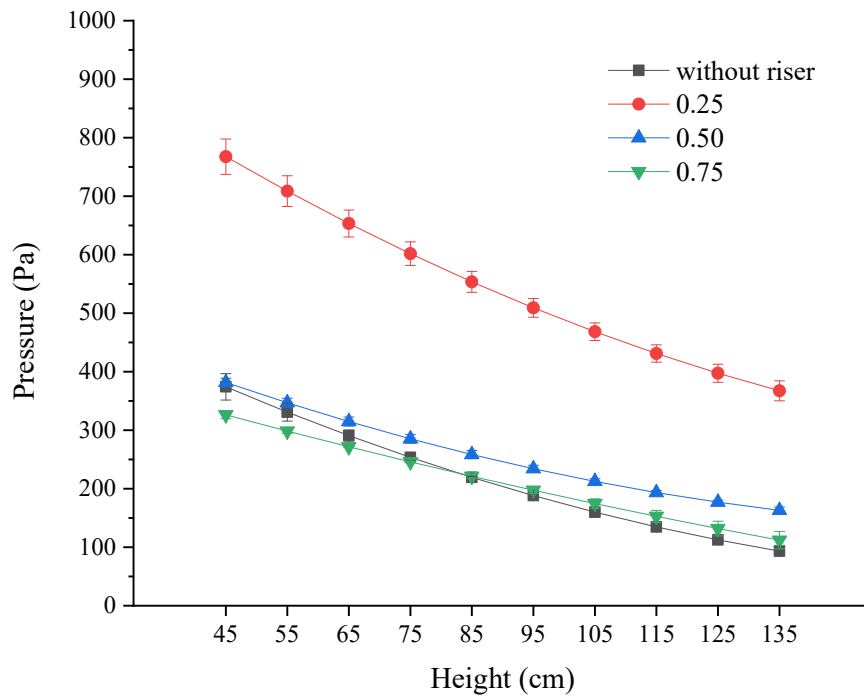


Figure 4. 13: Pressure and liquid fraction profiles of the foam at different heights within the column as a function of various constriction ratios (0.25, 0.50, and 0.75) of the foam riser. Data were obtained under the conditions: 35 mg L⁻¹ CTAB concentration, air flow rate of 1 L min⁻¹, feed flow rate of 0.1 L min⁻¹, column height of 146 cm, and liquid pool depth of 25 cm.

The volume of the final products (foam), as shown in **Figure 4.14**, was determined with the variation of the constriction ratio (0.25, 0.50 and 0.75) from the top of the column under the condition of 0.1 g L^{-1} algal biomass, 100 mg L^{-1} CTAB, 1 L min^{-1} air flow rate and 0.1 L min^{-1} feed flow rate, with 146 cm column height.

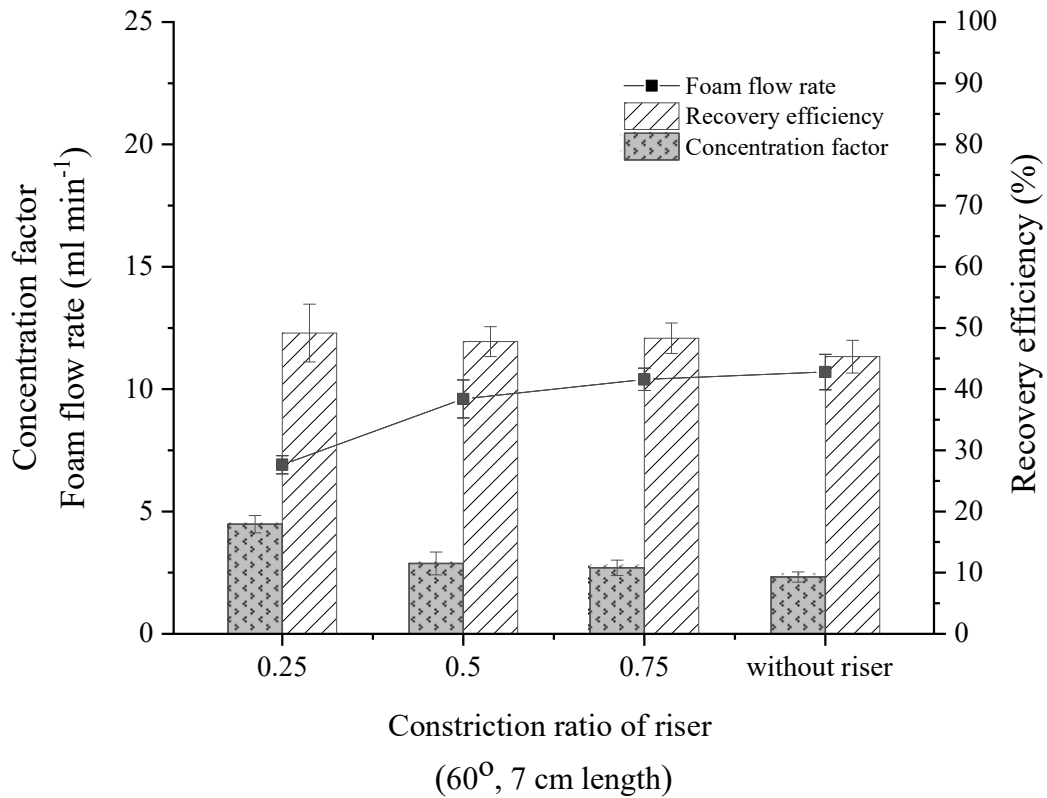


Figure 4. 14: The flotation efficiency as a function of the variations of the constriction ratios (0.25, 0.50 and 0.75) with an angle of 60° and a length of the foam riser of 7 cm.

Data were obtained under the conditions: 0.1 gL^{-1} algal biomass, 100 mgL^{-1} CTAB concentration under the condition of 1 L min^{-1} air flow rate, 0.1 L min^{-1} feed flow rate, 146 cm column height and 25 cm liquid pool depth.

This experiment was performed with a riser at 100 cm column height because the results from **Section 4.3 Foam Equilibrium (Figure 4.5)** indicate that the pressure profile is in the stability zone. Modules of the foam riser influenced the development of the total foam volume. The lowest foam volume was achieved at 6.9 ml min^{-1} when the foam riser constriction ratio of 0.25 was used. As the constriction ratios were increased to 0.50 and 0.75, the volume of the final products increased. On the other hand, it should be noted that there was no significant difference

between the concentration factors at 0.75 constriction ratios and without a riser at 10.4 and 10.7 ml min⁻¹, respectively.

During the experiments, the constriction factor decreased as the constriction ratio of the foam risers was increased from 0.25 to 0.75. The highest concentration factor was found with a restriction ratio of 0.25. As a result, the concentration factor in this study was approximately 95.6% higher than without the riser, resulting in a concentration factor of 4.5. Furthermore, the average concentration factors of 0.5 and 0.75 constriction ratios were 2.9 and 2.7, respectively, compared to 2.3 without risers. Higher volumes of final product with low cell concentration (due to the wetter foam) resulted in lower concentration factors. Nevertheless, it provides an approximate recovery efficiency of $48 \pm 3\%$ for all foam riser modules at an air flow of 1L min⁻¹.

From the results, it can be seen that the constriction ratio affected the microalgae concentration factor. The lower diameter ratio resulted in a reduction in foam water content as foam flowed through the riser, resulting in a lower volume in the final product. The small volume in the final product with a constriction ratio of 0.25, which has a high cell concentration, represented the highest concentration factor.

Therefore, the constriction ratio of 0.25 is more effective in algae separation than 0.50 and 0.75. The previous studies, Alkarawi *et al.* (2018) found that the liquid fraction and bubble size in the foam increased as the surface gas and liquid velocities increased as the foam flowed through the riser. Using the constriction ratio of 0.25 gave the highest concentration factor (752) at an air flow rate of 1 l.min⁻¹, while it decreased to 533 and 374 using the constriction ratios of 0.5 and 0.75.

4.4.2 Effect of angle

This experiment was conducted to investigate how different angles of the foam risers in a column would affect the flotation process.

The effect of the foam riser, as shown in **Figure 4.15**, was determined using the different angles of the riser (30°, 45°, 60° and 90°) with a constriction ratio of the foam riser of 0.25 at 5, 10 and 15 cm riser length and a placement at 100 cm of the 146 cm column height under the condition of 0.2 gL⁻¹ algal biomass, 150 mgL⁻¹ CTAB, 1 L min⁻¹ air flow rate and 0.1 L min⁻¹ feed flow rate.

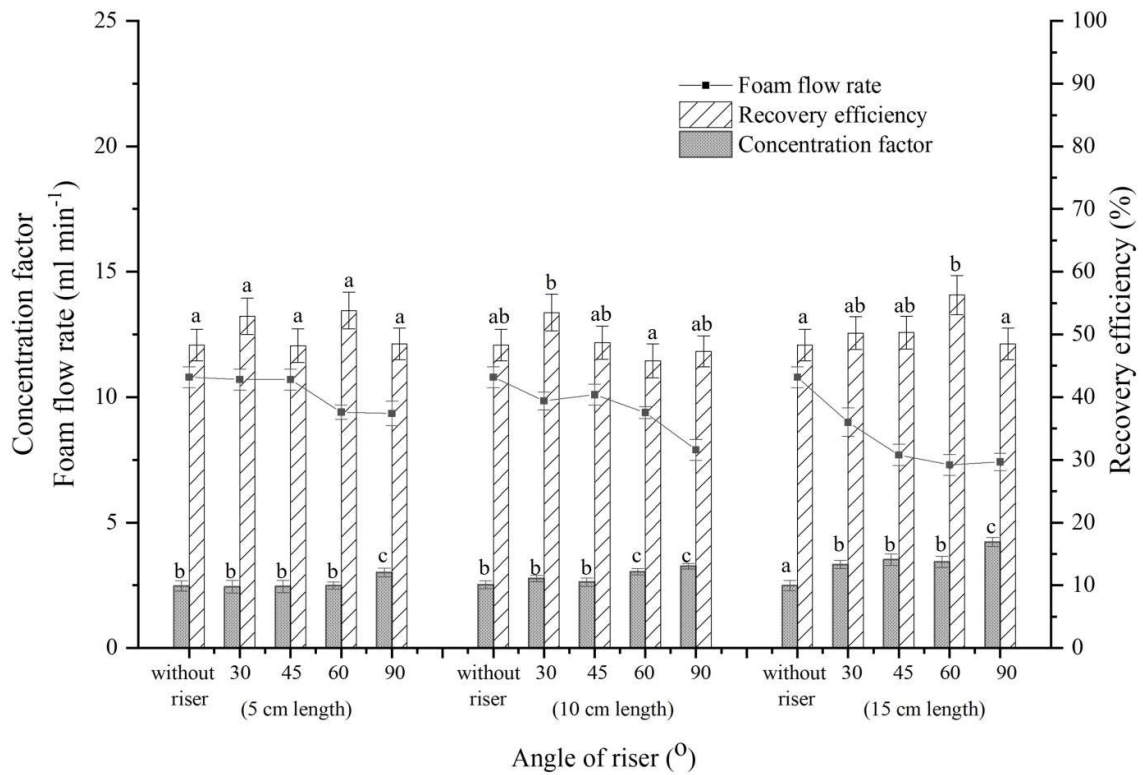


Figure 4. 15: The flotation efficiency profile as a function of the variation of the riser angle (30°, 45°, 60° and 90°) with 5, 10 and 15 cm riser length.

(Means within the same column followed by different letters are significantly different ($P \leq 0.05$)).

Data were obtained under the conditions: 0.2 g L⁻¹ algal biomass, 150 mg L⁻¹ CTAB, 1 L min⁻¹ air flow rate and 0.1 L min⁻¹ feed flow rate and 25 cm liquid pool depth. Mean \pm standard deviation.

No significant differences were observed between the concentration factor and the recovery efficiency (approximately $51 \pm 3\%$) at all angles. Nevertheless, the concentration factor at an angle of 90 was slightly higher and the final product flow rate was lower than the other modules with riser angles (2.9, 3.3 and 4.3 for 5 cm, 10 cm and 15 cm length, respectively).

As a result, it was obvious that the effect of the foam rise angle on the column was negligible. To achieve flotation, it is recommended to choose a foam riser in the column with a constriction ratio of 0.25 and an angle of 90 degrees due to its simplicity and ease of use.

4.4.3 Effect of riser length

As shown previously in **Figure 4.15**, the concentration factor of a 90 degrees angle with a constriction ratio of 0.25 was slightly higher than that of other riser angle modules. A study was conducted to determine how the length of the riser, including flat risers, 5, 7, 10 and 15 cm, affects the flotation process.

Two different feed cultures with an algae biomass concentration of 0.2 g L^{-1} and 0.4 g L^{-1} in 150 mg L^{-1} and 200 mg L^{-1} CTAB concentrations, respectively, were examined at a column height of 146 cm with an air flow rate of 1 L min^{-1} and feed flow rates of 0.1 L min^{-1} . **Figure 4.16 (A)** shows the separation profile for algal biomass at 0.2 g L^{-1} in 150 mg L^{-1} CTAB and **Figure 4.16 (B)** represents 0.4 g L^{-1} in 200 mg L^{-1} CTAB.

The efficiency of algal biomass removal appears to increase with the length of the riser up to 15 cm. It was found that the concentration factor was doubled compared to algae separation without a riser. However, it was found that the recovery efficiency was not significantly different at about $49 \pm 1.5\%$.

In summary, this study confirmed that foam risers increase flotation efficiency and thereby improve algae removal. In order to effectively and efficiently support the algae in harvesting from the culture medium, these can specify that such a riser should consist of a constriction ratio of 0.25, a 90 degree angle and a length of about 10-15 cm.

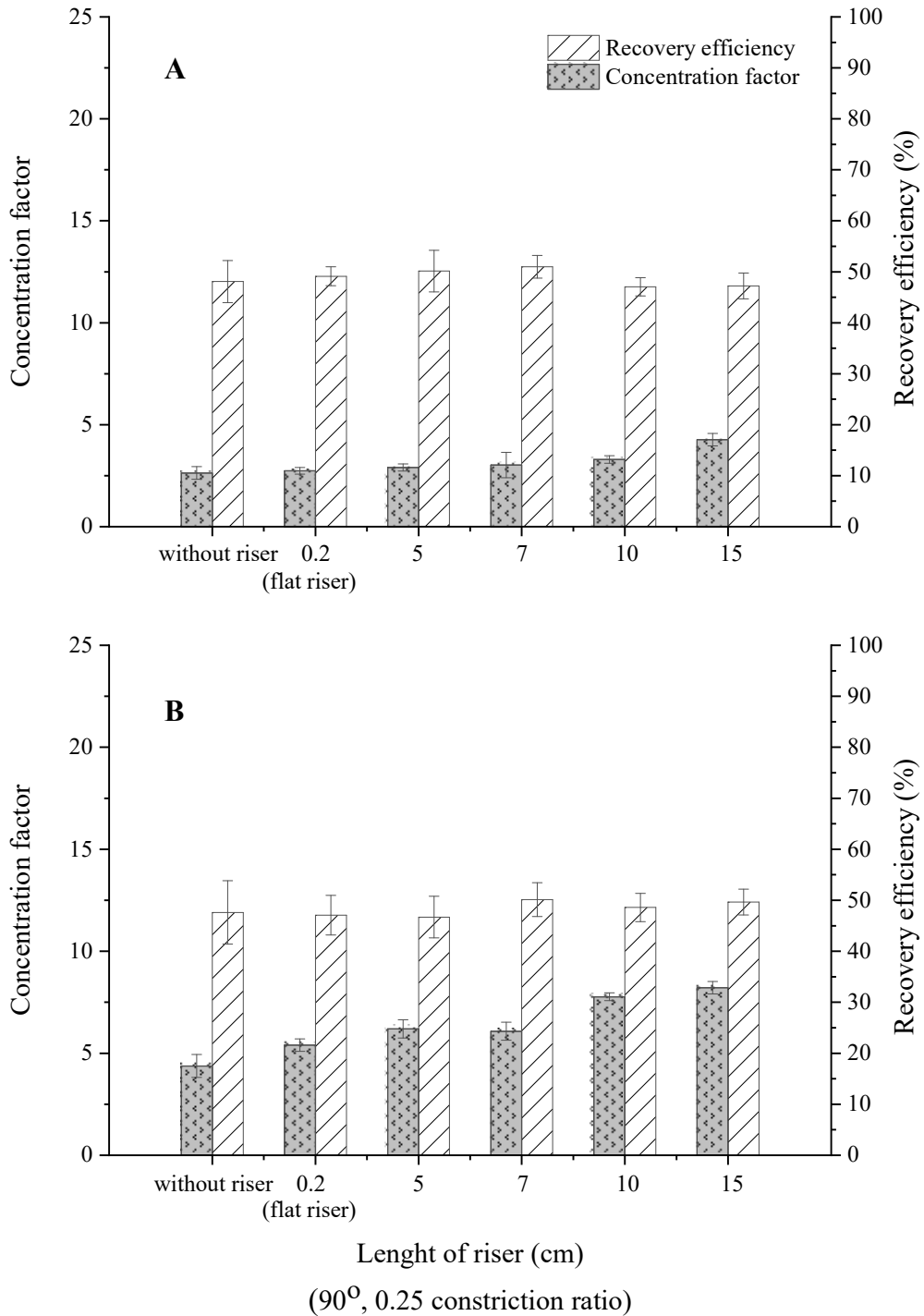


Figure 4. 16: The flotation efficiency profile as a function of variation of riser lengths (5, 7, 10, 15 cm and flat riser) between (A) 0.2 gL⁻¹ algal biomass and 150 mgL⁻¹ CTAB and (B) 0.4 gL⁻¹ algal biomass, 200 mgL⁻¹ CTAB.

Data were obtained under the conditions: air flow rate of 1 L min⁻¹ and feed flow rate of 0.1 L min⁻¹ and liquid pool depth of 25 cm with an angle of 90° and a constriction ratio of 0.25. Mean ± standard deviation.

4.5 Foam visualisation

4.5.1 Bubble formation and shape

The foam visualisation is used to study the formation and shape of the bubble in this work using an ultra-high molecular weight polyethylene with a thickness of 6.0 mm, a diameter of 51.5 mm and a pore size of 30 μm as an injector. This experiment was studied under the condition of an air flow rate of 1 L min^{-1} and a feed flow rate of 0.1 L min^{-1} and a liquid pool depth of 25 cm.

As shown in **Figure 4.17**, it was found that the bubble formed a symmetrical pattern on both sides in the column under the riser with a specification of 0.25 constriction ratio with 90° angle and 15 cm length before flowing through the riser channel. The foam bubbles exhibited hexagonal characteristics with an angle of 120° at all three-way junctions. At a distance of at least 5 cm below the riser, the rising bubbles were found to form vertically at a 90 degree angle to the riser.

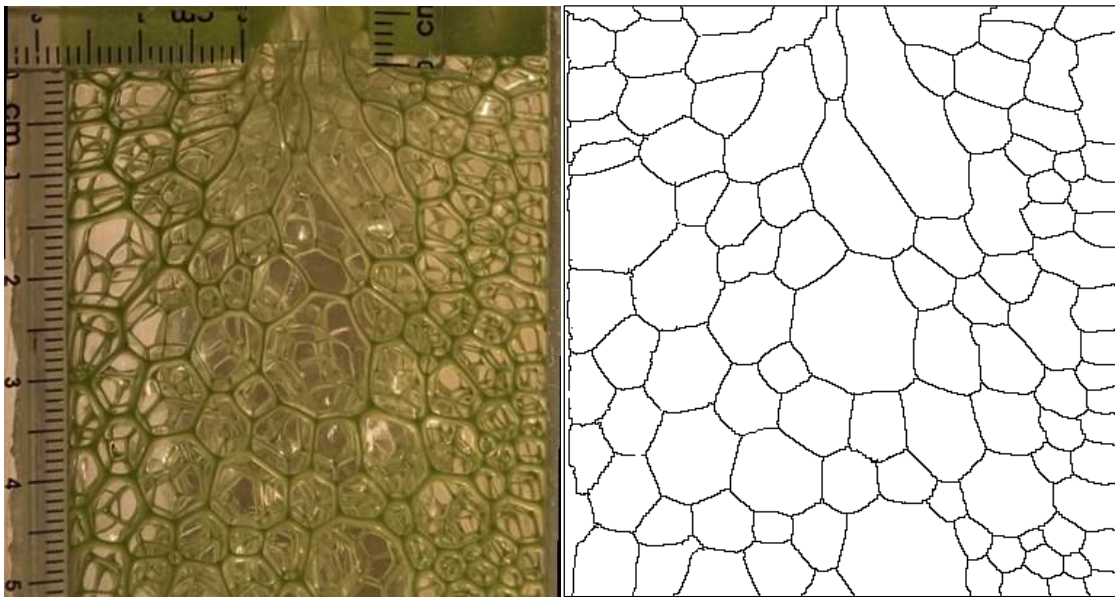


Figure 4. 17: The formation and shape of bubble appearance under the riser with a constriction ratio of 0.25, an angle of 90° and a length of 15 cm.

Data were obtained under the conditions: an air flow rate of 1 L min^{-1} and a supply flow rate of 0.1 L min^{-1} and 25 cm liquid pool depth.

As the bubble approached the riser, the angle decreased symmetrically toward the central of the column where the riser was located. The angle of the rising bubble was between 30 and 60 degrees overall over the entire 3 cm area below the riser.

The foam flow pattern transforms through the narrow channel within the riser, resulting in deformation. This phenomenon is due to the pressure gradient, velocity variations across the channel, and the influence of surface tension from the liquid film stabilising the bubbles.

Bubbles undergo deformation as they approach narrow channels or restricting risers. The foam undergoes compression as it enters the riser, the velocity is highest in the middle and the pressure is lowest, resulting in bubble coalescence and an increase in size. Khodaparast *et al.* (2018) studied the de-wetting process in micro channels, in which thin liquid films surround air bubbles. They showed that rupture occurs at specific locations within the cross-sectional plane and along the bubble. The initial rupture sites around the channel perimeter are between the channel corners and the centrelines of the walls because these areas have the thinnest liquid films.

From these observations, it is clear that the foam can spontaneously form angles before entering the riser channel. Based on these and other results, it is clear that the angles formed by the rising bubbles are independent of the angle of the riser. This is evidence that varying the rise angle does not affect the performance of the froth flotation process. There are therefore no different results for different riser angles, as described in **Part 4.4**, influence of the foam riser.

4.5.2 Bubbles size

In this study, a high-speed camera (Photron FASTCAM SA3, USA) with a Nikon AF Nikkor 24-85 mm lens was used to investigate foam drainage behaviour during dewatering experiments in the presence of a riser pipe. The riser had a constriction ratio of 0.25, an angle of 90° and a length of 15 cm. The operating conditions were 1 L min^{-1} air flow rate, 0.1 L min^{-1} feed flow rate and 25 cm liquid pool depth. The bubble sparger was made of an ultra-high molecular weight polyethylene with a thickness of 6.0 mm, a diameter of 51.5 mm and a pore size of $30 \mu\text{m}$. The riser was intended to improve the understanding of foam drainage behaviour during continuous foam flotation. Notably, the data also included observations of foam behaviour as a function of foam riser, including bubble size, velocity and shape. A typical bubble size distribution is shown in **Figure 4.18**.

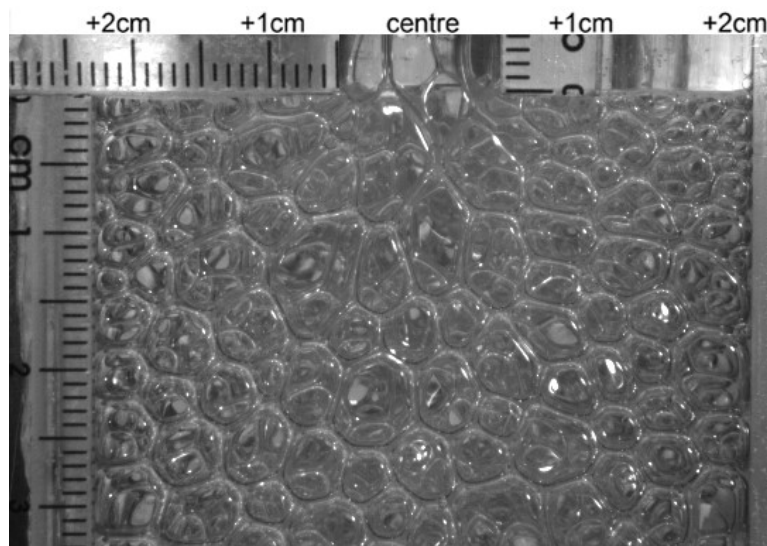


Figure 4. 18: Photo of the foam bubble under the riser with a constriction ratio of 0.25, an angle of 90° and a length of 15 cm

Data were obtained under the conditions: an air flow rate of 1 L min^{-1} , a feed flow rate of 0.1 L min^{-1} and a liquid pool depth of 25 cm.

Foam bubble images were captured and measured so that the following conclusions could be drawn:

1. The bubble at the centre of the column situated beneath the narrow channel of the constriction riser was the largest at a mean length of 10.3 mm. The length-to-diameter ratio of this bubble was the largest observed. Generally, the ratio increased with proximity to the centreline and to the constriction.
2. The average bubble size at 10 mm from the centre of the column was 4.8-5.3 mm whereas at 20 mm away (nearer the walls), the bubble size was smaller, at 3.1-3.5 mm on average. Clearly the bubble size increased toward the centre.
3. There was a symmetrical bubble size distribution across the column.

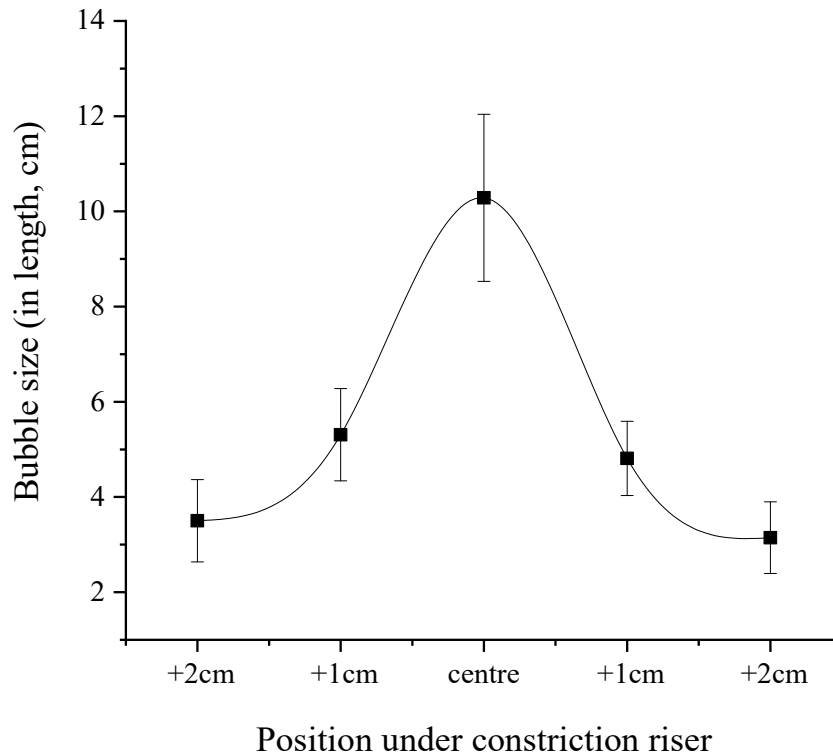


Figure 4. 19: Bubble size profile under the riser with a constriction ratio of 0.25, an angle of 90° and a length of 15 cm.

Data were obtained under the conditions: under the condition of an air flow rate of 1 L min^{-1} , a feed flow rate of 0.1 L min^{-1} and a liquid pool depth of 25 cm.

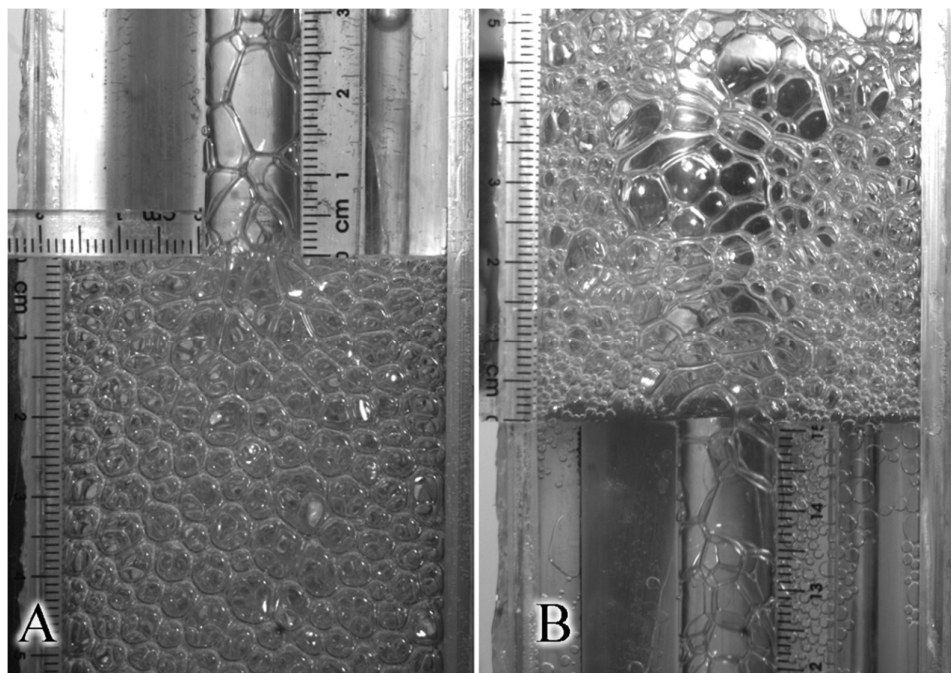
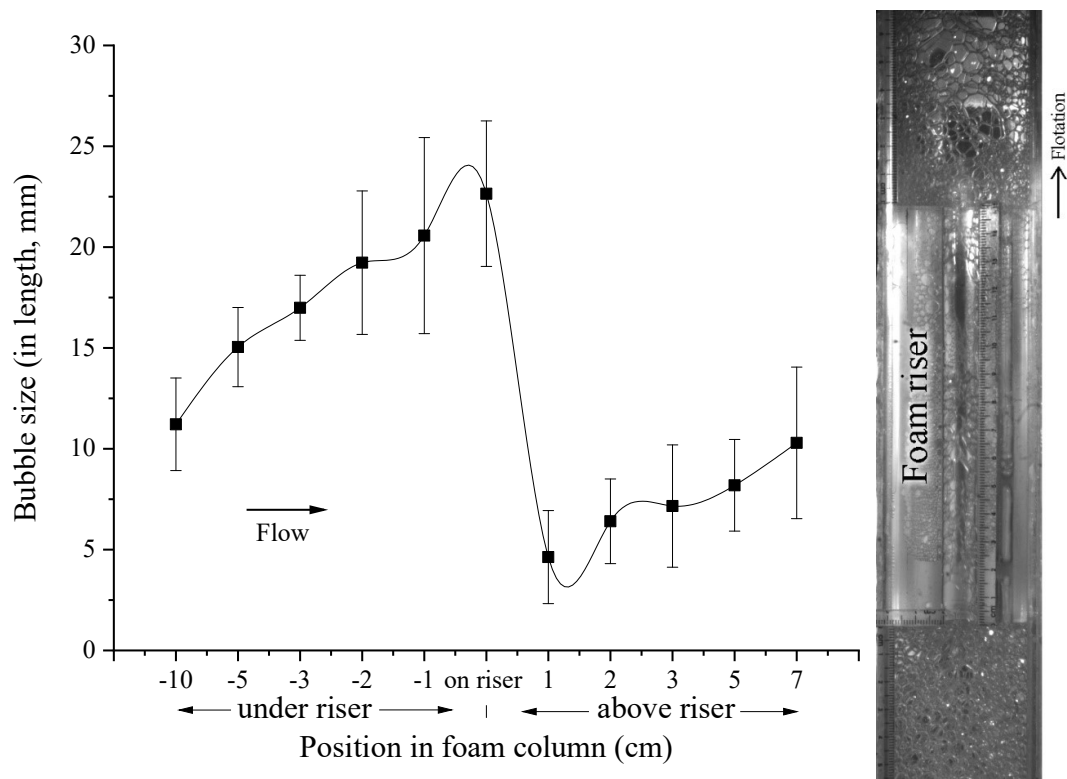


Figure 4. 20: Bubble size profile and the appearances, (A) before and (B) after passing through the riser of 0.25 constriction ratio, 90° of angle and 15 cm length.

Data were obtained under the conditions: 1 L min^{-1} air flow rate and 0.1 L min^{-1} feed flow rate and 25 cm liquid pool depth

However, **Figure 4.20 (B)** shows the bubble rearrangement over the constriction riser. As they passed through the riser, large bubbles formed ellipsoidal shapes, while smaller foams also regenerated near the side of the column. This is because the narrow channel of the riser effectively acts as an additional sparger, causing the particles above the riser to mix again and form new foam. Solarski (2019) demonstrated that the constriction could provoke foams to break, resulting in new bubbles in porous media, which reduces the bubble size distribution. In addition, bubbles are less likely to get stuck in corners, therefore these smaller bubbles gradually increase in bubble size and rise toward the collector at the top of the column. During this time, microalgae are likely to detach from the bubbles. Therefore, harvesting should occur after the foam has completely passed through the riser to maximize the accumulation of microalgae biomass.

Based on these results, it is clear that the riser plays a significant role in changing bubble sizes. As bubbles move closer to the riser, their size increases. Bubbles (at the centreline at least) reach their maximum size just before entering the narrow channel of the constriction riser, and their size continues to increase until they leave.

4.5.3 Foam Velocity

This experiment was conducted using a riser with constriction ratio of 0.25, an angle of 90° and a length of 15 cm. The operating conditions were 1 L min^{-1} air flow rate, 0.1 L min^{-1} feed flow rate and 25 cm liquid pool depth. The bubble sparger was made of an ultra-high molecular weight polyethylene with a thickness of 6.0 mm, a diameter of 51.5 mm and a pore size of $30 \mu\text{m}$. **Figure 4. 21** revealed the bubble velocity profile before and after passing through the riser. It was found that the foam velocity increases significantly as the foam approaches the riser and accelerates sharply once it is in the riser. However, a rapid decrease in foam velocity was observed after flowing through the riser.

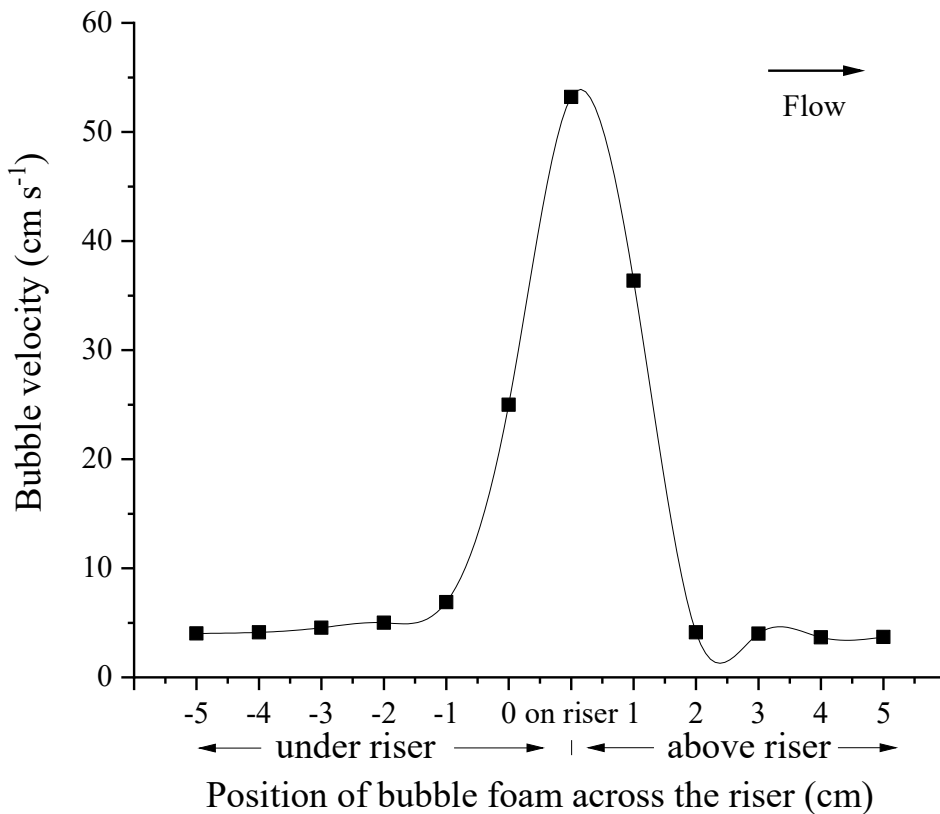


Figure 4. 21: Bubble velocity profile before and after passing through the riser with a constriction ratio of 0.25, an angle of 90° and a length of 15 cm.

Data were obtained under the conditions: an air flow rate of 1 L min^{-1} and a feed flow rate of 0.1 L min^{-1} and a liquid pool depth of 25 cm.

4.6 Process Development

In the previous **section, 4.4** it was suggested that a riser with a constriction ratio of 0.25 was the most efficient for algae harvesting. In addition, the riser length of achieved the highest concentration factor with an air flow rate of 1 Lmin^{-1} and a supply feed flow rate of 0.1 Lmin^{-1} . However, the experiments still showed that the separation efficiency was not satisfactory with 45-50 of recovery efficiency.

This clearly requires further investigation to achieve high recovery efficiency. In view of the practicality of installation for large-scale production, the principle is based on a simple design and convenient installation of the riser within the column. Therefore, this experiment investigated the effects of the 90 degree angled riser position and a multi-stage process in a column to address these concerns.

4.6.1 Riser position

In this study, a continuous flotation column was designed with different heights of riser position on the column, namely 45, 70, 95 and 120 cm. The harvest performance was evaluated when flotation reached the steady stage under the conditions of algal biomass concentration of 0.1 g L^{-1} , 100 mg L^{-1} CTAB, 1 L min^{-1} air flow rate, 0.1 L min^{-1} feed flow rate and 25 cm of the liquid pool depth. A flat riser with a 90 degree angle and a constriction ratio of 0.25 was used in this study.

The characteristics of algal cells that attached to bubbles in the column below the riser as they moved up between 50 and 90 cm above the pulp phase (solution mixing level) in the column as shown in **Figure 4.22**. The initial bubble was light green After rising, the pulp phase is formed in which the algae biomass is on the bubble, from 50 cm, and as the bubble rises, more green bubbles become visible, and a clear one at the top at a height of 100 cm of the column can see green bubble. This was due to the longer residence time of the foam, which resulted in increased liquid drainage in the bubble films.



Figure 4. 22: The characteristics of algal cells attached to bubbles in the column below the riser while rising between 50 and 90 cm above the pulp phase (mixed level solution).

Data were obtained under the conditions: 0.1 gL⁻¹ algal biomass, 100 mgL⁻¹ CTAB under the condition of 1 L min⁻¹ air flow rate and 0.1 L min⁻¹ feed flow rate and 25 cm liquid pool depth.

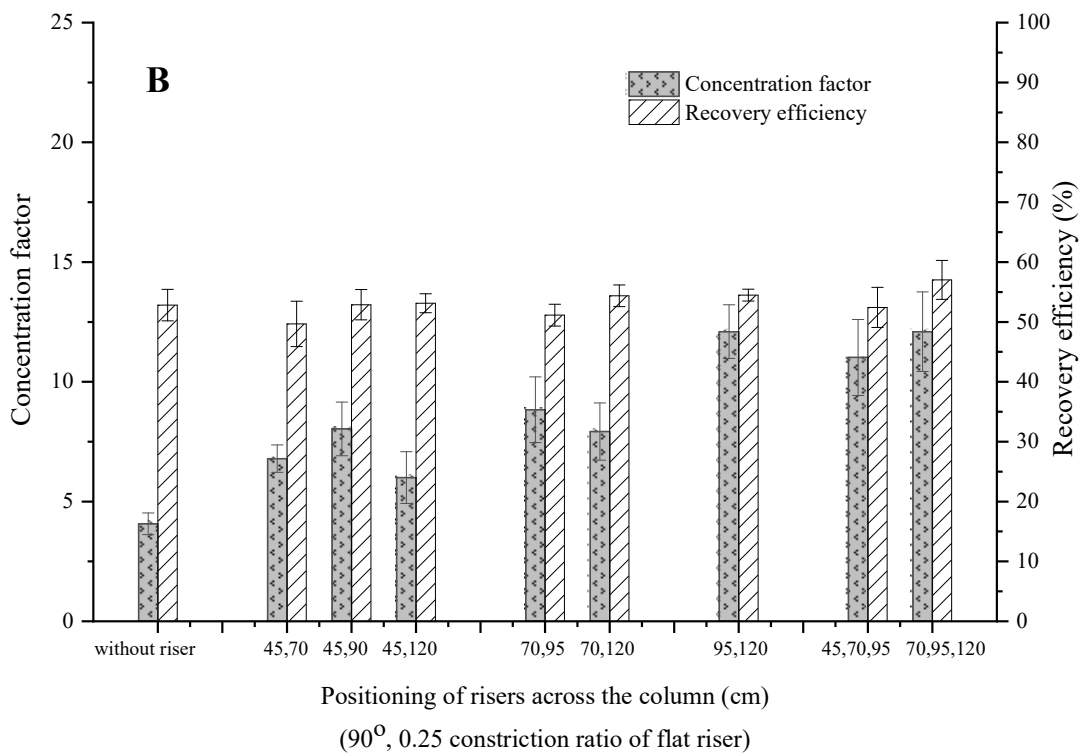
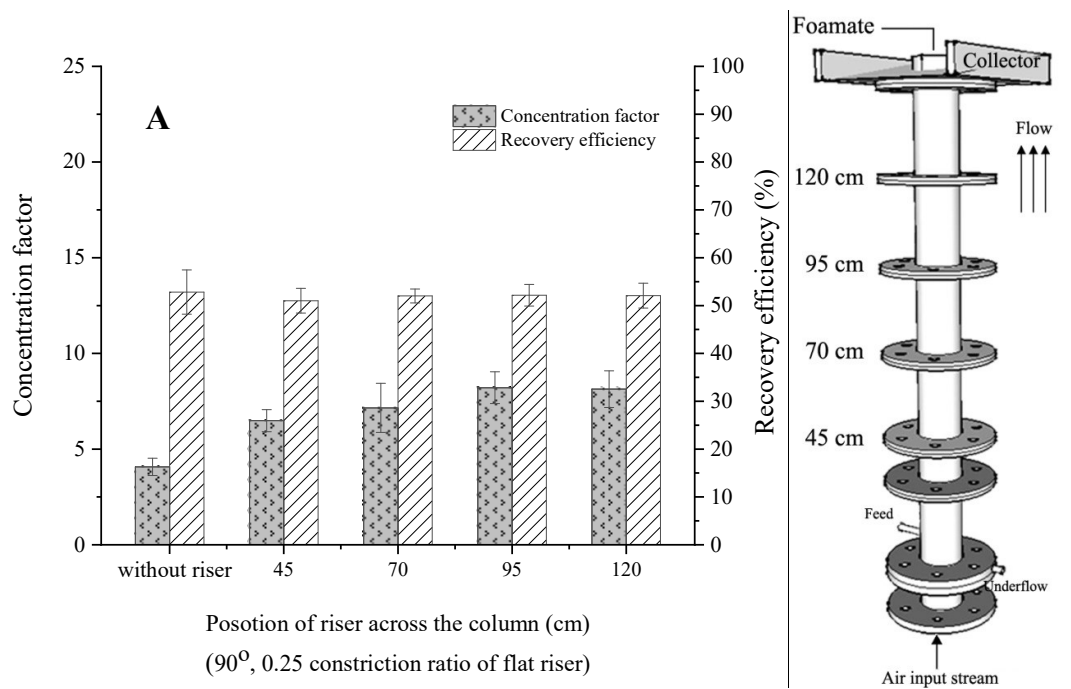


Figure 4. 23: The flotation efficiency profile as a function of the position of a flat riser with an angle of 90° and a constriction ratio of 0.25 at different heights on the column (A) and the sets of multiple risers (B) at 0.1 gL^{-1} algal biomass, 100 mgL^{-1} CTAB.

Data were obtained under the conditions: 1 L min^{-1} air flow rate and 0.1 L min^{-1} feed flow rate and 25 cm liquid pool depth. Mean \pm standard deviation.

Figure 4.23 (A) shows the effect of riser position at different heights in the column. Considering the position of a riser in the column, the foam height in the column corresponds to the position of the riser. It can be seen that the position of the riser significantly affects the concentration factor, with the concentration factor increasing as the height of the riser is increased. When placing the riser at 95 and 120 cm, the concentration factor was approximately doubled compared to the method without a riser. Due to the longer residence time of the foam, there is increased liquid drainage in the bubble film. However, the recovery efficiency is not significantly affected by the riser position, with 52.7±1.2% determined as an average for all riser positions. Therefore, as the foam height increases, the concentration of adsorbed algal biomass increases, resulting in a higher concentration factor.

In addition, several risers positioned at different heights in the column were combined for this experiment, as shown in **Figure 4.23 (B)**. As the number of risers increased, the concentration factor increased. There was also a connection between this and the positioning of the 95 and 120cm sets. This suggests that the addition of risers can increase the concentration factor by increasing turbulence in the column and providing additional surfaces for the reaction. This creates more contact between the gas and liquid phases. Additionally, the risers help advance the process by creating pressure differentials and also act as a support foam structure in the column. Despite the increased concentration factor, the recovery efficiency remains unchanged in this process. To maximize recovery efficiency, alternative processes such as multistage and residence times must be combined and adjusted accordingly.

4.6.2 Double-stage operation

This experiment aimed to demonstrate how optimizing the development of the foam flotation process could have further improved the recovery efficiency in microalgae harvesting.

4.6.2.1 Free CTAB contents

According to the foam balance and foam stability study presented in **session 4.3**, 30% of the free CTAB content remained in the system and approximately 70% was absorbed by the algal biomass. The free CTAB contents in the initial feed sample and discharge stream solutions of the multistage flotation process were measured as shown in **Figure 4.24**. The experiment was carried out with an operating condition of 0.1 L min^{-1} feed flow rate, 1 L min^{-1} air flow rate, 25 cm liquid pool depth, 0.2 g L^{-1} algal biomass, and 150 mg L^{-1} CTAB concentration.

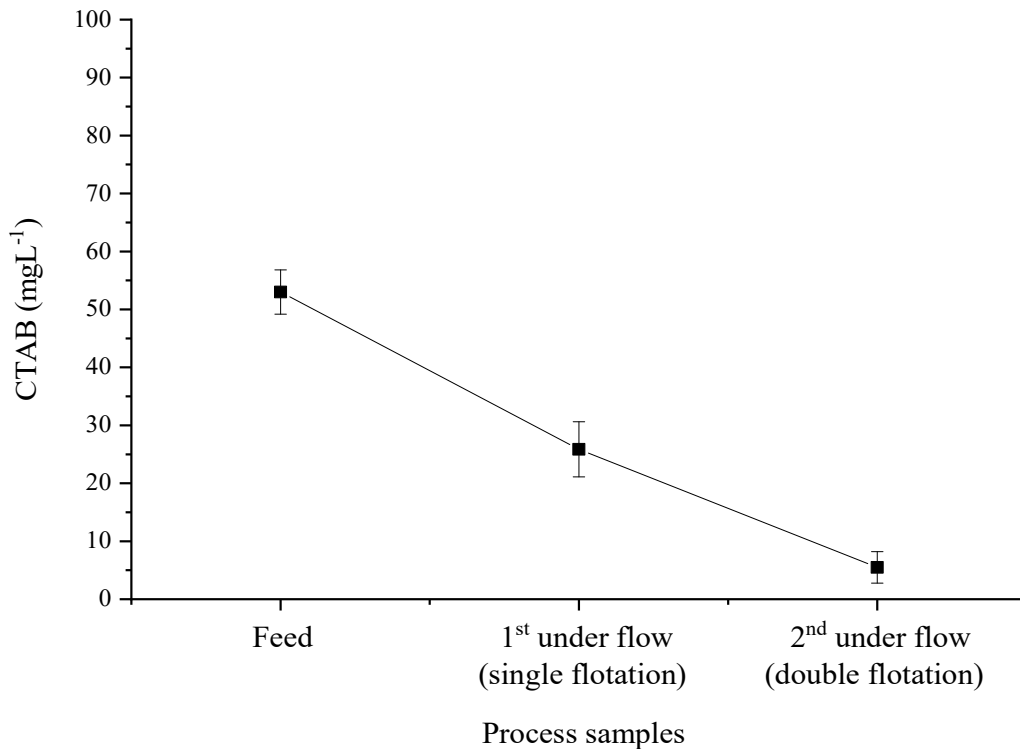


Figure 4. 24: Free CTAB profile in the multistage flotation process solution.

Data were obtained under the conditions: 0.1 L min^{-1} feed flow rate, 1 L min^{-1} air flow rate, 25 cm liquid pool depth with 0.2 g L^{-1} algal biomass and 150 mg L^{-1} CTAB concentration.

The initial sample solution used in this study had a free CTAB content of $53.0 \pm 3.8 \text{ mg L}^{-1}$. During the first process, single flotation, free CTAB was found in the discharge stream (underflow) at $25.9 \pm 4.6 \text{ mg L}^{-1}$. The free CTAB concentration in the discharge stream of the second process, called double flotation, was even lower, measuring less than 10 mg L^{-1} ($5.5 \pm 2.7 \text{ mg L}^{-1}$).

These results suggest that the double flotation process is more effective in removing CTAB from the solution than the single flotation process. Therefore, it is possible to harvest algal biomass from the culture medium or remove it from the culture medium with the remaining CTAB from the first process. Using an additional flotation process, this is a promising technique for recovering algal biomass and improving efficiency.

4.6.2.2 Flotation efficiency

A total of two columns were used for this study: one with the original column of this study, a total length of 145 cm and the other with half the length of the first column. The decision to use these column lengths was based on the free CTAB content in the discharge current solution. As shown in **Figure 4.24**, the initial feed sample had a free CTAB content of 53 mg L^{-1} , which allowed continuous foam flotation to be maintained through the columns. While after the flotation process, the first discharge stream (effluent solution) contained only 25.9 mg L^{-1} CTAB, which was half of the concentration in the feed solution.

Therefore, in order to maintain continuous foam flotation with this reduced CTAB concentration, the second column of this study was designed to be half the length of the first column, as shown in **Figure 3.5(B)** of the foam flotation process methodology in **section 3.53**.

The physical appearance of the multi-stage flotation process solution is shown in **Figure 4.25**. Two scenarios were performed with air flow rates at (A) 1 L min^{-1} and (B) 2 L min^{-1} . The process was carried out under the conditions of 0.1 L min^{-1} feed flow rate, 25 cm liquid pool depth with 0.2 g L^{-1} algal biomass and a 150 mg L^{-1} CTAB concentration with 0.25 constriction ratio, the riser has an entry angle of 90° and a length of 15 cm.

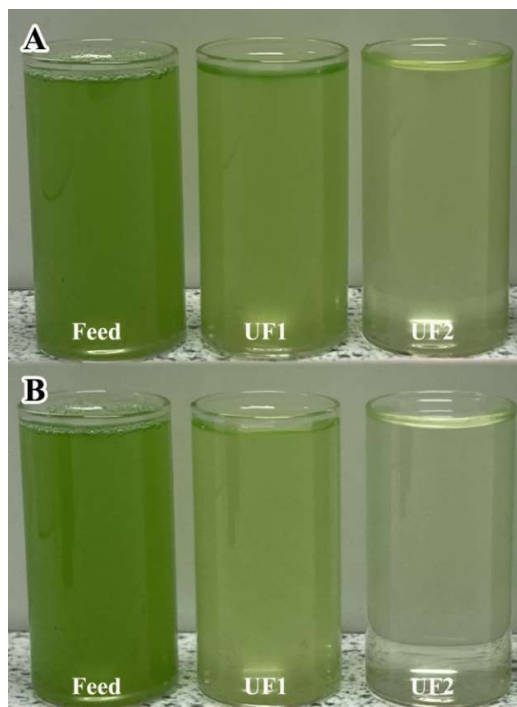


Figure 4. 25: *The physical appearance of the multi-stage flotation process solution at different air flow rates, (A) 1 L min^{-1} and (B) 2 L min^{-1}*

Data were obtained under the conditions: 0.1 L min^{-1} feed flow rate, 25 cm liquid pool depth with 0.2 g L^{-1} algal biomass and 150 mg L^{-1} CTAB concentration with a 0.25 constriction ratio, 90° angle and 15 cm length of the riser.

The results indicate that the second underflow sample exhibits a notable overall colour difference. At an airflow rate of 1 L min^{-1} (Scenario A), the absorbance at 680 nm supports a comparison between the feed sample, the first underflow (UF1) and the second underflow (UF2) with values of 1.75 and 0.96, respectively. 3.41. Likewise, the absorption values in scenario B (2 L min^{-1} air flow) were 3.72, 1.99 and 28.3, respectively.

This study (**Figure 4.26**) examined whether a multistage flotation process could improve recovery efficiency. For the experiment, an air flow rate of 1 L min^{-1} and 2 L min^{-1} was used to allow the foam to remain in the column for a comparable period of time, using a constriction ratio of 0.25 with an angle of 90° and a length of 15 cm at 0.2 g L^{-1} algal biomass, 150 mg L^{-1} CTAB under the condition of a feed flow rate of 0.1 L min^{-1} and a liquid pool depth of 25 cm. Despite the increased concentration factor, the recovery efficiency in the second multistage improved significantly, with the flotation air flow rate of 1 L min^{-1} and 2 L min^{-1} reaching at 85% and 95%, respectively. This means it can be increased by around 30% compared to a single-stage process. This indicates that increasing the total residence time through the multistage flotation process by using a low aeration flow rate effectively increased the recovery efficiency.

This suggests that optimizing the air feed flow rate for a multistage flotation process can be an efficient way to maximize recovery efficiency. Additionally, this could be a cost-effective strategy for processes to optimize the process to achieve optimal recovery efficiency for their overall process.

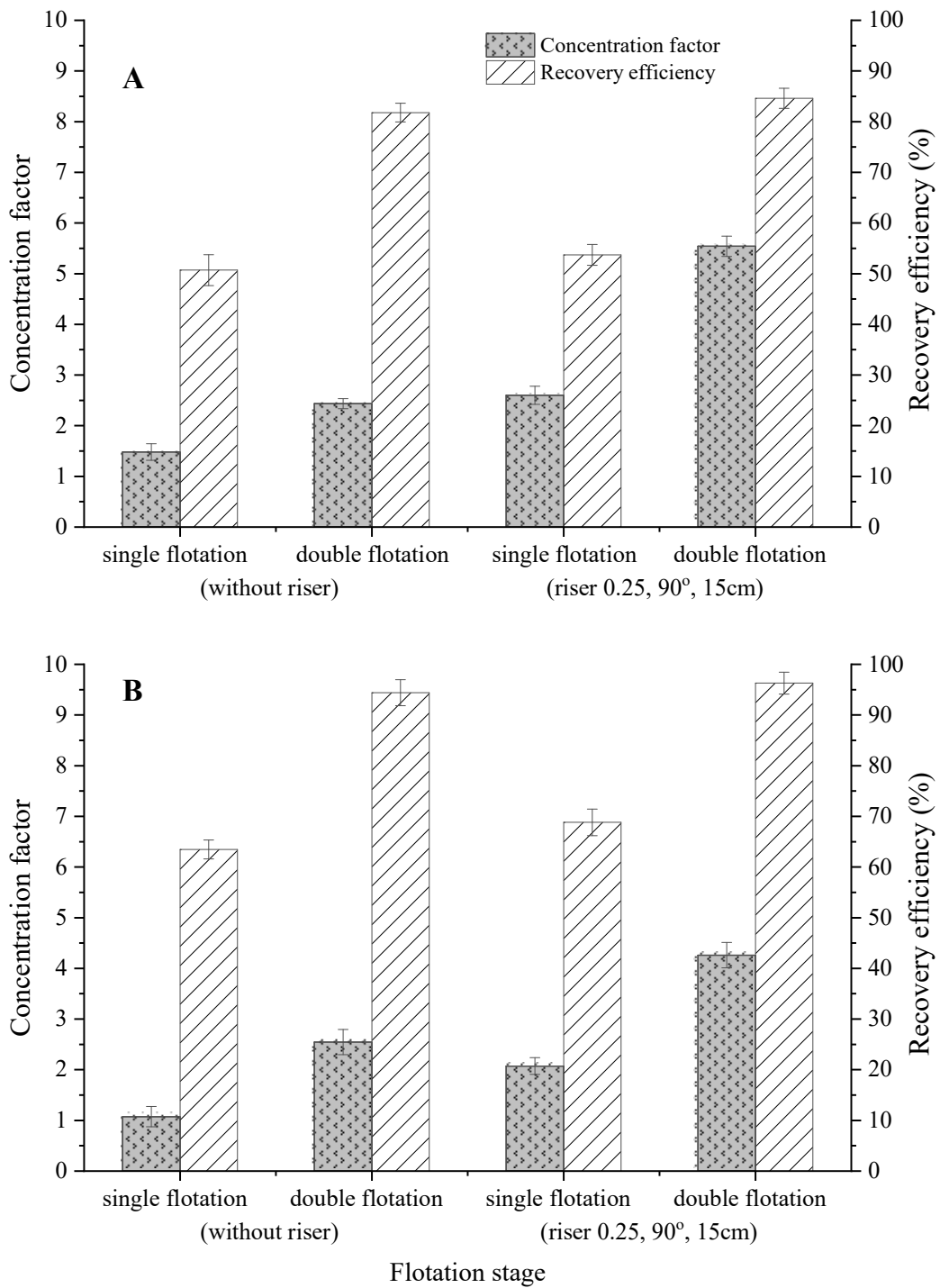


Figure 4. 26: The flotation efficiency profile as a function of multi-stage flotation using 90° of angle, 15 cm in length and 0.25 constriction ratio with 1 L min⁻¹ air flow rate (A) and 2 L min⁻¹ air flow rate (B) at 0.2 gL⁻¹ algal biomass, 150 mgL⁻¹ CTAB. Data were obtained under the conditions: 0.1 L min⁻¹ feed flow rate and 25 cm liquid pool depth. Mean ± standard deviation.

Chapter 5

Conclusions and Further Work

The chapter is divided into two sections; one is the conclusion and another is a suggestion. These sections will be described in more detail in the following.

5.1 Conclusions

This study investigated the feasibility of foam flotation with a focus on the issue of cost-effective microalgal harvesting using a column foam flotation design. The effectiveness, rapidity and smoothness of each step of the approach suggest its potential for scalability. The most important finding is that using the optimal riser, especially the constriction ratio and length within the column, significantly improves the efficiency of microalgae harvesting and biomass yield. In this work, the separation and concentration of algae was systematically investigated using a foam column. A flexible design allowed adaptation to various experimental requirements. The key findings include:

1. **Flow map optimization:** The study established a "flow map" in the context of the correlation among surfactant concentration, microalgae concentration and foam residence time in the column to optimise flotation efficiency.
2. **Foam riser design:** The influence of foam riser design on harvesting efficiency was investigated using the freshwater microalgae *Chlorella vulgaris*. The results indicate that an appreciated riser significantly enhances microalgae harvesting efficiency.
3. **Foam flotation mechanism:** High-resolution image visualization was used to study the mechanism of foam flotation through the foam riser, focusing on bubble size, shape and velocity. These findings provide valuable information for further process optimization.
4. **Double-stage flotation:** This study examined the double-stage flotation process as a potential method for further improving recovery efficiency.

The valuable outcomes have been figured out from this research, which can be divided into three main areas: (1) the identification of appropriate flow map conditions for algae/surfactant/flow rate combinations, (2) the evaluation of the optimal foam riser design and (3) Demonstrating how to optimise the development of the foam flotation process can further improve the recovery efficiency for microalgae harvesting.

5.1.1 *Algae/surfactant/flow rate “Flow map” and suitable conditions*

Pressure profiles (vs height) indicated that the stable zone of the foam in the column extended no higher than 145 cm. Hence, in all these experiments the column height was maintained at 145 cm for foam stability. A flow map was developed showing the relationships between foam structure (discontinuous/continuous) and air flow rate/surfactant (CTAB) concentration and algae concentration. It showed that more CTAB was required for higher concentrations of algae. Furthermore, it was found that approximately 30% of the free CTAB content still remained in the system, while approximately 70% was absorbed by the algae, resulting in a similar continuous foam flotation. Moreover, the final product volume decreased as residence time increased at all CTAB concentrations due to drainage and an increase in bubble size due to the higher flow rates required for shorter residence times.

Overall, the most suitable condition with the highest concentration factor for microalgae harvesting was achieved with the low air flow rate of 1 L min^{-1} . In addition, for each batch of concentrated algae samples used for harvesting, it is important to use the minimum surfactant concentration (this study used CTAB), ensuring that foam can flow continuously within the column.

5.1.2 *Foam riser design*

Foam riser models were created with diameter ratios of 0.25, 0.5 and 0.75 along with a wide range of riser angles (30° , 45° , 60° and 90°) and lengths (5, 10, 15 cm and a disc-shaped model with a height of 0.2 cm). These designs were drafted in Google SketchUp Make and subsequently fabricated using a uPrint SE Plus Desktop 3D printer using thermoplastic acrylonitrile butadiene styrene (ABS) as the building material. The evaluation of the optimal foam riser design revealed that risers significantly enhance the efficiency of microalgae harvesting. It has been shown that:

1. The constriction ratio affects the efficiency of froth flotation. A diameter ratio of 0.25 resulted in higher pressure and liquid fraction below the riser, which can be reduced the foam water content and increased the concentration factor. This phenomenon can be attributed to the observed foam flow mechanism through high-resolution image visualisation. It was found that the foam velocity increases significantly as the foam approaches the riser and accelerates sharply once it is in the riser. Regarding bubble size, the foam expands as it flows to reach the foam riser. At this point, the water content in the foam begins to decrease as large bubbles form in the middle under the riser and flow through. However, a rapid decrease in foam velocity and subsequent bubble

shrinks back to a small size were observed after flowing through the riser. Therefore, the bubble-solid particles, including microalgae biomass, should be collected after the foam has completely passed through the riser to accumulate and store microalgae biomass in the collection unit.

2. The angle of the foam riser had no significant influence on the flotation of the column. This was because the foam naturally formed its own angle beneath the riser. This was clearly observed via flow visualisation. Further observations revealed that individual bubbles from the edge of the column within the foam stream dynamically adjust their angles according to their movement pattern before entering the foam riser. The bubbles were observed to transition from nearly vertical (90 degrees) to a gradual reduction in angle as they approached the foam riser, with some angles falling below 30 degrees before entry.
3. The efficiency of algae removal appears to be improved when the length of the riser is increased to 15 cm.
4. The placement of the foam riser should be 70-100 cm above the liquid surface of the sample solution mixture, as this represents the foam stabilising zone in the column. This was directly observed in pressure profile measurements vs height experiments. At a steady state, the pressure profiles within this zone exhibited no fluctuations, confirming the presence of the foam stabilisation zone at this height.

5.1.3 *Process development*

Multiple risers in series were demonstrated to have no impact on recovery efficiency, so are not recommended. However, after the first flotation, the concentration of free CTAB in the discharged stream remained half that in the feed culture. This could therefore be used as a feed sample for the second flotation. The second-stage process can increase the recovery efficiency of the algae from the culture medium by approximately 30%. Hence, foam flotation of algae should instead be carried out in several stages, as this has been shown to improve the recovery efficiency of the flotation process. The number of stages required depends on the concentration of free CTAB remaining in the discharged stream.

Overall, due to its simplicity and ease of use, it is recommended to choose a foam riser in the column with a constriction ratio of 0.25, a length of 15cm (the longest used here) and an angle of 90 degrees to achieve flotation. The placement of the riser should be at 70-100 cm above the liquid surface of the sample solution mixture, representing the foam stabilise zone in the column.

5.2 Suggestions for future work

Thailand's Ministry of Agriculture and Cooperatives has prioritized promoting sustainable livelihood in rural communities through several innovative agricultural projects. As part of this strategy, they aim to both create new income opportunities and promote bio-based economic development. Microalgae cultivation in open pond is one of these choice that can offers a promising opportunity for biomass production in Thailand due to its low operating costs and the country's favourable year-round environmental conditions. The harvested microalgae can be used for various applications such as food, animal feed, fertilizer and renewable energy development and so on, depending on local needs and resource availability.

Integrating microalgae farms into local residences that exist in agricultural practices offers an alternative opportunity to create resilient and diversified agricultural systems at the local level. This integration would create employment and opportunities and promote entrepreneurship in the field of bio-based products. In particular, these farms can utilise an abundance of saline water that is unsuitable for conventional agriculture for microalgae production. Consequently, this approach could contribute to land rehabilitation and address the challenges of land degradation issue in northeast Thailand.

However, efficient harvesting of microalgae cells remains a significant bottleneck. An ideal harvesting technique would be characterised by effectiveness, rapidness, low cost, scalability and continuous operability. The investigation of this study, the column foam flotation technique, presents a potentially scalable solution that requires further research. In particular, exploring the scalability and cost-effective solution of foam column technology is crucial for continuously harvesting microalgae cells in open ponds. Therefore, future work will focus on developing a scalable and sustainable technology for microalgae cell harvesting, including process improvement, research into alternative foaming agents, and scaling-up considerations.

5.2.1 Process Improvement

The results of this study indicate that the lowest concentration ratio of 0.25 of foam riser was the most effective in achieving the highest concentration factor. Therefore, future studies will focus on evaluating the performance of the riser with a multi-channel of 0.25 dimension ratio to enhance the concentration factor. Additionally, multi-stage flotation processes are should be investigated beyond the current study for improvements in the recovery efficiency of microalgae harvesting.

5.2.2 *Foaming agents evaluation*

Other foaming substances, as well as foaming methods, should be further studied in the flotation process to harvest the microalgal biomass. This approach would provide broader applicability for various downstream applications.

5.2.3 *Scaling-up considerations*

Pilot-scale implementation and further optimization of the foam column technology should be investigated for continuous harvesting of microalgae cells in open pond systems. This should include:

1. ***Pilot plant design and construction:*** Design and construction of a pilot plant in Bangkok, Thailand, incorporating the optimized foam column technology for continuous microalgae harvesting with open ponds, as shown below, will be performed.



2. ***Performance evaluation:*** monitoring parameters such as harvesting efficiency, energy consumption and algal biomass quality.

A planned pilot plant installation in Bangkok, Thailand, provides an excellent opportunity to validate feasibility and optimize operating parameters to refine the technology and collect real-world data. The successful implementation could open up opportunities to establish microalgae farming projects in other locations, especially in north-eastern Thailand, where saline soils are a widespread problem.

Conferences attended and publication submitted

Conference

Title: process intensification for low-cost microalgae harvesting by using continuous foam flotation technique.

Oral Presentation at the AlgaEurope 2022, Rome, Italy

13-15 December 2022

Publication

With funding for one financial year, the Ministry of Agriculture and Cooperatives is currently installing an open raceway pond system in Bangkok, Thailand. The foam column of my thesis is implemented and optimized to increase the pilot scale of the algae harvesting process in an open channel pond in Thailand from 10,000 to 30,000 litres.

Furthermore, microalgae farming are likely to become established in northeastern Thailand, particularly in areas where saline soils are a significant problem. In addition, the prototype device and algae harvesting method that I acquired during my research are registered as a petty patent application for the cultivation of algae in open ponds with the School of Chemical Engineering and Advanced Materials, Newcastle University.

References

- Abdel-Raouf N, N., Al-Homaidan, A. & Ibraheem, I. (2012) 'Agricultural importance of algae', *AFRICAN JOURNAL OF BIOTECHNOLOGY*, 11(54), pp. 11648–11658.
- Ahmad, I., Abdullah, N., Koji, I., Yuzir, A. & Muhammad, S.E. (2021) 'Evolution of Photobioreactors: A Review based on Microalgal Perspective', *IOP Conference Series: Materials Science and Engineering*, 1142(1/012004), .
- Aikawa, S., Nishida, A., Ho, S.-H., Chang, J.-S., Hasunuma, T. & Kondo, A. (2014) 'Glycogen production for biofuels by the euryhaline cyanobacteria *Synechococcus* sp. strain PCC 7002 from an oceanic environment', *Biotechnology for Biofuels*, 7(1), p. 88.
- Al-Thyabat, S., Yoon, R.H. & Shin, D. (2011) 'Floatability of fine phosphate in a batch column flotation cell', *Minerals and Metallurgical Processing*, 28(2), pp. 110–116.
- Alam, M.A., Wang, Z. & Yuan, Z. (2017) 'Generation and Harvesting of Microalgae Biomass for Biofuel Production', in Bhumi Nath Tripathi & Dhananjay Kumar (eds.) *Prospects and Challenges in Algal Biotechnology*. [Online]. Singapore: Springer Singapore. pp. 89–111.
- Albijan, B., Zhou, Y., Tadesse, B., Dyer, L., Xu, G. & Yang, X. (2018) 'Influence of bubble approach velocity on liquid film drainage between a bubble and a spherical particle', *Powder Technology*, 338pp. 140–144.
- Alhattab, M. & Brooks, M.S.-L. (2017) 'Dispersed air flotation and foam fractionation for the recovery of microalgae in the production of biodiesel', *Separation Science and Technology*, 52(12), pp. 2002–2016.
- Alkarawi, M.A.S., Caldwell, G.S. & Lee, J.G.M. (2018) 'Continuous harvesting of microalgae biomass using foam flotation', *Algal Research*, 36pp. 125–138.
- Allnut, F.C.T. & Kessler, B.A. (2015) *Harvesting and Downstream Processing—and Their Economics*, in [Online]. Springer, Cham. pp. 289–310.
- Azwar, M.Y., Hussain, M.A. & Abdul-Wahab, A.K. (2014) 'Development of biohydrogen production by photobiological, fermentation and electrochemical processes: A review', *Renewable and Sustainable Energy Reviews*, 31pp. 158–173.
- Badary, A., Takamatsu, S., Nakajima, M., Ferri, S., Lindblad, P. & Sode, K. (2018) 'Glycogen Production in Marine Cyanobacterial Strain *Synechococcus* sp. NKBG 15041c.', *Marine biotechnology (New York, N.Y.)*, 20(2), pp. 109–117.

- Barbosa, M.J., Janssen, M., Südfeld, C., D'adamo, S. & Wijffels, R.H. (2023) 'Hypes, hopes, and the way forward for microalgal biotechnology', *Trends in Biotechnology*, 41pp. 452–471.
- Barkia, I., Saari, N. & Manning, S.R. (2019) 'Microalgae for high-value products towards human health and nutrition', *Mar Drugs*, 17(5), p. 304.
- Barros, A.I., Gonçalves, A.L., Simões, M. & Pires, J.C.M. (2015) 'Harvesting techniques applied to microalgae: A review', *Renewable and Sustainable Energy Reviews*, 41pp. 1489–1500.
- Barrut, B., Blancheton, J.-P., Muller-Feuga, A., René, F., Narváez, C., Champagne, J.-Y. & Grasmick, A. (2013) 'Separation efficiency of a vacuum gas lift for microalgae harvesting', *BIORESOURCE TECHNOLOGY*, 128pp. 235–240.
- Bashan, Y. & Perez-Garcia, O. (2015) 'Microalgal Heterotrophic and Mixotrophic Culturing for Bio-refining: From Metabolic Routes to Techno-economics', in *Algal biorefineries*. [Online]. pp. 61–131.
- Baweja, P. & Sahoo, D. (2015) 'Classification of Algae. In: The Algae World.', in Dinabandhu Sahoo & Joseph Seckbach (eds.) *Cellular Origin, Life in Extreme Habitats and Astrobiology*. 26th edition [Online]. Dordrecht: Springer Netherlands. pp. 31–55.
- Becker, W. (2007) 'Microalgae in Human and Animal Nutrition'. Handbook of Microalgal Culture
- Bertsch, P., Böcker, L., Mathys, A. & Fischer, P. (2021) 'Proteins from microalgae for the stabilization of fluid interfaces, emulsions, and foams', *Trends in Food Science & Technology*, 108pp. 326–342.
- Besagni, G., Brazzale, P., Fiocca, A. & Inzoli, F. (2016) 'Estimation of bubble size distributions and shapes in two-phase bubble column using image analysis and optical probes', *Flow Measurement and Instrumentation*, 52pp. 190–207.
- Bhakta, A. & Ruckenstein, E. (1997) 'Decay of standing foams: drainage, coalescence and collapse', *Advances in Colloid and Interface Science*, 70(1–3), pp. 1–124.
- Bhatia, S.C. & Bhatia, S.C. (2014) 'Algae fuel for future', *Advanced Renewable Energy Systems*, pp. 645–678.
- Bhondayi, C. (2020) 'Flotation Froth Phase Bubble Size Measurement', <https://doi.org/10.1080/08827508.2020.1854250>, 43(2), pp. 251–273.
- Biris-Dorhoi, E.S., Michiu, D., Pop, C.R., Rotar, A.M., Tofana, M., Pop, O.L., Socaci, S.A. & Farcas, A.C. (2020) 'Macroalgae - A Sustainable Source of Chemical Compounds with Biological Activities', *Nutrients*, 12(10), pp. 1–23.

- Blankenship, R. (2002) *Molecular Mechanism of Photosynthesis*.
- Bold, H.C. & Wynne, M.J. (1985) *Introduction to the algae: structure and reproduction*. Prentice-Hall.
- Borowitzka, M.A. (2005) 'Culturing microalgae in outdoor ponds', in R A Andersen (ed.) *Algal Culturing Techniques*. [Online]. Boston, USA: Academic Press. pp. 205–218.
- Borowitzka, M.A. (2013) 'Energy from Microalgae: A Short History', in *Algae for Biofuels and Energy*. [Online]. Dordrecht: Springer Netherlands. pp. 1–15.
- Brennan, L. & Owende, P. (2010) 'Biofuels from microalgae—A review of technologies for production, processing, and extractions of biofuels and co-products', *Renewable and Sustainable Energy Reviews*, 14(2), pp. 557–577.
- Brodie, J. & Lewis, J. (2007) *Unravelling the Algae: The Past, Present and Future of Algal Systematics*. London: CRC Press.
- Brooks, F., Rindi, F., Suto, Y., Ohtani, S. & Green, M. (2015) 'The Trentepohliales (Ulvophyceae, Chlorophyta): An Unusual Algal Order and its Novel Plant Pathogen—Cephaleuros', *Plant Disease*, 99(6), pp. 740–753.
- Brown, T.M., Duan, P. & Savage, P.E. (2010) 'Hydrothermal Liquefaction and Gasification of Nannochloropsis sp.', *Energy & Fuels*, 24(6), pp. 3639–3646.
- Brunner, C.A. & Lemlich, R. (1963) 'Foam fractionation', *Industrial and Engineering Chemistry Fundamentals*, 2(4), pp. 297–300.
- Bumbieris, J. (2020) *The effect of smooth successive constriction and expansion on the pressure and liquid fraction profiles of dry foam in a foam fractionation column*, (160107632), .
- Burghoff, B. (2012) 'Foam fractionation applications', *Journal of Biotechnology*, 161(2), pp. 126–137.
- Cai, J., Lovatelli, A., Gamarro, E.G., Geehan, J., Lucente, D., Mair, G., Miao, W., Reantaso, M., Roubach, R., Yuan, X., Aguilar-Manjarrez, J., Acadian, L.C., Dabbadie, L., Desrochers, A., Diffey, S., Tauati, M., Hurtado, A., Potin, P. & Przybyła, C. (2021) 'Seaweeds and microalgae : an overview for unlocking their potential in global aquaculture development'. FAO Fisheries and Aquaculture Circular No. 1229
- Callow, M.E., Callow, J.A., Ista, L.K., Coleman, S.E., Nolasco, A.C. & Lopez, G.P. (2000) 'Use of self-assembled monolayers of different wettabilities to study surface selection and primary adhesion processes of green algal (Enteromorpha) zoospores', *Applied and Environmental Microbiology*, 66(8), pp. 3249–3254.

- Calvert, J.R. & Nezhati, K. (1986) 'A rheological model for a liquid-gas foam', *International Journal of Heat and Fluid Flow*, 7(3), pp. 164–168.
- Del Campo, J.A., García-González, M. & Guerrero, M.G. (2007) 'Outdoor cultivation of microalgae for carotenoid production: current state and perspectives', *Applied Microbiology and Biotechnology*, 74(6), pp. 1163–1174.
- Cantat, I., Cohen-Addad, S., Elias, F., Graner, F., Höhler, R., Pitois, O., Rouyer, F., Saint-Jalmes, A. & Flatman, R. (2013) 'Foams: Structure and Dynamics', *Climate Change 2013 - The Physical Science Basis*, 1(9), pp. 1–278.
- Carrier, V. & Colin, A. (2003) 'Coalescence in draining foams'. *Langmuir* 19 (11) p.pp. 4535–4538.
- CG, J., Navarro, E., Malpartida, I., RM, R., Masojídek, J., Abdala, R. & L, F.F. (2014) 'Hydrodynamics and photosynthesis performance of *Chlorella fusca* (Chlorophyta) grown in a thin-layer cascade (TLC) system', *Aquatic Biology*, 22pp. 111–122.
- Chapman, Russell Leonard & Chapman, R L (2013) 'Algae: the world's most important "plants"-an introduction', *Mitig Adapt Strateg Glob Change*, 18pp. 5–12.
- Chapman, V.J. & Chapman, D.J. (1973) 'Classification', in V J Chapman & D J Chapman (eds.) *The Algae*. [Online]. London: Macmillan Education UK. pp. 1–12.
- Chaudhari, R. V. & Hofmann, H. (1994) 'Coalescence of gas bubbles in liquids', *Reviews in Chemical Engineering*, 10(2), pp. 131–190.
- Chen, C.-Y., Yeh, K.-L., Aisyah, R., Lee, D.-J. & Chang, J.-S. (2011) 'Cultivation, photobioreactor design and harvesting of microalgae for biodiesel production: A critical review', *Bioresource Technology*, 102(1), pp. 71–81.
- Chen, C.L., Chang, J.S. & Lee, D.J. (2015) 'Dewatering and Drying Methods for Microalgae', *Drying Technology*,
- Chen, Y.M., Liu, J.C. & Ju, Y.-H. (1998) 'Flotation removal of algae from water', *Colloids and Surfaces B: Biointerfaces*, 12(1), pp. 49–55.
- Chisti, Y. (2007) 'Biodiesel from microalgae', *Biotechnology Advances*, 25(3), pp. 294–306.
- Cohen-Addad, S. & Pitois, O. (2012) *Flow in Foams and Flowing Foams*,
- Cole, K.E. & Cole, K.E. (2011) *Bubble size, coalescence and particle motion in flowing foams*,

- Coward, T., Lee, J.G.M. & Caldwell, G.S. (2013) 'Development of a foam flotation system for harvesting microalgae biomass', *Algal Research*, 2(2), pp. 135–144.
- Coward, T., Lee, J.G.M. & Caldwell, G.S. (2014) 'Harvesting microalgae by CTAB-aided foam flotation increases lipid recovery and improves fatty acid methyl ester characteristics', *Biomass and Bioenergy*, 67pp. 354–362.
- Coward, T., Lee, J.G.M. & Caldwell, G.S. (2015) 'The effect of bubble size on the efficiency and economics of harvesting microalgae by foam flotation', *Journal of applied phycology*, 27(2), pp. 733–742.
- Crawford, C.B. & Quinn, B. (2017) 'Microplastic separation techniques', *Microplastic Pollutants*, pp. 203–218.
- Cruz, Y.R., Aranda, D.A.G., Seidl, P.R., Diaz, G.C., Carliz, R.G., Fortes, M.M., Ponte, D.A.M.P. da & Paula, R.C.V. de (2018) 'Cultivation Systems of Microalgae for the Production of Biofuels', in *Biofuels - State of Development*. [Online]. InTech.
- Csordas, A. & Wang, J.-K. (2004) 'An integrated photobioreactor and foam fractionation unit for the growth and harvest of *Chaetoceros* spp. in open systems', *Aquacultural Engineering*, 30(1–2), pp. 15–30.
- Danquah, M.K., Gladman, B., Moheimani, N. & Forde, G.M. (2009) 'Microalgal growth characteristics and subsequent influence on dewatering efficiency', *Chemical Engineering Journal*, 151(1–3), pp. 73–78.
- Dassey, A.J. & Theegala, C.S. (2013) 'Harvesting economics and strategies using centrifugation for cost effective separation of microalgae cells for biodiesel applications', *Bioresource Technology*, 128pp. 241–245.
- Diaz, C.J., Douglas, K.J., Kang, K., Kolarik, A.L., Malinovski, R., Torres-Tiji, Y., Molino, J. V., Badary, A. & Mayfield, S.P. (2023) 'Developing algae as a sustainable food source', *Frontiers in Nutrition*, 9.
- Dilia, P., Leila, K. & Rusdianasari (2018) 'Fatty Acids From Microalgae *Botryococcus braunii* For Raw Material of Biodiesel', *Journal of Physics: Conference Series*, 1095(1), p. 12010.
- Dineshbabu, G., Goswami, G., Kumar, R., Sinha, A. & Das, D. (2019) 'Microalgae–nutritious, sustainable aqua- and animal feed source', *Journal of Functional Foods*, 62p. 103545.

- Dragone, G. (2022) 'Challenges and opportunities to increase economic feasibility and sustainability of mixotrophic cultivation of green microalgae of the genus *Chlorella*', *Renewable and Sustainable Energy Reviews*, 160(112284), .
- Drenckhan, W. & Saint-Jalmes, A. (2015) 'The science of foaming', *Advances in Colloid and Interface Science*, 222pp. 228–259.
- Eckert, M. (2010) 'The troublesome birth of hydrodynamic stability theory: Sommerfeld and the turbulence problem', *The European Physical Journal H*, 35(1), .
- El-Khalek, M.H.A. (2012) *Performance of different surfactants in deinking flotation process*, in [Online]. 2012
- Etemad, S., Kantzas, A. & Bryant, S. (2022) 'A systematic analysis of foam drainage: Experiment and model', *Results in Engineering*, 15p. 100551.
- Fameau, A.L. & Salonen, A. (2014) 'Effect of particles and aggregated structures on the foam stability and aging', *Comptes Rendus Physique*, 15(8–9), pp. 748–760.
- FAO (2022) *The State of World Fisheries and Aquaculture 2022 : towards blue transformation*. Rome: Food and Agriculture Organization of the United Nations.
- Fernández, I., Acién, F.G., Berenguel, M. & Guzmán, J.L. (2014) 'First Principles Model of a Tubular Photobioreactor for Microalgal Production', *Industrial & Engineering Chemistry Research*, 53(27), pp. 11121–11136.
- Ferrell, J., Fishman, D., Majumdar, R., Morello, J., Pate, R., Yang, J., Darzins, A., Heffelfinger, G., Pezzullo, L., Pienkos, P., Roach, K. & Sarisky-Reed, V. (2010) 'National Algal Biofuels Technology Roadmap'. Biomass Program, U.S. Department of Energy, Office of Energy Efficiency and Renewable Energy
- Fogg, G.E. & Thake, B. (1987) *Algal cultures and phytoplankton ecology*. 3rd edition. University of Wisconsin Press.
- Fredriksson, S., Elwinger, K. & Pickova, J. (2006) 'Fatty acid and carotenoid composition of egg yolk as an effect of microalgae addition to feed formula for laying hens', *Food Chemistry*, 99(3), pp. 530–537.
- Garcia-Pichel, F. & Belnap, J. (2021) 'Cyanobacteria and algae', in Terry J Gentry, Jeffrey J Fuhrmann, & David A B T - Principles and Applications of Soil Microbiology (Third Edition) Zuberer (eds.) *Principles and Applications of Soil Microbiology*. 3rd edition [Online]. Elsevier. pp. 171–189.

- García Alba, L., Torri, C., Samori, C., van der Spek, J., Fabbri, D., Kersten, S.R.A. & Brillman, D.W.F. (Wim) (2012) 'Hydrothermal Treatment (HTT) of Microalgae: Evaluation of the Process As Conversion Method in an Algae Biorefinery Concept', *Energy & Fuels*, 26(1), pp. 642–657.
- García, J., Mujeriego, R. & Hernández-Mariné, M. (2000) 'High rate algal pond operating strategies for urban wastewater nitrogen removal', *Journal of Applied Phycology*, 12(3), pp. 331–339.
- Garg, S., Wang, L. & Schenk, P.M. (2014) 'Effective harvesting of low surface-hydrophobicity microalgae by froth flotation', *Bioresource Technology*, 159pp. 437–441.
- Gerardo, M.L., Van Den Hende, S., Vervaeren, H., Coward, T. & Skill, S.C. (2015) 'Harvesting of microalgae within a biorefinery approach: A review of the developments and case studies from pilot-plants', *Algal Research*, 11pp. 248–262.
- Ghernaout, D., Elboughdiri, N., Ghareba, S., Salih, A., Ghernaout, D., Elboughdiri, N., Ghareba, S. & Salih, A. (2020) 'Coagulation Process for Removing Algae and Algal Organic Matter—An Overview', *Open Access Library Journal*, 7(4), pp. 1–21.
- Ghosh, P. (2009) 'Coalescence of bubbles in liquid', *Bubble Sci. Engng Technol.*, 1(1–2), pp. 75–87.
- Ghosh, S. & Das, D. (2015) 'Improvement of Harvesting Technology for Algal Biomass Production', in *Algal Biorefinery: An Integrated Approach*. [Online]. Cham: Springer International Publishing. pp. 169–193.
- Grassia, P., Neethling, S.J., Cervantes, C. & Lee, H.T. (2006) 'The growth, drainage and bursting of foams', *Colloids and Surfaces A: Physicochemical and Engineering Aspects*, 274(1–3), pp. 110–124.
- Grivalský, T., Ranglová, K., da Câmara Manoel, J.A., Lakatos, G.E., Lhotský, R. & Masojídek, J. (2019) 'Development of thin-layer cascades for microalgae cultivation: milestones (review)', *Folia microbiologica*, 64(5), pp. 603–614.
- Guo, H., Hong, C., Zhang, C., Zheng, B., Jiang, D. & Qin, W. (2018) 'Bioflocculants' production from a cellulase-free xylanase-producing *Pseudomonas boreopolis* G22 by degrading biomass and its application in cost-effective harvest of microalgae', *Bioresource Technology*, 255pp. 171–179.
- Gupta, A.K., Banerjee, P.K., Mishra, A., Satish, P. & Pradip (2007) 'Effect of alcohol and polyglycol ether frothers on foam stability, bubble size and coal flotation', *International Journal of Mineral Processing*, 82(3), pp. 126–137.

- Gupta, P.L., Lee, S.-M. & Choi, H.-J. (2015) 'A mini review: photobioreactors for large scale algal cultivation', *World Journal of Microbiology and Biotechnology*, 31(9), pp. 1409–1417.
- Gupta, S., Gupta, C., Garg, A.P. & Prakash, D. (2017) 'Prebiotic Efficiency of Blue Green Algae on Probiotics Microorganisms', *Journal of Microbiology & Experimentation*, Volume 4(Issue 4), .
- Von Der Haar, D., Müller, K., Bader-Mittermaier, S. & Eisner, P. (2014) 'Rapeseed proteins – Production methods and possible application ranges', *OCL*, 21(1), p. D104.
- Hadley, K.B., Bauer, J. & Milgram, N.W. (2017) 'The oil-rich alga *Schizochytrium* sp. as a dietary source of docosahexaenoic acid improves shape discrimination learning associated with visual processing in a canine model of senescence', *Prostaglandins Leukotrienes and Essential Fatty Acids*, 118pp. 10–18.
- Han, O.H., Kim, M.K., Kim, B.G., Subasinghe, N. & Park, C.H. (2014) 'Fine coal beneficiation by column flotation', *Fuel Processing Technology*, 126pp. 49–59.
- Hanotu, J., Bandulasena, H.C.H. & Zimmerman, W.B. (2012) 'Microflotation performance for algal separation', *Biotechnology and Bioengineering*, 109(7), pp. 1663–1673.
- Hao, W., Yanpeng, L., Zhou, S., Xiangying, R., Wenjun, Z. & Jun, L. (2017) 'Surface characteristics of microalgae and their effects on harvesting performance by air flotation', *International Journal of Agricultural and Biological Engineering*, 10(1), pp. 125–133.
- Harvey, P.J. & Ben-Amotz, A. (2020) 'Towards a sustainable *Dunaliella salina* microalgal biorefinery for 9-cis β -carotene production', *Algal Research*, 50p. 102002.
- Hassanzadeh, A., Hassas, B.V., Kouachi, S., Brabcova, Z. & Çelik, M.S. (2016) 'Effect of bubble size and velocity on collision efficiency in chalcopyrite flotation', *Colloids and Surfaces A: Physicochemical and Engineering Aspects*, 498pp. 258–267.
- He, J. & Chen, J.P. (2014) 'A comprehensive review on biosorption of heavy metals by algal biomass: Materials, performances, chemistry, and modeling simulation tools', *Bioresource Technology*, 160pp. 67–78.
- Heasman, M., Diemar, J., Sushames, T. & Foulkes, L. (n.d.) *Development of extended shelf-life microalgae concentrate diets harvested by centrifugation for bivalve molluscs ± a summary*.
- Henderson, R.K., Parsons, S.A. & Jefferson, B. (2008) 'Surfactants as Bubble Surface Modifiers in the Flotation of Algae: Dissolved Air Flotation That Utilizes a Chemically Modified Bubble Surface', *Environmental Science & Technology*, 42(13), pp. 4883–4888.

- Hey, M.J., Hilton, A.M. & Bee, R.D. (1994) 'The formation and growth of carbon dioxide gas bubbles from supersaturated aqueous solutions', *Food Chemistry*, 51(4), pp. 349–357.
- Hilgenfeldt, S., Koehler, S.A. & Stone, H.A. (2001) 'Dynamics of Coarsening Foams: Accelerated and Self-Limiting Drainage', *Physical Review Letters*, 86(20), p. 4704.
- Hilton, A.M., Hey, M.J. & Bee, R.D. (1993) 'Nucleation and Growth of Carbon Dioxide Gas Bubbles', *Food Colloids and Polymers*, pp. 365–375.
- Hoef-Emden, K. & Archibald, J.M. (2017) *Cryptophyta (Cryptomonads) BT - Handbook of the Protists*, in John M Archibald, Alastair G B Simpson, & Claudio H Slamovits (eds.) [Online]. Cham: Springer International Publishing. pp. 851–891.
- Hoffmann, L. (1989) 'Algae of Terrestrial Habitats', *Botanical Review*, 55(2), pp. 77–105.
- Hosseini, M., Starvaggi, H.A. & Ju, L.-K. (2016) 'Additive-free harvesting of oleaginous phagotrophic microalga by oil and air flotation', *Bioprocess and Biosystems Engineering*, 39(7), pp. 1181–1190.
- Hu, B., Min, M., Zhou, W., Li, Y., Mohr, M., Cheng, Y., Lei, H., Liu, Y., Lin, X., Chen, P. & Ruan, R. (2012) 'Influence of exogenous CO₂ on biomass and lipid accumulation of microalgae *Auxenochlorella protothecoides* cultivated in concentrated municipal wastewater.', *Applied biochemistry and biotechnology*, 166(7), pp. 1661–1673.
- Hu, Q., Sommerfeld, M., Jarvis, E., Ghirardi, M., Posewitz, M., Seibert, M. & Darzins, A. (2008) 'Microalgal triacylglycerols as feedstocks for biofuel production: perspectives and advances', *The Plant Journal*, 54(4), pp. 621–639.
- Huang, G., Chen, F., Wei, D., Zhang, X. & Chen, G. (2010) 'Biodiesel production by microalgal biotechnology', *Applied Energy*, 87(1), pp. 38–46.
- Huang, W.-C. & Kim, J.-D. (2013) 'Cationic surfactant-based method for simultaneous harvesting and cell disruption of a microalgal biomass', *Bioresource Technology*, 149pp. 579–581.
- Hutzler, S., Weaire, D., Saugey, A., Cox, S. & Peron, N. (2005) *The physics of foam drainage*,
- Ireland, P.M. & Jameson, G.J. (2007) 'Liquid transport in a multi-layer froth', *Journal of Colloid and Interface Science*, 314(1), pp. 207–213.
- Jena, U., Das, K.C. & Kastner, J.R. (2011) 'Effect of operating conditions of thermochemical liquefaction on biocrude production from *Spirulina platensis*', *Bioresource Technology*, 102(10), pp. 6221–6229.

- Johnson, M.B. & Wen, Z. (2009) *Production of Biodiesel Fuel from the Microalga Schizochytrium limacinum by Direct Transesterification of Algal Biomass*,
- Joubert, J.J. & Rijkenberg, F.H.J. (1971) 'Parasitic Green Algae', *Annual Review of Phytopathology*, 9(1), pp. 45–64.
- Jung, F., Krüger-Genge, A., Waldeck, P. & Küpper, J.-H. (2019) 'Spirulina platensis, a super food?', *Journal of Cellular Biotechnology*, 5pp. 43–54.
- Kang, R., Wang, J., Shi, D., Cong, W., Cai, Z. & Ouyang, F. (2004) 'Interactions between organic and inorganic carbon sources during mixotrophic cultivation of *Synechococcus* sp.', *Biotechnology letters*, 26(18), pp. 1429–1432.
- Khan, M.I., Shin, J.H. & Kim, J.D. (2018) 'The promising future of microalgae: current status, challenges, and optimization of a sustainable and renewable industry for biofuels, feed, and other products', *Microbial cell factories*, 17(1), p. 36.
- Khodaparast, S., Atasi, O., Deblais, A., Scheid, B. & Stone, H.A. (2018) 'Dewetting of Thin Liquid Films Surrounding Air Bubbles in Microchannels', *Langmuir*, 34(4), pp. 1363–1370.
- Kittirattanachai, V. (2016) *Demand Side Management* .
- Koehler, S.A., Hilgenfeldt, S. & Stone, H.A. (2000) 'A Generalized View of Foam Drainage: Experiment and Theory', *Langmuir*, 16(15), pp. 6327–6341.
- Koehler, S.A., Hilgenfeldt, S. & Stone, H.A. (1999) 'Liquid Flow through Aqueous Foams: The Node-Dominated Foam Drainage Equation', *Physical Review Letters*, 82(21), p. 4232.
- Kroes, R., Schaefer, E.J., Squire, R.A. & Williams, G.M. (2003) 'A review of the safety of DHA45-oil', *Food and Chemical Toxicology*, 41(11), pp. 1433–1446.
- Kuech, A., Breuer, M. & Popescu, I. (2023) *Research for PECH Committee - The future of the EU algae sector*.
- Kulkarni, A.A. & Joshi, J.B. (2005) *Bubble Formation and Bubble Rise Velocity in Gas-Liquid Systems: A Review*,
- Kumar, A. (2021) 'Current and Future Perspective of Microalgae for Simultaneous Wastewater Treatment and Feedstock for Biofuels Production', *Chemistry Africa 2021 4:2*, 4(2), pp. 249–275.

- Kumar, B., Das, B., Garain, A., Rai, S., Begum, W., Inamuddin, M., Mondal, M.H., Bhattarai, A. & Saha, B. (2022) 'Diverse utilization of surfactants in coal-floatation for the sustainable development of clean coal production and environmental safety: a review', *RSC Advances*, 12(37), pp. 23973–23988.
- Kumar, N., Banerjee, C., Negi, S. & Shukla, P. (2022) 'Microalgae harvesting techniques: updates and recent technological interventions', *Critical Reviews in Biotechnology*,
- Kurniawati, H.A., Ismadji, S. & Liu, J.C. (2014) 'Microalgae harvesting by flotation using natural saponin and chitosan', *Bioresource Technology*, 166pp. 429–434.
- Kwak, D.H. & Kim, M.S. (2015) 'Flotation of algae for water reuse and biomass production: role of zeta potential and surfactant to separate algal particles', *Water science and technology : a journal of the International Association on Water Pollution Research*, 72(5), pp. 762–769.
- Langevin, D. (2019) 'Coalescence in foams and emulsions: Similarities and differences', *Current Opinion in Colloid & Interface Science*, 44pp. 23–31.
- Laurens, L. (2017) *State of Technology Review - Algae Bioenergy*.
- Lavens, P. & Sorgeloos, P. (1996) *Manual on the Production and Use of Live Food for Aquaculture*. Rome: FAO.
- Lee, A.K., Lewis, D.M. & Ashman, P.J. (2009) 'Microbial flocculation, a potentially low-cost harvesting technique for marine microalgae for the production of biodiesel', *Journal of Applied Phycology*, 21(5), pp. 559–567.
- Lee, K., Eisterhold, M.L., Rindi, F., Palanisami, S. & Nam, P.K. (2014) 'Isolation and screening of microalgae from natural habitats in the midwestern United States of America for biomass and biodiesel sources.', *Journal of natural science, biology, and medicine*, 5(2), pp. 333–339.
- Lee, R.E. (2018) *Phycology*. 5th edition. Cambridge: Cambridge University Press.
- Lee, R.E. (2008) *Phycology*. 4th edition. Cambridge: Cambridge University Press.
- Leliaert, F. (2019) 'Green Algae: Chlorophyta and Streptophyta', *Encyclopedia of Microbiology*, pp. 457–468.
- Leliaert, F., Smith, D.R., Moreau, H., Herron, M.D., Verbruggen, H., Delwiche, C.F. & De Clerck, O. (2012) 'Phylogeny and Molecular Evolution of the Green Algae', *Critical Reviews in Plant Sciences*, 31(1), pp. 1–46.

- Lewin, R.A. (1995) 'Symbiotic Algae: Definitions, Quantification and Evolution', *Symbiosis*, 19pp. 31–37.
- Lewis, L.A. & Mccourt, R.M. (2004) 'Green algae and the origin of land plants', *American Journal of Botany*, 91(10), .
- Li, H., Wang, J., Luo, Y., Bai, B. & Cao, F. (2022) 'pH-Responsive Eco-Friendly Chitosan–Chlorella Hydrogel Beads for Water Retention and Controlled Release of Humic Acid', *Water* 2022, Vol. 14, Page 1190, 14(8), p. 1190.
- Li, X., Evans, G.M. & Stevenson, P. (2011) 'Process intensification of foam fractionation by successive contraction and expansion', *Chemical Engineering Research and Design*, 89(11), pp. 2298–2308.
- Liu, J.C., Chen &, Y.M. & Ju, Y.-H. (1999) 'Separation of Algal Cells from Water by Column flotation', *Separation Science and Technology*, 34(11), pp. 2259–2272.
- LIU, J.C., CHEN, Y.M. & JU, Y.-H. (1999) 'Separation of Algal Cells from Water by Column flotation', *Separation Science and Technology*, 34(11), pp. 2259–2272.
- López Barreiro, D., Ronsse, F. & Brilman, W. (2013) 'Hydrothermal liquefaction (HTL) of microalgae for biofuel production: State of the art review and future prospects', *Biomass and Bioenergy*, 53pp. 113–127.
- Loughland, R.A., Qasem, A.M., Burwell, B. & Prihartato, P.K. (2018) 'Coastal Sabkha (Salt Flats) of the Southern and Western Arabian Gulf', in C Max Finlayson, G Randy Milton, R Crawford Prentice, & Nick C Davidson (eds.) *The Wetland Book: II: Distribution, Description, and Conservation*. [Online]. Dordrecht: Springer Netherlands. pp. 1173–1183.
- Loy, C.W. & Chu, W.-L. (2012) 'Biotechnological applications of microalgae', *IeJSME*, 6(Suppl 1), pp. S24–S37.
- Machado, L., Carvalho, G. & Pereira, R.N. (2022) 'Effects of Innovative Processing Methods on Microalgae Cell Wall: Prospects towards Digestibility of Protein-Rich Biomass', *Biomass* 2022, Vol. 2, Pages 80-102, 2(2), pp. 80–102.
- Marrucci, G. (1969) 'A theory of coalescence', *Chemical Engineering Science*, 24(6), pp. 975–985.
- Martin, P.J., Dutton, H.M., Winterburn, J.B., Baker, S. & Russell, A.B. (2010) 'Foam fractionation with reflux', *Chemical Engineering Science*, 65(12), pp. 3825–3835.

- Masojídek, J., Kopecký, J., Giannelli, L. & Torzillo, G. (2011) 'Productivity correlated to photobiochemical performance of *Chlorella* mass cultures grown outdoors in thin-layer cascades', *Journal of Industrial Microbiology and Biotechnology*, 38(2), pp. 307–317.
- Masojídek, J., Lhotský, R., Štěrbová, K., Zittelli, G.C. & Torzillo, G. (2023) 'Solar bioreactors used for the industrial production of microalgae', *Applied Microbiology and Biotechnology*, 107(21), pp. 6439–6458.
- Masojídek, J. & Torzillo, G. (2014) 'Mass Cultivation of Freshwater Microalgae☆', in *Reference Module in Earth Systems and Environmental Sciences*. [Online]. Elsevier.
- Masojídek, J. & Torzillo, G. (2014) 'Mass Cultivation of Freshwater Microalgae☆', in *Reference Module in Earth Systems and Environmental Sciences*. [Online]. Elsevier.
- Mata, T.M., Martins, A.A. & Caetano, N.S. (2010) 'Microalgae for biodiesel production and other applications: A review', *Renewable and Sustainable Energy Reviews*, 14(1), pp. 217–232.
- Medipally, S.R., Yusoff, F.M., Banerjee, S. & Shariff, M. (2015) 'Microalgae as Sustainable Renewable Energy Feedstock for Biofuel Production', *BioMed Research International*,
- Merz, J., Zorn, H., Burghoff, B. & Schembecker, G. (2011) 'Purification of a fungal cutinase by adsorptive bubble separation: A statistical approach', *Colloids and Surfaces A: Physicochemical and Engineering Aspects*, 382(1–3), pp. 81–87.
- Miettinen, T., Ralston, J. & Fornasiero, D. (2010) 'The limits of fine particle flotation', *Minerals Engineering*, 23(5), pp. 420–437.
- Milledge, J.J. & Heaven, S. (2013) 'A review of the harvesting of micro-algae for biofuel production'. *Reviews in Environmental Science and Biotechnology*
- Milledge, J.J. & Heaven, S. (2011) 'Disc Stack Centrifugation Separation and Cell Disruption of Microalgae: A Technical Note', *Environment and Natural Resources Research*,
- Moheimani, N.R., Borowitzka, M.A., Isdepsky, A. & Sing, S.F. (2013) 'Standard Methods for Measuring Growth of Algae and Their Composition', in *Algae for Biofuels and Energy*. [Online]. Dordrecht: Springer Netherlands. pp. 265–284.
- Molina Grima, E., Belarbi, E.-H., Acien Fernández, F., Robles Medina, A. & Chisti, Y. (2003) 'Recovery of microalgal biomass and metabolites: process options and economics', *Biotechnology Advances*, 20(7–8), pp. 491–515.

- Möllers, K.B., Cannella, D., Jørgensen, H. & Frigaard, N.-U. (2014) 'Cyanobacterial biomass as carbohydrate and nutrient feedstock for bioethanol production by yeast fermentation', *Biotechnology for Biofuels*, 7(1), p. 64.
- Moolman, D.W., Aldrich, C., Schmitz, G.P.J. & Van Deventer, J.S.J. (1996) 'The interrelationship between surface froth characteristics and industrial flotation performance', *Minerals Engineering*, 9(8), pp. 837–854.
- Mutanda, T., Naidoo, D., Bwapwa, J.K. & Anandraj, A. (2020) 'Biotechnological Applications of Microalgal Oleaginous Compounds: Current Trends on Microalgal Bioprocessing of Products', *Frontiers in Energy Research*, 8(598803), .
- Nash, M.C., Diaz-Pulido, G., Harvey, A.S. & Adey, W. (2019) 'Coralline algal calcification: A morphological and process-based understanding', *PLOS ONE*, 14(9), p. e0221396.
- Nguyen, A. & Schulze, H.J. (2003) 'Colloidal Science of Flotation', *Colloidal Science of Flotation*,
- Niecikowska, A., Zawala, J. & Malysa, K. (2011) 'Influence of adsorption of nalkyltrimethylammonium bromides (C8, C12, C16) and bubble motion on kinetics of the bubble attachment to mica surface', *Physicochemical Problems of Mineral Processing*, 47(1), pp. 237–248.
- Nozzi, N., Oliver, J. & Atsumi, S. (2013) 'Cyanobacteria as a Platform for Biofuel Production', *Frontiers in Bioengineering and Biotechnology*, 1.
- Nzayisenga, J.C., Niemi, C., Ferro, L., Gorzszas, A., Gentili, F.G., Funk, C. & Sellstedt, A. (2020) 'Screening Suitability of Northern Hemisphere Algal Strains for Heterotrophic Cultivation and Fatty Acid Methyl Ester Production'. *Molecules* 25 (9).
- Oh, H.-M., June Lee, S., Park, M.-H., Kim, H.-S., Kim, H., Yoon, J.-H., Kwon, G.-S. & Yoon, B.-D. (2001) *Harvesting of Chlorella vulgaris using a bioflocculant from Paenibacillus sp. AM49*. Vol. 23.
- Olaizola, M. (2003) 'Commercial development of microalgal biotechnology: from the test tube to the marketplace', *Biomolecular Engineering*, 20(4–6), pp. 459–466.
- Ometto, F., Pozza, C., Whitton, R., Smyth, B., Torres, A.G., Henderson, R.K., Jarvis, P., Jefferson, B. & Villa, R. (2014) 'The impacts of replacing air bubbles with microspheres for the clarification of algae from low cell-density culture', *Water Research*, 53pp. 168–179.

- van Oss, C.J. (1995) 'Hydrophobicity of biosurfaces — Origin, quantitative determination and interaction energies', *Colloids and Surfaces B: Biointerfaces*, 5(3–4), pp. 91–110.
- Ozkan, A. & Berberoglu, H. (2013) 'Physico-chemical surface properties of microalgae', *Colloids and Surfaces B: Biointerfaces*, 112pp. 287–293.
- Packer, M. (2009) 'Algal capture of carbon dioxide; biomass generation as a tool for greenhouse gas mitigation with reference to New Zealand energy strategy and policy', *Energy Policy*, 37(9), pp. 3428–3437.
- Pahl, S.L., Lee, A.K., Kalaitzidis, T., Ashman, P.J., Sathe, S. & Lewis, D.M. (2013) 'Harvesting, Thickening and Dewatering Microalgae Biomass', in Michael A Borowitzka & Navid R Moheimani (eds.) *Algae for Biofuels and Energy*. [Online]. Dordrecht: Springer Netherlands. pp. 165–185.
- Paria, S. & Khilar, K.C. (2004) 'A review on experimental studies of surfactant adsorption at the hydrophilic solid–water interface', *Advances in Colloid and Interface Science*, 110(3), pp. 75–95.
- Pawlik, M. (2022) 'Fundamentals of froth flotation', *ChemTexts*, 8(4), pp. 1–40.
- Pires, J.C.M. (2017) *Microalgae as a Source of Bioenergy : products, processes and economics*, in José Carlos Magalhães Pires (ed.) 1st edition [Online]. Sharjah: Bentham Science Publishers Sharjah.
- Plączek, M., Patyna, A. & Witczak, S. (2017) 'Technical evaluation of photobioreactors for microalgae cultivation', in *International Conference on Energy, Environment and Material Systems*. [Online]. 2017
- Pothong, P., Chawaloephonsiya, N., Puprasert, C. & Painmanakul, P. (2012) 'Treatment of Cutting Oily Wastewater by Dissolved Air Flotation (DAF) process', *Engineering Journal*, 3(4), pp. 1–14.
- Prakash, R., Majumder, S.K. & Singh, A. (2018) 'Flotation technique: Its mechanisms and design parameters', *Chemical Engineering and Processing - Process Intensification*, 127pp. 249–270.
- Prates, A.D.S., Schorer, M., Moura, G.S., Lanna, E.A.T., Castro, G.F. & Pedreira, M.M. (2018) 'Microalgae *Schizochytrium* sp. in Feed for Piau *Leporinus friderici*', *American Journal of Animal and Veterinary Sciences Original Research Paper*,
- Pugh, R.J. (2016a) 'Basic principles and concepts', in *Bubble and Foam Chemistry*. [Online]. Cambridge University Press. pp. 1–53.

- Pugh, R.J. (2016b) 'Bubble and Foam Chemistry', *Bubble and Foam Chemistry*,
- Pugh, R.J. (2016c) 'Particle-stabilized foams', in *Bubble and Foam Chemistry*. [Online]. Cambridge University Press. pp. 269–306.
- Pugh, R.J. (2016d) 'Processes in foaming', in *Bubble and Foam Chemistry*. [Online]. Cambridge University Press. pp. 112–154.
- Qi, S., Chen, J., Hu, Y., Hu, Z., Zhan, X. & Stengel, D.B. (2022) 'Low energy harvesting of hydrophobic microalgae (*Tribonema* sp.) by electro-flotation without coagulation', *Science of The Total Environment*, 838p. 155866.
- Qin, L., Alam, M.A. & Wang, Z. (2019) 'Open Pond Culture Systems and Photobioreactors for Microalgal Biofuel Production', in *Microalgae Biotechnology for Development of Biofuel and Wastewater Treatment*. [Online]. Singapore: Springer Singapore. pp. 45–74.
- Ralston, J., Fornasiero, D. & Hayes, R. (1999) 'Bubble–particle attachment and detachment in flotation', *International Journal of Mineral Processing*, 56(1–4), pp. 133–164.
- Raven, J.A. & Giordano, M. (2014) 'Algae', *Current Biology*, 24(13), pp. R590–R595.
- Reis, A.S., Mendes, T.F., Petri Júnior, I., S Barrozo, M.A. & Petri unior, I.J. (2023) 'Influence of bubble size on performance of apatite flotation of different particle sizes', <https://doi.org/10.1080/02726351.2023.2170840>, pp. 1–9.
- Reis, A.S., Reis Filho, A.M., Demuner, L.R. & Barrozo, M.A.S. (2019) 'Effect of bubble size on the performance flotation of fine particles of a low-grade Brazilian apatite ore', *Powder Technology*, 356pp. 884–891.
- Rosa, P.T. V., Santana, C.C. & Carbonell, R.G. (2007) 'Determination of the liquid pool surfactant and protein concentration for semi-batch foam fractionation columns', *Brazilian Journal of Chemical Engineering*, 24(1), pp. 1–14.
- Rösch, C., Roßmann, M. & Weickert, S. (2019) 'Microalgae for integrated food and fuel production', *GCB Bioenergy*, 11(1), pp. 326–334.
- Roselet, F., Vandamme, D., Muylaert, K. & Abreu, P.C. (2019) 'Harvesting of Microalgae for Biomass Production', in Md. Asraful Alam & Zhongming Wang (eds.) *Microalgae Biotechnology for Development of Biofuel and Wastewater Treatment*. [Online]. Singapore: Springer Singapore. pp. 211–243.
- Rosen, M.J. & Kunjappu, J.T. (2012) 'Characteristic Features of Surfactants', *Surfactants and Interfacial Phenomena*, 4pp. 1–38.

- Rosenberg, J.N., Oyler, G.A., Wilkinson, L. & Betenbaugh, M.J. (2008) 'A green light for engineered algae: redirecting metabolism to fuel a biotechnology revolution', *Current Opinion in Biotechnology*, 19(5), pp. 430–436.
- Ruth, D.J., Vernet, M., Perrard, S. & Deike, L. (2021) 'The effect of nonlinear drag on the rise velocity of bubbles in turbulence', *Journal of Fluid Mechanics*, 924p. A2.
- Saadaoui, I., Rasheed, R., Aguilar, A., Cherif, M., Al Jabri, H., Sayadi, S. & Manning, S.R. (2021) 'Microalgal-based feed: promising alternative feedstocks for livestock and poultry production', *Journal of Animal Science and Biotechnology*, 12(1), p. 76.
- Saint-Jalmes, A. (2006) 'Physical chemistry in foam drainage and coarsening', *Soft Matter*, 2(10), pp. 836–849.
- Saint-Jalmes, A., Zhang, Y. & Langevin, D. (2004) 'Quantitative description of foam drainage: Transitions with surface mobility', *The European Physical Journal E 2004 15:1*, 15(1), pp. 53–60.
- Saliu, T.D., Lawal, I.A., Akinyeye, O.J., Bulu, Y.I., Klink, M., Ololade, I.A. & Oladoja, N.A. (2022) 'Biocoagulant with Frother Properties for Harvesting Invasive Microalgae Colonies from the Eutrophicated System', *ACS Sustainable Chemistry & Engineering*, 10(15), pp. 5024–5034.
- Sarker, P.K., Kapuscinski, A.R., Lanois, A.J., Livesey, E.D., Bernhard, K.P. & Coley, M.L. (2016) 'Towards Sustainable Aquafeeds: Complete Substitution of Fish Oil with Marine Microalga *Schizochytrium* sp. Improves Growth and Fatty Acid Deposition in Juvenile Nile Tilapia (*Oreochromis niloticus*)', *PLOS ONE*, 11(6), p. e0156684.
- Sathasivam, R., Radhakrishnan, R., Hashem, A. & Abd_Allah, E.F. (2017) 'Microalgae metabolites: A rich source for food and medicine', *Saudi Journal of Biological Sciences*,
- Scardina, P. & Edwards, M. (2000) 'The Fundamentals of Bubble Formation in Water Treatment', *Virginia Polytechnic Institute and State University*,
- Schenk, Peer M, Thomas-Hall, Skye R, Stephens, Evan, Marx, Ute C, Mussgnug, Jan H, Posten, Clemens, Kruse, Olaf, Hankamer, Ben, Schenk, P M, Thomas-Hall, S R, Stephens, E, Marx, U C, Hankamer, B, Mussgnug, J H, Kruse, O & Posten, C (2008) 'Second Generation Biofuels: High-Efficiency Microalgae for Biodiesel Production', *BioEnergy Research*, 1(1), pp. 20–43.
- Seneesrisakul, K., Kanokkarn, P., Charoensaeng, A. & Chavadej, S. (2021) 'Motor oil removal from water by continuous froth flotation: The influence of surfactant structure on interfacial adsorption and foam properties', *Colloids and Surfaces A: Physicochemical and Engineering Aspects*, 618p. 126499.

- Shammas, N.K. & Bennett, G.F. (2010) 'Principles of Air Flotation Technology', in *Flotation Technology*. [Online]. Totowa, NJ: Humana Press. pp. 1–47.
- Shaw, R., Evans, G.M. & Stevenson, P. (2011) 'Start-up transients in a pneumatic foam', *Asia-Pacific Journal of Chemical Engineering*, 6(4), pp. 613–623.
- Sheath, R.G. & Wehr, J.D. (2015) 'Introduction to the Freshwater Algae', *Freshwater Algae of North America: Ecology and Classification*, pp. 1–11.
- Sheehan, J., Dunahay, T., Benemann, J. & Roessler, P. (1998) *A Look Back at the U.S. Department of Energy's Aquatic Species Program: Biodiesel from Algae Close-Out Report*,
- Shen, Z., Li, Y., Wen, H., Ren, X., Liu, J. & Yang, L. (2018) 'Investigation on the role of surfactants in bubble-algae interaction in flotation harvesting of *Chlorella vulgaris*', *Scientific Reports 2018* 8:1, 8(1), pp. 1–10.
- Show, K.-Y. & Lee, D.-J. (2014) 'Algal Biomass Harvesting', in Ashok Pandey, Duu-Jong Lee, Yusuf Chisti, & Carlos R B T - Biofuels from Algae Soccol (eds.) *Biofuels from Algae*. [Online]. Amsterdam: Elsevier. pp. 85–110.
- Singh, R.N. & Sharma, S. (2012) 'Development of suitable photobioreactor for algae production – A review', *Renewable and Sustainable Energy Reviews*, 16(4), pp. 2347–2353.
- Solarski, M.M. (2019) *Flow of bubbles and foams in narrow microfluidic geometries*,
- Sommerfeld, A.J.W. (1908) 'A Contribution to Hydrodynamic Explanation of Turbulent Fluid Motions', *International Congress of Mathematicians*, 3pp. 116–124.
- Spolaore, P., Joannis-Cassan, C., Duran, E. & Isambert, A. (2006) 'Commercial applications of microalgae', *Journal of Bioscience and Bioengineering*, 101(2), pp. 87–96.
- Srirathchatchawarn, S. & Petiruksakul, A. (2016) 'Dissolved Air Flotation Processes', *The Journal of King Mongkut's University of Technology North Bangkok*,
- Stachowiak, B. & Szulc, P. (2021) 'Astaxanthin for the Food Industry'. *Molecules* 26 (9).
- Stamatis, H., Xenakis, A., Provelegiou, M. & Kolisis, F.N. (1993) 'Esterification reactions catalyzed by lipases in microemulsions: The role of enzyme localization in relation to its selectivity', *Biotechnology and Bioengineering*, 42(1), pp. 103–110.
- Stanier, R.Y., Kunisawa, R., Mandel, M. & Cohen-Bazire, G. (1971) 'Purification and properties of unicellular blue-green algae (order Chroococcales).', *Bacteriological reviews*, 35(2), pp. 171–205.

- Stevenson, P. (2012) 'Foam Engineering: Fundamentals and Applications', *Foam Engineering: Fundamentals and Applications*,
- Stevenson, P. & Li, X. (2014) *Foam Fractionation : Principles and Process Design*. CRC Press.
- Stevenson, P., Li, X. & Evans, G.M. (2008) 'A mechanism for internal reflux in foam fractionation', *Biochemical Engineering Journal*, 39(3), pp. 590–593.
- Suganya, T., Varman, M., Masjuki, H.H. & Renganathan, S. (2016) 'Macroalgae and microalgae as a potential source for commercial applications along with biofuels production: A biorefinery approach', *Renewable and Sustainable Energy Reviews*, 55pp. 909–941.
- Sullivan, J.M. (1999) 'The Geometry of Bubbles and Foams', *Foams and Emulsions*, pp. 379–402.
- Sumi, Y. (2009) 'Microalgae Pioneering the Future - Application and Utilization'. SCIENCE & TECHNOLOGY TRENDS p.pp. 9–21.
- Swamy, J.N., Crofcheck, C.L. & Mengüç, M.P. (2010) 'Polarized light based scheme to monitor column performance in a continuous foam fractionation column', *Journal of Biological Engineering*, 4(1), p. 5.
- Tan, X.B., Lam, M.K., Uemura, Y., Lim, J.W., Wong, C.Y. & Lee, K.T. (2018) 'Cultivation of microalgae for biodiesel production: A review on upstream and downstream processing', *Chinese Journal of Chemical Engineering*, 26(1), pp. 17–30.
- Tao, D. (2010) 'Role of Bubble Size in Flotation of Coarse and Fine Particles—A Review', <https://doi.org/10.1081/SS-120028444>, 39(4), pp. 741–760.
- Tao, X., Liu, Y., Jiang, H. & Chen, R. (2019) 'Microbubble generation with shear flow on large-area membrane for fine particle flotation', *Chemical Engineering and Processing - Process Intensification*, 145p. 107671.
- Taylor, F.J.R., Hoppenrath, M. & Saldarriaga, J.F. (2008) 'Dinoflagellate diversity and distribution', *Biodiversity and Conservation*, 17(2), pp. 407–418.
- Team group (2012) *Port Waste Management in Thai Ports*.
- Teo, C.L. & Idris, A. (2014) 'Evaluation of direct transesterification of microalgae using microwave irradiation', *Bioresource Technology*, 174pp. 281–286.
- Tiwari, M. & Tripathy, D.B. (2023) 'Soil Contaminants and Their Removal through Surfactant-Enhanced Soil Remediation: A Comprehensive Review', *Sustainability 2023, Vol. 15, Page 13161*, 15(17), p. 13161.

- Tobin, S.T., Weaire, D. & Hutzler, S. (2014) 'Theoretical analysis of the performance of a foam fractionation column', *Proceedings of the Royal Society A: Mathematical, Physical and Engineering Sciences*, 470(2165), .
- Trentacoste, E.M., Martinez, A.M. & Zenk, T. (2015) 'The place of algae in agriculture: policies for algal biomass production.', *Photosynthesis research*, 123(3), pp. 305–15.
- Uduman, N., Qi, Y., Danquah, M.K., Forde, G.M. & Hoadley, A. (2010) 'Dewatering of microalgal cultures: A major bottleneck to algae-based fuels', *J. Renewable Sustainable Energy*, 2p. 12701.
- Vahidi, K., Jalili, Y.S. & Salar Elahi, A. (2017) 'The effect of varying the introduction mode of reactants on electrical, physical and thermal stability properties of polypyrrole synthesized with CTAB', *AIP Advances*, 7(10), p. 105222.
- Vandamme, D. (2017) 'Harvesting, Thickening and Dewatering Processes', in *Microalgae as a Source of Bioenergy: Products, Processes and Economics*. TA - TT -. [Online]. pp. 202–223.
- Vazquez Calderon, F. & Sanchez Lopez, J. (2022) *An overview of the algae industry in Europe. Producers, production systems, species, biomass uses, other steps in the value chain and socio-economic data* Jordi Guillen & Marios Avraamides (eds.). (JRC130107).
- Vidu, R., Matei, E., Predescu, A.M., Alhalaili, B., Pantilimon, C., Tarcea, C. & Predescu, C. (2020) 'Removal of Heavy Metals from Wastewaters: A Challenge from Current Treatment Methods to Nanotechnology Applications', *Toxics 2020, Vol. 8, Page 101*, 8(4), p. 101.
- Walstra, P. (1989) *Principles of Foam Formation and Stability*, pp. 1–15.
- Wang, B., Lan, C.Q. & Horsman, M. (2012) 'Closed photobioreactors for production of microalgal biomasses', *Biotechnology Advances*, 30(4), pp. 904–912.
- Wang, J., Cao, Y., Li, G., Deng, L. & Li, S. (2018) 'Effect of CTAB Concentration on Foam Properties and Discussion Based on Liquid Content and Bubble Size in the Foam', *International Journal of Oil, Gas and Coal Engineering*, 6(1), p. 18.
- Wang, J., Nguyen, A. V. & Farrokhpay, S. (2016) 'A critical review of the growth, drainage and collapse of foams', *Advances in Colloid and Interface Science*, 228pp. 55–70.
- Wang, J., Yang, H. & Wang, F. (2014) 'Mixotrophic Cultivation of Microalgae for Biodiesel Production: Status and Prospects', *Applied Biochemistry and Biotechnology*, 172(7), pp. 3307–3329.

- Wang, L. & Jonikas, M.C. (2020) 'The pyrenoid', *Current Biology*, 30pp. R456–R458.
- Wang, L. & Langley, D. (1975) 'Determining Cationic Surfactant Concentration', *Industrial & Engineering Chemistry Product Research and Development*, 14(3), pp. 210–212.
- Wang, L.K., Fahey, E.M. & Wu, Z. (2005) 'Dissolved Air Flotation', in Lawrence K Wang, Yung-Tse Hung, & Nazih K Shammam (eds.) *Physicochemical Treatment Processes*. [Online]. Totowa, NJ: Humana Press. pp. 431–500.
- Wang, L.K., Shammam, N.K., Selke, W.A. & Aulenbach, D.B. (eds.) (2010) *Flotation Technology*. Totowa, NJ: Humana Press.
- Ward, O.P. & Singh, A. (2005) 'Omega-3/6 fatty acids: Alternative sources of production', *Process Biochemistry*, 40(12), pp. 3627–3652.
- Weeks, N.C., Timmons, M.B. & Chen, S. (1992) 'Feasibility of using foam fractionation for the removal of dissolved and suspended solids from fish culture water', *Aquacultural Engineering*, 11(4), pp. 251–265.
- Wehr, J., Sheath, R. & Kociolek, P. (2015) *Freshwater Algae of North America: Ecology and Classification*. 2nd edition.
- Wehr, J.D. & Sheath, R.G. (2015) 'Habitats of Freshwater Algae', *Freshwater Algae of North America: Ecology and Classification*, pp. 13–74.
- Wierenga, P.A., Basheva, E.S. & Delahaije, R.J.B.M. (2023) 'Variations in foam collapse and thin film stability with constant interfacial and bulk properties', *Advances in Colloid and Interface Science*, 312p. 102845.
- Wiley, P.E., Brenneman, K.J. & Jacobson, A.E. (2009) 'Improved Algal Harvesting Using Suspended Air Flotation', *Water Environment Research*, 81(7), pp. 702–708.
- Wilkie, A.C., Edmundson, S.J. & Duncan, J.G. (2011) 'Indigenous algae for local bioresource production: Phycoprospecting', *Energy for Sustainable Development*, 15(4), pp. 365–371.
- Williams, P.J. le B. & Laurens, L.M.L. (2010) 'Microalgae as biodiesel & biomass feedstocks: Review & analysis of the biochemistry, energetics & economics', *Energy & Environmental Science*, 3(5), pp. 554–590.
- Wunsch, N.-G. (2020) *Algae products: market value worldwide 2018-2025* | *Allied Market Research*. [Online] [online]. Available from: <https://www.statista.com/statistics/1029897/market-size-algae-products-global/> (Accessed 12 November 2023).

- Y. Shen, W. Yuan, Z. J. Pei, Q. Wu & E. Mao (2009) 'Microalgae Mass Production Methods', *Transactions of the ASABE*,
- Yaminsky, V. V., Ohnishi, S., Vogler, E.A. & Horn, R.G. (2010) 'Stability of aqueous films between bubbles. Part 1. the effect of speed on bubble coalescence in purified water and simple electrolyte solutions', *Langmuir*, 26(11), pp. 8061–8074.
- Yan, C., Fan, J. & Xu, C. (2013) 'Chapter 5 - Analysis of Oil Droplets in Microalgae', in Hongyuan Yang & Peng B T - Methods in Cell Biology Li (eds.) *Lipid Droplets*. [Online]. Academic Press. pp. 71–82.
- Yazhgur, P., Rio, E., Rouyer, F., Pigeonneau, F. & Salonen, A. (2016) 'Drainage in a rising foam', *Soft Matter*, 12(3), pp. 905–913.
- Yin, Z., Zhu, L., Li, S., Hu, T., Chu, R., Mo, F., Hu, D., Liu, C. & Li, B. (2020) 'A comprehensive review on cultivation and harvesting of microalgae for biodiesel production: Environmental pollution control and future directions', *Bioresource Technology*, 301p. 122804.
- Yoon, R.H. (2000) 'The role of hydrodynamic and surface forces in bubble–particle interaction', *International Journal of Mineral Processing*, 58(1–4), pp. 129–143.
- Yoon, R.H. & Luttrell, G.H. (1989) 'The Effect of Bubble Size on Fine Particle Flotation', *Mineral Processing and Extractive Metallurgy Review*, 5(1–4), pp. 101–122.
- Yu, K., Li, B., Zhang, H., Wang, Z., Zhang, W., Wang, D., Xu, H., Harbottle, D., Wang, J. & Pan, J. (2021) 'Critical role of nanocomposites at air–water interface: From aqueous foams to foam-based lightweight functional materials', *Chemical Engineering Journal*, 416p. 129121.
- Yu, W., Zhou, X. & Kanj, M.Y. (2022) 'Microfluidic Investigation of Foam Coarsening Dynamics in Porous Media at High-Pressure and High-Temperature Conditions', *Langmuir*, 38(9), pp. 2895–2905.
- Zamanikherad, M., Montazeri, A., Gheibi, M., Fathollahi-Fard, A.M. & Behzadian, K. (2023) 'An efficient design of primary sedimentation tanks using a combination of the response surface, metaheuristic, and scenario building methods', *International Journal of Environmental Science and Technology*, 20(2), pp. 1215–1246.
- Zawala, J. & Malysa, K. (2011) 'Influence of the impact velocity and size of the film formed on bubble coalescence time at water surface', *Langmuir*, 27(6), pp. 2250–2257.
- Zhang, H. & Zhang, X. (2019) 'Microalgal harvesting using foam flotation: A critical review', *Biomass and Bioenergy*, 120pp. 176–188.

- Zhang, X., Gu, X., Han, Y., Parra-Álvarez, N., Claremboux, V. & Kawatra, S.K. (2019) 'Flotation of Iron Ores: A Review', *Mineral Processing and Extractive Metallurgy Review*, 42(3), pp. 184–212.
- Zhao, F., Li, Zhichao, Han, X., Shao, Z. & Li, Zongxue (2022) 'Optimization of Air Flotation and the Combination of Air Flotation and Membrane Filtration in Microalgae Harvesting', *Processes* 2022, Vol. 10, Page 1594, 10(8), p. 1594.
- Zhao, H., Zheng, L., Li, X., Chen, P. & Hou, Z. (2020) 'Hydrogenolysis of glycerol to 1,2-propanediol over Cu-based catalysts: A short review', *Catalysis Today*, 355pp. 84–95.
- Zhou, G., Zhang, H., Yang, W., Wu, Z., Liu, W. & Yang, C. (2020) 'Biobleaching assisted foam fractionation for recovery of gold from the printed circuit boards of discarded cellphone', *Waste Management*, 101pp. 200–209.
- Zhou, W., Min, M., Hu, B., Ma, X., Liu, Y., Wang, Q., Shi, J., Chen, P. & Ruan, R. (2013) 'Filamentous fungi assisted bio-flocculation: A novel alternative technique for harvesting heterotrophic and autotrophic microalgal cells', *Separation and Purification Technology*, 107pp. 158–165.
- Zullaikah, S., Utomo, A.T., Yasmin, M., Ong, L.K. & Ju, Y.H. (2019) 'Ecofuel conversion technology of inedible lipid feedstocks to renewable fuel', in Kalam Azad (ed.) *Advances in Eco-Fuels for a Sustainable Environment*. Woodhead Publishing Series in Energy. [Online]. Woodhead Publishing. pp. 237–276.